Synthesis, Structural Characterization, and Subsequent Applications of Salicyldiminato Pd (II) Complexes as Efficient Catalysts for C-C Bond-forming Reactions.

Submitted in fulfilment of the academic requirements for the degree of Master of Science in Chemistry

College of Agriculture, Engineering, and Science,

School of Chemistry and Physics

University of KwaZulu-Natal

Pietermaritzburg

South Africa

by

Khethukuthula Petronella Mallecia Khoza

219034150

Supervisor: Dr. S. Sithebe

August 2024

DECLARATION 1

I, Khethukuthula Petronella Mallecia Khoza, hereby declare that:

1. The research report in this thesis, except where otherwise indicated, is my original research.
2. This thesis has not been submitted for any degree or examination at any other university.
3. This thesis does not contain other persons' data, pictures, graphs, or other information, unless specifically acknowledged as being sourced from other persons.
4. This thesis does not contain other persons' writing, unless specifically acknowledged as being sourced from other researchers. Where other written sources have been quoted, then:

a) Their words have been re-written, but the general information attributed to them has been referenced.

b) Where their exact words have been used then their writing has been placed in italics and inside quotation marks and referenced.

5. This thesis does not contain text, graphics or tables copied and pasted from the internet, unless specifically acknowledged and the source being detailed in the thesis and in the References sections.

[redacted]

Khethukuthula Petronella Mallecia Khoza (Student)

As trithe supervisor of the student, I approve the submission of this MSc Thesis for examination.

[redacted]

Dr S. Sithebe (Supervisor)

DECLARATION 2 – CONFERENCE PRESENTATIONS

Some parts of this research have been presented in the following conferences:

1. Khethukuthula Petronella Mallecia Khoza and Dr Siphamandla Sithebe. College of Agriculture, Engineering and Science. Postgraduate Research and Innovation Symposium (PRIS). November 2023. Flash Presentation. Synthesis, Structural Characterization, and Subsequent Applications of Salicyldiminato Pd (II) Complexes as Efficient Catalysts for C-C Bond-forming Reactions.

2. Khethukuthula Petronella Mallecia Khoza and Dr Siphamandla Sithebe. The South African Chemical Institute-KwaZulu-Natal Section (SACI-KZN) with ChemBurg and the School of Chemistry and Physics (UKZN-PMB). November 2023. Poster Presentation. Synthesis, Structural Characterization, and Subsequent Applications of Salicyldiminato Pd (II) Complexes as Efficient Catalysts for C-C Bond-forming Reaction.

ABSTRACT

Palladium-catalysed cross-coupling reactions (i.e., Heck, Stille, Liebeskind Strogl, and Suzuki-Miyaura) are perceived as one of the most prominent, successful, and widely used strategies for the construction of complex organic compounds such as biaryls from simple precursors. Amongst the known carbon-carbon bond-forming reactions, the Suzuki-Miyaura (SM) cross-coupling reaction has emerged as one of the most efficient and powerful methodologies due to its high versatility, use of non-toxic reagents, mild reaction conditions, broad substrate scope, and functional group tolerance. The SM cross-coupling has not only greatly changed the landscape of the field of organic chemistry, but also profoundly impacted pharmaceuticals, agrochemicals, natural products, material science, and various related industries. Stable supporting ligands are key in the catalytic activities of Pd complexes. The design and development of supporting ligands that will result in stable Pd complexes while maintaining high catalytic activity and catalytic turnover through stereo-electronic effect alteration are highly desirable. With the aim of developing stable highly catalytic Pd complexes, our research focus is directed towards the synthesis, characterisation, and application of novel *N, O*-bis Schiff base chelated Pd (II) complexes (**PdC1** - **PdC7**) from Schiff base ligands (**L1** - **L7**).

The synthesis of *(E)-2-((phenylimino)methyl) phenol* (**L1**), *(E)-2-((4-tolylimino)methyl) phenol* (**L2**), *(E)-2-(((4-ethylphenyl)imino)methyl) phenol* (**L3**), *(E)-2-(((4-methoxyphenyl) imino)methyl) phenol* (**L4**), *(E)-2-(((4-fluorophenyl)imino)methyl) phenol* (**L5**), *(E)-2-(((4-bromophenyl)imino)methyl) phenol* (**L6**), and *(E)-4-((2-hydroxybenzylidene)amino) benzonitrile* (**L7**) was achieved in excellent yields (80% - 94%) through a condensation reaction of salicyldehyde with various electron-withdrawing and donating *para*-substituted anilines. The reaction between **L1** - **L7** and Palladium acetate Pd $(OAc)_2$) afforded **PdC1** - **PdC7** with yields ranging from 78% - 95%. The successful synthesis of **L1** - **L7** was verified by NMR, FTIR, and MS analyses, while all complexes (**PdC1** - **PdC7**) were characterised using NMR, FTIR, MS, and Single X-ray crystallography. However, a comprehensive X-ray data report was only obtained for **PdC2**, as the X-ray crystallographic structures of **PdC3** - **PdC7** proved difficult to solve. The crystallographic analysis of **PdC2** revealed that **L2** is coordinated to the Pd metal center in a bidentate mode *via* the *N*-donor of the imine bond and the *O*-donor of the phenolic group. The complex displayed a distorted square planar geometry and crystallised in a monoclinic crystal system with a P21/c space group.

All the complexes were tested for catalytic activity in the SM cross-coupling reaction between sodium (trihydroxy)phenylborate salt and 4-bromotoluene. The reactions were catalysed with a catalyst loading of 2 mol% for 24 hours in ethanol, yielding 18% - 32% of the desired biaryl product.

Motivated by the successful cross-coupling reaction between sodium (trihydroxy)phenylborate salt and 4-bromotoluene, we opted to broaden the application scope of the complexes using the established reaction conditions in SM cross-coupling acylation reaction. We used the most active catalysts, **PdC2** and **PdC6** for constructing biaryl ketones through the reaction of benzoyl chloride with sodium (trihydroxy)phenylborate salt in toluene for 24 hours. The reactions yielded 15% and 30% of the desired products, respectively.

DEDICATION

I dedicate this thesis to my mother, whose love, support, and encouragement have sustained me throughout my educational journey.

ACKNOWLEDGEMENTS

Firstly, I would like to express my deep and sincere gratitude to my research supervisor, Dr Siphamandla Sithebe, for his professional guidance, enthusiastic encouragement, patience, motivation, and support.

I would also like to thank the technical staff of the Chemistry department for their assistance. I'm also grateful to the Mining Qualification Authorities (MQA) for financial support.

To my caring, loving, and supportive family who never ceased to believe in me, my heartfelt thanks for always being there to strengthen me with confidence every time I felt weak or discouraged. And as for my mom, ngilangikhona kungenca yakho. Ngiyabonga Gogo Tilela wami. Ngikutsandza kundlula imali, Vungandze!

I would also like to thank Patience Molefe, Dr Sibonelo Hlengwa and Dr Mncedisi Mazibuko for always being willing to assist me whenever I had questions or needed their help.

Finally, I thank all my friends, namely: Mmangeryzo, Mpinkeryzo, Narty, Berls, Pakman, Angel, and Thabie for their support and laughter.

Above all, praises and thanks to God, the Almighty, who has always been my guidance and support in every step of the way.

TABLE OF CONTENTS

LIST OF ABBREVIATIONS

BF_3•OEt_2	Boron trifluoride etherate
C–C	Carbon-carbon
C–N	Carbon-nitrogen
$CDCl_3$	Deuterated chloroform
$(CD_3)_2CO$	Deuterated acetone
D_2O	Deuterated water
d	Doublet
ESI-MS	Electrospray ionization mass spectrometry
FTIR	Fourier-transform infrared spectroscopy
GC-MS	Gas chromatography-mass spectrometry
H_2O	Water
hrs	Hours
L	Ligand
MS	Mass spectrometry
m	Multiplet
NHC	*N*-heterocyclic carbene
NMR	Nuclear magnetic resonance
OH	Hydroxyl
ppm	parts per million
Pd	Palladium
Pd $(OAc)_2$	Palladium acetate
$PdCl_2COD$	Dichloro(1,5-cyclooctadiene) palladium
q	Quartet

s	Singlet
SM	Suzuki-Miyaura
TLC	Thin Layer Chromatography
TMS	Tetramethylsilane
TOF-MS	Time-of-flight mass spectrometry
t	Triplet

LIST OF FIGURES

LIST OF SCHEMES

LIST OF TABLES

CHAPTER 1

1. Introduction

Ligand systems have been shown to play a significant role in influencing the reactivity, effectiveness and efficiency of catalytic systems.[1] Thus, the design of new ligand systems and their transition metal complexes that are effective in C–C bond-forming reactions with high conversion and selectivity has emerged as an exciting and challenging area of research.[2] Ligands serve not only to stabilize the metal center but also to enhance the activity and selectivity of the metal center by inducing stereochemistry and altering electronic and steric properties.[3] Chelating ligands containing both soft donor atoms such as Phosphorus (P) and Sulfur (S) as well as hard atoms such Nitrogen (N) and Oxygen (O) donor sites are not only of academic interest but are also attractive industrially for catalyst design due to their hemilabile behaviour, which enables facile and reversible generation of coordinatively unsaturated metal centers.[4] Unsaturated transition metals with open coordination sites typically serve as excellent catalysts in various catalytic processes.[5] Understanding how ligands influence the activity and structural properties of metal species has led to the discovery of new and improved catalysts. As a result, efforts have been made towards developing effective and efficient ligand systems (Discussed in **Chapter 2**). Among these ligands, Schiff bases have gained much attention since their discovery in 1864 when Hugo Schiff reported the condensation reaction of primary amines with carbonyl compounds.[6] They present an important class of organic compounds that contain an azomethine or imine (C=N) functional group in their structure (**Figure 1.1**).[7]

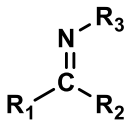

R_1 & R_2 = Alkyl/ Aryl/ H
R_3 = Alkyl/Aryl

Figure 1.1: General structure of Schiff base.

Schiff bases are recognized as popular prevalent ligands in coordination chemistry owing to their facile synthesis, availability, electronic characteristics, remarkable adaptability, selectivity towards transition metal ions, and ability to form highly stable Palladium (II) complexes.[8] The greater stability of Pd (II) can be attributed to its lower tendency to undergo one-electron or radical reactions.[9] In addition, it easily reacts in two-electron oxidation or

reduction reactions.[10] Schiff bases also serve as an extremely significant class of organic compounds due to being extensively employed in numerous fields such as industry, pharmaceuticals, analytical chemistry, and biology.[11,12]

Palladium complexes derived from Schiff base ligands have been the most extensively studied coordination compounds, primarily because of their crucial function as catalysts in forming carbon-carbon bonds.[13] Pd (II) complexes are also utilized in dental fillings, electrical components, jewellery, automotive catalytic converters, and fuel cells for power generation.[14,15]The structure of Schiff base ligands affects the steric and electronic properties of the palladium catalyst, thereby significantly influencing the efficiency of the carbon-carbon bond-forming reactions.[16]

Carbon-carbon bond-forming reactions are one of the most significant reactions in the realm of organic chemistry due to their ability to produce highly complex molecules such as biaryls from simple substrates which are an important class of organic compounds.[17] The biaryl unit is a recurrent building block in numerous compounds that have profoundly changed many aspects of the modern era, from natural and synthetic bioactive compounds to new organic materials, in all fields of chemistry.[18] As a structural component in agrochemicals, organic electronic devices, and pharmaceuticals, the biaryl moiety is a highly desirable synthetic target for both industry and academia.[19]

The most well-known efficient and powerful methodology for the construction of C-C bonds is the palladium-catalysed Suzuki-Miyaura (SM) cross-coupling reaction.[20] Its popularity stems from the environmentally benign nature of the organoboron reagents used such as aryl boronates, trifluoroborates and boronic acids which are readily available and less toxic.[21] In addition, the SM reaction can be carried in one pot strategy under mild conditions and proceeds with high regio- and stereoselectivity with a wide tolerance for a broad range of functional groups.[22] Although this method has many benefits, it also has drawbacks related to the organoboron compounds used as nucleophiles. Most organoboranes are sensitive to air and moisture (e.g. catechol borane, boranes, mono- and disubstituted halo boranes). The more stable organoboron compounds (boronic acids) slowly decompose to form di- and trisubstituted cyclic borane which makes it difficult to calculate, accurately, the stoichiometric ratios.[23] In addition, the major disadvantage of boronic acids lies in their nature as tri-coordinated organoboron compounds, hence they do not induce sufficient nucleophilicity to the organic

moiety directly bonded to them.[24] As a result, the addition of a base is essential to facilitate the transmetallation step.[24]

Researchers have reported several different methodologies (**Discussed in Chapter 2**) under Suzuki-Miyaura cross-coupling reactions. However, there have been few efforts directed towards the development of new nucleophiles that will efficiently facilitate SM cross-coupling reactions. One facile SM cross-coupling procedure for the synthesis of biaryl ketones was reported by Sithebe and Molefe, where they used sodium (trihydroxy) aryl boronate salts as nucleophiles which displayed numerous advantages over boronic acids.[25]

Based on the authors' findings, it has been observed that sodium (trihydroxy) aryl boronate salts are easy to synthesise and isolate, have high stability, can be coupled under base-free SM mild reaction conditions, and have a high tolerance for a wide range of functionalities including base sensitive substrates as they do not require a base to be activated for transmetallation.

This innovation has prompted us to implement the use of a small library of *N, O*-bis Schiff base chelated Pd (II) complexes as catalysts in SM cross-coupling reaction to explore the stereo-electronic effects of the ligand substituents on the Pd complexes and determine whether sodium (trihydroxy) aryl borate salts will transmetallate in Suzuki-Miyaura cross coupling reaction without the addition of a base thereby produce high yields of the desired biaryl products.

References

1. R.J. Lundgren, and M. Stradiotto, *John Wiley & Sons*, 1-14 (**2016**).
2. F. Chen, T. Wang, and N. Jiao, *Chemical Reviews*, 114(17), 8613-8661 (**2014**).
3. P.W.V. Leeuwen, P.C. Kamer, C. Claver, O. Pamies, and M. Dieguez, *Chemical Reviews*, 111(3), 2077-2118 (**2011**).
4. R.G. Cavell, R.G., *Current Science*, (78)(4), 440-451 (**2000**).
5. M. Hartings, *Nature Chemistry*, 4(9), 764-764 (**2012**).
6. H. Schiff, *Ann. Chem. Suppl*, 3, 343-349 (**1864**).
7. A. Kajal, S. Bala, S. Kamboj, N. Sharma, and V. Saini, *Journal of Catalysts*, 2013, 1-14 (**2013**).
8. M.S. More, P.G. Joshi, Y.K. Mishra, and P.K. Khanna, *Materials Today Chemistry*, 14,100195 (**2019**).
9. E.M. Beccalli, G. Broggini, M. Martinelli, and S. Sottocornola, *Chem. Rev*, 107(11), 5318-5365 (**2007**).
10. E. Negishi, and A.de. Meijere, *John Wiley & Sons*, 127-147 (**2003**).
11. J. Xu, Y. Liu, and S.H. Hsu, *Molecules*, 24(16), 3005 (**2019**).
12. P. Ghanghas, A. Choudhary, D. Kumar, and K. Poonia, *Inorganic Chemistry Communications*, 130, 108710 (**2021**).
13. M.P. Conley, R.F. Jordan, *Angewandte Chemie*, 123(16), 3828-3830 (**2011**).
14. T. Fleetham, G. Li, J. Li, *Advanced Materials*, 29(5), 1601861 (**2017**).
15. K.N. Nigussa, *Materials Research Express*, 6(10), 105540 (**2019**).
16. M. Schmidt, H. Görls, and W. Plass, *RSC advances*, 6(79), 75844-75854 (**2016**).
17. S. Kotha, K. Lahiri, D. Kashinath, *Tetrahedron*, 58(48), 9633-9695 (**2002**).
18. A.J.J. Lennox, G.C Lloyd-Jones, *Chem. Soc. Rev*, 43(1), 412-443 (**2014**).
19. M. Simonetti, D. Cannas, I. Larrosa, *Adv. Organomet. Chem*, 67, 299-399 (**2017**).
20. N. Miyaura, A. Suzuki, Miyaura, K. Yamada, *Tetrahedron Letters*, **20**(36), 3437-3440 (**1979**).
21. A.L. Casalnuovo, J.C. Calabrese, *Journal of the American Chemical Society*, 112(11), 4324-4330 (**1990**).
22. H.H. Rau, N.S. Werner, *Chem. Lett*, 28(16), 2693-2696 (**2018**).
23. S. Lai, N. Takaesu, W.X. Lin, and D.M. Perrin, 2021. *Tetrahedron Letters*, 74, 153147 (**2021**).
24. N.A. Bumagin, and D.N. Korolev, *Tetrahedron letters*, 40(15), 3057-3060 (**1999**).
25. S. Sithebe, and P. Molefe, *Journal of Organometallic Chemistry*, 846, 305-311 (**2017**)

CHAPTER 2

2. Literature review

2.1. Ligand systems influencing C-C bond-forming reactions

Ligands are atoms, molecules, or ions with non-bonded pair of electrons (lone pairs) that form a coordination complex with the central transitional metal atom(s) *via* coordinate bonds. [1] They are classified based on their proclivity to form coordinate bonds. This tendency of ligands is known as denticity.[2] Denticity of a ligand refers to the total number of donor groups (pairs of electrons) that bind to the central transition metal atom in a coordination complex.[3] There are various types of ligands with varying denticities used in coordination chemistry. Some of the most widely utilized common types of ligands include monodentate ligands, bidentate ligands, bridging ligands, polydentate ligands (chelate ligands), and so forth.[4]

Ligand systems have been shown to play an important role in affecting the reactivity and effectiveness of particular catalytic systems.[5] The application of ligands such as *N*-heterocyclic-ligands,[6-8] *P, O*-based ligands,[9] bipyridines,[10] phosphines,[11] Schiff base ligands,[12-17] bis(thiourea) ligands, [18] acyclic diaminocarbene [19] and others have recently broadened the scope of C-C bond forming reactions. However, the practical application of these ligands remains challenging due to the ligand's donor atom system which consists of not only soft bases like phosphorous (P) and sulfur (S) but also hard donors such as nitrogen (N) and oxygen (O) which affects the ligand's stability as well as their synthetic methodologies which require complicated and costly chemical organic precursors.[20] Moreover, the majority of them are susceptible to oxidation, which reduces their reactivity in most catalytic reactions.[21] As a result, the search for suitable ligands with higher reactivity and selectivity is still an ongoing research goal.

Tertiary phosphines have been extensively employed in the design and production of transition metal catalysts, notably for late transition metals including nickel (Ni), rhodium (Rh), ruthenium (Ru), platinum (Pt), and palladium (Pd).[22,23] Such catalysts are utilized in a variety of processes, such as hydroformylation, allylic alkylation, amination, Heck reaction, Suzuki-Miyaura cross-coupling, and hydrogenation of olefins.[24-26] Particularly, Pd complexes produced from phosphine ligands serve as highly effective catalysts for the formation of carbon-carbon bonds which is the key for the synthesis of complex organic molecules from simple precursors.[27]

2.1.1. Phosphine ligands

Phosphines are dative, L-type ligands that formally contribute a pair of electrons to the metal center[28] (**Figure 2.1**). They are crucial in homogeneous catalysis, organometallic chemistry, coordination chemistry, and organic synthesis due to their wide applications as ligands and reagents in the synthesis of bulk chemicals and fine chemical intermediates.[29,30] They are generally the ligands of choice due to their superior donor capability and stabilization effects as well as the alterability of their electronic and steric properties.[31] However, there are major limitations with phosphine ligands in catalytic reactions, one of which is the formation of stable phosphido bridged dimers[32] (**Figure 2.2**). These dimers are catalytically inactive which severely restricts the effectiveness of phosphines as supporting ligands.[33]

R can be any bulky or non-bulky substituent

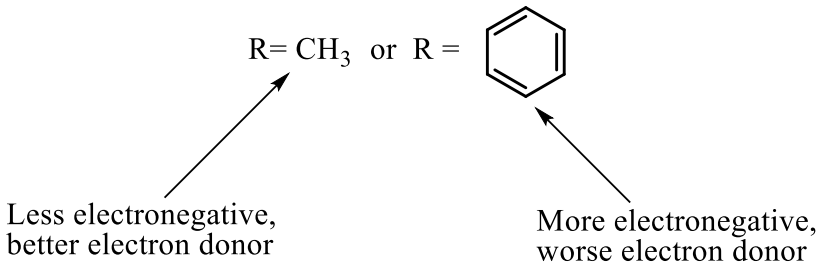

Figure 2.1: General structure of phosphine ligand.

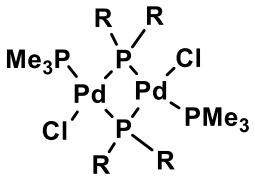

A (R = iPr), **31%**
B (R = Cy), **45%**

Figure 2.2: Phosphido bridged dimers.

Biricik *et al*.[34] reported an aminophosphine ligand (**3**) produced *via* an aminolysis reaction of diphenylphosphine chloride (**1**) and 2-picolylamine (**2**), in yield of 98 % (**Scheme 2.1**). They

discovered that the ligand is stable in air, probably due to the presence of the bulky phenyl groups which induce steric hindrance to the ligand. However, they observed that the ligand gradually decomposes in solution making it a challenge to use the ligand in prolonged reactions.

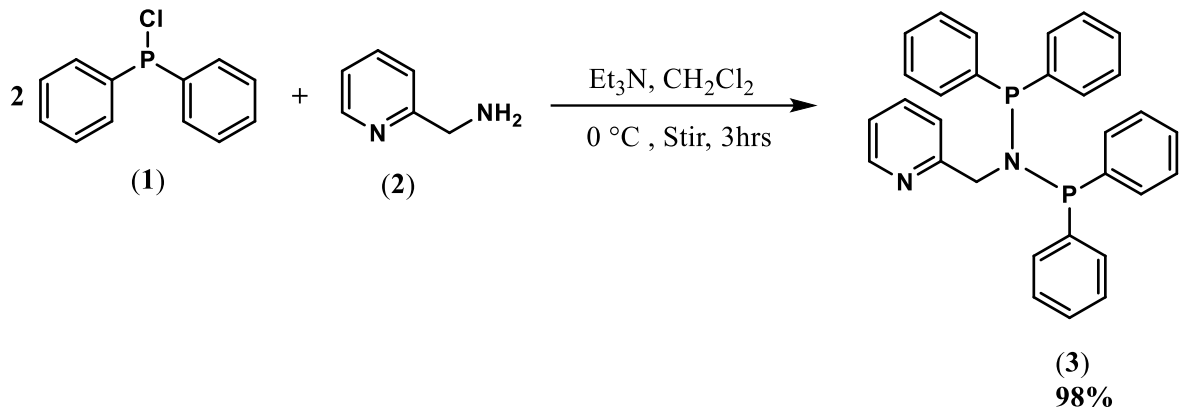

Scheme 2.1:Synthesis of an aminophosphine ligand.

Biricik and colleagues coordinated the resulting aminophoshine ligand (**3**) with Dichloro(1,5-cyclooctadiene) palladium (II) ($PdCl_2$(cod)) (**4**), affording a Pd (II) complex (**5**) in good yield (**Scheme 2.2**).

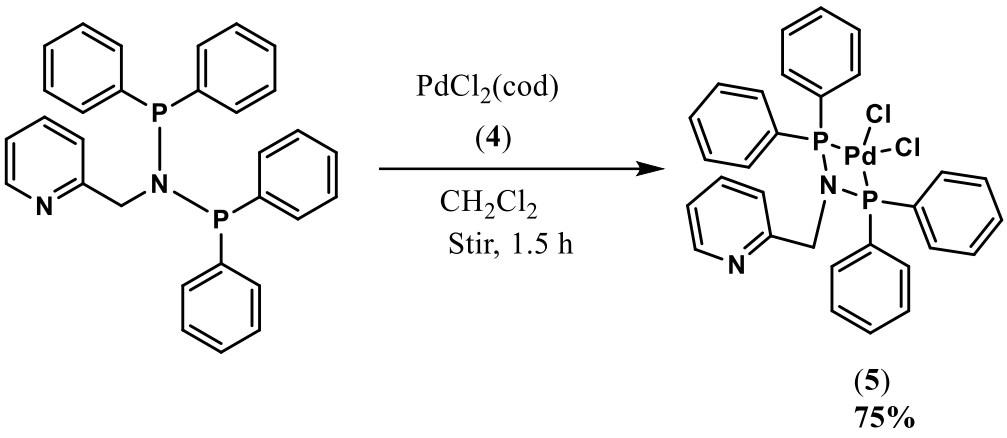

Scheme 2.2: Synthesis of an aminophosphine complex.

After characterization, they reported that Single X-ray crystallographic studies of the Pd complex (**5**) revealed that the nitrogen atom in the pyridyl group was not involved in any coordination with the metal center due to the phosphorus atom which is a stronger donor than

the nitrogen donor and thus, coordination to the metal center occurred preferentially at the phosphorus atoms.

To explore the potential applications of the synthesised Pd complex (**5**), the authors initially investigated the catalytic activity of (**5**) in Heck cross-coupling reaction. Substituted 4-bromoacetophenones (**7**) were reacted with styrene (**6**) in the presence of 1 mmol% Pd complex (**5**) affording the desired alkenes in poor 9% - 41% yields (**Scheme 2.3**).

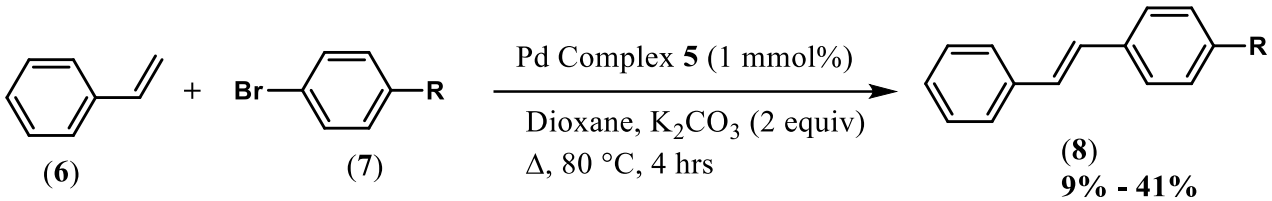

Scheme 2.3: Heck cross-coupling reactions of Pd complex **5**.

As a result of the low yields obtained in the Heck cross-coupling reactions, Biricik and co-workers further investigated the catalytic activity of (**5**) in Suzuki-Miyaura (SM) cross-coupling reactions of different aryl bromides (**10**) and boronic acid (**9**) (**Scheme 2.4**) with the aim of obtaining high yields of the converted biaryl products. They discovered that the complex exhibited excellent catalytic activity towards the SM cross-coupling reaction, revealing its efficacy as a catalyst.

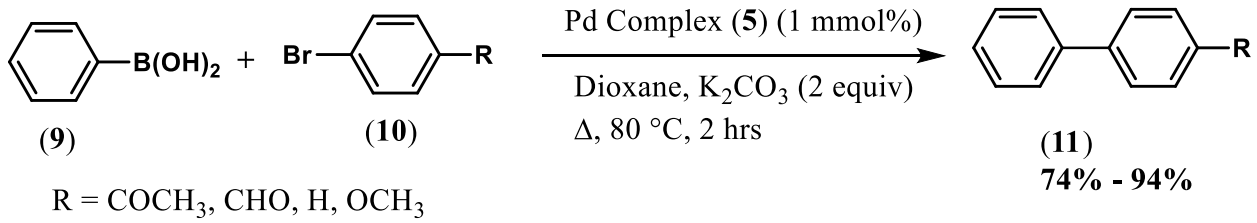

Scheme 2.4: SM cross-coupling reactions using Pd complex **5**.

With phosphine-based ligands having numerous drawbacks, several phosphine-free ligands have been introduced.[35] Therefore, researchers have been interested in investigating catalytic systems with ligands comprising various heteroatoms such as *N*-heterocyclic ligands with an objective of improving the ligand/catalytic systems *via* ligand design.[36]

2.1.2. *N*-heterocyclic carbene (NHC) ligands

N-heterocyclic carbenes (NHCs) (**13**) are electron-rich nucleophilic species in which the divalent carbenic center is directly bonded to at least one nitrogen atom within the heterocycle [37], (**Figure 2.3**). They are typically synthesized by deprotonating azolium salts (**12**) with strong anionic bases [38] (**Scheme 2.5**). Wanzlick *et al.*[39] discovered NHC in 1968, and Arduengo *et al.*[40] isolated and determined the first structure of NHC in 1991.

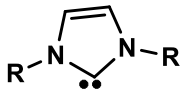

R= Any bulky substituent

e.g. 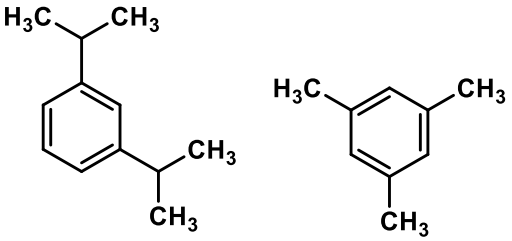

Figure 2.3:General structure of *N*-heterocyclic carbenes.

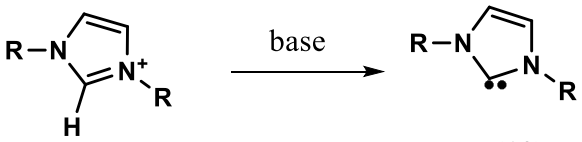

(**12**) (**13**)

R= Any bulky substituent

e.g. 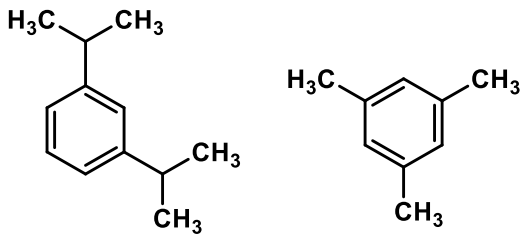

Scheme 2.5: Synthesis of *N*-heterocyclic carbenes.

N-heterocyclic carbenes are stabilized *via* a push-push mesomeric action in which both nitrogen lone pairs interact strongly with the π -orbital of the carbene center[41] (**Figure 2.4**). The stability of NHC is additionally aided by the nitrogen atoms' σ-electron-withdrawing effect and its π-electron-donating capacity (compared to the carbon atom).[42] The adjacent σ- electron-

withdrawing and π-electron-donating nitrogen atoms stabilize this structure both inductively by lowering the energy of the occupied π-orbital and mesomerically by donating electron density into the empty π-orbital.[43]

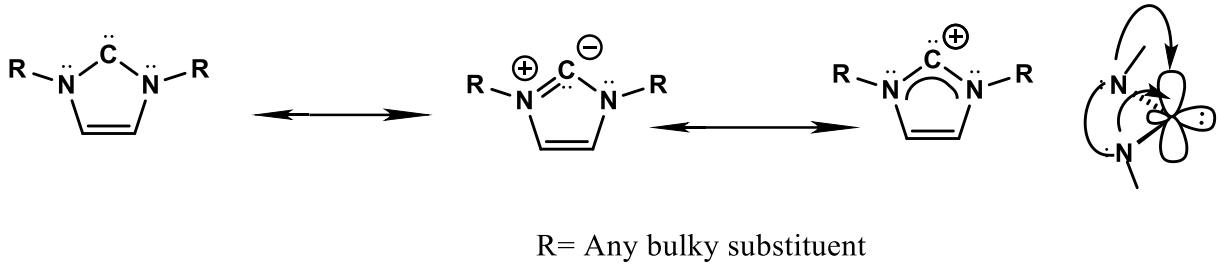

R= Any bulky substituent

Figure 2.4: Mesomeric structures of NHCs and mesomeric stabilization of the singlet ground state.

N-heterocyclic carbenes have drawn a lot of attention as ligands in coordination chemistry and homogeneous catalysis due to their high versatility in terms of easy tuning of their stereo-electronic properties.[44] They serve as advantageous mimics of phosphines in transition-metal coordination because of their strong σ-donor and relatively weak π-acceptor properties.[45] One of NHCs' primary drawback is that they are hydrolytically sensitive.[46] As a result, they easily dimerize or degrade which makes it challenging to separate them as individual carbene monomers.[47]

Karatus and colleagues synthesized an *N*-heterocyclic carbene ligand (**16**) from *N*-(n-butyl)imidazole (**14**) and 9-chloromethylanthracene (**15**) (**Scheme 2.6**).[48]

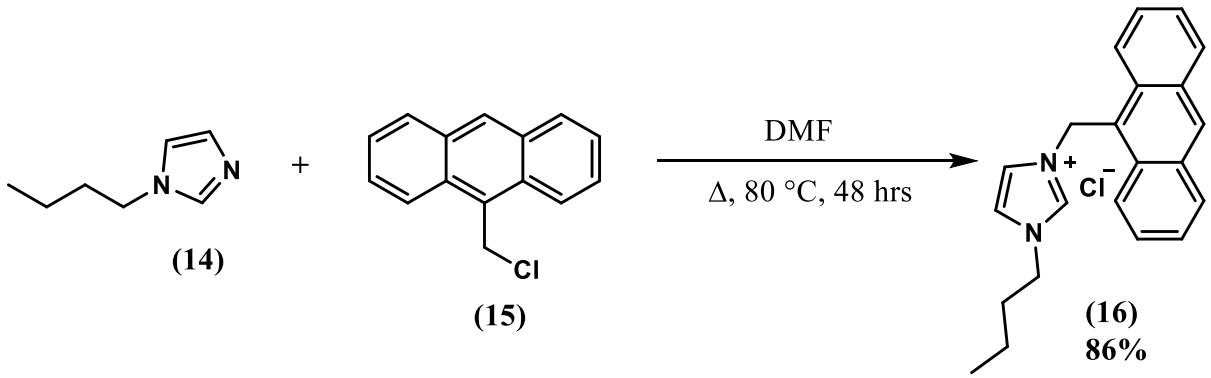

Scheme 2.6: Synthesis of an *N*-heterocyclic carbene ligand.

The interaction of the carbene ligand (**16**) and palladium (II) acetate with three equivalents of pyridine resulted in a Pd complex (**18**) with a moderate yield of 54% (**Scheme 2.7**). According

to the authors' observations, the complex exhibited excellent stability in the presence of water and oxygen.

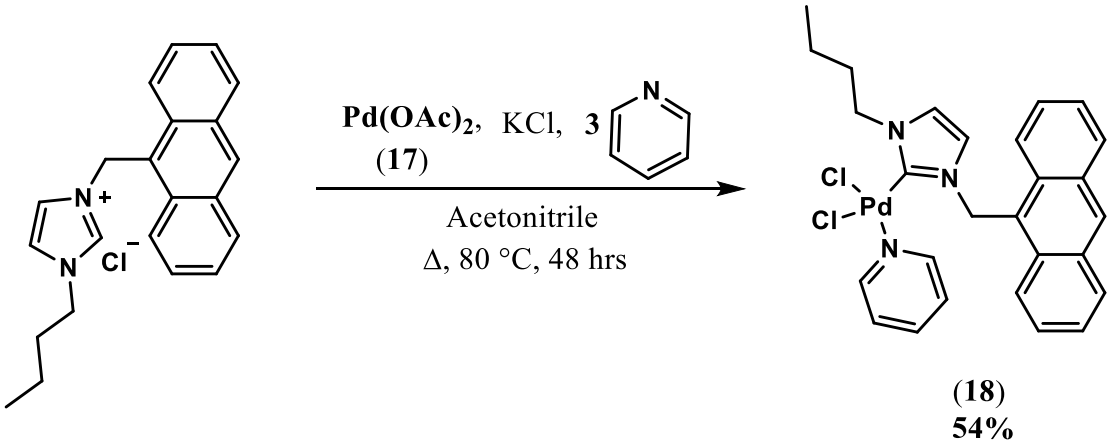

Scheme 2.7: Synthesis of an *N*-heterocyclic carbene Pd complex.

Karatus and colleagues examined the catalyst properties of the Pd complex (**18**) in the SM cross-coupling reaction between aryl chlorides (**20**) and phenylboronic acid (**19**) (**Scheme 2.8**). However, they obtained low to moderate yields of the coupled biaryl products. They hypothesized that the poor catalytic activity of the complex may be attributed to the imidazole's stronger coordination ability to pyridine, potentially delaying the oxidative addition step.

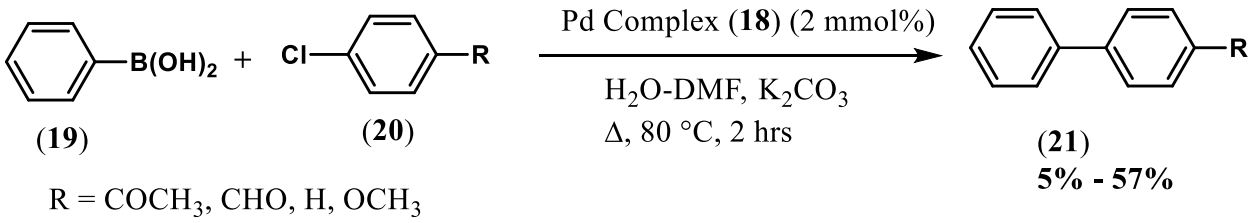

Scheme 2.8: The SM cross-coupling reaction using Pd complex **18**.

As excellent ligands for transition metals, NHCs have found extensive use in some of the most prominent catalytic transformations in the chemical industry.[49] However, their shortcomings have opened up new fields of research with an objective of improving ligand activity and stability by altering both steric and electronic properties of the ligand systems.[50] This has prompted scientists to delve into the chemistry of Schiff bases by investigating their effect and influence in organic synthetic transformations.[51, 52]

2.1.3. Schiff base ligands

Schiff bases are compounds characterized by an imine or azomethine (C=N) functional group[53] (**Figure 2.5**). Hugo Schiff, a German chemist, first synthesized and reported them in 1864, hence they are named after him.[54] Schiff bases are produced *via* the condensation reaction of primary amines with carbonyl compounds, mainly ketones, and aldehydes[55] (**Scheme 2.9**). Aldehydes are, however, extensively used in Schiff base condensation reactions due to their high reactivity and less steric hindrance compared to ketones.[56] In addition, the additional carbon in ketones donates electron density, which reduces its electrophilicity in comparison to aldehydes.[57,58] Schiff base reactions are reversible, and they typically occur under both acidic and basic catalysed reaction conditions.[59] Due to their reversibility, the formation of Schiff bases is facilitated by the constant elimination of water from the reaction mixture to drive the reaction to completion.[60]

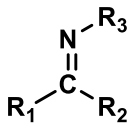

R_1 & R_2 = Alkyl/ Aryl/ H
R_3 = Alkyl/Aryl

Figure 2.5: General structure of Schiff base.

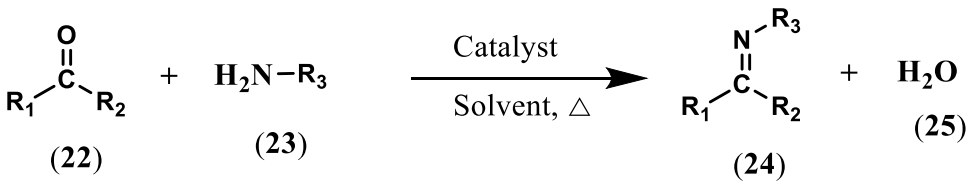

(**22**) + H_2N-R_3 (**23**) → (**24**) + H_2O (**25**)

R_1 & R_2 = Alkyl/Aryl/H
R_3 = Alkyl/Aryl

Scheme 2.9: General scheme for the formation of Schiff bases.

There are two steps in the mechanistic formation of an imine. In the first step, the amine acts as a nucleophile, attacking the aldehyde or ketone's electrophilic carbonyl carbon through an addition reaction resulting in an unstable hemiaminal adduct known as a carbinolamine (**29**).[61] The protonation of the hydroxyl group followed by the delocalisation of the lone pair on the nitrogen atom eliminates water molecule to form a N-C double bond (**31**), which ultimately

leads to the formation of an imine compound (**32**) and a water molecule as a by-product in the last step[62] (**Scheme 2.10**).

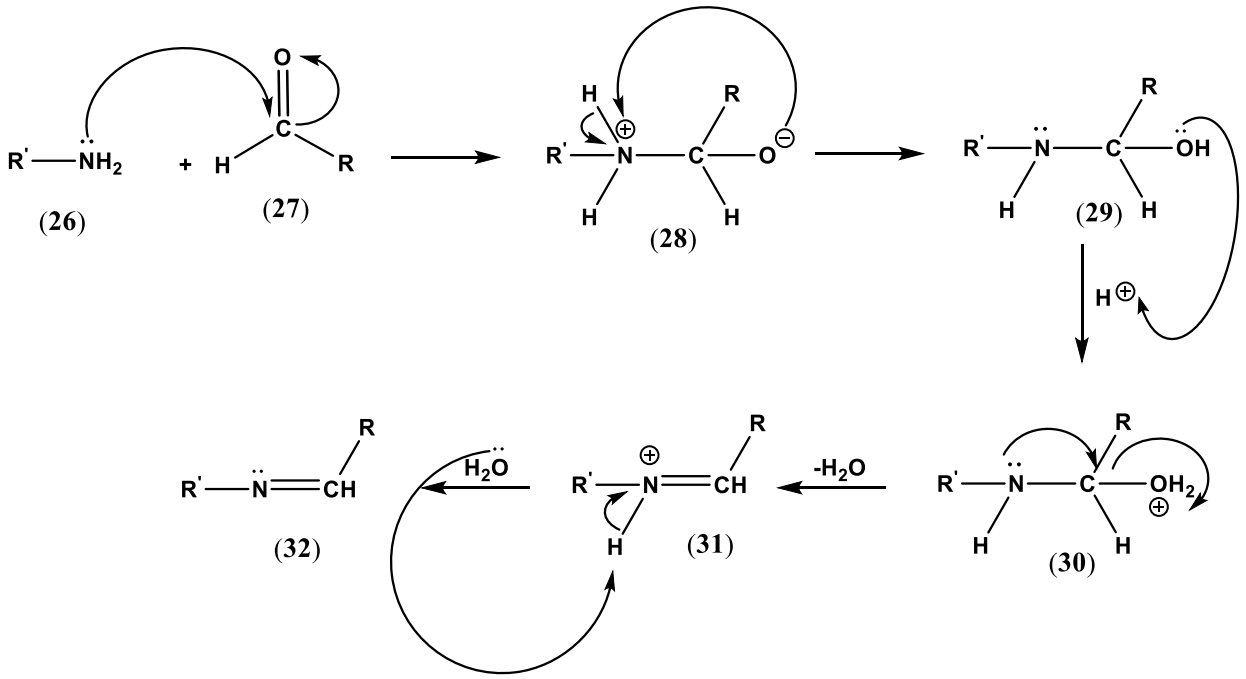

Scheme 2.10: Mechanistic pathway for Schiff base production.

Schiff bases are one of the most widely used *N*-donor organic ligands.[63-65] They are utilized in industry as organic synthetic intermediates, pigments and dyes, polymer stabilizers, corrosion inhibitors to mention just a few.[66-70] Most importantly, Schiff base ligands have found applications in catalysis and organic synthesis both as ligands and catalysts in organic reactions.[71,72] Their wide scope of applications is derived from their facile synthesis, remarkable adaptability, availability, excellent stability, high solubility in most organic solvents, and ability to coordinate with different transition metals.[73.74] Schiff bases have made significant contributions to the fundamental and practical advances of coordination chemistry, where they are extensively employed as common chelating ligands for *p, d,* and *f* block transition metals to form coordination complexes.[75] They have gained a lot of attention in the field of coordination chemistry due to their electronic and steric properties which modify the metal's steric and electronic environment while stabilizing and regulating its reactivity.[76] They coordinate with the metal center through the azomethine nitrogen which allows them to bind with different transition metals in a variety of oxidation states and geometries.[77]

There are different types of Schiff base chelates used in coordination chemistry. These are generally classified into bidentate, tridentate, tetradentate, or polydentate ligands that can form highly stable complexes with transition metal ions.[78-81]

2.1.3.1. Tetradentate Schiff base ligands

a) *N, N, O, O*-donor ligands

Tetradentate Schiff-base ligands are ligands that form a coordination complex by binding four donor atoms to a transition central atom.[82] They are well-known to chemists for their versatility, structural flexibility, as well as biological and industrial significance.[83]

Given the relevance of tetradentate Schiff base ligands, Kargar and co-workers constructed an unsymmetric *N, N, O, O*-Schiff base ligand (**35**) from excess 3-ethoxysalicylaldehyde (**33**) and 4,5-dimethylbenzene-1,2-diamine (**34**) (**Scheme 2.11**).[84]

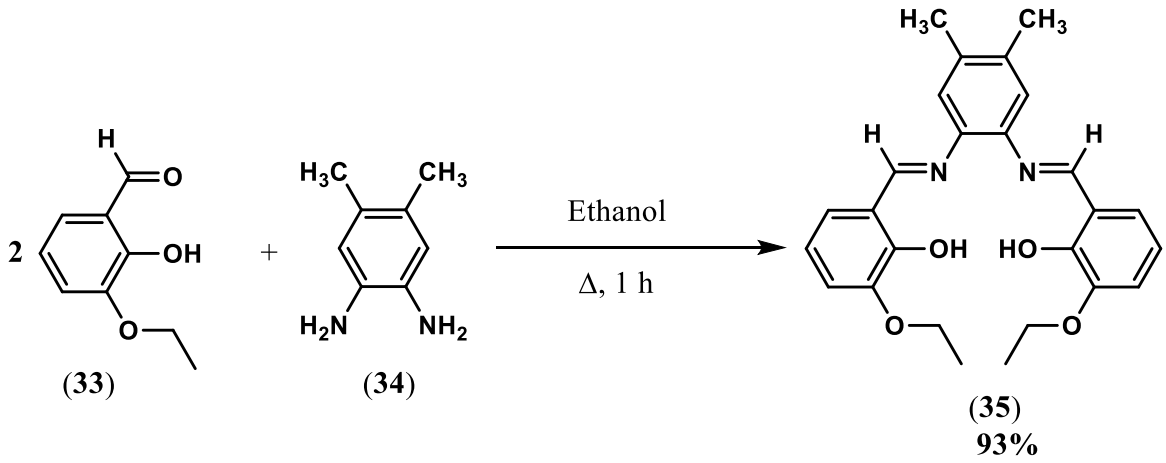

Scheme 2.11: Synthetic route of *N, N, O, O*-tetradentate Schiff base ligand.

To synthesize a Pd-complex, the authors reacted equimolar amounts of the synthesized Schiff base ligand (**35**) and palladium acetate (**36**) (**Scheme 2.12**). They discovered that the Pd complex exhibited greater stability as a result of the stronger π→π* intramolecular electronic interactions from the Schiff base ligand.

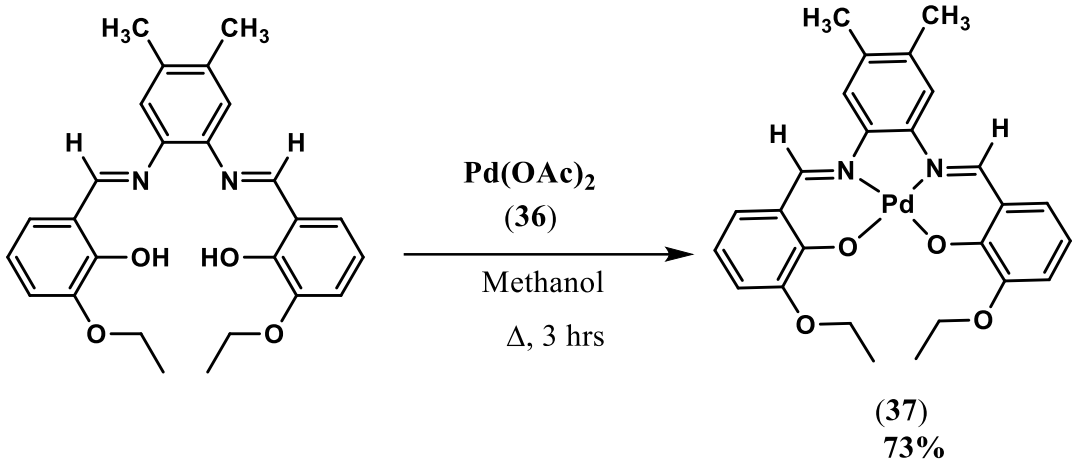

Scheme 2.12: Synthesis of Pd coordination complex **37**.

The authors further investigated the effectiveness and activity of the Pd complex in SM cross-coupling reaction of various substituted aryl iodides, aryl bromides, and aryl chlorides (**39**) with boronic acids (**38**) (**Scheme 2.13**).

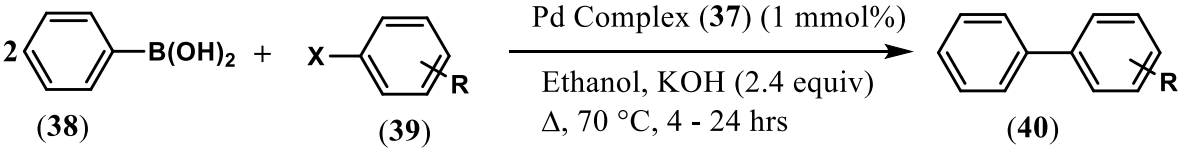

Aryl iodides: X = I
R = H, 4-CH_3, 4-OCH_3
Aryl bromides: X = Br
R = H, 4-OCH_3, 3-CN
Aryl chlorides: X = Cl
R = 4-NO_2, 2-NO_2, 4-CN

Aryl iodides: **91% - 99%**
Aryl bromides: **82% - 97%**
Aryl chlorides: **47% - 59%**

Scheme 2.13: SM cross-coupling reaction catalysed by Pd complex **37**.

With the exception of aryl chlorides, which displayed modest yields (47 % - 59%) of the biaryl products because of the stronger C to Cl bond strength, outstanding yields were obtained for aryl iodides (91% - 99%) and aryl bromides (82% - 97%), revealing the Pd complex's excellent performance in SM cross-coupling reaction.

To improve the yields of biaryls produced from aryl chlorides reported by Kargar and colleagues, Sedighipoor *et al.*[85] constructed an *N, N, O, O*-Schiff base ligand (**45**) by modulating the steric properties of the ligand using 1-(2-hydroxyphenyl)ethan-1-one (**41**), benzene-1,2-diamine (**42**), and 3-hydroxy-2-naphthaldehyde (**44**) (**Scheme 2.14**) hoping that

this would have a greater influence on the Pd complex's stereo-electronic properties, thereby enhancing the SM catalytic reaction.

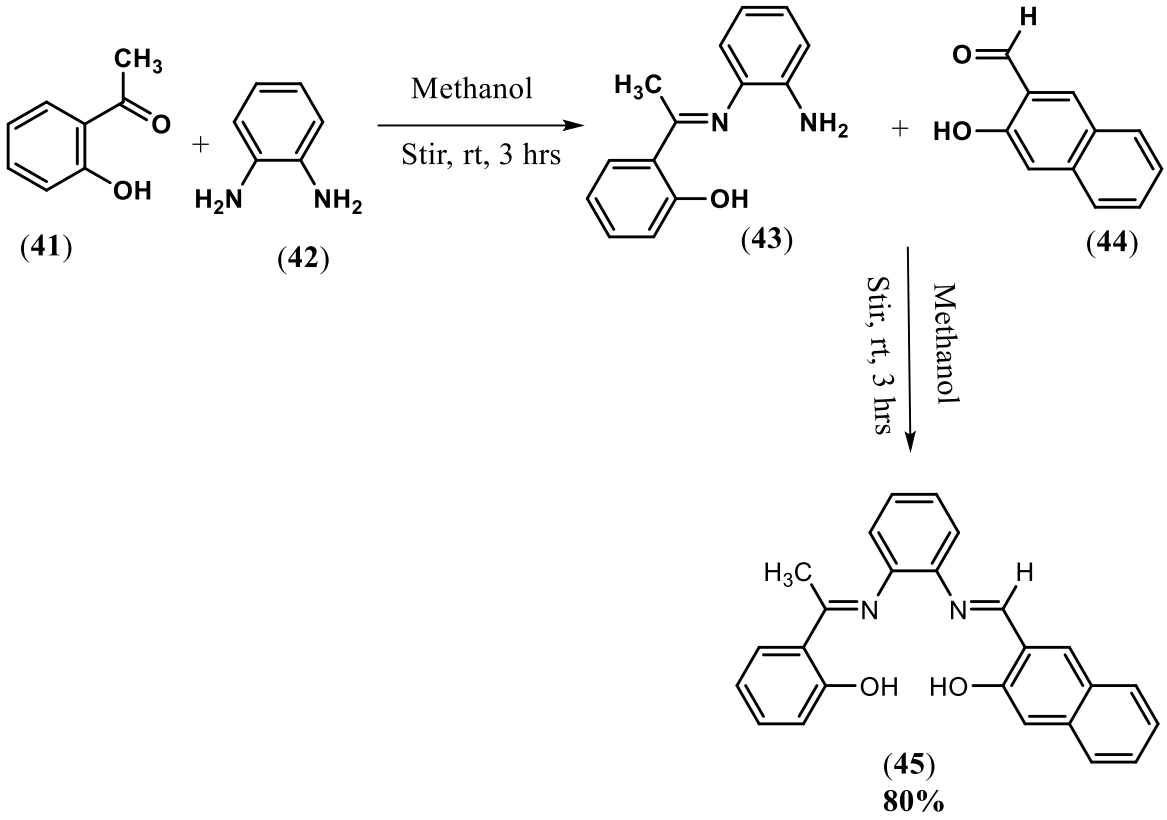

Scheme 2.14: Synthesis of an *N, N, O, O*-tetradentate Schiff base ligand.

Sedighipoor *et al.* synthesized Pd complex (**47**) from the tetradentate Schiff base ligand (**45**) and Palladium acetate (**46**) (**Scheme 2.15**) and further tested the catalytic activity of the Pd complex in SM cross-coupling reaction of substituted aryl chlorides (**49**) and boronic acid (**48**) (**Scheme 2.16**). To their disappointment, the complex also displayed poor yields (28% - 43%) of the biaryl products from the aryl chlorides.

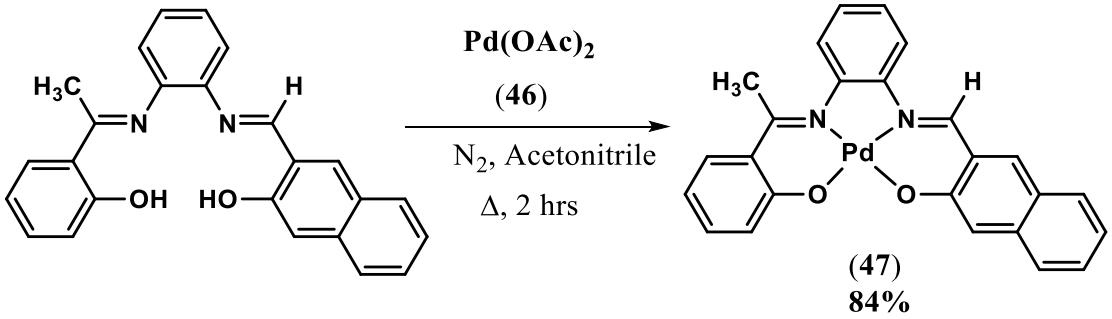

Scheme 2.15: Synthesis of *N, N, O, O*-tetradentate chelate Pd complex.

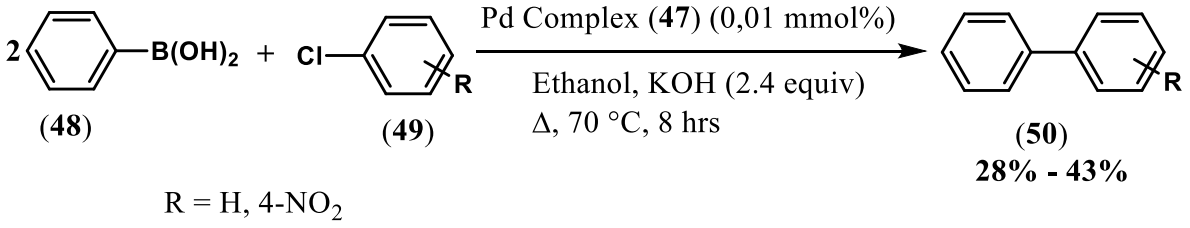

Scheme 2.16: SM cross-coupling reaction using Pd complex **47**.

The main obstacle in the preparation of unsymmetrical Schiff bases is that numerous symmetrical Schiff base ligands are guaranteed to form as by-products.[86] This is because condensation of the two amino groups frequently proceeds with comparable rates, resulting in an average yield of 60-85% desired unsymmetric Schiff base ligand and 15-40% undesired symmetric Schiff base ligand.[86] Furthermore, in the SM coupling processes of aryl chlorides, Pd complexes derived from *N, N, O, O*-tetradentate Schiff base ligands were shown to be less efficient.[87] These unsatisfactory results have led scientists to explore other chelating systems with varying denticities that can be effective in organic catalysis, particularly in SM cross-coupling reactions.

2.1.3.2. Bidentate Schiff base ligands

a) *N, N*-donor ligands

Bidentate Schiff-base ligands are Lewis bases that bind to the central metal *via* two donor atoms.[88] In the following section the synthesis, and coordination of *N, N*-donors, *N, P*-donors, and *N, O*-donors with Pd metal precursors and their applications will be discussed.

Kylmälä *et al*.[89] synthesized a series of *N, N*-symmetrical diimine Schiff base ligands (**53**) (**Scheme 2.17**) and subsequently converted them into their corresponding Pd complexes (**55**) (**Scheme 2.18**).

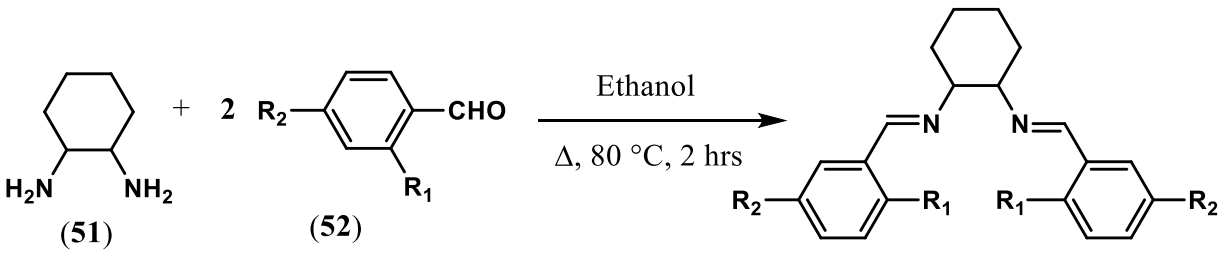

L1: R1 = CF_3, R2 = H
L2: R1 = F, R2 = H
L3: R1 = R2 = OMe

Scheme 2.17: Synthesis of *N, N* symmetrical diimine bidentate Schiff base ligands.

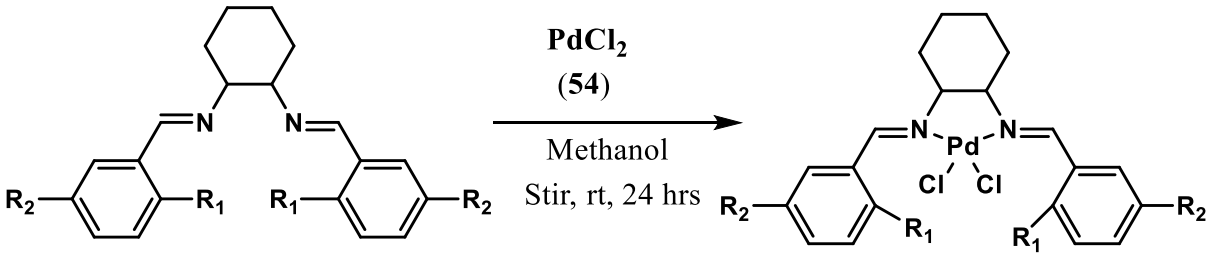

C1: R1 = CF_3, R2 = H
C2: R1 = F, R2 = H
C3: R1 = R2 = OMe

Scheme 2.18: Synthesis of *N, N* symmetrical diimine bidentate Pd complexes.

The use of the isolated Pd-complexes as a catalyst yielded very poor conversions of the biaryl products in the SM cross-coupling reaction of substituted boronic acids (**56**) and 4-Bromoacetophenone (**57**) (**Scheme 2.19**).

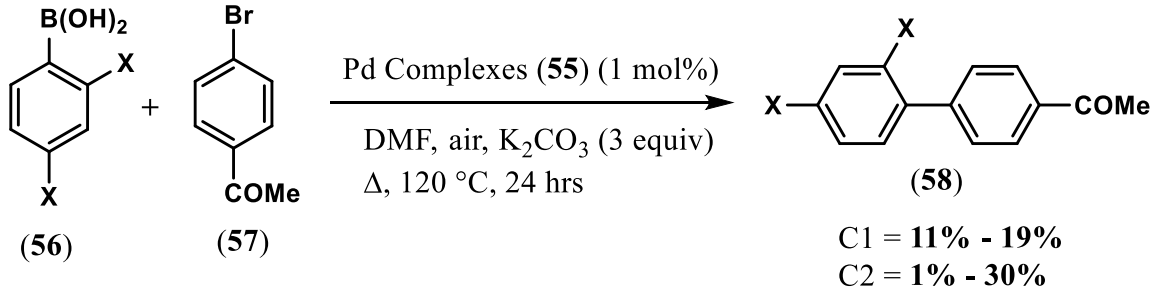

X = H, F, Cl

Scheme 2.19: SM cross-coupling reaction using Pd complexes **55**.

To introduce a different class of *N, N*-donor bidentate ligands, Vanbellingen *et al*.[90] reported ligand (**61**) which was synthesized by a condensation reaction between tyramine (**59**) and di(2-pyridyl)ketone (**60**) (**Scheme 2.20**). The authors evaluated the ability of the ligand to complex a palladium precursor by reacting ligand (**61**) with $PdCl_2COD$ (COD = cyclooctadiene) to afford a Pd complex (**63**) in good yield (**Scheme 2.21**). However, one disadvantage they discovered in using this type of ligand is that it is difficult to determine which nitrogen atoms are involved in the complexation since the complexation may occur either between the two pyridines, to form a 6-membered ring, or between the imine and one pyridine, to form a 5-membered ring. Therefore, failure to obtain crystals of the complex implies that it's going to be a challenge to identify which nitrogen atoms participated in the coordination.

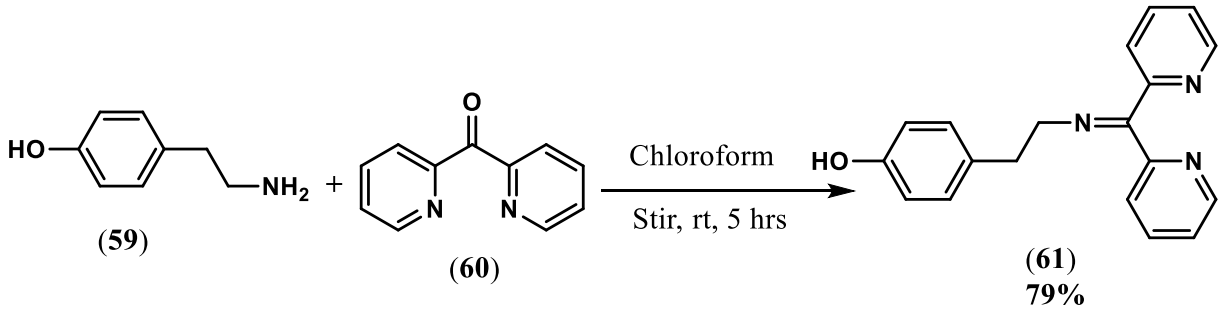

Scheme 2.20: Synthesis of an *N, N*–bidentate Schiff base ligand.

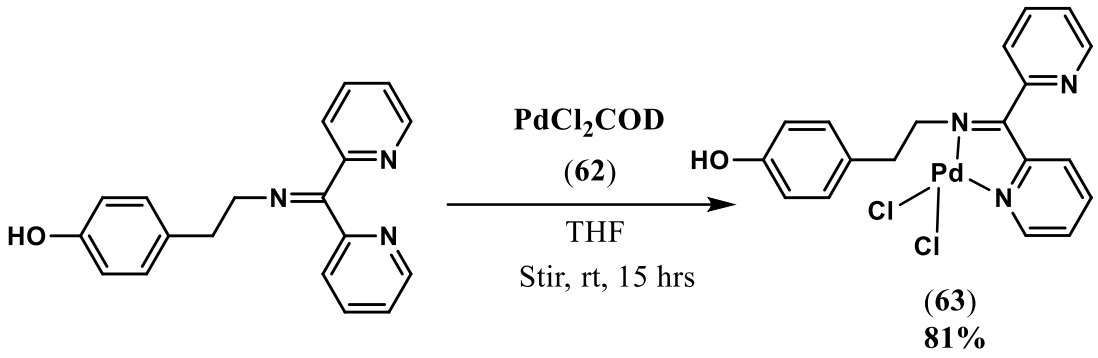

Scheme 2.21: Synthesis of an *N, N*–bidentate Pd complex.

The authors examined the activity of the complex in Heck cross-coupling reaction as a catalyst between the reaction of styrene (**64**) and iodobenzene (**65**) (**Scheme 2.22**). Initially, their temperature was 40 °C and resulted in no product. They subsequently increased the temperature to 70 °C and they were able to isolate the desired alkenes in 98% yields. Thus, revealing a remarkable efficiency of the complex towards the Heck cross-coupling reaction.

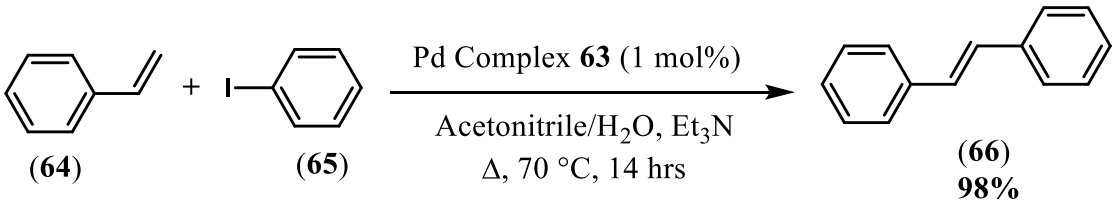

Scheme 2.22: Heck cross-coupling reaction using Pd complex **63**.

The general chemistry of nitrogen explains that the π-orbital of nitrogen is half-filled whereas its σ-orbitals are completely occupied.[91] As a result, elements having half-filled and full-filled orbitals are the most stable and have the least energy, hence they are less reactive. This implies that in most cases, Schiff base ligands comprising *N, N*-donors are overly stable and tend to have an extremely lower reactivity due to the nitrogen donor atoms which are more stable and have less energy.[91] All the abovementioned drawbacks of Schiff bases containing *N, N*-donor system provides prospects for improvement in the field of Schiff base synthesis. Therefore, this has motivated researchers to investigate the development of mixed donor atoms such as *N, P*- and *N, O*-donor systems with the goal of balancing the reactivity as well as stability effect brought by the ligand.

b) *N, P*-donor ligands

Although phosphine ligands and their Pd-complexes are extensively utilized to catalyse the cross-coupling reactions for a variety of substrates, not enough research has been done on the use of imino phosphines and their palladium-complexes in C-C coupling reactions.

With that being stated, Mahamo *et al* [92] reported an *N, P*-Schiff base ligand (**69**) from 2-(diphenylphosphino) benzaldehyde and 2-thionylamine (**Scheme 2.23**) and its corresponding Pd-complex (**71**) (**Scheme 2.24**). The authors discovered that this ligand has the ability to stabilize metal complexes in a variety of oxidation states and geometries that occur during the catalytic cycle. Furthermore, the hard imine donor site is weakly coordinated to the soft metal center and easily dissociates in solution, providing a vacant site when required, whereas the chelate effect stabilizes the catalyst precursor (**71**) in the absence of substrate, preventing catalyst decomposition. Moreover, the π-acceptor of the soft phosphine donor site stabilizes the metal center in low oxidation states, while the nitrogen σ-donor makes the metal center more susceptible to oxidative addition reactions.

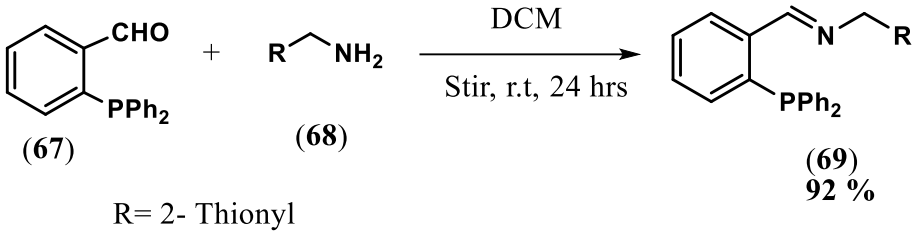

Scheme 2.23: Synthesis of an *N, P*-bidentate Schiff base ligand.

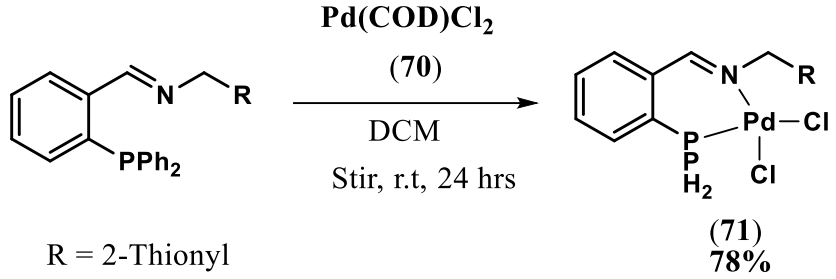

Scheme 2.24: Synthesis of an *N, P* Pd-complex.

Mahamo *et al*. evaluated the activity of the complex in SM cross-coupling reaction between aryl bromide or aryl chloride (**73**) and boronic acid (**72**) (**Scheme 2.25**). The authors reported that high yields were only achieved for the biphenyl from aryl bromides (90%) whereas extremely poor yields were obtained for the biphenyl from aryl chlorides (16%), implying that the catalyst is highly efficient in coupling aryl bromides than aryl chlorides.

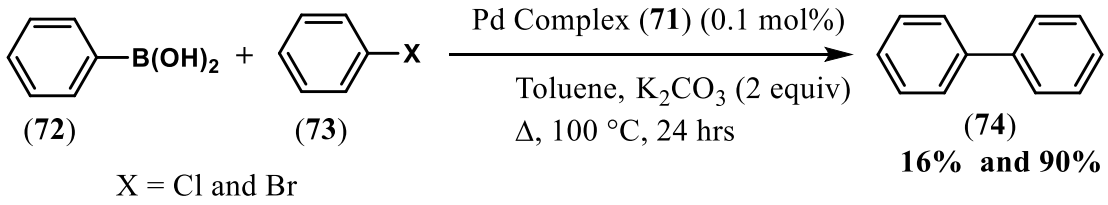

Scheme 2.25: SM coupling reaction catalysed by Pd complex **71**.

Owing to the poor yields of the products from aryl chlorides isolated by Mahamo *et al*, Kaushal and colleagues [93] reported another *N, P*-bidentate ligand (**77**) (**Scheme 2.26**) and its corresponding complex in an attempt of improving the catalytic activity of the complex, with the hope that it will result in excellent conversions of the biaryls from aryl chlorides.

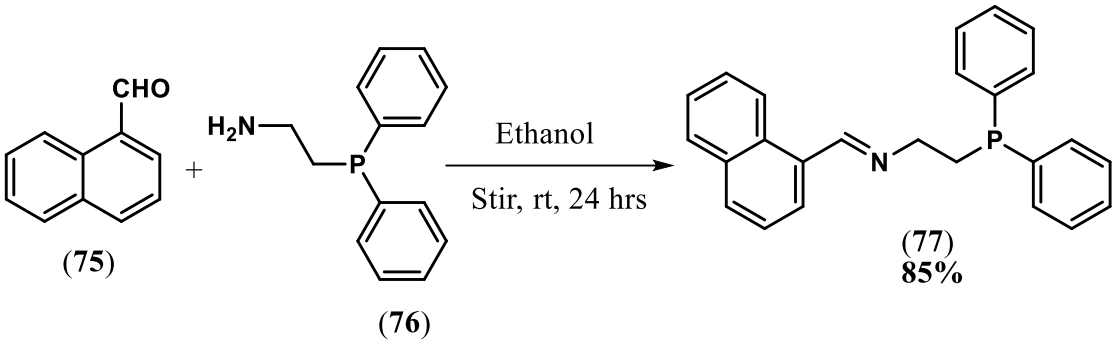

Scheme 2.26: Synthesis of an *N, P*-bidentate Schiff base ligand.

This ligand is distinctive in that it contains both naphthalene and diphenylphosphine (- PPh2) functionality within the same framework. The authors reported that the ligand demonstrated a strong binding ability with transition metals due to the presence of both soft (nitrogen) and hard (phosphorus) donors. These properties allowed Kaushal and colleagues to coordinate the ligand with sodiumtetrapalladate (**78**) to afford a Pd complex (**79**) (**Scheme 2.27**). The authors investigated the efficiency of the catalyst in SM coupling reaction of substituted aryl halides (**81**) (aryl bromides and aryl chlorides) with boronic acid (**80**) (**Scheme 2.28**). However, high yields of the coupled products from aryl bromides have been reported, yet minimal conversions of the products from aryl chlorides were still obtained.

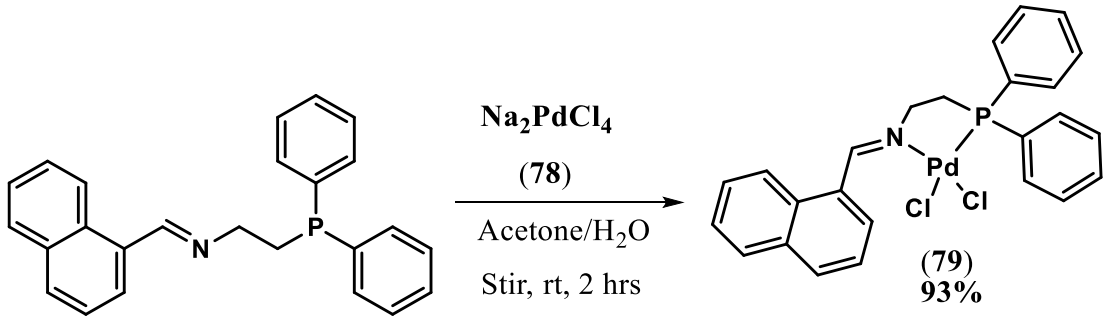

Scheme 2.27: Synthesis of an *N, P* Pd complex.

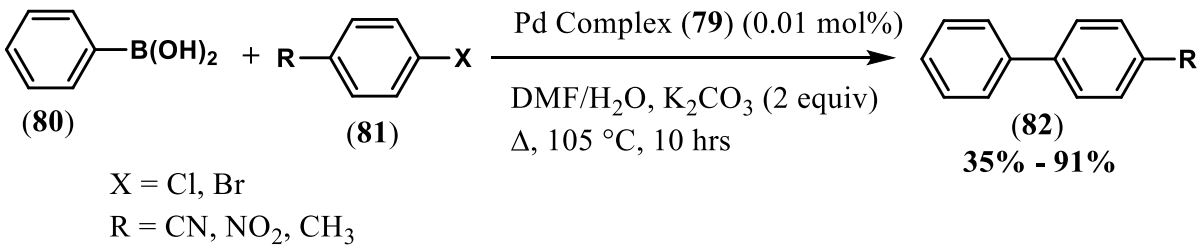

Scheme 2.28: SM coupling reaction using Pd complex **79**.

In brief, Schiff base ligands with *N, P*-donor systems showed exceptional stability and reactivity. This is attributed to the combination of *N* and *P* donor atoms, where the nitrogen hard donor nature provides great stability whereas the phosphorus soft donor induces the ligand's excellent reactivity.[94] However, the major drawback in this class of ligands is the susceptibility of phosphorus to oxidation, which restricts their application in industry and academia.[95]

Based on literature search, *N, O*-bidentate donor ligands have emerged as one of the most efficient and powerful chelates due to their numerous advantages such as their facile and simple preparation as well as the ease tuning of both electronic and steric properties.[96]

c) *N, O*-donor ligands

Bowes *et al.*[97] synthesised an *N, O*-bidentate ligand (**85**) from substituted benzene amine and substituted salicylic aldehyde (**Scheme 2.29**).

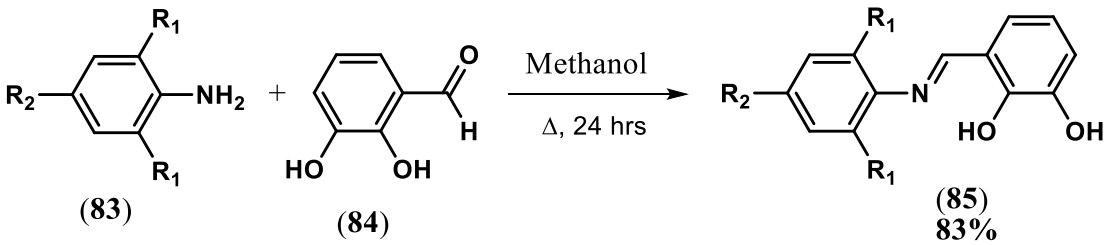

R_1 = Me, R_2 = H

Scheme 2.29: Synthesis of an *N, O*-bidentate ligand.

Bowes *et al.* reported that the complexation of the ligand (**85**) with palladium acetate (**86**) afforded a highly stable and reactive Pd-complex (**87**) in good yield (**Scheme 2.30**).

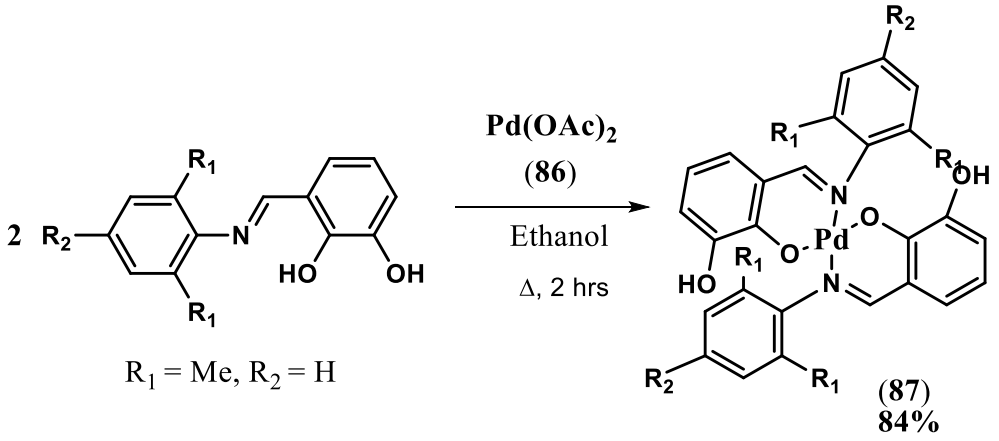

Scheme 2.30: Synthesis of an *N, O,* Pd complex.

The authors tested the ability of the catalyst (**87**) in catalysing the SM cross-coupling reaction of aryl chlorides and bromides (**89**) with phenyl boronic acid (**88**) (**Scheme 2.31**). They noticed that there was no significant activity observed with aryl chlorides, whereas the complex moderately catalysed the coupling of aryl bromides and aryl iodides with phenylboronic acid. This demonstrates that the complex was ineffective in the catalytic system of aryl chlorides as substrates.

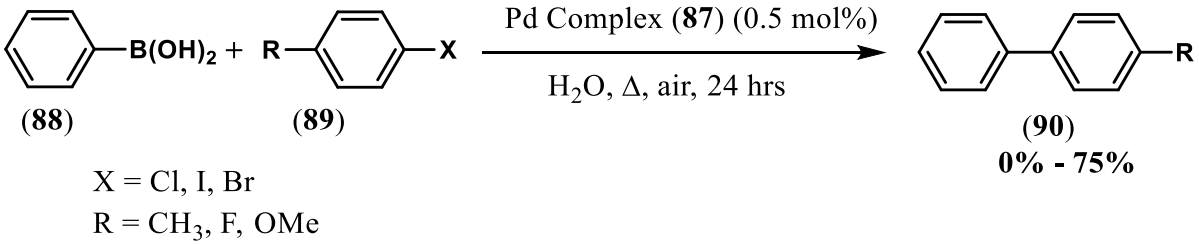

Scheme 2.31: SM cross-coupling reaction catalysed by Pd complex **87**.

Cui *et al*.[98] noticed that the results obtained by Bowes *et al* were promising therefore they developed an *N, O*-bidentate ligand (**93**) (**Scheme 2.32**) and its corresponding Pd-complex (**95**) from a reaction of the ligand (**93**) and Bis (acetonitrile)dichloropalladium (II) (**94**) (**Scheme 2.33**) with efforts to introduce an efficient catalytic system for the cross coupling reaction of aryl chlorides as substrates in the SM cross-coupling reaction.

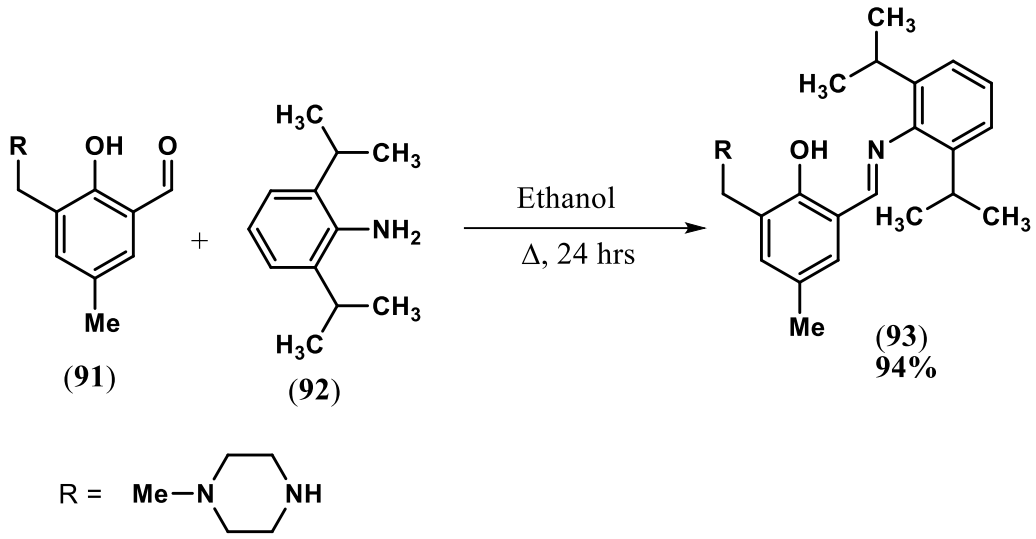

Scheme 2.32: Synthesis of an *N, O*-bidentate ligand.

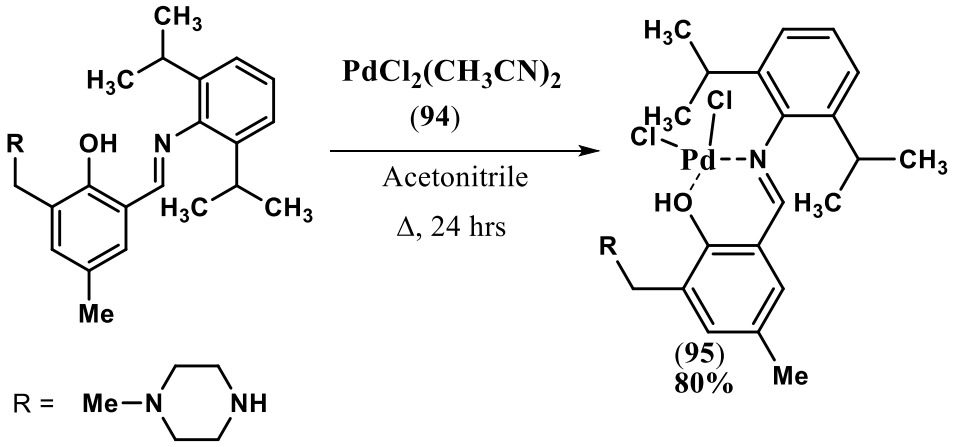

Scheme 2.33: Synthesis of an *N, O,* Pd complex.

The resulting Pd-complex (**95**) showed high efficacy in activating numerous structurally different aryl chlorides with good to excellent yields in SM cross-coupling reaction of substituted aryl chlorides (**97**) and boronic acid (**96**) (**Scheme 2.34**). However, extremely low yields were generated from sterically hindered *Ortho*-substituted aryl chlorides.

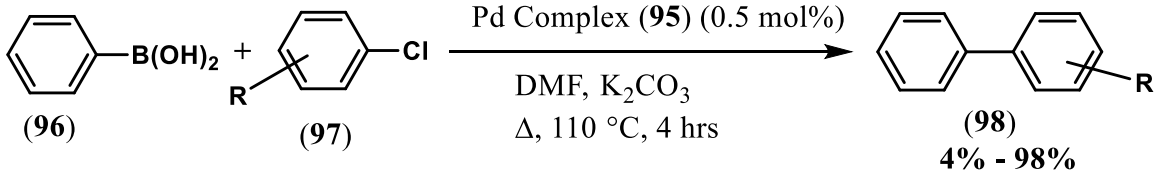

R = 2-CH_3, 2-NO_2, 4-OH, 4-CH_3

Scheme 2.34: SM cross-coupling reaction utilising Pd complex **95**.

The chemistry described in this chapter has demonstrated the significant role played by ligands in the reactivity and the efficiency of Pd complexes as catalysts in promoting carbon-carbon bond-forming reactions. Different types of ligands with various denticities such as *N, N- and N, P*-donors with their Pd complexes have been documented extensively in the literature owing to their superior reactivity and efficiency in organic catalysis. On the other hand, the chemistry of *N, O*-donor ligands with their corresponding Pd-complexes have been given limited attention. As a result, the design and development of supporting *N, O*-donor ligands with their Pd-complexes and subsequently their catalytic application in Suzuki-Miyaura cross-coupling reaction is still highly desirable in organic catalysis.

Interested in the chemistry of stable and highly active Pd-complexes and their application in Suzuki-Miyaura cross-coupling reaction, we have developed novel *N, O*-based Pd-complexes and investigated their catalytic activities in SM cross-coupling reaction. We hypothesize that using *Para* substituted *N, O*-bis Schiff base chelated Pd (II) complexes as catalysts while scrutinising the electronic effect of ligand substituents will exhibit high catalytic activity and efficiency in SM cross-coupling reactions.

2.4. Aims and Objectives

- This study aims to report the synthesis of *N, O*-bidentate Schiff base ligands (**L1 - L7**) (**Scheme 2.35**) and their corresponding novel Pd (II) complexes (**PdC1 - PdC7**) (**Scheme 2.36**).
- To characterise the *N, O*-bidentate Schiff base ligands (**L1 - L7**) and their novel Pd (II) complexes (**PdC1 - PdC7**) using NMR, FTIR, MS and Single X-ray crystallography.
- To investigate their catalytic activities in SM cross-coupling reaction for the formation of biaryls and biaryl ketones (**Scheme 2.37**).

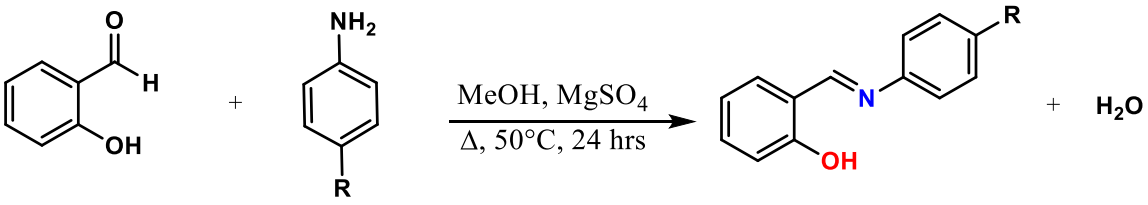

(80% - 94%)

R = H (**L1**), R = CH_3 (**L2**),
R = CH_2CH_3 (**L3**), R = OCH_3 (**L4**),
R = F (**L5**), R = Br (**L6**), R = CN (**L7**)

Scheme 2.35: Synthesis of *N, O*-bidentate Schiff base ligands.

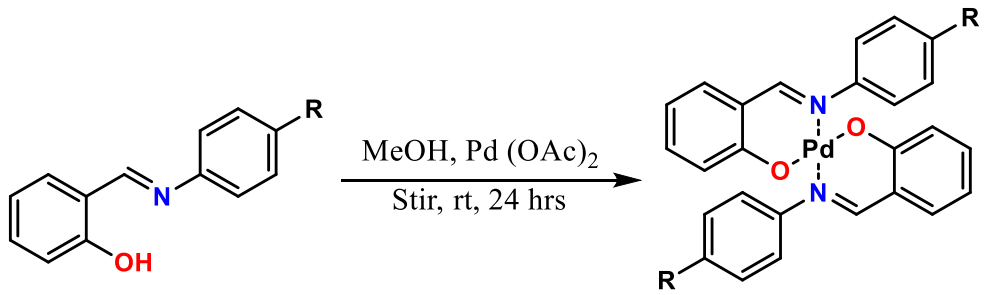

(78% - 95%)

R = H (**PdC1**), R = CH_3 (**PdC2**),
R = CH_2CH_3 (**PdC3**), R = OCH_3 (**PdC4**),
R = F (**PdC5**), R = Br (**PdC6**), R = CN (**PdC7**)

Scheme 2.36: Synthesis of *N, O*-bis Schiff base chelated Pd (II) complexes.

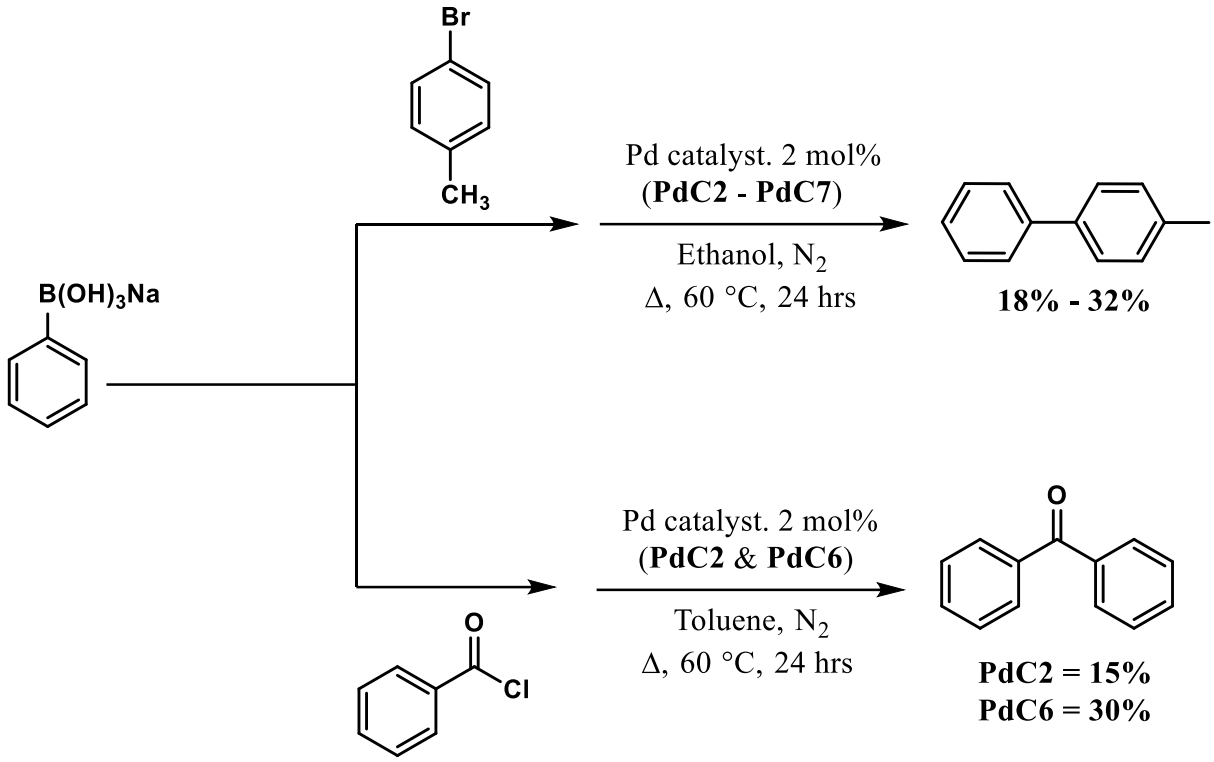

Scheme 2.37: Synthesis of Biaryls and biaryl ketones.

References

1. D.J. Goss, and R.H. Petrucci, *Pearson Prentice Hall* (**2007**).
2. C.L Wagner, G. Herrera, Q. Lin, C.T Hu, and T. Diao, *Journal of the American Chemical Society*, 143(14), 5295-5300 (**2021**).
3. A.D McNaught, and A. Wilkinson, *Blackwell Science*, 200 -201 (**1997**).
4. F. Basolo, and J.L. Burmeister, 13, *World Scientific*, (**2003**).
5. M. Siddiqui, M. Waheed, S. A. Bhat, and M.J. Balakrishna, *Chem. Sci*., 127(5), 879-884 (**2023**).
6. C.M. Zhang, J.K. Huang, M.L. Trudell, and S. Nolan, *Journal of organic chemistry*, 64(11), 3804-3805 (**1999**).
7. İ. Özdemir, B. Çetinkaya, S. Demir, and N. Gürbüz, *Catalysis letters*, 97, 37 - 40 (**2004**).
8. V.A. Glushkov, M.S. Valieva, O.A. Maiorova, E.V. Baigacheva, and A.A. Gorbunov, *Russian journal of organic chemistry*, 47, 230 - 235 (**2011**).
9. W.M. Dai, and Y. Zhang, *Tetrahedron letters*, 46(8), 1377-1381 (**2005**).
10. F. Christoffel, and T.R. Ward, *Catalysis Letters*, 148, 489-511 (**2018**).
11. G.Z. Wang, R. Shang, and Y. Fu, *Organic letters*, 20(3), 888-891 (**2018**).
12. G.C. Fortman, and S.P. Nolan, *Chemical Society Reviews*, 40(10), 5151-5169 (**2011**).
13. P. Das, C. Sarmah, A. Tairai, and U. Bora, *Applied Organometallic Chemistry*, 25(4), 283-288 (**2011**).
14. L. Botella, and C. Nájera, *Chem. Int. Ed*, 41(1), 179-181 (**2002**).
15. A.O. Eseola, D. Geibig, H. Görls, W.H. Sun, X. Hao, J.A. O Woods, and W. Plass, *Journal of Organometallic Chemistry*, 754, 39-50 (**2014**).
16. M. Wang, H. Zhu, K. Jin, D. Dai, and L. Sun, *Journal of Catalysis*, 220(2), 392-398 (**2003**).
17. F. Marchetti, C. Pettinari, R. Pettinari, A. Cingolani, D. Leonesiand and A. Lorenzotti, *Polyhedron*,18(23) 3041-3050 (**1999**).
18. W. Chen, R. Li, B. Han, B.J. Li, Y. C. Chen, Y. Wu, L. Ding, and D. Yang, *European Journal of Organic Chemistry,* 1177-1184 (**2006**).
19. A.I. Moncada, S. Manne, J.M. Tanski, and L.M. Slaughter, *Organometallics*, 25(2), 491-505 (**2006**).
20. B. Dede, F. Karipcin, and M. Cengiz, *Journal of Hazardous Materials*, 163(2-3), 1148-1156 (**2009**).
21. G. Wilke, H. Schott, H. and P. Heimbach, *Ang. Chem. Int.*, 6(1), 92-93 (**1967**).
22. A.L. Clevenger, R.M. Stolley, J. Aderibigbe, and J. Louie, *Chemical Reviews*, 120(13), 6124-6196 (**2020**).
23. G.R. Cairns, R.J. Cross, and D. Stirling, *Journal of Molecular Catalysis*, 172(1-2), 207-218 (**2001**).
24. S. Bhakta, and T. Ghosh, *Advanced Synthesis & Catalysis*, 362(23), 5257-5274 (**2020**).
25. E.A. Ziemann, S. Baljak, S. Steffens, T. Stein, N. Van Steerteghem, I. Asselberghs, K. Clays. and J. Heck, *Organometallics*, 34(9), 1692-1700 (**2015**).
26. L.C. Liang, P.S. Chien, and M.H. Huang, *Organometallics*, 24(3), 353-357 (**2005**).
27. J.P. Wolfe, R.A. Singer, B.H. Yang, and S.L. Buchwald, *Journal of the American Chemical Society*, 121(41), 9550-9561 (**1999**).
28. L.C. Liang, *Coordination chemistry reviews*, 250(9-10), 1152-1177 (**2006**).
29. M.M. Pereira, M.J. Calvete, R.M. Carrilho, and A.R. Abreu, *Chemical Society Reviews*, 42(16), 6990 -7027 (**2013**).

30. J.G. de Vries, *Topics in Catalysis*, 57(17),1306-1317 (**2014**).
31. K. Billingsley and S.L. Buchwald, *Journal of the American Chemical Society*, 129(11), 358-3366 (**2007**).
32. C. Mealli, A. Ienco, A. Galindo, and E.P. Carreno, *Inorganic chemistry*, 38(21), 4620-4625 (**1991)**
33. F. Leca, M. Sauthier, V. Deborde, V., Toupet, L. and R. Réau, *Chemistry–A European Journal*, 9(16), 3785-3795 (**2003**).
34. N. Biricik, F. Durap, C. Kayan, B. Gümgüm, N. Gürbüz, I. Oezdemir, W.H. Ang, Z. Fei, and R. Scopelliti, *Journal of Organometallic Chemistry*, 693(16), 2693-2699 (**2008**).
35. T. Mino, Y. Shirae, Y Sasai, M. Sakamoto and T. Fujita, *The Journal of OrganicChemistry*, 71(18),6834-6839 (**2006**).
36. O. Kühl, *Chemical Society Reviews*, 36(4), 592-607 (**2007**).
37. P. De Fremont, N. Marion, and S.P Nolan, *Coordination Chemistry Reviews*, *253*(7-8), 862-892 (**2009**).
38. M.N Hopkinson, C. Richter, M. Schedler, and F. Glorius., *Nature*, 510(7506), 485-496 (**2014**).
39. H.W. Wanzlick, and H.J. Schönherr, *Angewandte Chemie International Edition in English*, 7(2), 141-142 (1**968**).
40. A.J. Arduengo. R.L. Harlow, and M. Kline, *Journal of the American Chemical society*, 113(1), 361-363 (**1991**).
41. B. Maji, M. Breugst, and H. Mayr, *Angewandte Chemie-International Edition*, 50(30), 6915- 9619 (**2011**).
42. S. Díez-González, and S.P. *Coordination chemistry reviews,* 251(5-6), 874-883, (**2007**)**.**
43. L. Benhamou, E. Chardon, G. Lavigne, S. Bellemin-Laponnaz, and V. César, *Chemical reviews*, 111(4), 2705-2733 (**2011**).
44. F.E. Hahn, and M.C. Jahnke, *Angewandte Chemie International Edition*, 47(17), 3122-3172 (**2008**).
45. T. Dröge, and F. Glorius, *Angewandte Chemie International Edition*, 49(39), 6940-6952 (**2010**).
46. A.J. Arduengo, R.L. Harlow, M.J. Kline, *Chem*. *Soc* 113(1) 361-363) (**1991**).
47. R.W. Alder, M.E. Blake, L. Chaker, J.N, Harvey, F. Paolini, and J. Schütz, *Angewandte Chemie*, 116(44), .6020-6036 (**2004**).
48. M.O. Karataş, N. Özdemir, B. Alıcı, and I. Özdemir, *Polyhedron*, 176, 114271 (**2020**).
49. N.U.D. Reshi, and J.K. Bera, *Coordination Chemistry Reviews*, 422, 213334 (**2020**).
50. D. Enders, O. Niemeier, and A. Henseler, *Chemical Reviews*, 107(12), 5606-5655 (**2007**).
51. S. De, A. Jain. and P. Barman, *ChemistrySelect*, 7(7), e202104334 (**2022**).
52. M. Kaur, S. Kumar, S.A. Younis, M. Yusuf, J. Lee, S. Weon, K.H. Kim, and A.K. Malik, 2021. *Chemical Engineering Journal*, 423,130230 (**2021**).
53. P.G. Cozzi, *Chem. Soc. Rev*, 33(7) 410-421 (**2004**).
54. W. Qin, S. Long, M. Panunzio, S. Biondi. *Molecules*, 18(10), 12264 (**2013**).
55. M. Chaurasia, D. Tomar, S. Chandra, *Egypt. J. Chem*, 62(2), 357-372 (**2019**).
56. N. R. Bader, *J. Chem*, 3(4), 660-670 (**2010**).
57. J. Hine, C.Y. Yeh, *Journal of the American Chemical Society*, 89(11), 2669-2676 (**1967**).
58. R.J. Fessenden, J.S. Fessenden, *The Journal of Organic Chemistry*, 32(11), 3535-3537 (**1967**).
59. M. Mesbah et al., *Journal of Molecular Structure*, 1151, 41-48 (**2018**).

60. C. Erdal, A. Ayşe, Ş. Hakan, K. Mehmet, *Sci J (CSJ)*, 37(1), 65-73 (**2016**).
61. J. Hao-Ran, L. Jing, S. Yin-Xia, G. Jian-Qiang, Y. Bin, W. Na, X. Li, *Crystals*, 7(8), 1-15 (**2017**).
62. AM. Franz, CF. Roland, S. Mark, RA. Andres, HT. Diana, SM. Salah, *Crystals*, 6(8), 1-17 (**2016**).
63. B. Banik, A. Tairai, N. Shahnaz, and P. Das, *Tetrahedron Letters*, 53(42), 5627-5630 (**2012**).
64. A. Dewan, U. Bora, and G. Borah, *Tetrahedron Letters*, 55(10), 1689-1692 (**2014**).
65. X. Liu, C. Manzur, N. Novoa, S. Celedón, D. Carrillo, and J.R. Hamon, *Coordination Chemistry Reviews*, 357, 144-172 (**2018**).
66. A. Kanwal, B. Parveen, R. Ashraf, N. Haider, K.G. Ali, *Journal of Coordination Chemistry*, 75(19-24), 2533-2556 (**2022**).
67. E. Pahontu, F. Julea, T. Rosu, V. Purcarea, Y. Chumakov, P. Petrenco, A. Gulea. *J. Cell Mol. Med*, 19(4), 865 (**2015**).
68. J.A. Lara-Cerón, V.M.J. Pérez, L. Xochicale-Santana, M.E. Ochoa, A. Chávez-Reyes, B.M. Muñoz-Flores, *RSC advances*, 10(53), 31748-31757 (**2020**).
69. W. Al Zoubi, M.J. Kim, A.A. Salih Al-Hamdani, Y.G. Kim, Y.G. Ko. *Appl. Organomet. Chem*., 33(11), 5210 (**2019**).
70. A. Madani, I. Kaabi, L. Sibous, E. Bentouhami. *J. Iran. Chem. Soc*., 18 (11), 3077-3095 (**2021**).
71. R.M. Ansari, and B.R. Bhat, *Journal of Chemical Sciences*, 129, 1483-1490 (**2017**).
72. M. Dolaz, V. McKee, S. Uruş, N. Demir, A.E. Sabik, A. Gölcü, and M. Tümer, *Spectrochimica Acta Part A: Molecular and Biomolecular Spectroscopy*, 76(2), 174-181 (**2010**).
73. K. Sundaravel, E. Suresh, and M. Palaniandavar, *Inorganica Chimica Acta*, 362(1), 199-207 (**2009**).
74. M.S. More, P.G. Joshi, Y.K. Mishra, and P.K. Khanna, *Materials Today Chemistry*, 14, 100195 (**2019**).
75. L. Fabbrizzi, *The Journal of Organic Chemistry*, 85(19), 12212-12226 (**2020**).
76. Y. Shibuya, K. Nabari, M. Kondo, S. Yasue, K. Maeda, F. Uchida, and H. Kawaguchi, *Chemistry letters*, 37(1), 78-79 (**2008**).
77. M. Ashfaq, K.S. Munawar, M.N. Tahir, N. Dege, M. Yaman, S. Muhammad, S.S. Alarfaji, H. Kargar. and M.U. Arshad, *ACS omega*, 6(34), 22357-22366 (**2021**).
78. J. Anandakumaran M.L. Sundararajan, T. Jeyakumar, and M.N. Uddin, *Chem. Sci. Int. J.* 11(3), 1-14 (**2016**).
79. D.A. Chowdhury, M.N. Uddin, and F. Hoque, *Chiang Mai Univ J Nat Sci*, 10(2), 261-268 (**2011**).
80. M.N. Uddin D.A. Chowdhury M.M. Rony and M.E. Halim, *Mod. Chem,* 2(2), 6-14 (**2014**).
81. X.X. Sun, C.M. Qi, S.L. Ma, H.B. Huang, W.X. Zhu, Y.C. Liu, *Inorg. Chem. Commun*, 9(9), 911- 914 (**2006**).
82. M. Kumar, A.K. Singh, A.K. Singh, R.K. Yadav, S. Singh, A.P. Singh, and A. Chauhan, *Coordination Chemistry Reviews*, 488, 215176 (**2023**).
83. A.S. Munde, A.N. Jagdale, S.M. Jadhav, and T.K. Chondhekar, *Journal of the Serbian Chemical Society*, 75(3), 349-359 (**2010**).
84. H. Kargar, M. Fallah-Mehrjardi, R. Behjatmanesh-Ardakani, M. Bahadori, M. Moghadam, J. Javid, and K.S. Munawar, *Journal of the Iranian Chemical Society*, 19(9), 3981-3992 (**2022**).
85. M. Sedighipoor, A.H. Kianfar, G. Mohammadnezhad, H. Görls, and W. Plass, *Inorganica Chimica Acta*, 476, 20-26 (**2018**).

86. M. Holbach, X. Zheng, C. Burd, C.W Jones, M. Weck, *The Journal of Organic Chemistry*, 71(7), 2903-2906 (**2006**).
87. G.C. Fu, *Accounts of chemical research*, 41(11),1555-1564 (**2008**).
88. D. I. Ugwu, an J. Conradie, *Inorganica Chimica Acta*, 553, 121518 (**2023**).
89. T. Kylmälä, N. Kuuloja, Y. Xu, K. Rissanen, and R. Franzén, *European Journal of Organic Chemistry*, 2008(23), 4019-4024 (**2008**).
90. Q. Vanbellingen, P. Servin, A. Coinaud, S. Mallet-Ladeira, R. Laurent, and A.M. Caminade, *Molecules*, 26(8), 2333 (**2021**).
91. J.E. House, and K.A. House, *Academic Press*, 197 (**2015**).
92. T. Mahamo, M.M. Mogorosi, J.R. Moss, S.F. Mapolie, J.C. Slootweg, K. Lammertsma, and G.S. Smith, *Journal of Organometallic Chemistry*, 703, 34-42 (**2012**).
93. J. Kaushal, S. Singh, P. Oswal, A. Arora, D. Nautiyal, and A. Kumar, *Journal of Molecular Structure*, 1253, 132099 (**2022**).
94. P. Espinet, and K. Soulantica, *Coordination Chemistry Reviews*, 193, 499-556 (**1999**).
95. T.G. Santiago, C. Urbaneja, E. Álvarez, E. Ávila, P. Palma, and J. Cámpora, *Dalton Transactions*, 49(2), 322-335 (**2020**).
96. D.R. Meena, S. Meena, and S. Singh, *Polyhedron*, 245, 116655 (**2023**).
97. E.G. Bowes, G.M. Lee, C.M. Vogels, A. Decken, and S.A. Westcott, *Inorganica Chimica Acta*, 377(1), 84-90 (**2011**).
98. J. Cui, M. Zhang, and Y. Zhang, *Inorganic Chemistry Communications*, 13(1), 81-85 (**2010**).

CHAPTER 3

3. Results and discussion

3.1 The synthesis of Schiff base ligands

Schiff base ligands are known as privileged ligands due to their ease of preparation through condensation of aldehydes/ketones and amines starting materials, both of which are inexpensive and readily available.[1] The wide application and diversity of Schiff bases stems from the ease in which they can be functionalised with either electron-withdrawing or electron-donating substituents either on *ortho, meta,* or *para*-positions relative to the imine group.[2] These characteristics have encouraged us to synthesize several *para*-substituted Schiff base ligands with the aim of investigating whether the *para* substituents will have any influence on the catalytic activity of the corresponding Pd (II) complexes.

To begin our investigation, a series of different electron-withdrawing and electron-donating functionalised *para*-substituted Schiff base ligands were successfully synthesized following modified reported procedures.[3] The condensation reaction of salicylaldehyde (**99**) with anilines (**100**) in a 1:1.2 stoichiometric ratio afforded a yellow solution after 24 hrs (**Scheme 3.1**).

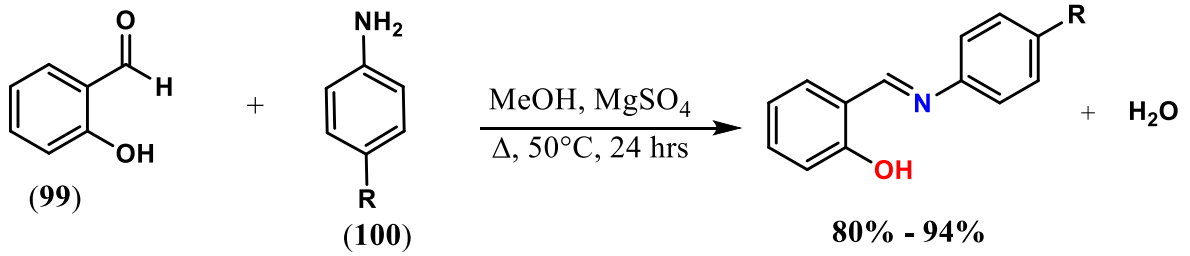

R = H (**L1**), R = CH_3 (**L2**),
R = CH_2CH_3 (**L3**), R = OCH_3 (**L4**),
R = F (**L5**), R = Br (**L6**), R = CN (**L7**)

Scheme 3.1: Synthesis of Schiff base ligands.

The progress of the condensation reaction was monitored using a Thin Layer Chromatography (TLC). The TLC analysis displayed only one spot which revealed that both the starting materials were completely consumed suggesting that the reaction went to completion with no undesired by-products present. Upon completion of the reaction, the evaporation of the solvent, under vacuum, followed by recrystallization using a slow diffusion technique of hexane and dichloromethane, afforded the desired Schiff base ligand (**L1**) in 92% yield.

The successful synthesis of the desired Schiff base ligand (**L1**) was confirmed using ^{1}H NMR spectroscopy. The ^{1}H NMR spectrum (**Figure 3.1**) exhibited 5 signals in the range of 7.29-7.48 ppm which are assigned to the aromatic protons of the compound. Additionally, a distinctive signal resonating as a singlet peak at 8.66 ppm was assigned to the imine proton (H_e) which confirms the successful formation of an imine functional group. Furthermore, another peak resonating as a broad singlet at 13.25 ppm which is attributed to the hydroxyl proton of the ligand was observed (**Figure 3.1**). The absence of the aldehyde and amine hydrogens (of the starting materials) which usually resonate at approximately 10 ppm and 4-6 ppm respectively, further confirmed the complete conversion of the starting materials to the desired product.

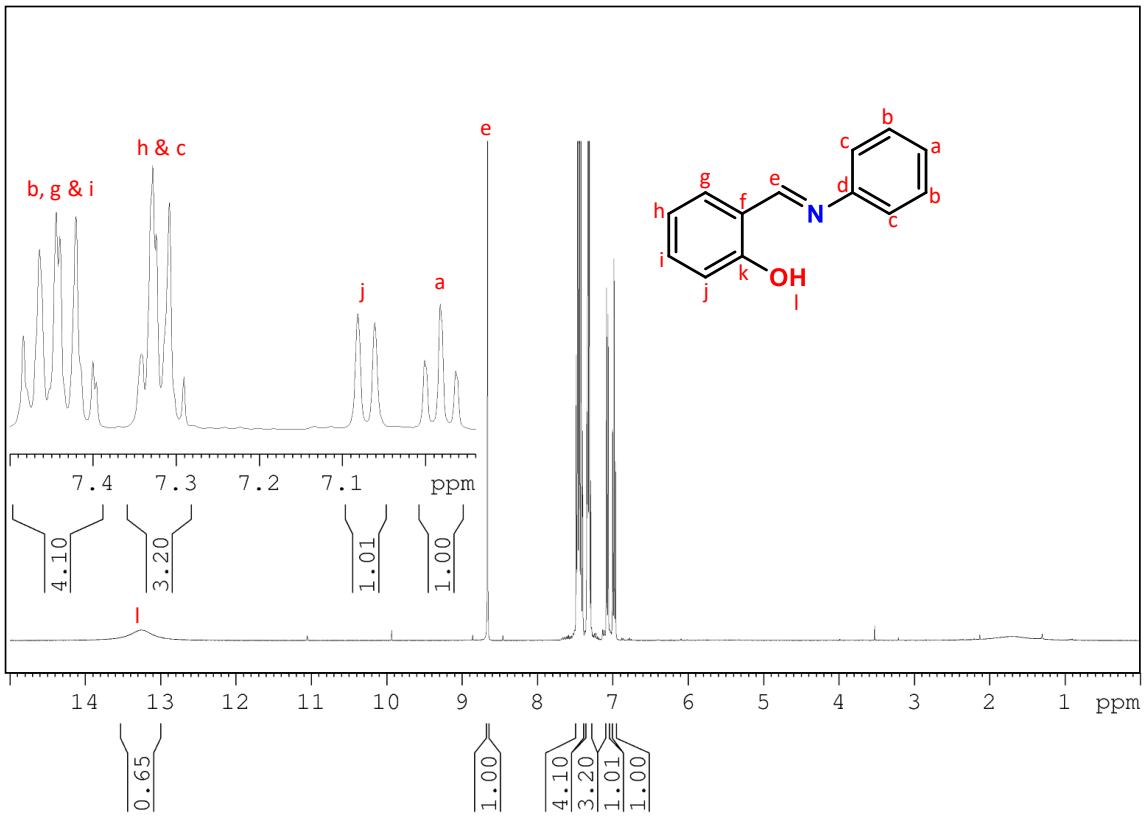

Figure 3.1: ^{1}H NMR spectrum of Schiff base **L1**.

The ^{13}C NMR spectrum (**Figure 3.2**) of **L1** shows a total of 13 carbon resonances (some overlapped), which correlate to the total number of carbon atoms of the compound. In addition, the distinctive carbon imine peak assigned as C_e resonates at 161.19 ppm which further confirms the formation of the imine functional group.

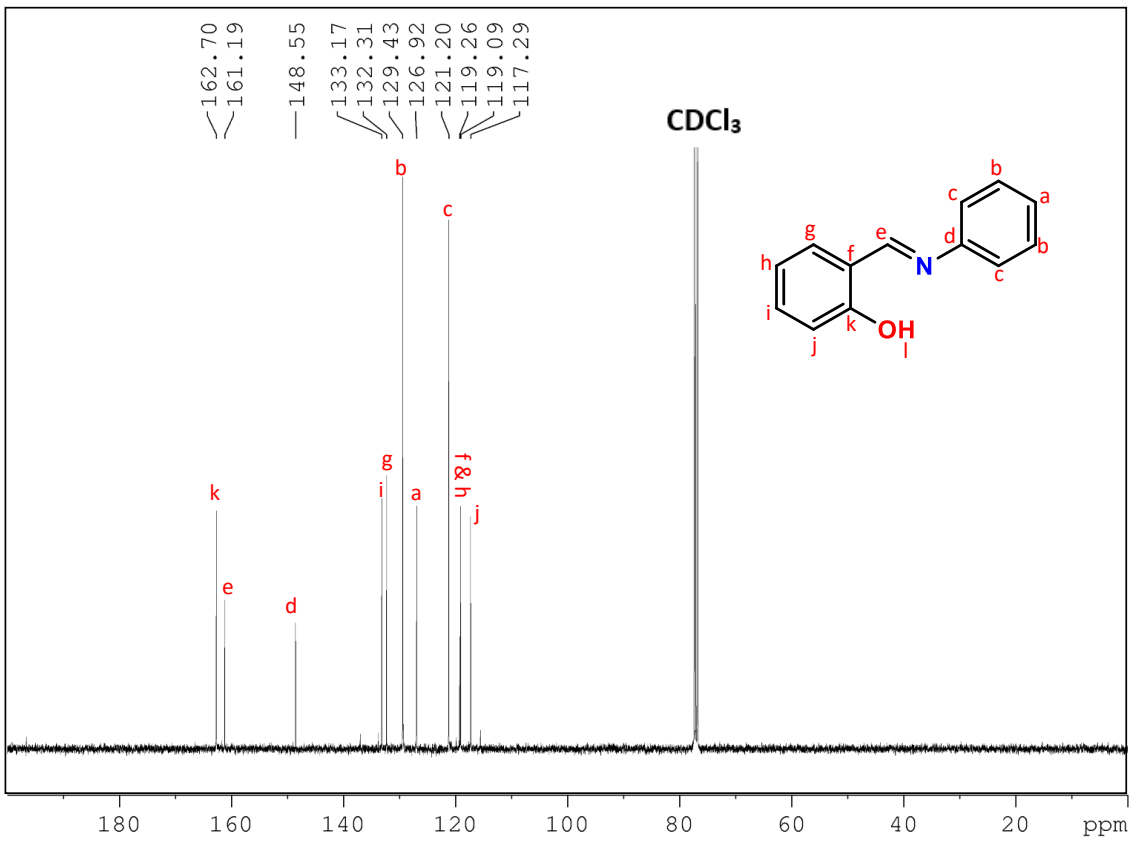

Figure 3.2: ^{13}C NMR spectrum of **L1**.

The transformation of a carbonyl carbon of salicylaldehyde to an imine moiety was confirmed using IR spectroscopy through the appearance of an imine bond stretching frequency at 1656.74 cm^{-1} (**Figure 3.3**). The IR spectrum of **L1** showed a broad absorption band at about 3433.03 cm^{-1} that may be assigned to the phenolic hydroxyl (O-H) group stretching vibration. To further confirm the successful synthesis of **L1**, electrospray ionization mass spectrometry (ESI^+- MS) (**Figure A4**) was used which revealed a base peak at *m/z* 197.24. This base peak corresponded to the protonated adduct $[M + H]^+$ of the compound with a molecular formula ($C_{14}H_{11}NO$). The melting point temperature of the product (**L1**) was found to be 49.6 - 51.7 °C which is close to the melting point temperature reported by Petrović *et al*.[3]

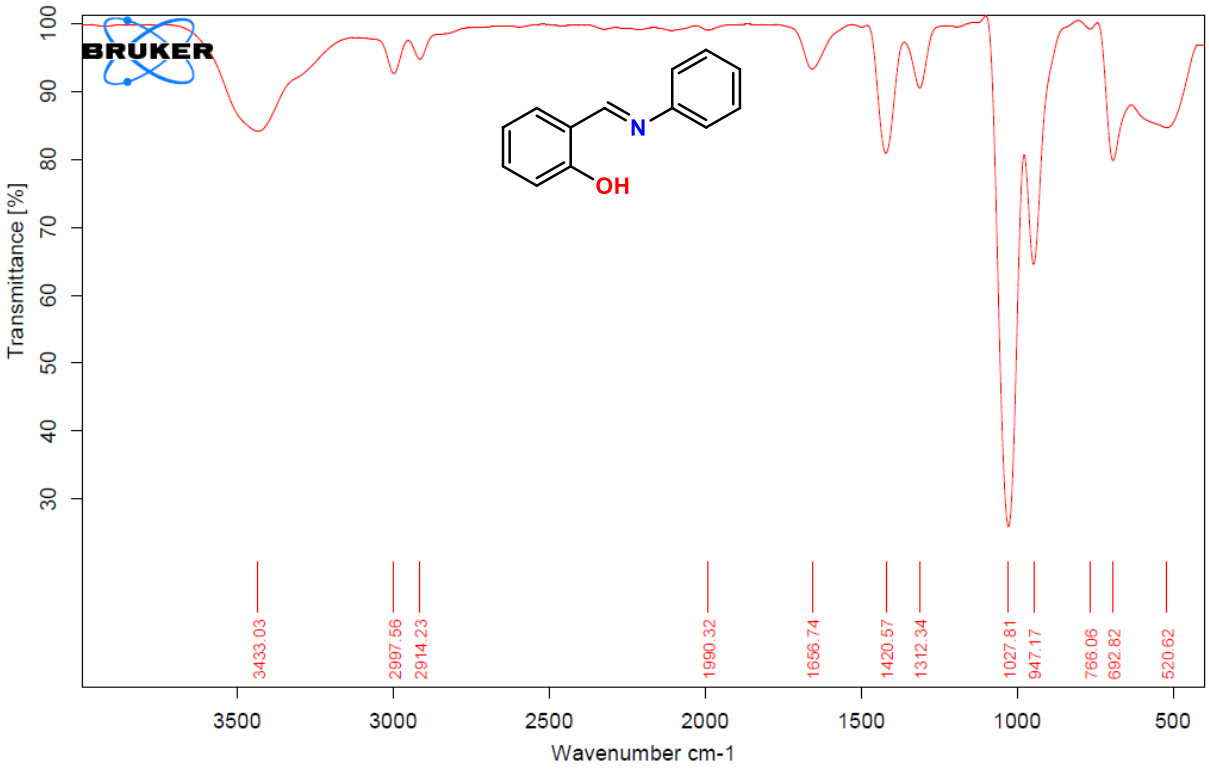

Figure 3.3: IR spectrum of **L1**.

Since Schiff base ligands can be functionalised easily, Schiff base ligands with electron-donating substituents such as -OCH_3, -CH_3, and -CH_2CH_3 on the *para*-position relative to the imine were synthesised. This allowed us to investigate the influence of the electron-donating *para* substituents on the ligands' behaviour and reactivity.

To synthesise Schiff base **L4**, 4-methoxyanaline (**100**) was reacted with salicylaldehyde (**99**) to afford the desired product as orange crystals in 80% yield after 24 hours (**Scheme 3.1**). The successful synthesis of **L4** was confirmed by its ^{1}H NMR spectrum (**Figure 3.4**) which revealed a singlet peak resonating at 3.87 ppm attributed to the methoxy functional group. The spectrum showed an upfield shift of the aromatic protons labelled as $H_{c, d}$ resonating at a range of 6.94 - 7.31ppm compared to the same protons in **L1** which resonated at 7.29 - 7.48 ppm. This shift may be attributed to the shielding effect of the methoxy substituent. An upfield shift is also observed for the distinctive imine signal assigned as H_f resonating as a singlet at 8.64 ppm when compared with the same signal in **L1** which resonated at 8.66 ppm.

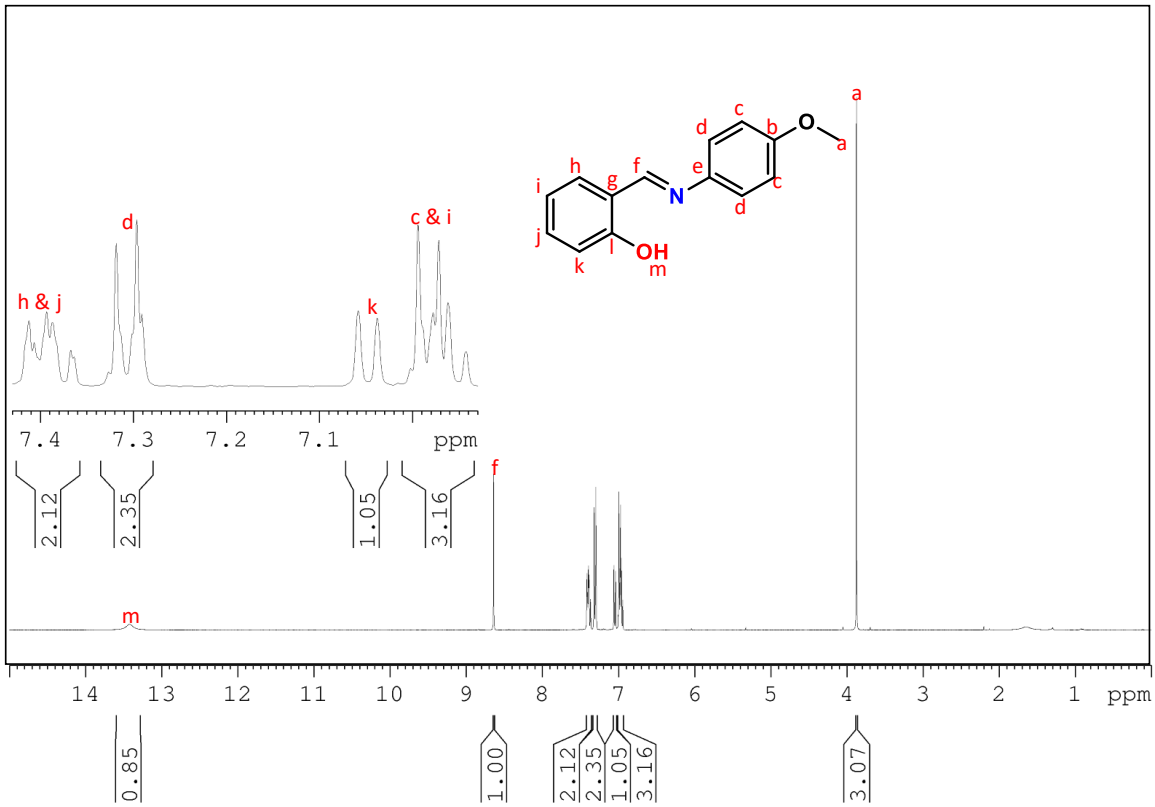

Figure 3.4: ^{1}H NMR spectrum of Schiff base **L4**.

^{13}C NMR spectrum (**Figure 3.5**) of ligand **L4** showed a carbon resonance peak at 55.53 ppm that is assigned to the carbon atom from the methoxy functional group. The distinctive imine carbon peak observed at 160.53 ppm is slightly shifted upfield when compared to **L1** as a result of the methoxy substituent which donates more electrons to the ligand than the H atom in **L1**. The IR spectrum of **L4** confirms the formation of the imine bond and the absence of the carbonyl group (C=O) of the salicylaldehyde starting material (**Figure 3.6**). The actual band at 1655.61 cm^{-1} is assigned to the stretching vibration of the imine functional group and the vibrational band of the hydroxyl group is observed in the range of 3425.13 cm^{-1}. The molecular mass of the compound was confirmed by MS which showed a base peak at *m/z* 228 (**Figure A16**, **Appendix**) corresponding to the protonated adduct $[M + H]^{+}$ of the compound with a molecular formula ($C_{14}H_{13}NO_2$).

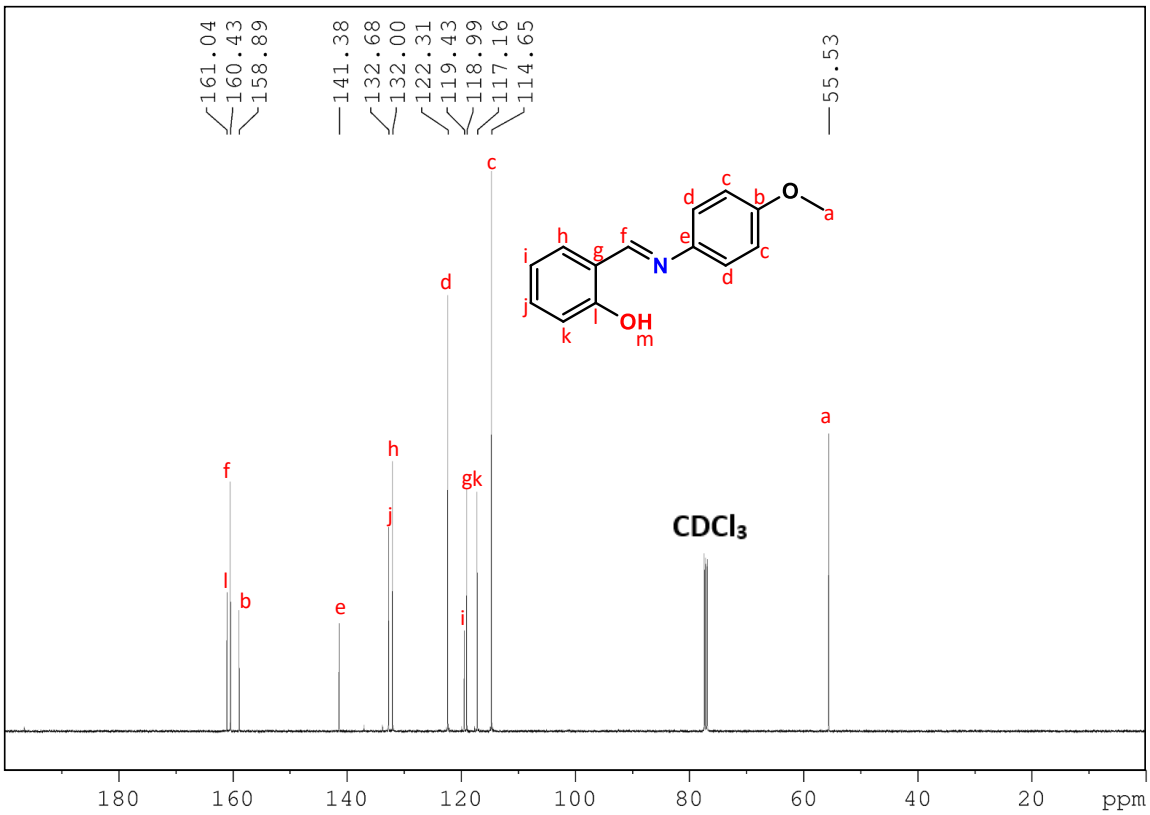

Figure 3.5: ^{13}C NMR spectrum of **L4**.

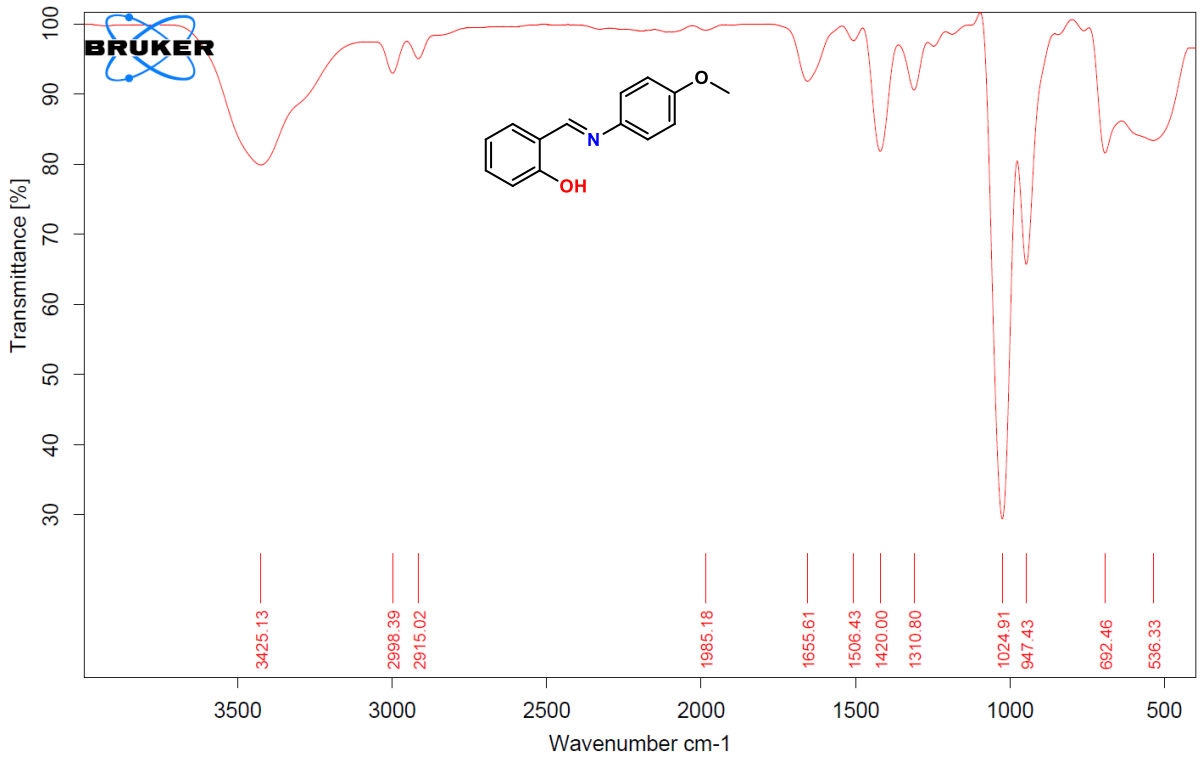

Figure 3.6: IR spectrum of **L4**.

Schiff bases **L2** and **L3** were successfully synthesised following the same procedure as mentioned above (**Scheme 3.2**). **L2** was obtained in 87% yield which is 7% lower than the yield obtained for **L3**. The spectroscopic characterisation of both **L2** and **L3** (^{1}H, ^{13}C NMR, IR, and MS) were ran, analysed and are corresponding to the predicted structures of the ligands (**Figure A5 - A12**, **Appendix**).

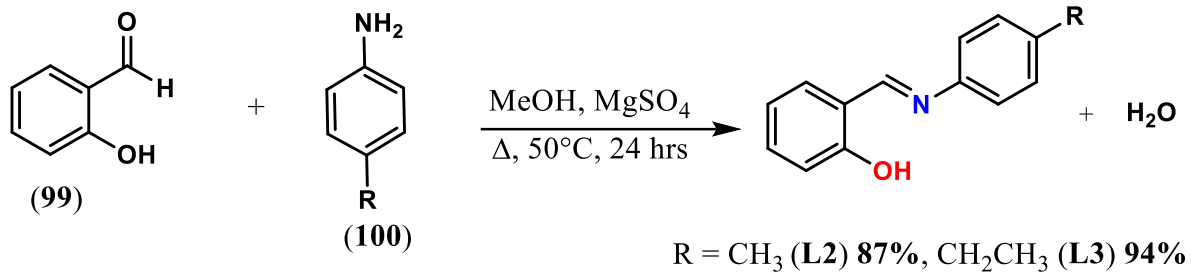

R = CH_3 (**L2**) **87%**, CH_2CH_3 (**L3**) **94%**

Scheme 3.2: Synthesis of L2 and **L3**.

Motivated by the influence exhibited by the electron-donating *para*-substituents, we modified the ligand systems with the objective of investigating how the electron-withdrawing *para*-substituents will affect the reactivity and stability of the Schiff base as well as their corresponding Pd (II) complexes. Schiff base ligands with moderate electron-withdrawing substituents such as halogens (-Br and -F), and with a strong electron-withdrawing substituent such as the cyano (-CN) on the *para*-position relative to the imine group were synthesised.

The synthesis of Schiff base ligands **L5**, **L6**, and **L7** was achieved by reacting the appropriate *para*-substituted aniline (4-fluoro aniline, 4-bromo aniline, and 4-cyano aniline) with salicylaldehyde (**99**) (**Scheme 3.3**) in methanol. The ligands were characterised by ^{1}H NMR, ^{13}C NMR, FTIR as well as MS.

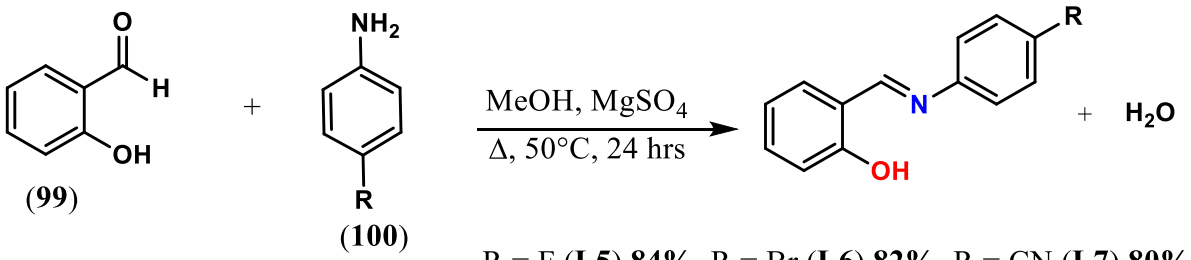

R = F (**L5**) **84%**, R = Br (**L6**) **82%**, R = CN (**L7**) **80%**

Scheme 3.3: Synthesis of **L5, L6,** and **L7.**

The ^{1}H NMR spectra of **L5** and **L6** showed distinctive signals resonating at 8.62 ppm and 8.63 ppm respectively which are assigned to the imine functional groups, verifying the successful synthesis of the ligands (**Figure A17 & A21, Appendix**). The broad signals observed at 13.12 ppm and 13.01 ppm on the ^{1}H NMR spectra correspond to the hydroxyl group of **L5** and **L6**, respectively. The ^{13}C NMR spectra of both ligands show 11 sets of carbon signals (some overlapped) that can be assigned to the compound's aromatic carbons (**Figure A18 & A22, Appendix**). The IR spectrum of **L5** reveals vibrational bands at 3439.9 cm^{-1} and 1654.78 cm^{-1} which are attributed to the imine bond and the phenolic hydroxy group, respectively (**Figure A19**, **Appendix**). The ESI^{+}- MS spectrum of **L5** displays a protonated adduct corresponding to the molecular mass of the ligand (**Figure A20, Appendix**).

The IR spectrum of **L6** displays a stretching band that is assigned to the imine bond observed at approximately 1651.54 cm^{-1}, which confirmed that the amine and aldehyde moieties starting materials successfully reacted to completion (**Figure 3.7**). The stretching band found at the 3422.91 cm^{-1} region was assigned to the phenolic (O-H) group. The strong band at 690.70 cm^{-1} was assigned as a C-Br bond stretching vibration. The molecular mass and formula of the ligand were confirmed by electrospray ionization mass spectrometry (ESI^{+}- MS). The ESI^{+}- MS spectrum of **L6** reveals two base peaks observed at *m/z* 276 and *m/z* 278 which correspond to the molecular mass and the molecular formula of the ligand ($C_{13}H_{10}BrNO$) (**Figure 3.8**). Since a bromine atom can exist as two stable isotopes (^{79}Br and ^{81}Br), the *m/z* values of the peaks agree with the molecular formula and molecular mass of the respective brominated compound isotopes hence the difference of *m/z* 2 is observed in the base peaks.

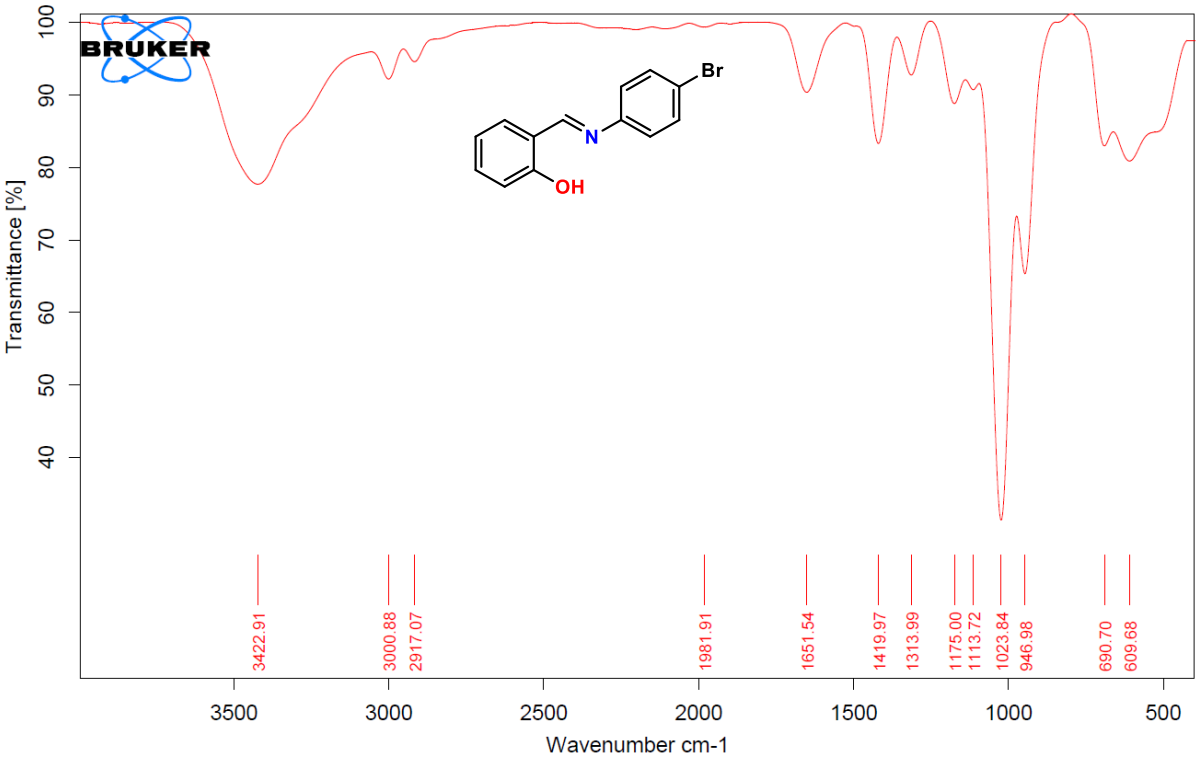

Figure 3.7: IR spectrum of **L6**.

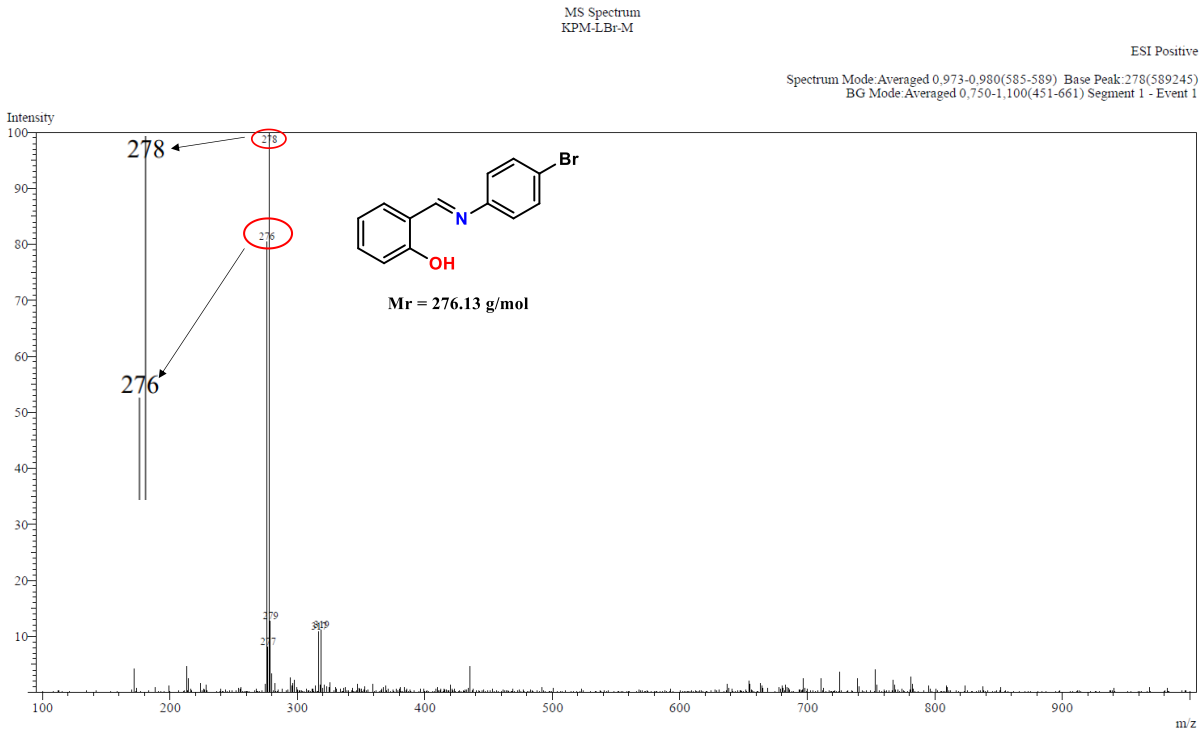

Figure 3.8: MS spectrum of **L6**.

The ^{1}H NMR spectrum of **L7** (**Figure 3.9**) shows a multiplets signal in an aromatic region from 6.99 - 7.06 ppm and 7.58 - 7.67 ppm. Singlet peaks for the imine proton and the phenolic proton

are observed at 8.97 ppm and 12.69 ppm, respectively. These significant downfield shifts (compared to the same protons on the unsubstituted **L1** Schiff base) are attributed to the nitrile group which is known for its stronger electron-withdrawing ability, thus inducing a deshielding effect on the ligand. The ^{13}C NMR spectrum (**Figure 3.10**) of the ligand reveals a signal resonating at 118.34 ppm which is assigned to the nitrile carbon atom. The imine and hydroxyl carbons are observed at 161.32 ppm and 166.38 ppm, respectively. IR and MS were also used to confirm the successful synthesis of **L7** (**Figure A27 & A28, Appendix**), and the results obtained corresponded to the functional groups and molecular mass of the ligand.

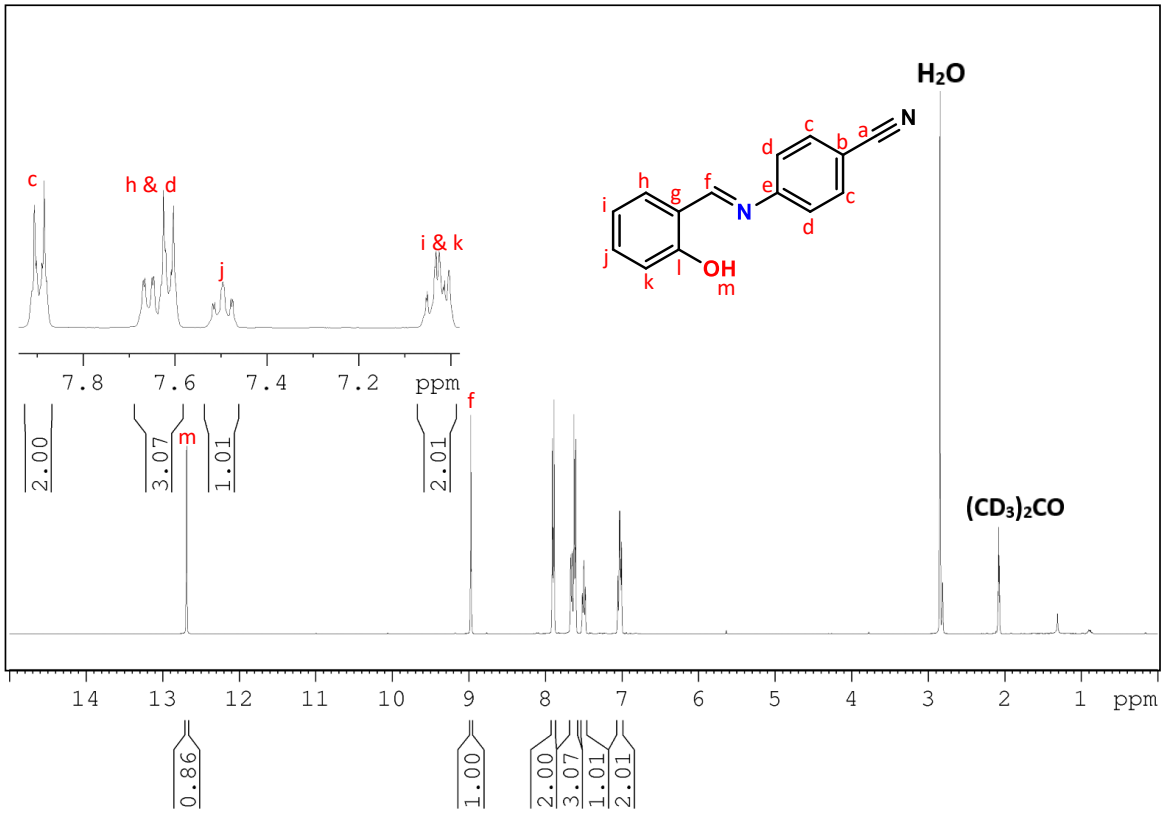

Figure 3.9: ^{1}H NMR spectrum of **L7**.

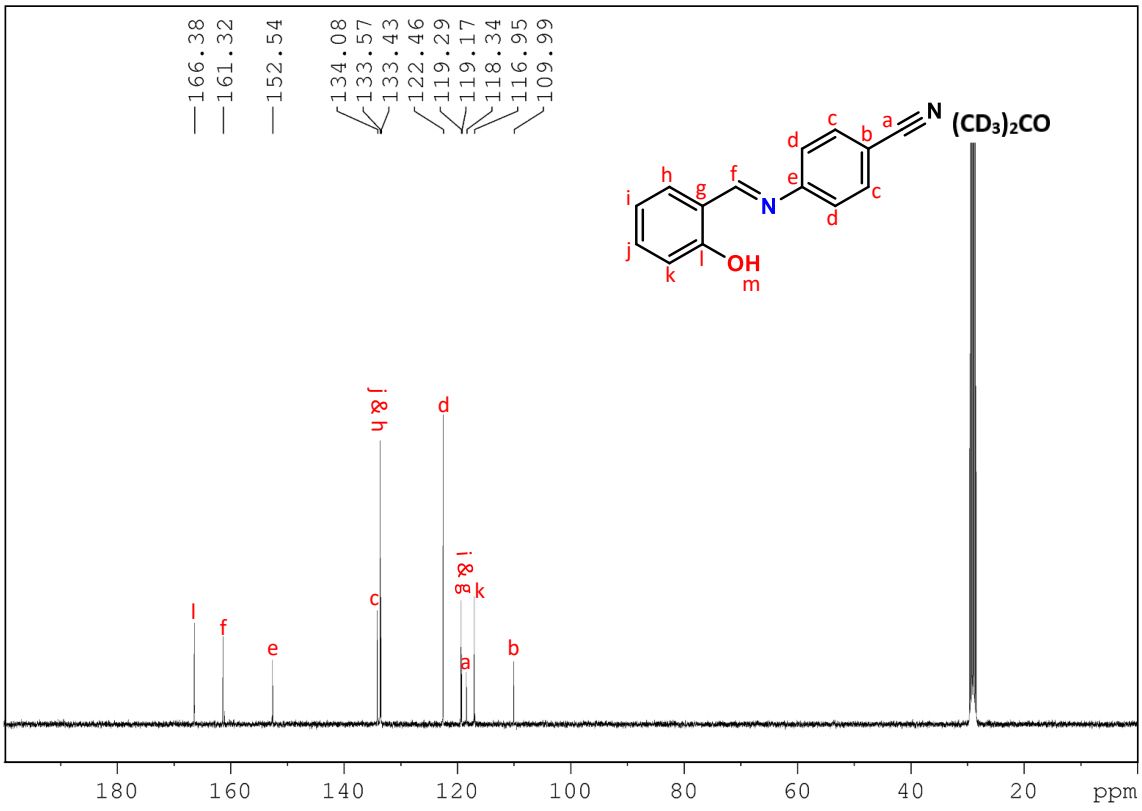

Figure 3.10: ^{13}C NMR spectrum of **L7**.

Having successfully synthesized Schiff base ligands (**L1-L7**) in excellent yields (80% - 94%) and fully characterised them, our next step was to coordinate the synthesized ligands with Pd (II) precursor to form the corresponding Schiff base Pd (II) complexes.

Pd (II) complexes have widespread applications in organic catalysis and have emerged as one of the most powerful and convenient catalysts for C–C and C–N bond-forming processes in pharmaceutical chemistry, materials, and synthetic chemistry. Therefore, developing facile innovative methodologies for the construction of stable and reactive Pd (II) complexes in high yields is of high interest in industry and academia.

A large number of recent studies have reported on the use of Palladium acetate (Pd $(OAc)_2$) as a precursor in the production of stable Pd (II) complexes because of its high reactivity and solubility in most volatile organic solvents such as dichloromethane, chloroform, methanol and ethanol. For instance, Akiri *et al* [4] and Name *et al* [5] demonstrated the successful synthesis of

bis-chelated Schiff base Pd (II) complexes derived from palladium acetate and Schiff base ligands exhibiting good yields, stability, and reactivity.

This discovery has prompted us to design novel *N, O*-bis Schiff base chelated Pd (II) complexes employing the modified method reported by Akiri *et al*. Schiff base ligands **L1-L7** were reacted in a 2:1 stoichiometric ratio with Pd $(OAc)_2$ (**101**) to afford the corresponding complexes **PdC1-PdC7** in excellent yields (78% - 95%) (**Scheme 3.4**).

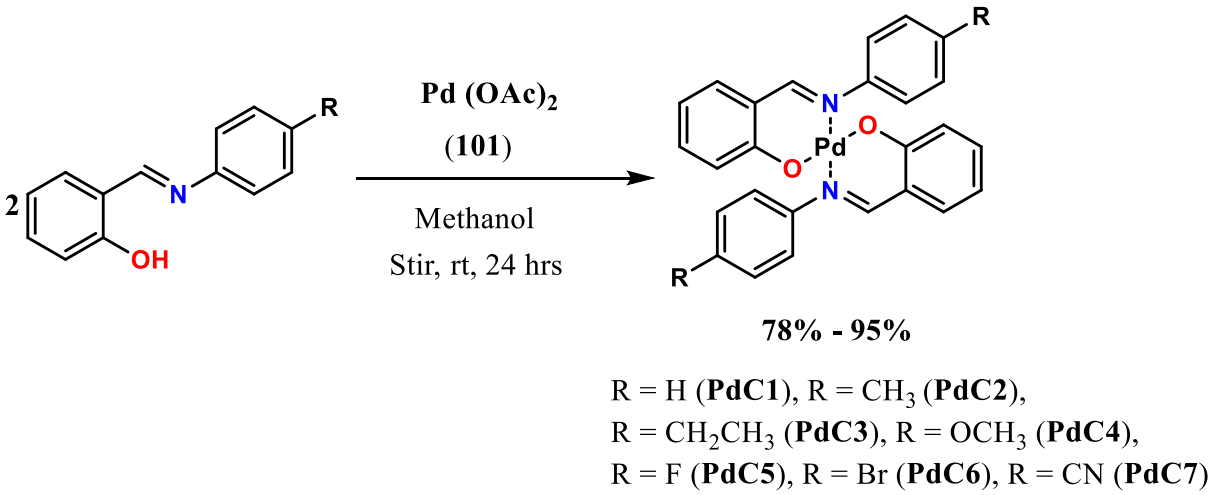

Scheme 3.4: Synthesis of *N, O*-bis chelated Pd (II) complexes.

For the synthesis of Pd (II) complex 1 (**PdC1**), to a methanolic solution of (Pd $(OAc)_2$) (**101**) was added a methanolic solution of **L1**. The resulting mixture was stirred under a nitrogen atmosphere for 24 hours, producing an orange solution. The use of inert atmosphere (nitrogen atmosphere) in palladium complexation is intended to suppress the oxidation of Pd by eliminating oxygen in the flask. The evaporation of solvent under vacuum followed by recrystallisation, using small amounts of hexane and chloroform by a slow diffusion process, resulted in the formation of an orange solid identified as Palladium complex 1 (**PdC1**) in 88% yield (**Scheme 3.4**).

The successful formation of the desired Pd (II) complex (**PdC1**) was confirmed using ^{1}H NMR spectroscopy. The overlayed ^{1}H NMR spectra (**Figure 3.11**) of **L1** and **PdC1** revealed that there is a noticeable upfield shift in all the signals observed in the spectrum of **PdC1** when compared to **L1**. An upfield shift is observed in the range of 6.15 - 7.47 ppm which is assigned to the aromatic signals of the complex **PdC1** when compared to the aromatic protons of **L1**

which resonates at 7.29 -7.48 ppm. The distinctive imine signal shifted to an upfield region of 7.76 ppm when compared to the same imine signal of **L1** which was observed at 8.64 ppm. These significant upfield shifts prove that the coordination between (Pd $(OAc)_2$) and the *N*-and *O*-donors of ligand **L1** was successful. Additionally, the disappearance of the broad phenolic signal in the spectrum of **PdC1** which appeared at 13.25 ppm in the ^{1}H NMR spectrum of **L1** indicates that complexation between the Pd precursor and **L1** was successfully achieved through the deprotonation of the phenol proton upon coordination.

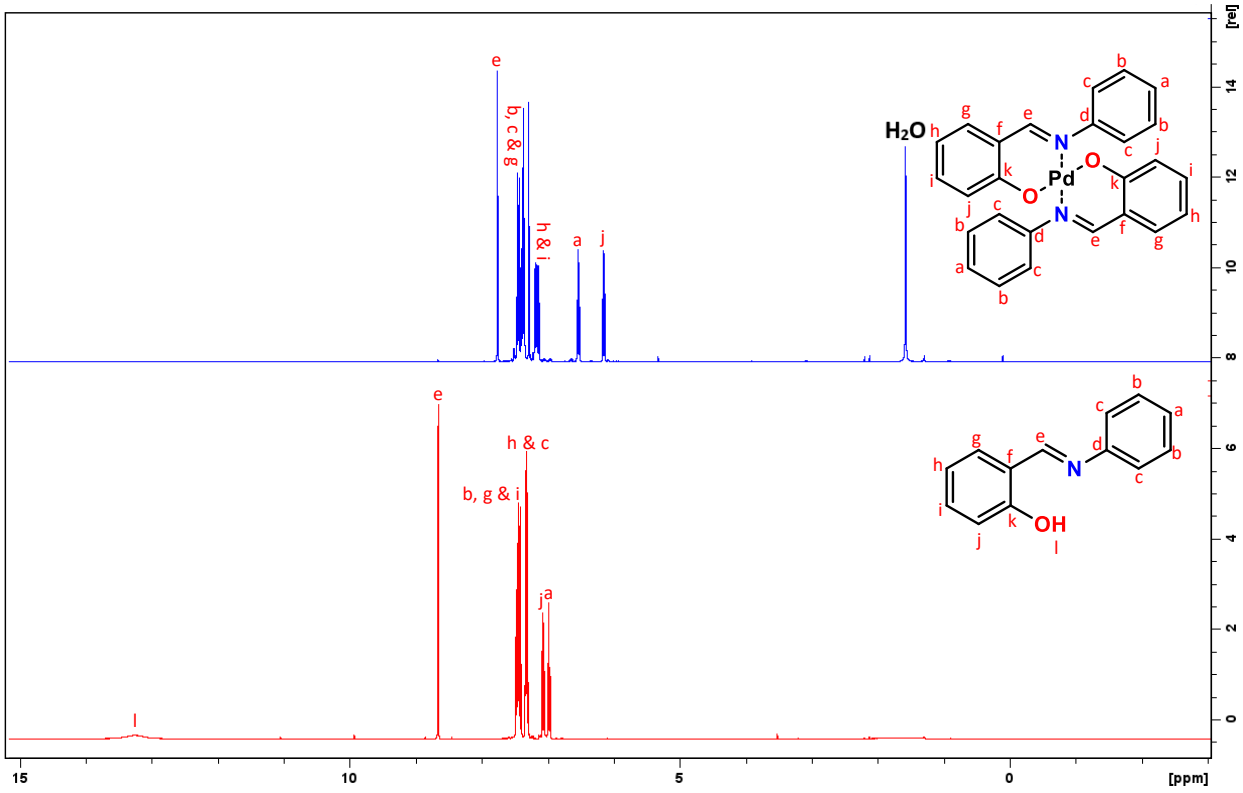

Figure 3.11: ^{1}H NMR spectra of **L1** and **PdC1**.

The ^{13}C NMR spectrum of **PdC1** displays a total number of 11 carbon resonances some of which are overlapped (**Figure 3.12**). This can be attributed to the complex's bis-chelation binding fashion, which results in its symmetric manner. The signals for the imine and phenolic carbons of the complex assigned as C_e and C_k resonate at 165.13 ppm and 162.76 ppm, respectively. When compared to ligand **L1**, these signals shifted to an upfield region of 161.19 ppm for the imine carbon and 162.70 ppm for the phenolic carbon. These observations indicate the successful coordination of the Pd precursor and **L1**. These alterations in the chemical shifts are undoubtedly brought about by the donation of the nitrogen's lone pair to the vacant *d* orbital

of the Pd transition metal center. These up-field shifts of the signals upon coordination of the ligand with Pd metal are consistent with the reported literature.[3]

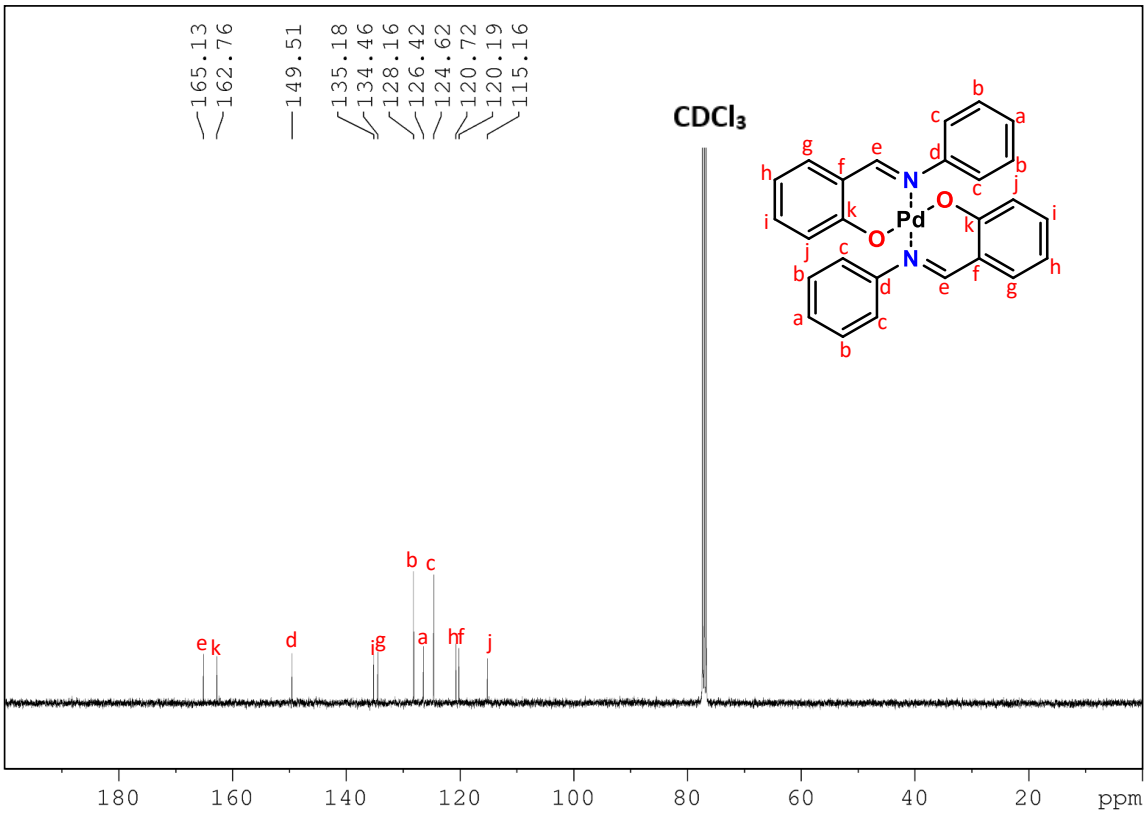

Figure 3.12: ^{13}C NMR spectrum of **PdC1**.

The successful synthesis of **PdC1** was also confirmed by FTIR. The IR spectrum revealed slight shifts in the vibrational bands of the functional groups present in the complex (**Figure A31**, **Appendix**) which proved the coordination of the metal precursor and the ligand. The molecular mass of the complex was verified by ESI$^+$- MS which showed a base peak at *m/z* 499 (**Figure A32**, **Appendix**) corresponding to the protonated adduct $[M + H]^+$ of the complex with a molecular formula ($C_{26}H_{20}N_2O_2Pd$).

Pd complexes coordinated to Schiff bases with *para*-electron donating substituents (**PdC2, PdC3, and PdC4**) were synthesized from (Pd $(OAc)_2$) (**101**) and Schiff base with *Para* electron-donating substituents (**L2, L3, and L4**) in 95%, 93%, and 78% yields, respectively (**Scheme 3.4**). To verify the successful synthesis of these Pd (II) complexes, their samples were fully characterised using ^{1}H and ^{13}C NMR, IR, and MS techniques. ^{1}H NMR spectra of **PdC2**

and **L2** (**Figure 3.13**) display the chemical shift for the methyl proton appearing at 2.41 ppm as a singlet in **L2** whereas the same signal shifted to the downfield region of 2.45 ppm in its respective complex **PdC2**. The aromatic signals of the complex are observed at 7.13 - 7.24 ppm which revealed an upfield shift when compared to the same protons that appeared at 7.29-7.48 ppm in the ^{1}H NMR spectrum of **L2**. The imine proton in **L2** resonates at 8.65 ppm, whereas, in the corresponding complex **PdC2**, the same proton shifted upfield to 7.73 ppm. These shifts prove the successful reaction between the Pd precursor and **L1**. The successful coordination between *O*-donor of the ligand and the Pd metal center was also verified by the disappearance of the hydroxyl proton in **PdC2** which resonated at 13.39 ppm in the ^{1}H NMR spectrum of **L2**.

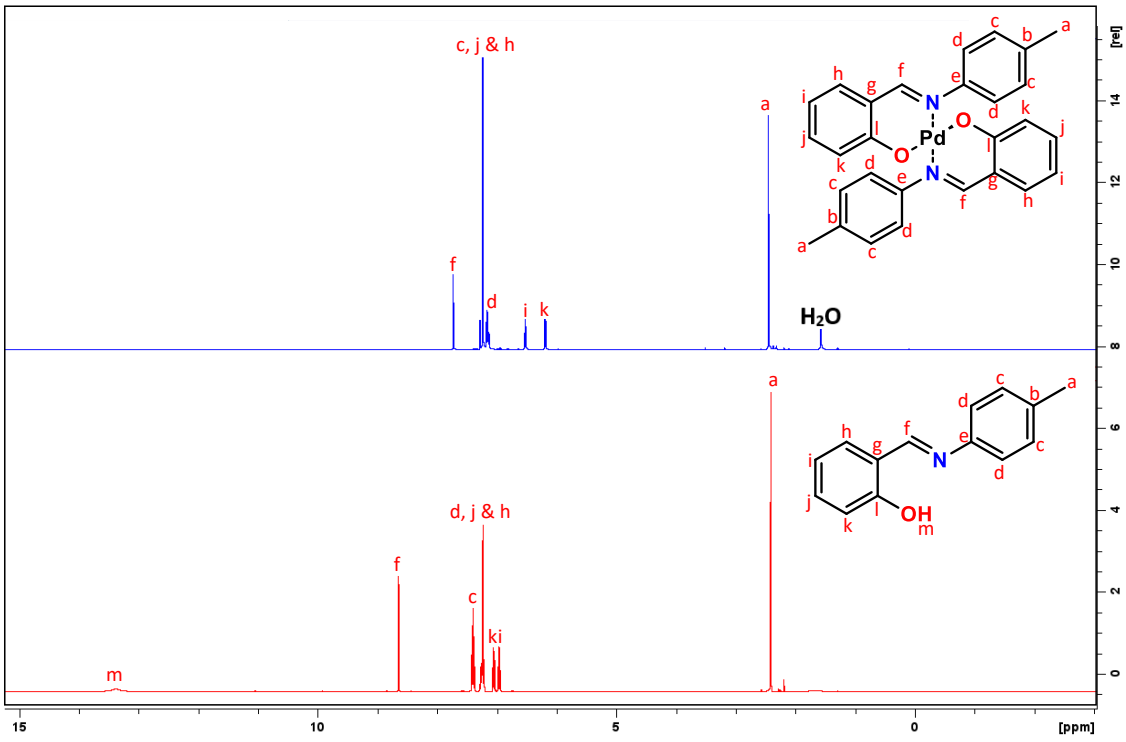

Figure 3.13: ^{1}H NMR spectra of **L2** and **PdC2**.

The ^{13}C NMR spectrum analysis of **PdC2** (**Figure 3.14**) shows downfield shifts in the imine and the hydroxyl carbon signals resonating at 165.18 ppm and 162.67 ppm, respectively. These signals resonated at 161.15 ppm and 161.71 ppm respectively in the ^{1}H NMR spectrum of **L2** suggesting that the *N*-and *O*-donors of the ligand indeed coordinated with the Pd metal center.

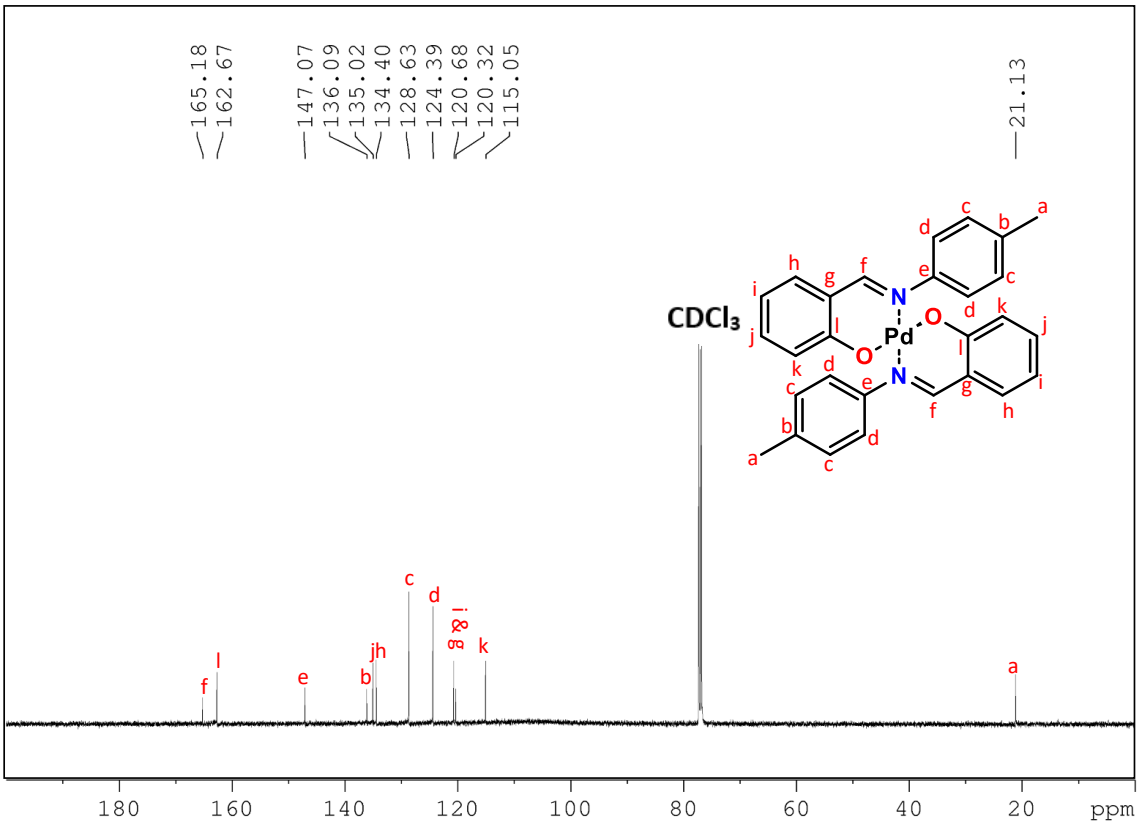

Figure 3.14: ^{13}C NMR spectrum of **PdC2**.

The IR spectrum of complex **PdC2** shows a vibrational band at 1658.08 cm^{-1} which is assigned to the imine bond of the complex (**Figure 3.15**). The positive electrospray ionisation time-of-flight mass spectrometry (TOF-MS ES^{+}) reveals a protonated mass-to-charge ratio corresponding to the molecular weight of the complex (**Figure A36**, **Appendix**).

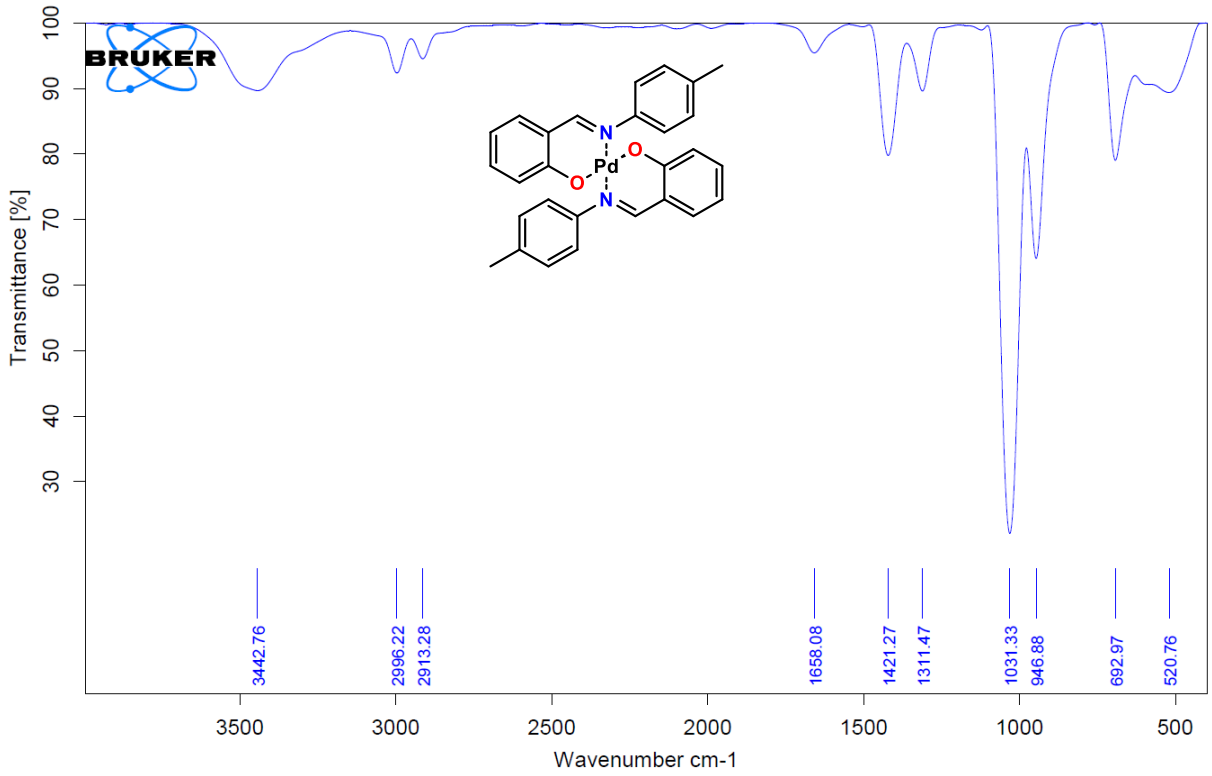

Figure 3.15: IR spectrum of **PdC2**.

The coordination and formation of **PdC2** was also confirmed by single X-ray crystallography (**Figure 3.16**). The crystal structure analysis of **PdC2** shows that the **L2** ligand coordinates to the Pd metal center in a bidentate mode *via* the nitrogen atom of the imine and the oxygen atom of the phenolic group. The crystallographic structure also reveals that the complex exhibits a distorted square planar geometry. This is consistent with most Pd (II) complexes which adopt a square planar geometry.[6] The obtained crystallographic data highlighted that **PdC2** crystallises in the monoclinic crystal system with a P21/c space group and a Z value of 2, indicating specific symmetry and packing arrangements within the crystal lattice of the complex. The Z value of 2 indicates that there are two molecular units of the complex per unit cell, providing insight into the structural arrangement of the complex within the crystal lattice (**Figure 3.16**). **Table 3.1** presents the crystallographic data and refinement parameters of **PdC2**, corresponding to the expected structure of the complex.

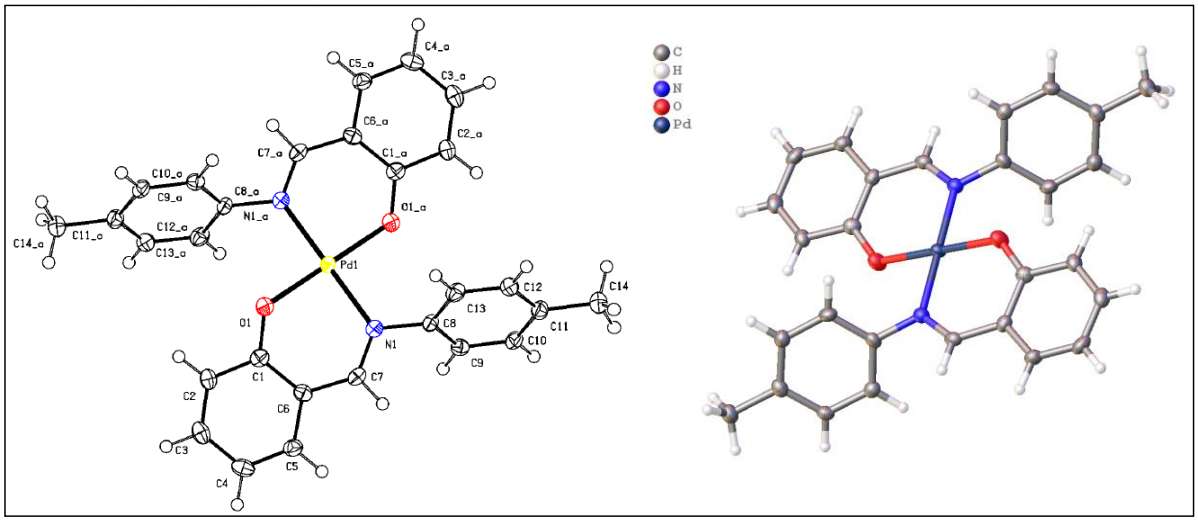

Figure 3.16: X-ray crystallographic structure of **PdC2**.

Table 3.1: Crystallographic data and refinement parameters of **PdC2**.

Empirical formula	$C_{28}H_{24}N_2O_2Pd$
Formula weight	526.89
Temperature/K	100.03
Crystal system	Monoclinic
Space group	$P2_1/c$
Unit cell dimensions	a = 9.745 (3) Å
	b = 10.946 (3) Å
	c = 10.820 (3) Å
	α = 90°
	β = 104.680 (4) °
	γ = 90°
Volume/Å^3	1116.5 (6)
Z	2
ρ_{calc}g/cm^3	1.567
μ/mm^{-1}	0.860
F (000)	536.0
Crystal size/mm^3	0.3 × 0.175 × 0.14
Radiation	MoKα (λ = 0.71073)
2Θ range for data collection/°	4.32 to 55.054

Index ranges	$-12 \leq h \leq 12, -14 \leq k \leq 14, -14 \leq l \leq 14$
Reflections collected	49114
Independent reflections	2562 [$R_{int} = 0.1284$, $R_{sigma} = 0.0489$]
Data/restraints/parameters	2562/0/152
Goodness-of-fit on F^2	1.063
Final R indexes [I>=2σ (I)]	$R_1 = 0.0333$, $wR_2 = 0.0804$
Final R indexes [all data]	$R_1 = 0.0562$, $wR_2 = 0.0886$
Largest diff. peak/hole / e $Å^{-3}$	0.67/-0.58

Complex **PdC3** was synthesised and was fully characterised by ^{1}H and ^{13}C NMR, IR, and MS. All the spectroscopic characterisations of the complex were analysed and corresponded to the predicted structure of the complex (**Figure A38 – A41**, **Appendix**).

Pd complexes coordinated to Schiff bases with *para*-electron withdrawing substituents i.e. Cl, Br and CN, (**PdC5, PdC6, and PdC7**) were synthesized from (Pd $(OAc)_2$) (**101**) and Schiff base ligands functionalised with *para* electron-donating substituents (**L2, L3, and L4**) in 86%, 81%, and 91% yields, respectively (**Scheme 3.4**). To verify the successful synthesis, the complexes were fully characterised using ^{1}H and ^{13}C NMR, IR, and MS.

The ^{1}H NMR spectrum of **PdC5** (**Figure 3.17**) exhibits upfield shifts of the aromatic protons within the range of 7.10 - 7.32 ppm, along with a signal at 7.75 ppm attributed to the imine functional group. These signals were observed at 7.11 - 7.44 ppm and 8.62 ppm when compared to the same signals in the ^{1}H NMR spectrum of **L5**. The spectrum also revealed the disappearance of the hydroxyl proton signal which resonated at 13.12 ppm in the ligand. These altered chemical shifts indicate the coordination of the imine nitrogen and hydroxyl oxygen to the palladium center in the complex. The ^{13}C NMR spectrum of the complex shows 11 sets of carbon signals (some overlapped) that correspond to the complex's aromatic carbons (**Figure A47**, **Appendix**). The imine and hydroxyl carbon signals resonated at 165.11 ppm and 160.21 ppm, respectively which displays a downfield shift when compared to the same carbon signals in the ^{1} H NMR spectrum of **L5**. The vibrational bands displayed by the IR spectrum of the complex corresponded to the molecular structure of the complex (**Figure A48, Appendix**). The

TOF- MS ES$^+$ spectrum of the complex reveals an *m/z* value of 557.03 which corresponds to the sodium adduct [M + Na]$^+$ of the complex (**Figure 3.18**).

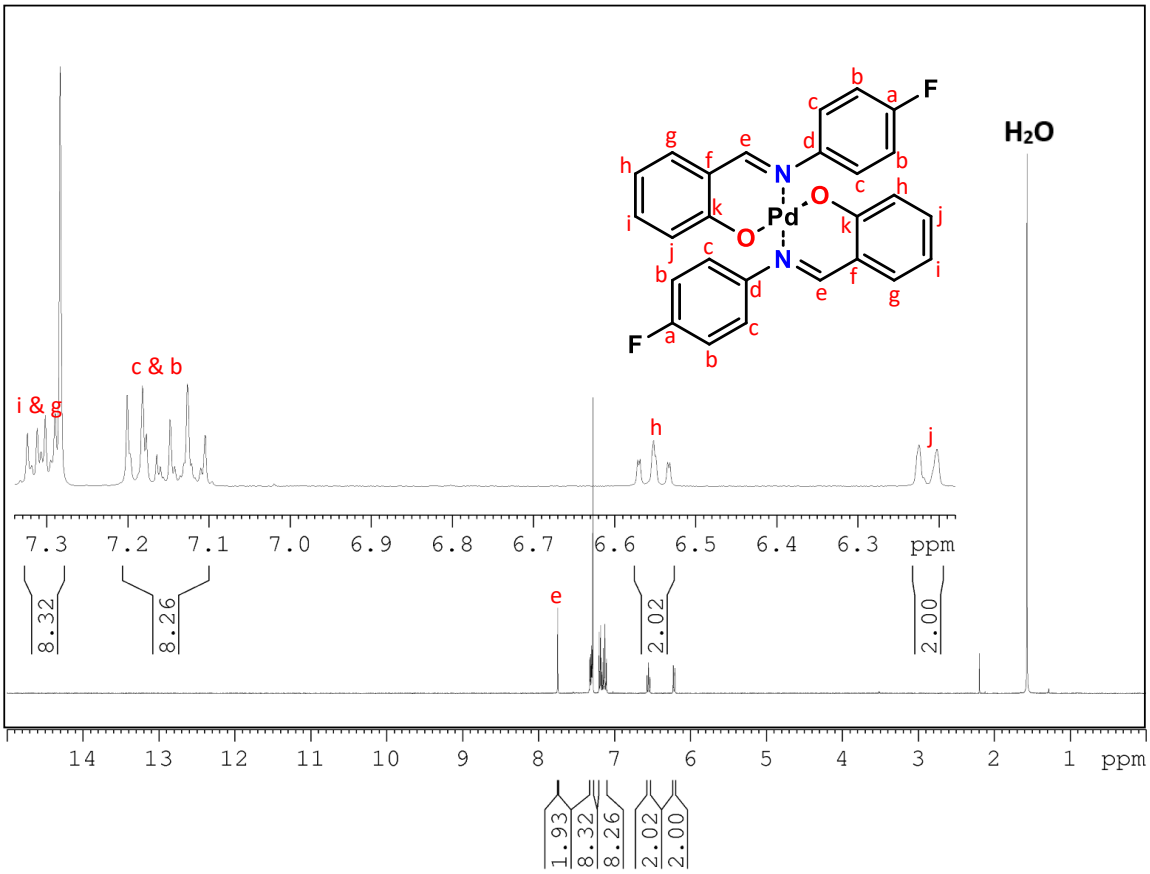

Figure 3.17: ^{1}H NMR spectrum of **PdC5**.

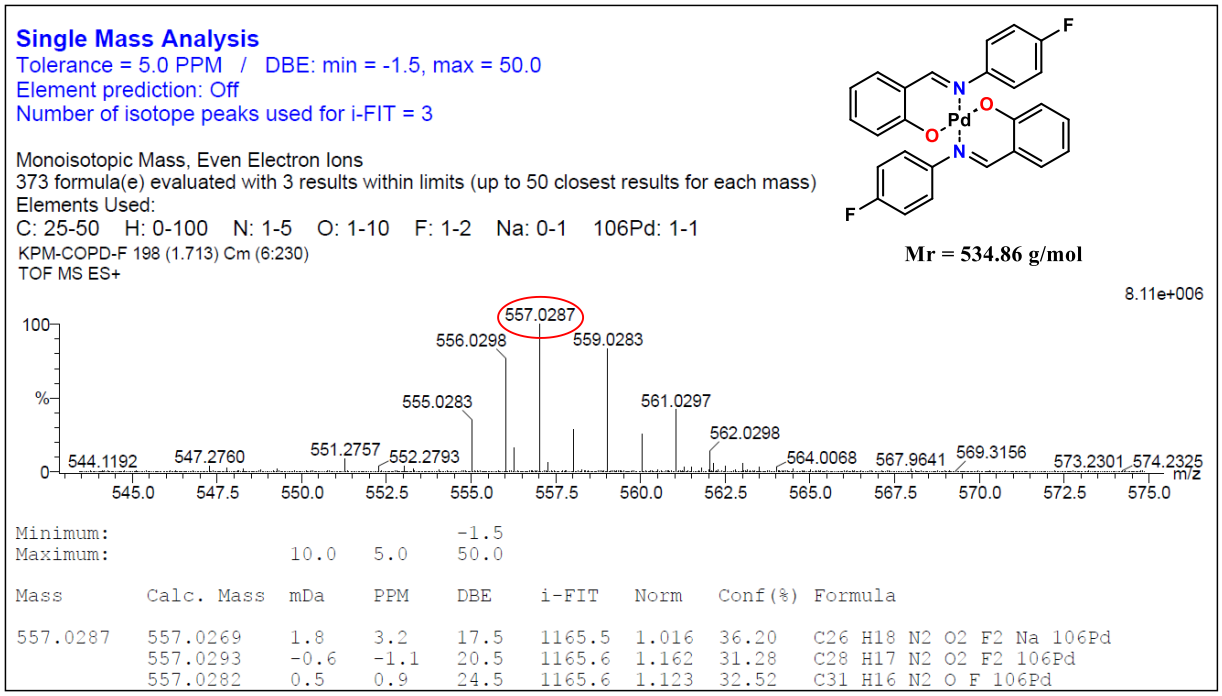

Figure 3.18: MS spectrum of **PdC5**.

Complex **PdC6** was fully characterised by ^{1}H and ^{13}C NMR, IR, and MS (**Figure A50 - A52**, **Appendix)**. The TOF- MS ESI^{+} spectrum (**Figure 3.19**) of the complex depicts an *m/z* value of 674.30 which corresponds to the hydrated adduct $[M+ H_2O]^{+}$ of the complex. All the other spectroscopic characterisations of the complex were analysed and corresponded to the predicted structure of the complex (**Figure A50 - A52**, **Appendix**).

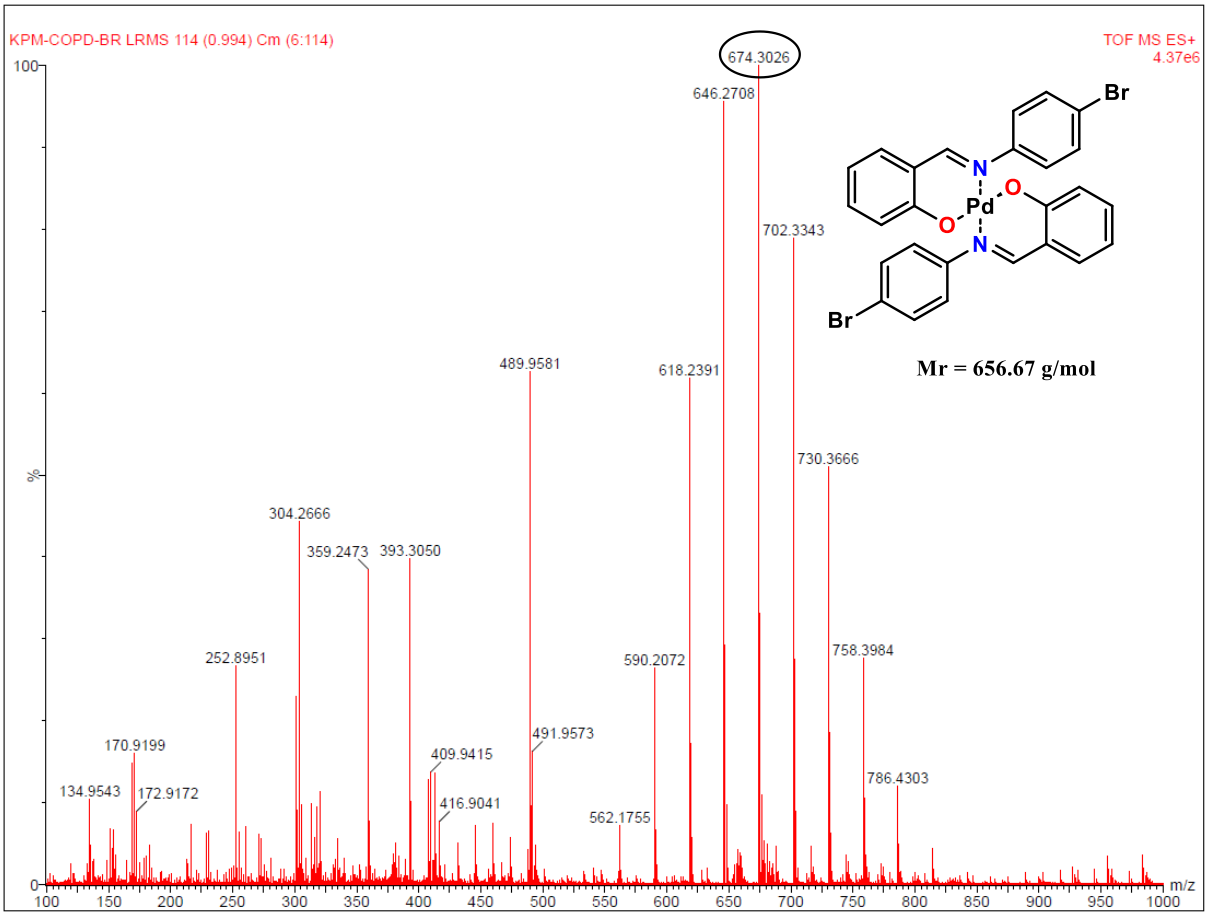

Figure 3.19: MS spectrum of **PdC6**.

On one hand, complex **PdC7** was synthesized, isolated and it was fully characterized using ^{1}H and ^{13}C NMR, IR, and MS techniques (**Figure A54 – A57**, **Appendix**). Analysis of the ^{1}H NMR spectrum (**Figure 3.20**) revealed a disappearance of the hydroxyl proton which confirmed the successful coordination of the Pd precursor and the ligand. All spectroscopic characterizations of the complex were examined and corresponded to the predicted structure of the complex (**Figure A54 – A57**, **Appendix**).

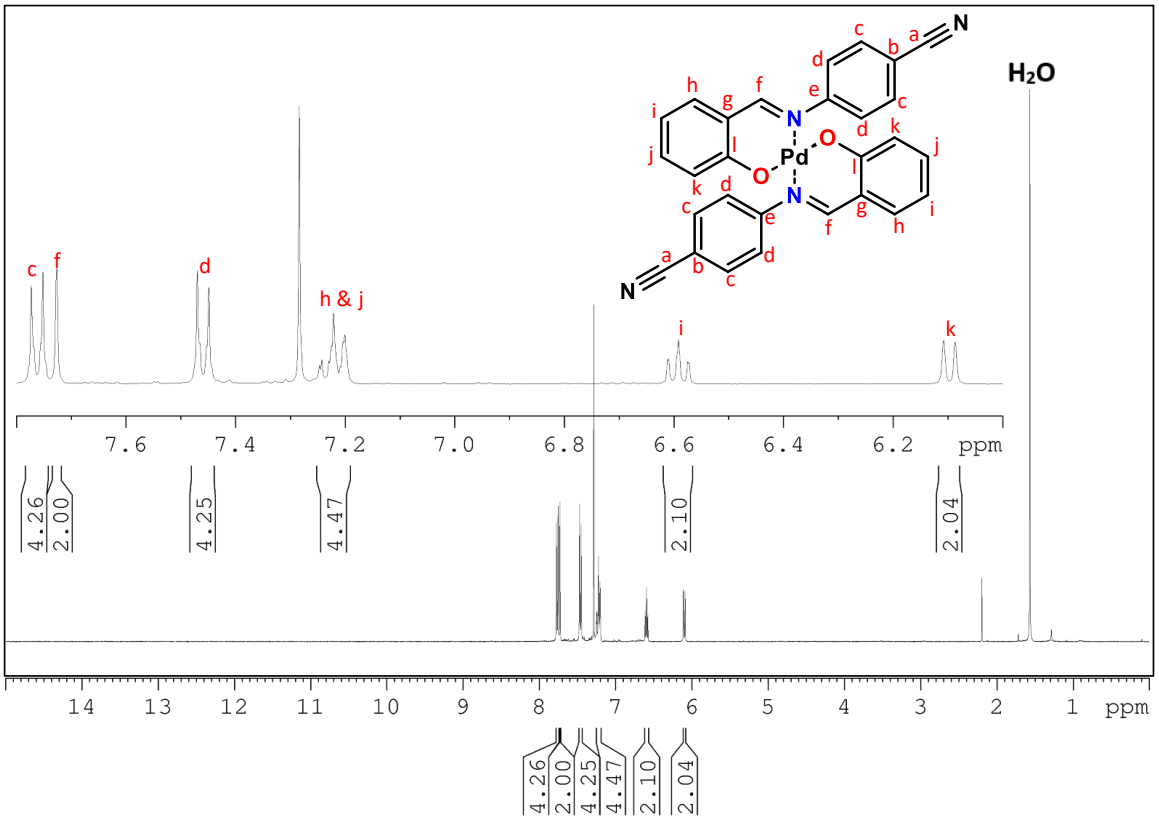

Figure 3.20: ^{1}H NMR spectrum of **PdC7**.

Using the reported procedures, we have successfully synthesised Schiff base ligands (**L1- L7**) and also successfully coordinated them to Pd (II) acetate to form the corresponding bidentate Pd (II) complexes (**PdC1 - PdC7**) in excellent yields (78% - 95%). Having successfully achieved the synthesis of both the ligands and the Pd (II) complexes, our next objective was to investigate the catalytic activities of the synthesised Pd (II) complexes in the Suzuki-Miyaura cross-coupling reaction to synthesise functionalised biaryl and biaryl ketones.

3.2. Application of the Pd (II) complexes in Suzuki-Miyaura cross-coupling reaction

Carbon-carbon bond-forming cross-coupling reactions are one of the most significant reactions in the realm of organic chemistry due to their ability to produce highly complex organic molecules from simple substrates which are in turn easily accessible or commercially available.[7]

The SM cross-coupling reaction has experienced significant growth since its discovery in 1975 and is widely recognized as one of the most extensively versatile methodologies for the construction of C−C bonds (**104**) using nucleophilic organoboron compounds such as boronic acids (**102**) and organic electrophiles (**103**) like aryl halides or pseudohalides. This reaction is catalysed by Pd complexes in the presence of a base (**Scheme 3.5**).[8]

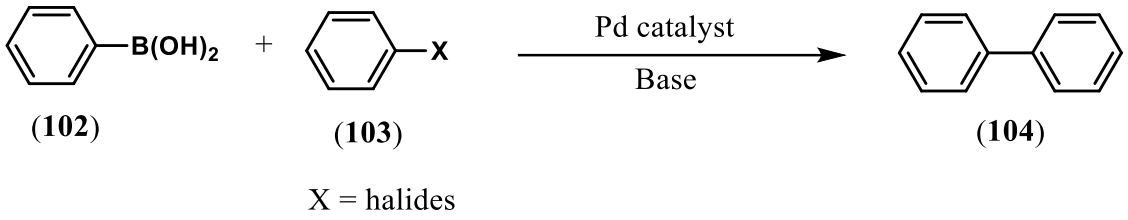

Scheme 3.5: General scheme for Pd catalysed SM cross-coupling reaction.

The SM cross-coupling reaction follows a well-defined catalytic cycle which mainly involves three steps namely: oxidative addition, transmetallation, and reductive elimination (**Scheme 3.6**).[9]

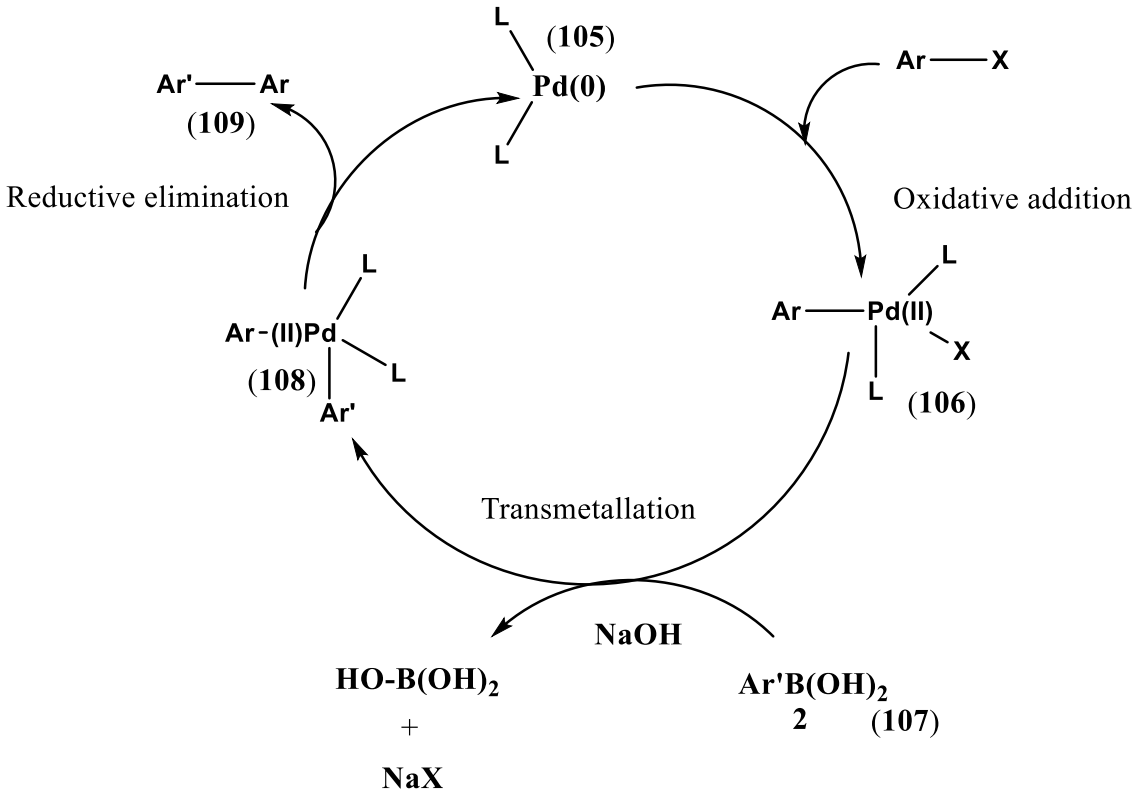

X = Halides (i.e. Br, Cl, I)
Ar = Ar' = Aryl

Scheme 3.6: General SM cross-coupling mechanism.

The first step in the catalytic cycle of SM cross-coupling reaction is oxidative addition. During this step, the palladium catalyst (**105**) is oxidised from Pd (0) to generate a Pd (II) intermediate (**106**). Under the participation of a base, the Pd (II) intermediate (**106**) undergoes transmetallation with the organoboron compound (**107**) to afford the bi-aryl Pd (II) intermediate (**108**). The final step is reductive elimination where the bi-aryl Pd (II) species proceed to eliminate the desired product (**109**) and regenerate the Pd (0) catalyst.

Aryl boronates, trifluoroborates, and boronic acids are among the most frequently utilised organoboron compounds in SM cross-coupling reactions, largely due to their commercial availability.[10,11] However, despite their widespread use as nucleophiles in SM cross-coupling reaction, they exhibit several drawbacks and limitations. The main drawback associated with aryl boronates is their inherent instability, often resulting in the formation of various side products.[12] These side reactions not only reduce the yield of the desired biaryl product but also complicate the purification process.[13]

On the other hand, a significant disadvantage of trifluoroborates arises from their high electronegativity.[14] Since trifluoroborates are fluorinated, they are unstable in the presence of bases, often resulting in the loss of their boronate substituent and subsequent decomposition. [15] In addition, they can exhibit poor solubility in some organic solvents, making it impractical to purify them using conventional column chromatographic methods.[16] Boronic acids are susceptible to hydrolysis, posing a significant obstacle in their use.[17] Additionally, they do not exist solely as monomeric compounds but also undergo equilibrium with dimers and cyclic trimers, such as boroxines.[18] These byproducts can be challenging to remove from the boronic acid starting materials, complicating the purification and isolation process as well as stoichiometric calculations.[19] Moreover, boronic acids are tri-coordinated organoboron compounds, hence they do not induce sufficient nucleophilicity to the organic moiety directly bonded to them.[20] As a result, the addition of a base, to form active four coordinates, is essential to facilitate the transmetallation step.[20]

Based on the limitations associated with the abovementioned organoboron compounds, there have been significant efforts directed towards the development of new nucleophiles that will efficiently facilitate SM cross-coupling reactions.

Interested in developing stable organoboron nucleophiles, Sithebe's research group has reported a facile SM cross-coupling procedure for the synthesis of biaryl ketones.[21] In their study, they found that using various sodium aryl boronate salts (**110**), as nucleophiles with different substituted aryl acyl chlorides (**111**) catalysed by Tetrakis(triphenylphosphine)palladium (0) (**112**), afforded biaryl ketones (**113**) in excellent yields (**Scheme 3.7**). The authors also found that the use of sodium aryl boronate salts displayed numerous advantages over boronic acids. These advantages include their ease in synthesis and isolation, high stability, capability to be coupled under base-free SM cross-coupling reaction conditions, and a high tolerance for a wide range of functionalities including base-sensitive substrates as they do not require a base to be activated for transmetallation.

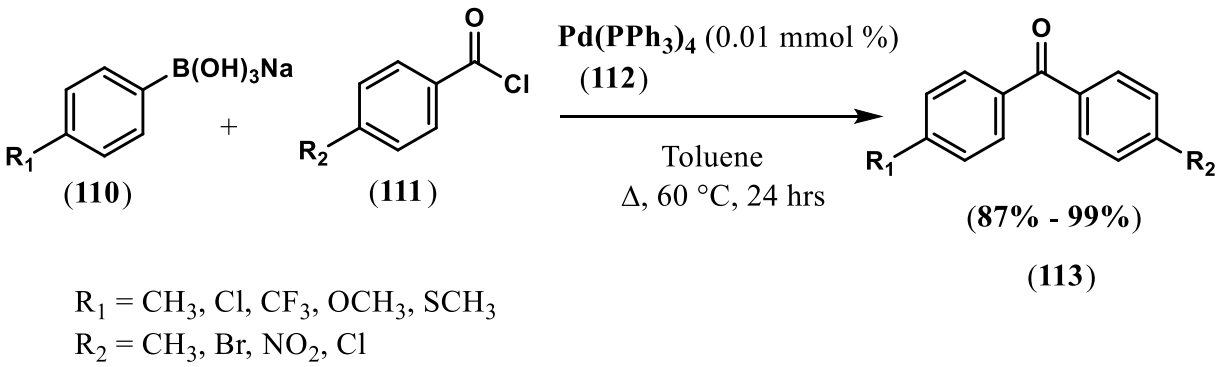

$R_1 = CH_3$, Cl, CF_3, OCH_3, SCH_3
$R_2 = CH_3$, Br, NO_2, Cl

Scheme 3.7: SM cross-coupling reaction for the synthesis of biaryl ketones.

Expanding on the previous work done in our research group working with sodium aryl boronates nucleophiles, this project is also aimed to extend the scope of sodium aryl boronates to the synthesis of biaryls as well as biaryl ketones using novel *N, O*-bindentate Pd (II) complexes as catalysts in SM cross-coupling reaction.

To begin our investigation, we synthesised sodium aryl borate salt (**115**) from commercially available starting material, boronic acid (**114**) using the procedure reported by Sithebe and Molefe[21] (**Scheme 3.8**). The salt was obtained as a pure white solid with a yield of 98%, and further purification was deemed unnecessary. Confirmation of the successful synthesis of the

salt was achieved through the utilisation of ^{1}H, ^{13}C, ^{11}B NMR, and MS, with the obtained data corresponding to the molecular structure of the compound (**Figure A58 - 61**, **Appendix**).

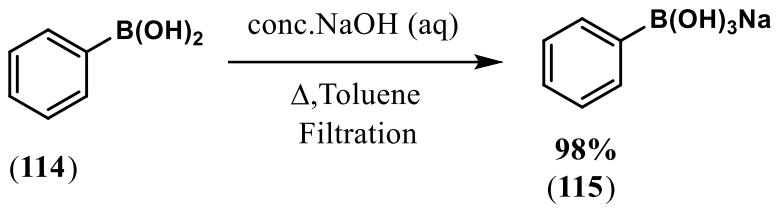

Scheme 3.8: Synthesis of sodium (trihydroxy)phenylborate salt **115**.

After the successful synthesis of the sodium aryl boronate salt, our next objective was to find suitable reaction conditions for the synthesis of biaryls *via* SM cross-coupling reaction. To achieve this, an optimisation study was conducted using equimolar amounts of the synthesised sodium (trihydroxy)phenylborate salt (**115**) and 4-bromotoluene (**116**) catalysed by one of our novel *N, O*-bindentate Pd (II) complexes (**PdC1**) under different reaction conditions and solvent combinations (**Scheme 3.9**). Throughout this step, we monitored and studied the impact of solvent, temperature, and catalyst loading in the SM model cross-coupling reaction (**Table 2**).

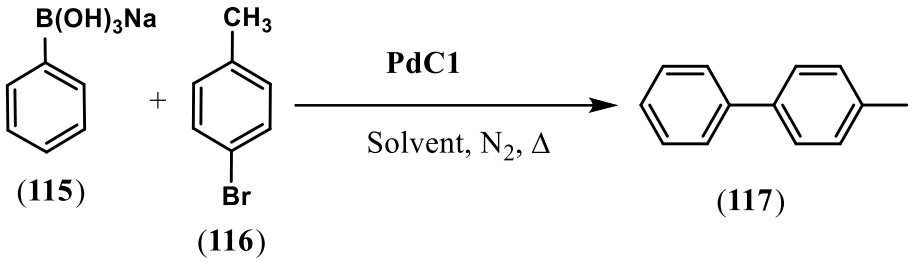

Scheme 3.9: Optimisation of SM cross-coupling reaction catalysed by **PdC1.**

Table 3.2: Optimisation of **PdC1** under various reaction conditions.

Entry	Solvents	Time (h)	Temperature (°C)	Catalyst loading (mol%)	Yield (%)
1	Acetone/H_2O	24	60	-	0
2	Acetone/H_2O	24	60	0.005	2
3	Ethylacetate/H_2O	24	60	0.5	3
4	Toluene/H_2O	24	60	0.5	1

5	DMF/H_2O	24	60	0.5	10
6	Toluene/H_2O	24	60	1	31
7	DCM/H_2O	24	40	2	4
8	**Ethanol/H_2O**	**24**	**60**	**2**	**47**
9	Methanol/H_2O	24	60	3	21
10	Acetone/H_2O	24	60	4	12
11	Acetone/H_2O	24	60	5	26
12	Acetone/H_2O	24	60	6	1

The bold text indicates the optimized reaction conditions for the developed biaryl procedure.

Reaction conditions: sodium (trihydroxy)phenylborate (1mmol), 4-bromotoluene (1mmol), Pd catalyst (2 mol%), water (3 drops), ethanol (3 ml), N_2, Reflux, 24 hrs. Isolated yields after column and radial chromatography (chromatotron).

Entry 1 in **Table 3.2** confirms that no product was obtained when the model reaction was conducted without a catalyst, highlighting the necessity of the catalyst in this cross-coupling reaction. The use of organic solvents such as ethyl acetate, acetone, toluene and DMF in combination with water did not seem to promote the cross-coupling reaction (**Table 3.2, entries 2-5).** However, doubling the catalytic loading from 0.5 mol % to 1 mol % improved the yield of the product (**Table 3.2, entry 6**). The combination of methanol and acetone with water produced yields of 21% and 26% of the desired products, respectively (**Table 3.2, entries 9 and 11**). The only highest yield was achieved in **entry 8** from the combination of ethanol and water which produced 47% of the desired product. Even though 47% is not regarded as a high yield, the fact that the reaction was working and the conversion approaches 50% was encouraging.

Having established the optimized reaction conditions (**Table 3.2**, **entry 8**), we investigated the effect of the substituents *(para*-electron-withdrawing and *para*-electron-donating) on the reactivity of all the synthesised catalysts. Therefore, **PdC2 – PdC7** were used to catalyse the reaction between sodium (trihydroxy)phenylborate salt (**115**) and 4-bromotoluene (**116**) using the established optimum reaction conditions resulting in the desired biaryls with poor yields ranging from 18% - 32% (**Scheme 3.10**).

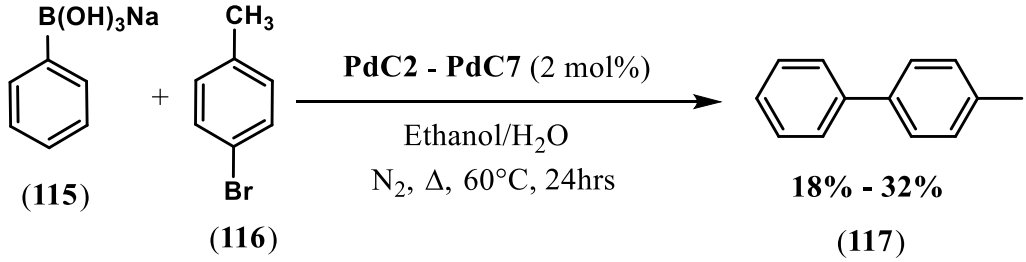

Scheme 3.10: SM cross-coupling reaction catalysed by **PdC2-PdC7** for the synthesis of biaryls.

Table 3.3: SM cross-coupling reaction catalysed by **PdC2-PdC7** under the optimized reaction conditions.

Entry	Catalyst	Solvents	Time (h)	Temperature (°C)	Catalyst loading (mol%)	Yield (%)
1	**PdC2**	Ethanol/H_2O	24	60	2	31
2	**PdC3**	Ethanol/H_2O	24	60	2	18
3	**PdC4**	Ethanol/H_2O	24	60	2	29
4	**PdC5**	Ethanol/H_2O	24	60	2	29
5	**PdC6**	Ethanol/H_2O	24	60	2	32
6	**PdC7**	Ethanol/H_2O	24	60	2	22

A comparative analysis of catalytic activity was conducted, examining complexes **PdC2**, **PdC3**, and **PdC4** to determine the effect of the *para* electron-donating substituents on the activity of the Pd catalysts. Comparing the results obtained for **PdC2**, **PdC3**, and **PdC4** (**entries 1 - 3, Table 3.3**), it's apparent that the **PdC2** complex exhibits higher activity than **PdC3** and **PdC4**. This observation is based on the 31% conversion of the biaryl product achieved by **PdC2**, which is 2% and 13% higher than those produced by **PdC4** and **PdC3**, respectively. This difference in activity is attributed to the nature of the substituents present on the complexes. The methyl substituent on **PdC2** is less electron-donating compared to the methoxy substituent on **PdC4**, which, in turn, is less electron-donating than the ethyl substituent on **PdC3**. This hierarchy in electron-donation renders **PdC2** more reactive, leading to its higher catalytic activity in the cross-coupling reaction.

The effect of the *para* electron-withdrawing substituents on the reactivity of **PdC5**, **PdC6**, and **PdC7** were also compared (**entries 4 - 6**, **Table 3.3**). It is observed that complex **PdC6** displayed a higher reactivity, yielding a desired product of 32% compared to **PdC5** and **PdC7** which exhibited a yield of 29% and 22%, respectively. These results can be explained by the fact that the bromine substituent on **PdC2** withdraws electrons less readily than the nitrile and fluorine substituents on **PdC5** and **PdC7**.

Despite exhibiting poor catalytic activities in the SM cross-coupling reaction, all the catalysts proved to be active since they successfully yielded the desired product. These catalytic activities may be attributed to the strong sigma donors from the Schiff base ligands, which enhanced the electron density at the metal center of the complexes, thereby facilitating the oxidative addition step. Increased electron densities at the metal center are recognized to facilitate the oxidative addition step.[22] Hence, both the steric and electronic characteristics of the Schiff base ligand systems contribute to stabilizing the active Pd (0) catalyst. The low product conversions may be attributed to the nature of the organo halide substrate used (**116**) which decreased the rate of the oxidative addition step due to the electron-donating substituent (methyl group) attached to the aromatic ring. It should also be noted that more investigation in order to increase the yields of the desired product is underway, especially the use of microwave radiation which is well known for decreasing activation energy barrier in SM cross coupling, thus enhancing the yields.

The structure of the biaryl product (**117**) was confirmed with ^{1}H and ^{13}C NMR spectroscopy as well as Gas Chromatography-Mass Spectrometry (GC-MS). The ^{1}H NMR spectrum of **117** exhibits a singlet peak at 2.42 ppm, assigned to the methyl proton (**Figure 3.21**). Doublet peaks are evident at 7.27 ppm and 7.52 ppm which are attributed to H_c and H_d signals, respectively. Additionally, a triplet peak is observed at 7.45 ppm, corresponding to the H_h signal. The H_i and H_g signals appear as multiplets within the range of 7.33 - 7.37 ppm and 7.60 - 7.62 ppm, respectively.

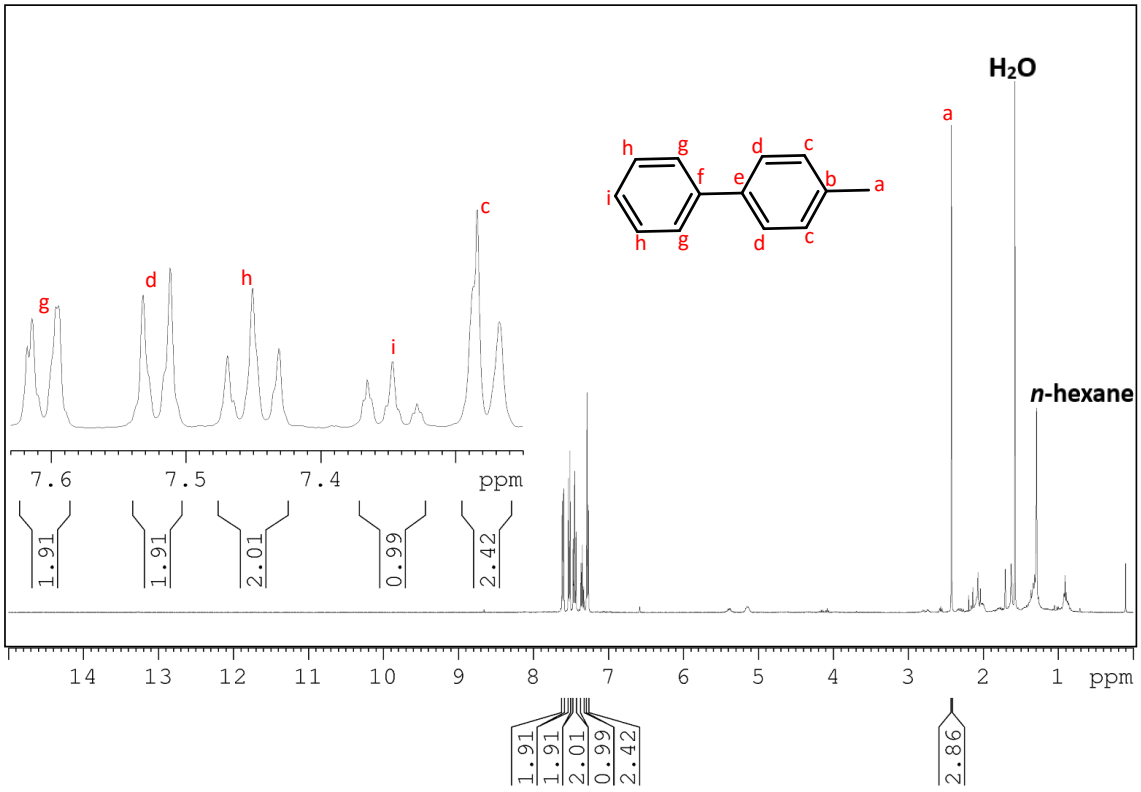

Figure 3.21: ^{1}H NMR spectrum of **117**.

The ^{13}C NMR spectrum of the biaryl displays a total of 8 carbon resonances, some of which overlap. Among these, a peak is observed at 29.70 ppm, assigned to the methyl carbon (**Figure A63**, **Appendix**). The GC-MS chromatogram reveals a single peak at a retention time of 12.939 minutes indicating that the analyte took 12.939 minutes to pass through the column and reach the mass spectrometer detector (**Figure 3.22**) The MS-spectrum (**Figure 3.22**) underneath the GC-MS chromatogram exhibited an exceptional similarity index (SI) of 95, affirming that the most likely compound that matches the expected compound from the GC-MS library is 1,1'biphenyl, 4-methyl which corresponds to the anticipated compound (**117**). In addition, the successful formation of the biaryl is further confirmed by the deprotonated peak $[M - H]^-$ of 167 displayed on the MS spectrum which corresponds to the molecular mass of the expected compound (**117**).

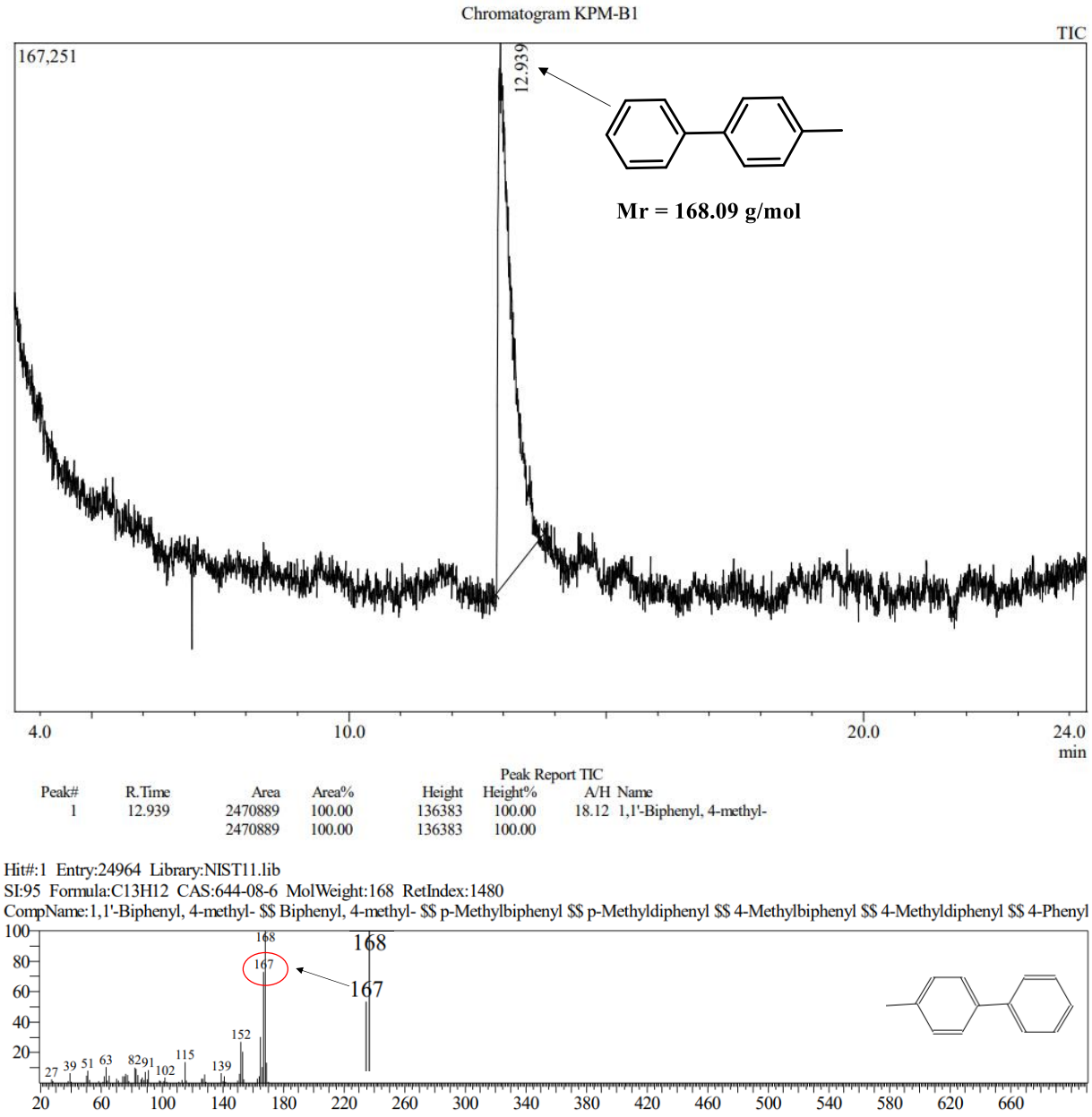

Figure 3.22: GC-MS chromatogram and MS spectrum of **117**.

As **PdC2** and **PdC6** exhibited superior catalytic activity in the formation of biaryls compared to the other catalysts, we broadened the scope of our study and evaluated their catalytic effectiveness in SM-acylation reactions to assess their potential suitability as catalysts for the synthesis of biaryl ketones using the optimised reaction conditions achieved for biaryls (**Table 3.2**, **entry 8**). The biaryl ketones (**119**) were synthesised using sodium (trihydroxy)phenylborate salt (**115**) and benzoyl chloride (**118**) (**Scheme 3.11**).

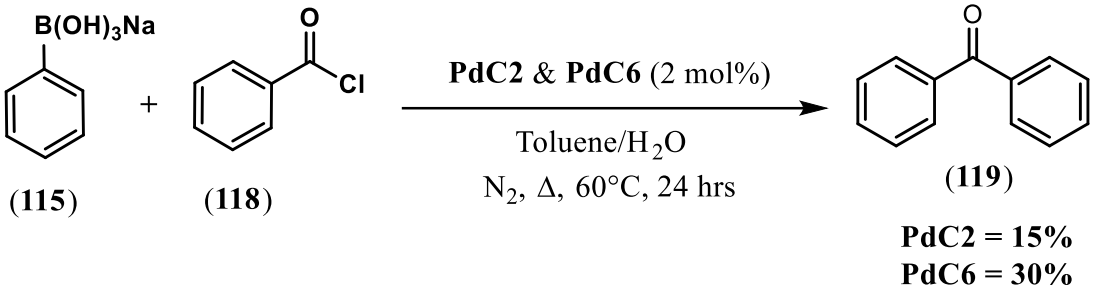

Scheme 3.11: SM-acylation reaction catalysed by **PdC2** and **PdC6** for the synthesis of biaryl ketones.

The yield achieved (15%) using **PdC2** suggests that the catalyst is less reactive for the synthesis of biaryl ketones compared the synthesis of biaryl. Conversely, the higher yield (30%) observed with **PdC6** is consistent for the synthesis of both biaryl and ketones.

To verify the successful synthesis of the biaryl ketone ^{1}H NMR, ^{13}C NMR spectroscopy and GC-MS techniques were used. The ^{1}H NMR spectrum of the compound shows two triplet peaks resonating around 7.51 ppm and 7.61 ppm assigned to the H_b and H_a protons, respectively. A doublet signal is also observed at 7.83 ppm which is assigned to the H_c signal (**Figure 3.23**).

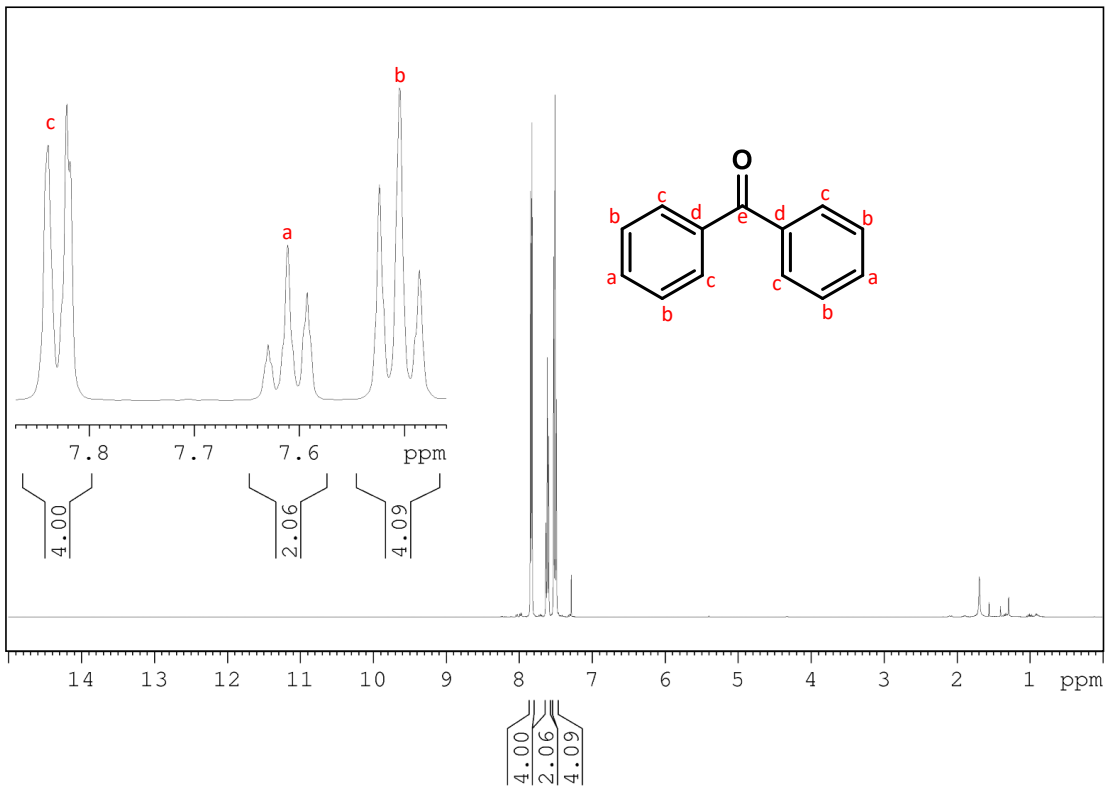

Figure 3.23: ^{1}H NMR spectrum of benzophenone **119**.

The ^{13}C NMR spectrum of **119** exhibits carbon signals corresponding to the total number of carbon atoms present in the compound (**Figure 3.24**). The carbonyl carbon of the ketone resonates at 196.74 ppm. The GC-MS data corresponds to the molecular mass and structure of the coupled desired product (**Figure A67**, **Appendix**).

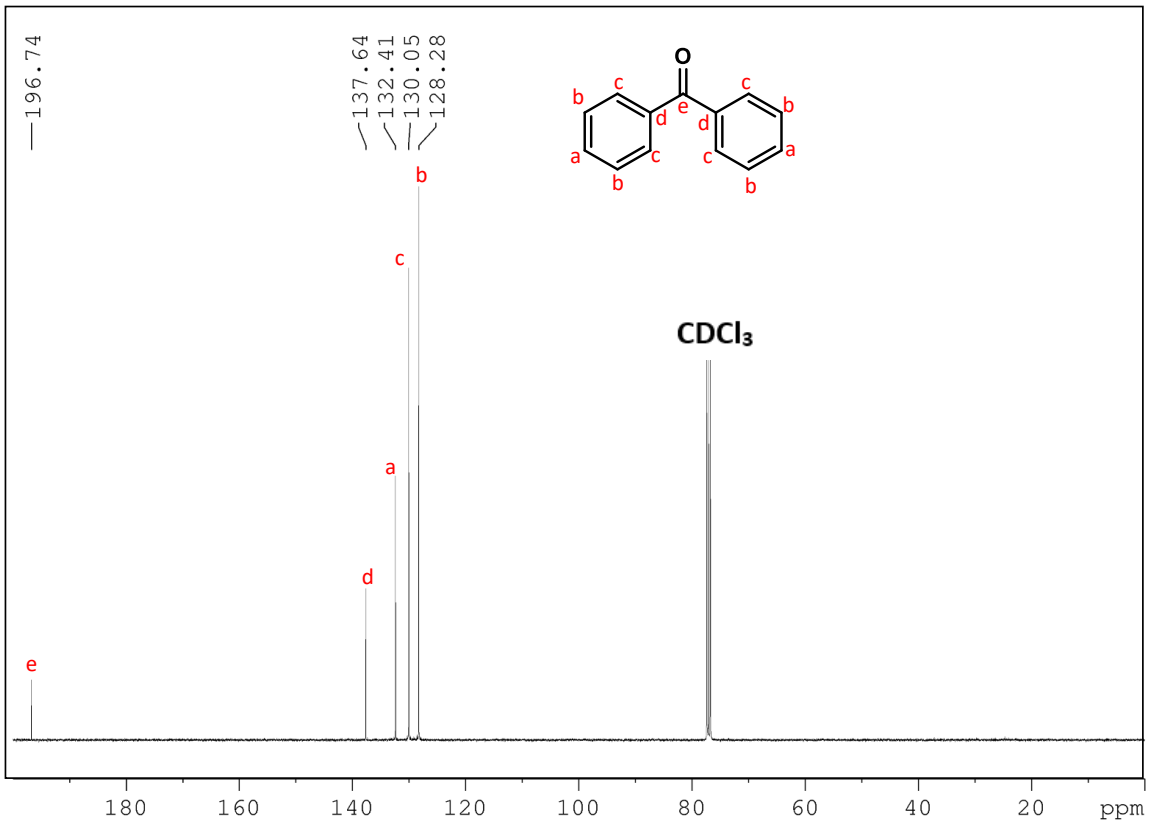

Figure 3.24: ^{13}C NMR spectrum of **119**.

3.3. Conclusion

In conclusion, we have successfully synthesised a series of *N, O*-Schiff base ligands (**L1**-**L7**) with excellent yields ranging from 80% - 94% and were fully characterised by NMR spectroscopy, FTIR spectroscopy and Mass spectrometry techniques. Reactions of the Schiff base ligands (**L1**- **L7**) with Palladium acetate afforded the corresponding *N, O*-bis Schiff base chelated Pd (II) complexes (**PdC1** - **PdC7**) in good yields (78% - 95%). The complexes were fully characterised by NMR spectroscopy, FTIR spectroscopy, Mass spectrometry, and single X-ray crystallography. However, a comprehensive X-ray report was only obtained for **PdC2** whereas only data was obtained for **PdC3 - PdC7** due to the difficulty in solving their crystallographic structures**.** The crystallographic analysis of **PdC2** revealed that **L2** is coordinated to the Pd metal center in a bidentate mode *via* the *N* donor of the imine bond and the *O* donor of the phenolic group. The complex displayed a distorted square planar geometry and crystallised in the monoclinic crystal system with a P21/c space group.

All the complexes exhibited poor catalytic activity in the SM cross-coupling reaction. However, comparative analysis revealed that the complexes bearing *para* electron-donating substituents with lower electron donating density are more active than those bearing *para* electron-donating substituents with high electron donating density. Conversely, complexes bearing *para* electron-withdrawing substituents with less electron-withdrawing density showed greater activity than those bearing *para* electron-withdrawing substituents with more electron-withdrawing density. As a result, the stereo-electronic effects greatly impacted the catalytic behaviour of the Pd (II) complexes.

Although these results are promising, further research is imperative to extend the scope of this study to investigate the catalytic activities of the synthesised catalysts (**PdC1** - **PdC7**) with different leaving groups (such as iodine and triflates) and nucleophiles bearing electron-donating and electron-withdrawing substituents thereby improving the yields of the desired coupled products.

This study highlights that the synthesised novel palladium complexes (**PdC1** - **PdC7**) are active as SM cross-coupling catalysts. A lot of improvement is, however, needed in order to increase the yields of the desired product. The use of microwave irradiation will be considered as well as the use of aryl iodides, with a good leaving iodine group, will also be investigated.

3.4. Future work

This study highlights the potential use of the synthesised *N, O*-bis Schiff base chelated Pd (II) complexes (**PdC1** - **PdC7**) as catalysts for Suzuki-Miyaura cross-coupling reactions. Therefore, to further explore their catalytic activity and expand the scope/applicability of the methodology, we intend to use various aryl halides and aryl sodium (trihydroxy)phenylborate salts for future work.

References

1. A.A. Alothman, E.S. Al-Farraj, W.A. Al-Onazi, Z.M. Almarhoon, and A.M. Al-Mohaimeed, *Arabian Journal of Chemistry*, 13(2), 3889-3902 (**2020**).
2. V.K. Juyal, A. Pathak, M. Panwar, S.C. Thakuri, O. Prakash, A. Agrwal, and V. Nand, *Journal of Organometallic Chemistry*, 999, 122825 (**2023**).
3. Z. D. Petrović, J. Đorović, D. Simijonović, V. P. Petrović and Z. Marković, *RSC Advances*, 5(31), 24094-24100 (**2015**).
4. S.O. Akiri, S.O. and Ojwach, *Journal of Organometallic Chemistry*, 942, 121812 (**2021**).
5. J. Name, A. Zianna, G.D. Geromichalos, A. Pekou, A.G. Hatzidimitriou, and G. Psomas, *Journal of Organometallic Chemistry*, 199, 110792 (**2019**).
6. A.P. McKay, W.K. Lo, D. Preston, G.I. Giles, J.D. Crowley, J.E. Barnsley, K.C. Gordon, and D.A. McMorran, *Inorganica Chimica Acta*, 446, 41-53 (**2016**).
7. K.C. Nicolaou, P.G. Bulger, D. Sarlah, Angew. Chem. Int. Ed., 44(29), 4442-4489 (**2005**).
8. Miyaura, K. Yamada, A. Suzuki, *Tetrahedron. Lett*, 20(36), 3437-3440 (**1979**).
9. C. Amatore, G. Le Duc, and A. Jutand, *Chemistry–A European Journal*, 19(31), 10082-10093 (**2013**).
10. S.R. Chemler, D. Trauner, and S.J. Danishefsky, *Angewandte Chemie International Edition*, 40(24), 4544-4568 (**2001**).
11. M. Blangetti, H. Rosso, C. Prandi, A. Deagostino, and P. Venturello, *Molecules*, 18(1), 1188-1213 (**2013**).
12. C. Len, S. Bruniaux, F. Delbecq, and V.S. Parmar, *Catalysts*, 7(5), 146 (**2017**).
13. S. Lai, N. Takaesu, W.X. Lin, and D.M. Perrin, 2021. *Tetrahedron Letters*, 74, 153147 (**2021**).
14. G.A. Molander, and B. Canturk, *Angewandte Chemie International Edition*, 48(49), 9240-9261 (**2009**).
15. S.D. Dreher, S.E. Lim, D.L. Sandrock, and G.A. Molander, *The Journal of organic chemistry*, 74(10), 3626-3631 (**2009**).
16. J. El-Maiss, T. Mohy El Dine, C.S. Lu, I. Karamé, A. Kanj, K. Polychronopoulou, and J. Shaya, *Catalysts*, 10(3), 296 (2020).
17. A.A Thomas, A.F. Zahrt, C.P. Delaney, and S.E. Denmark, *Journal of the American Chemical Society*, 140(12), 4401-4416 (**2018**).
18. Z.Z. Song, and H.N. Wong, *The Journal of Organic Chemistry*, 59(1), 33-41 (**1994**).
19. N.A. Bumagin, and D.N. Korolev, *Tetrahedron letters*, 40(15), 3057-3060 (**1999**).
20. A.J. Lennox, and G.C. Lloyd-Jones, *Chemical Society Reviews*, 43(1), 412-443 (**2014**).
21. S. Sithebe, and P. Molefe, *Journal of Organometallic Chemistry*, 846, 305-311 (**2017**).
22. E. Bratt, O. Verho, M.J. Johansson, and J.E. Backvall, *The Journal of Organic Chemistry*, 79(9), 3946-3954 (**2014**).

CHAPTER 4

4. Experimental

4.1 Materials and Instrumental Information

All commercially available reagents (amines, salicylaldehyde, magnesium sulfate anhydrous, sodium hydroxide, phenylboronic acid, and palladium acetate) were purchased from Merck and were used without further purification. All solvents were also purchased from Merck; hexane and methanol were distilled, and methanol was stored in molecular sieves before use.

^{1}H NMR and ^{13}C NMR as well as ^{11}B NMR spectra were recorded on a Bruker Avance III 400 spectrometer at frequencies of 400 MHz for ^{1}H NMR, 100 MHz for ^{13}C NMR, and 128 MHz for ^{11}B NMR. The measurements were conducted in deuterated solvents ($CDCl_3$, $(CD_3)_2CO$, and D_2O) at 25 °C. All chemical shifts in the spectra are reported in ppm (δ) and referenced to internal standard tetramethylsilane (TMS), except for the ^{11}B NMR, which was referenced to boron trifluoride etherate (BF_3•OEt_2). All proton and carbon chemical shifts are reported relative to their corresponding deuterated solvent signal. Proton resonances have been assigned in accordance with their integration and multiplicity pattern and the signals observed are described as s (singlet), d (doublet), t (triplet), q (quartet) and m (multiplets). All coupling constants (*J*) are reported in Hz.

The infrared spectra were recorded using a Bruker Alpha II infrared spectrometer instrument. ATR Diamond-1 Bounce was employed for data acquisition, with 31 background scans and 31 sampling scans conducted within the 4000 - 400 cm^{-1} range at a resolution of 4 cm^{-1}. The collected data was processed using Opus Spectroscopy Software to perform smoothing, baseline correction, and peak labelling.

Mass spectral analyses were conducted using Shimadzu LCMS-200, Waters Synapt Xs w Acquit LCT Premier TOF-MS and Shimadzu GC MS -QP2010 SE instruments. For GC MS data acquisition, the parameters included a Column Zebron ZB-5MSplus of dimensions 30m x 0.25mm (0.25 um), with a column temperature set at 40 °C, an injection temperature of 200 °C, and a split injection mode. X-ray data was captured using a Mo source on a Bruker APEX-

II CCD (Bruker Apex Duo) diffractometer, with the crystal kept/maintained at 100.03 K during data collection. All Melting points were determined using a Stuart SMP3 Melting Point Apparatus and are uncorrected.

4.2 Synthesis of Schiff-base ligands

4.2.1 Synthetic procedure of Schiff-bases (P1)

Schiff bases (**L1 - L7**) were prepared following the procedure in the literature with some modifications.[1] In our experiment, aldehyde (salicylaldehyde) (1 mmol), with corresponding aromatic amine (aniline, 4-methylaniline, 4-ethylaniline, 4-methoxy aniline, 4-fluoroaniline, 4-bromoaniline, 4-cyanoaniline) (1.2 mmol), and 20 mL of methanol were placed in a 1 neck 100 mL round-bottom flask equipped with a magnetic stirrer bar and reflux condenser. The contents were refluxed while stirred at 50 °C in an oil bath for 24 hours in the presence of a 300 mg dehydrating agent (Magnesium sulphate anhydrous) and monitored by TLC. After completion of the reaction, the solvent was *vacuum* evaporated, and the final product was obtained and further purified by recrystallisation in a slow diffusion process of hexane in DCM. Schiff bases were obtained in 80% - 94% yield. All Schiff bases (**L1 - L7**) were characterised with ^{1}H NMR and ^{13}C NMR, FTIR and MS.

4.2.1.1 Synthesis of *(E)-2-((phenylimino)methyl) phenol* (L1)

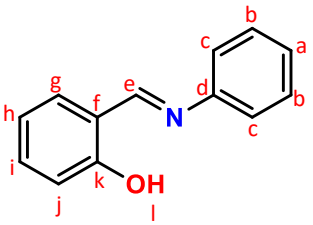

(E)-2-((phenylimino)methyl) phenol **(L1)**: Following procedure (**P1**), **L1** was synthesised by reacting 1 mmol (0.11 ml) of salicylaldehyde and 1.2 mmol (0.11 ml) of aniline and was obtained as orange crystals (182.4 mg, 92%, ; mp: 49.6 - 51.7 °C): ^{1}H (400 MHz, $CDCl_3$) δppm: 6.98 (t, 1H, J = 7.53 Hz, -**H$_a$**-), 7.08 (d, 1H, J = 8.26 Hz, -**H$_j$**-), 7.29 - 7.34 (m, 3H, -**H$_{h,\ \&\ c}$**-), 7.40 - 7.48 (m, 4H, -**H$_{b,\ g\ \&\ i}$**-) 8.66 (s, 1H, -**H$_e$**-), 13.25 (s, 1H, -**H$_l$**-). ^{13}C (100 MHz, $CDCl_3$)

δppm: 117.29 (-**C**$_{j}$-), 119.09 (-**C**$_{f}$-), 119.26 (-**C**$_{h}$-), 121.20 (-**C**$_{c}$-), 126.92 (-**C**$_{a}$-), 129.43 (-**C**$_{b}$-), 132.31 (-**C**$_{g}$-), 133.17 (-**C**$_{i}$-), 148.55 (-**C**$_{d}$-), 161.19 (-**C**$_{e}$-), 162.70 (-**C**$_{k}$-). FTIR (Liquid neat) cm^{-1}: 3433.03 (ν_{O-H}), 1656.74 ($\nu_{HC=N}$), 1420.57 ($\nu_{C=C}$), 1312.34 (ν_{C-N}), 1027.81 (ν_{C-O}). ESI^{+}-MS $[M + H]^{+}$, *m/z* = 198 (calculated *m/z* = 197.24).

4.2.1.2 Synthesis of *(E)-2-((4-tolylimino)methyl) phenol* (L2)

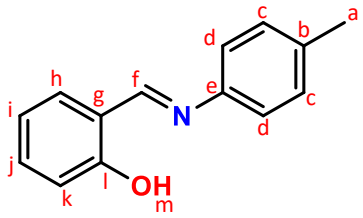

***(E)-2-((4-tolylimino)methyl) phenol* (L2)**: Following procedure (**P1**), **L2** was synthesized by reacting 1 mmol (0.11 ml) of salicylaldehyde and 1.2 mmol (223.36 mg) of 4-methylamine and was obtained as yellow crystals (183.5 mg, 87% ; mp: 97.4 - 99.1 °C): ^{1}H NMR (400 MHz, $CDCl_3$) δppm: 2.41 (s, 3H, -**H**$_{a}$-), 6.96 (t, 1H, *J* = 7.48 Hz, -**H**$_{i}$-), 7.05 (d, 1H, *J* = 8.20 Hz, -**H**$_{k}$-), 7.21 - 7.28 (m, 4H, -**H**$_{d, j \& h}$-), 7.37 - 7.42 (m, 2H, -**H**$_{c}$-), 8.65 (s, 1H, -**H**$_{f}$-), 13.39 (s, 1H, -**H**$_{m}$-). ^{13}C NMR (100 MHz, CD_3COCD_3) δppm: 21.05 (-**C**$_{a}$-), 117.22 (-**C**$_{k}$-), 119.00 (-**C**$_{g}$-), 119.33 (-**C**$_{i}$-), 121.01 (-**C**$_{d}$-), 130.02 (-**C**$_{c}$-), 132.12 (-**C**$_{h}$-), 132.91 (-**C**$_{j}$-), 136.91 (-**C**$_{b}$-), 145.92 (-**C**$_{e}$-), 161.15 (-**C**$_{f}$-), 161.71 (-**C**$_{l}$-). FTIR (Liquid neat) cm^{-1}: 3438.31 (ν_{O-H}), 1655.22 ($\nu_{HC=N}$), 1420.45 ($\nu_{C=C}$), 1311.67 (ν_{C-N}), 1030.85 (ν_{C-O}). TOF-MS ES^{-} $[M - H]^{-}$, *m/z* = 210.09 (calculated *m/z* = 211.26).

4.2.1.3 Synthesis of *(E)-2-(((4-ethylphenyl)imino)methyl) phenol* (L3)

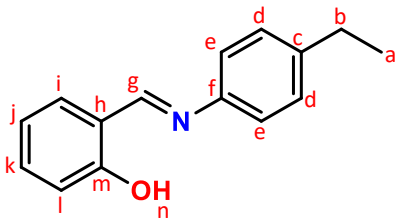

(E)-2-((((4-ethylphenyl)imino)methyl) phenol **(L3)**: Following procedure (**P1**), **L3** was synthesized by reacting 1 mmol (0.11 ml) of salicylaldehyde and 1.2 mmol (1.15 ml) of 4-ethylamine and was obtained as orange crystals (212.7 mg, 94%; mp: 56.8 - 57.3 °C): ^{1}H NMR (400 MHz, $CDCl_3$) δppm: 1.31 (t, 3H, *J* = 7.64 Hz, -**H$_a$**-), 2.72 (q, 2H, *J* = 7.61 Hz, -**H$_b$**-), 6.97 (t, 1H, *J* = 7.46 Hz, -**H$_j$**-), 7.07 (d, 1H, *J* = 8.14 Hz, -**H$_l$**-), 7.25 - 7.30 (m, 4H, -**H$_{e, k\&\ i}$**-), 7.38 - 7.43 (m, 2H, -**H$_d$**-), 8.66 (s, 1H, -**H$_g$**-), 13.38 (s, 1H, -**H$_n$**-). ^{13}C NMR (100 MHz, $CDCl_3$) δppm: 15.62 (-**C$_a$**-), 28.49 (-**C$_b$**-), 117.24 (-**C$_l$**-), 119.00 (-**C$_h$**-), 119.35 (-**C$_j$**-), 121.10 (-**C$_e$**-), 128.84 (-**C$_d$**-), 132.14 (-**C$_i$**-), 132.92 (-**C$_k$**-), 143.33 (-**C$_c$**-), 146.13 (-**C$_f$**-), 161.17 (-**C$_g$**-), 161.78 (-**C$_m$**-). FTIR (Liquid neat) cm^{-1}: 3438.66 (ν $_{O-H}$), 1656.04 (ν $_{HC=N}$), 1420.52 (ν $_{C=C}$), 1311.27 (ν $_{C-N}$), 1031.36 (ν $_{C-O}$). ESI$^+$- MS $[M+H]^+$, *m/z* = 226 (calculated *m/z* = 225.29).

4.2.1.4 Synthesis of *(E)-2-((((4-methoxyphenyl)imino)methyl) phenol* (L4)

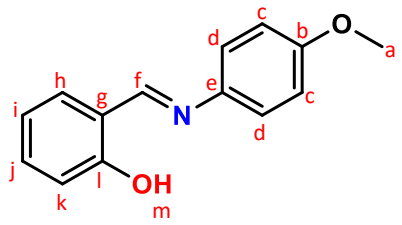

(E)-2-((((4-methoxyphenyl) imino)methyl) phenol **(L4)**: Following procedure (**P1**), **L4** was synthesized by reacting 1 mmol (0.11 ml) of salicylaldehyde and 1.2 mmol (272.71 mg) of 4-methoxyamine. **L4** was obtained as pale yellow crystals (181.3 mg, 80%; mp: 89.4 - 90.7 °C): ^{1}H NMR (400 MHz, $CDCl_3$) δppm: 3.87 (s, 3H, -**H$_a$**-), 6.94 - 7.01 (m, 3H, -**H$_{c\ \&\ i}$**-), 7.05 (d, 1H, *J* = 8.07 Hz, -**H$_k$**-), 7.29 - 7.32 (m, 2H, -**H$_d$**-), 7.36 - 7.41 (m, 2H, -**H$_{h\ \&\ j}$**-), 8.64 (s, 1H, -**H$_f$**-), 13.42 (s, 1H, -**H$_m$**-). ^{13}C NMR (100 MHz, $CDCl_3$) δppm: 55.53 (-**C$_a$**-), 114.65 (-**C$_c$**-), 117.16 (-**C$_k$**-), 118.99 (-**C$_g$**-), 119.43 (-**C$_i$**-), 122.31 (-**C$_d$**-), 132.00 (-**C$_h$**-), 132.68 (-**C$_j$**-), 141.38 (-**C$_e$**-), 158.89 (-**C$_b$**-), 160.43 (-**C$_f$**-), 161.04 (-**C$_l$**-). FTIR (Liquid neat) cm^{-1}: 3425.13 (ν $_{O-H}$), 1655.61 (ν $_{HC=N}$), 1420.00 (ν $_{C=C}$), 1310.80 (ν $_{C-N}$), 1024.91 (ν $_{C-O}$). ESI$^+$- MS $[M+H]^+$, *m/z* = 228 (calculated *m/z* = 227.26).

4.2.1.5 Synthesis of *(E)-2-(((4-fluorophenyl)imino)methyl) phenol* (L5)

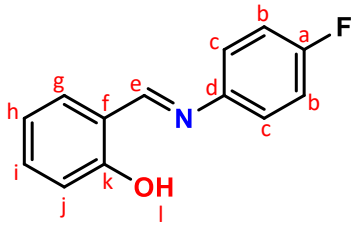

***(E)-2-(((4-fluorophenyl)imino)methyl) phenol* (L5)**: Following procedure (**P1**), **L5** was synthesized by reacting 1 mmol (0.11 ml) of salicylaldehyde and 1.2 mmol (0.11 ml) of 4-fluoroaniline. **L5** was obtained as yellow crystals (180.6 mg, 84%; mp: 85.4 - 86.7 °C): ^{1}H NMR (400 MHz, $CDCl_3$) δppm: 6.98 (t, 1H, J = 7.56 Hz, -**H$_h$**-), 7.06 (d, 1H, J = 8.66 Hz, -**H$_j$**-), 7.11 - 7.17 (m, 2H, -**H$_c$**-), 7.27 - 7.32 (m, 2H, -**H$_b$**-), 7.39 - 7.44 (m, 2H, -**H$_{g\ \&\ i}$**-), 8.62 (s, 1H, -**H$_e$**-), 13.12 (s, 1H, -**H$_l$**-). ^{13}C NMR (100 MHz, $CDCl_3$) δppm: 116.12 (-**C$_b$**-), 116.30 (-**C$_j$**-), 117.29 (-**C$_f$**-), 119.15 (-**C$_h$**-), 122.57 (-**C$_c$**-), 132.29 (-**C$_g$**-), 133.22 (-**C$_i$**-), 144.69 (-**C$_d$**-), 160.69 (-**C$_e$**-), 161.07 (-**C$_k$**-), 162.45 (-**C$_a$**-). FTIR (Liquid neat) cm^{-1}: 3439.92 (ν $_{O-H}$), 1654.78 (ν $_{HC=N}$), 1420.59 (ν $_{C=C}$), 1311.08 (ν $_{C-N}$), 1031.73 (ν $_{C-O}$). ESI^{+}- MS $[M + H]^{+}$, *m/z* = 216 (calculated *m/z* = 215.23).

4.2.1.6 Synthesis of *(E)-2-(((4-bromophenyl)imino)methyl) phenol* (L6)

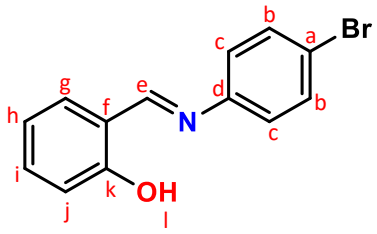

***(E)-2-(((4-bromophenyl)imino)methyl) phenol* (L6)**: Following procedure (**P1**), **L6** was synthesized by reacting 1 mmol (0.11 ml) of salicylaldehyde and 1.2 mmol (206.42 mg) of 4-bromoaniline. **L6** was obtained as orange crystals (223.8 mg, 82%; mp: 101.8 - 102.4 °C): ^{1}H NMR (400 MHz, $CDCl_3$) δppm: 6.98 (t, 1H, J = 7.51 Hz, -**H$_h$**-), 7.06 (d, 1H, J = 8.64 Hz, -**H$_j$**-

), 7.17 - 7.21 (m, 2H, -**H$_{c}$**-), 7.40 - 7.45 (m, 2H, -**H$_{g\ \&\ i}$**-), 7.55 - 7.59 (m, 2H, -**H$_{b}$**-), 8.63 (s, 1H, -**H$_{e}$**-), 13.01 (s, 1H, -**H$_{l}$**-). ^{13}C NMR (100 MHz, $CDCl_3$) δppm: 117.35 (-**C$_{j}$**-), 119.07 (-**C$_{h}$**-), 119.24 (-**C$_{f}$**-), 120.40 (-**C$_{a}$**-), 122.84 (-**C$_{c}$**-), 132.44 (-**C$_{g}$**-), 132.52 (-**C$_{i}$**-), 133.50 (-**C$_{b}$**-), 147.56 (-**C$_{d}$**-), 161.15 (-**C$_{e}$**-), 163.05 (-**C$_{k}$**-). FTIR (Liquid neat) cm^{-1}: 3422.91 (ν $_{O-H}$), 1651.54 (ν $_{HC=N}$), 1419.97 (ν $_{C=C}$), 1313.99 (ν $_{C-N}$), 1023.84 (ν $_{C-O}$), 690.70 (ν $_{C-Br}$), ESI^{+}- MS [M + Br isotopes (^{79}Br & ^{81}Br)]$^{+}$, *m/z* = 276 & 278 (calculated *m/z* = 276.13).

4.2.1.7 Synthesis of *(E)-4-((2-hydroxybenzylidene)amino) benzonitrile* (L7)

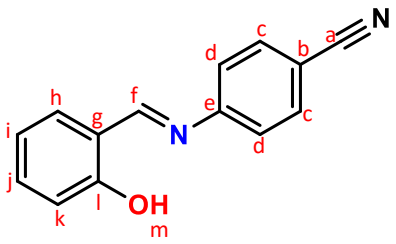

(E)-4-((2-hydroxybenzylidene)amino) benzonitrile **(L7)**: Following procedure (**P1**), **L7** was synthesized by reacting 1 mmol (0.11 ml) of Salicylaldehyde and 1.2 mmol (141.77 mg) of 4-cyanoamine and obtained as orange crystals (177.3 mg, 80%; mp: 124.8 - 125.4 °C): ^{1}H NMR (400MHz, CD_3COCD_3) δppm: 6.99 - 7.06 (m, 2H, -**H$_{i\ \&\ k}$**-), 7.50 (t, 1H, *J* = 7.65 Hz, -**H$_{j}$**-), 7.58 - 7.67 (m, 3H, -**H$_{h\ \&\ d}$**-),7.89 (d, 2H, *J* = 8.50 Hz, -**H$_{c}$**-), 8.97 (s, 1H, -**H$_{f}$**-), 12.69 (s, 1H, -**H$_{m}$**-). ^{13}C NMR (100 MHz, CD_3COCD_3) δppm: 109.99 (-**C$_{b}$**-), 116.95 (-**C$_{k}$**-), 118.34 (-**C$_{a}$**-), 119.17 (-**C$_{g}$**-), 119.29 (-**C$_{i}$**-), 122.46 (-**C$_{d}$**-), 133.43 (-**C$_{h}$**-), 133.57 (-**C$_{j}$**-), 134.08 (-**C$_{c}$**-), 152.54 (-**C$_{e}$**-), 161.32 (-**C$_{f}$**-), 166.38 (-**C$_{l}$**-). FTIR (Liquid neat) cm^{-1}: 3437.83 (ν $_{O-H}$), 1655.83 (ν $_{HC=N}$), 1420.37 (ν $_{C=C}$), 1311.66 (ν $_{C-N}$), 1030.18 (ν $_{C-O}$). TOF-MS ES [M - H]$^{-}$, *m/z* = 221.07 (calculated *m/z* = 222.25).

4.3 Synthesis of *N, O*-bis Schiff base chelated Pd (II) complexes

4.3.1 Synthetic procedure of Pd (II) complexes (P2)

N, O-bis Schiff base chelated Pd (II) complexes (**PdC1 - PdC7**) were synthesised following a modified procedure in the literature.[2] In our experiment, palladium acetate (Pd $(OAc)_2$) (0.25 mmol) was dissolved in 10 ml dry methanol. In another separate vial, 0.5 mmol of the corresponding Schiff base ligand (**L1 - L7**) was dissolved in 5 ml dry methanol. To the methanolic solution of (Pd $(OAc)_2$) was added the methanolic solution of the corresponding ligand. The resulting mixture was stirred under a nitrogen atmosphere for 24 hours. Afterward, the mixture was *vacuum* filtered and recrystallised using small amounts of hexane and chloroform by a slow diffusion process. The Pd (II) complexes were obtained in a 78%–95% yield. All the Pd (II) complexes (**PdC1 - PC7**) were characterised using ^{1}H NMR and ^{13}C NMR, FTIR, MS and. Single X-ray crystallography was also used to characterise **PdC2**.

4.3.1.1 Synthesis of *Bis ((E)-2-((phenylimino)methyl) phenol) Palladium (II)* (PdC1)

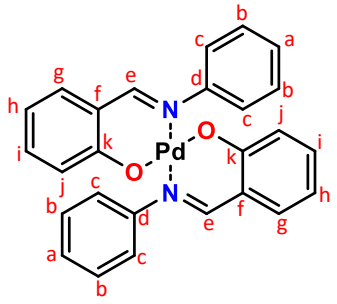

Bis ((E)-2-((phenylimino)methyl) phenol) Palladium (II) **(PdC1)**: Following procedure (**P2**), **PdC1** was synthesized by reacting 0.5 mmol (98.62 mg) of **L1** and 0.25 mmol (56.13 mg) of palladium acetate (Pd $(OAc)_2$). **PdC1** was obtained as orange crystals (109.9 mg, 88%; mp: 287.6 - 288.4°C (> 290°C = Decomposition)): ^{1}H (400 MHz, $CDCl_3$) δppm: 6.15 (d, 2H, J = 8.50 Hz, -**H$_j$**-), 6.54 (t, 2H, J = 7.36 Hz, -**H$_a$**-), 7.13 - 7.20 (m, 4H, -**H$_{h\ \&\ i}$**-), 7.34 - 7.47 (m, 10H, -**H$_{b,\ c\ \&\ g}$**-), 7.76 (s, 2H, -**H$_e$**-). ^{13}C (100 MHz, $CDCl_3$) δppm: 115.16 (-**C$_j$**-), 120.19 (-**C$_f$**-), 120.72 (-**C$_h$**-), 124.62 (-**C$_c$**-), 126.42 (-**C$_a$**-), 128.16 (-**C$_b$**-), 134.46 (-**C$_g$**-), 135.18 (-**C$_i$**-), 149.51 (-**C$_d$**-), 162.76 (-**C$_k$**-), 165.13 (-**C$_e$**-). FTIR (Liquid neat) cm^{-1}: 3443.52 (ν_{O-H}), 1658.63 ($\nu_{HC=N}$),

1421.66 (ν $_{C=C}$), 1311.96 (ν $_{C-N}$), 1031.81 (ν $_{C-O}$). ESI^{+}- MS $[M + H]^{+}$, *m/z* = 499 (calculated *m/z* = 498.88).

4.3.1.2 Synthesis of *Bis ((E)-2-((4-tolylimino) methyl) phenol) Palladium (II)* (PdC2)

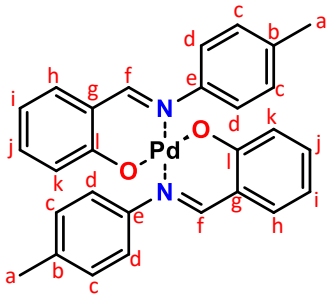

Bis ((E)-2-((4-tolylimino) methyl) phenol) Palladium (II) **(PdC2)**: Following procedure (**P2**), **PdC2** was synthesized by reacting 0.5 mmol (105.63 mg) of **L2** and 0.25 mmol (56.13 mg) of palladium acetate (Pd $(OAc)_2$). **PdC2** was obtained as orange crystals (125.4 mg, 95%; mp: 256.3 - 257.9°C (> 260°C = Decomposition)): ^{1}H NMR (400 MHz, $CDCl_3$) δppm: 2.45 (s, 6H, -**H$_a$**-), 6.19 (d, 2H, *J* = 8.52 Hz, -**H$_K$**-), 6.53 (t, 2H, *J* = 7.36 Hz, -**H$_I$**-), 7.13 - 7.18 (m, 4H, -**H$_{h\ \&\ j}$**-), 7.24 (m, 8H, -**H$_{c\ \&\ d}$**-), 7.73 (s, 2H, -**H$_f$**-). ^{13}C NMR (100 MHz, $CDCl_3$) δppm: 21.13 (-**C$_a$**-), 115.03 (-**C$_k$**-), 120.32 (-**C$_g$**-), 120.68 (-**C$_i$**-), 124.39 (-**C$_d$**-), 128.63 (-**C$_c$**-), 134.40 (-**C$_h$**-), 135.02 (-**C$_j$**-), 136.09 (-**C$_b$**-), 147.07 (-**C$_e$**-), 162.67 (-**C$_l$**-), 165.18 (-**C$_f$**-). FTIR (Liquid neat) cm^{-1}: 3442.76 (ν $_{O-H}$), 1658.08 (ν $_{HC=N}$), 1421.27 (ν $_{C=C}$), 1311.47 (ν $_{C-N}$), 1031.33 (ν $_{C-O}$). TOF-MS ES^{+} $[M + H]^{+}$, *m/z* = 527.10 (calculated *m/z* = 526.93).

4.3.1.3 Synthesis of *Bis ((E)-2-(((4-ethylphenyl)imino)methyl) phenol) Palladium (II)* (PdC3)

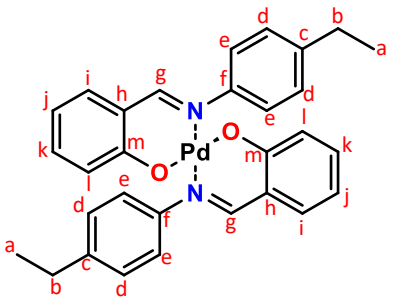

Bis ((E)-2-(((4-ethylphenyl)imino)methyl) phenol) Palladium (II) **(PdC3)**: Following procedure (**P2**), **PdC3** was synthesized by reacting 0.5 mmol (112.62 mg) of **L3** and 0.25 mmol (56.13 mg) of palladium acetate (Pd $(OAc)_2$). **PdC3** was obtained as orange crystals (128.8 mg, 98%; mp: 285.6 – 286.8°C. (> 290°C = Decomposition)): ^{1}H NMR (400 MHz, $CDCl_3$) δppm: 1.34 (t, 6H, J = 7.60 Hz, -**H$_a$**-), 2.76 (q, 4H, J = 7.60 Hz, -**H$_b$**-), 6.17 (d, 2H, J = 8.58 Hz, -**H$_l$**-), 6.53 (t, 2H, J = 7.33 Hz, -**H$_j$**-),7.12 - 7.19 (m, 4H, -**H$_{i\ \&\ k}$**-), 7.27 (m, 8H, -**H$_{d\ \&\ e}$**-), 7.75 (s, 2H, -**H$_g$**-). ^{13}C NMR (100 MHz, $CDCl_3$) δppm: 15.89 (-**C$_a$**-), 28.59 (-**C$_b$**-), 115.04 (-**C$_l$**-), 120.33 (-**C$_h$**-), 120.62 (-**C$_j$**-), 124.47 (-**C$_e$**-), 127.47 (-**C$_d$**-), 134.40 (-**C$_i$**-), 135.00 (-**C$_k$**-), 142.59 (-**C$_c$**-), 147.21 (-**C$_f$**-), 162.61 (-**C$_m$**-), 165.17 (-**C$_g$**-). FTIR (Liquid neat) cm^{-1}: 3436.17 (ν_{O-H}), 1659.36 ($\nu_{HC=N}$), 1422.95 ($\nu_{C=C}$), 1311.38 (ν_{C-N}), 1028.96 (ν_{C-O}). TOF- MS ES$^+$ [M + H]$^+$, m/z = 555.13 (calculated m/z = 554.99).

4.3.1.4 Synthesis of *Bis ((E)-2-(((4-methoxyphenyl) imino) methyl) phenol) Palladium (II)* (PdC4)

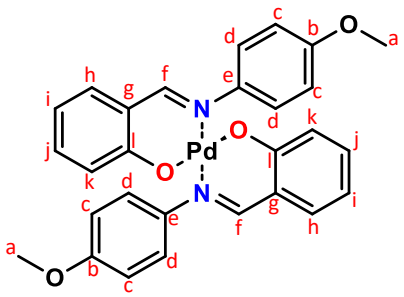

Bis ((E)-2-(((4-methoxyphenyl)imino)methyl) phenol) Palladium (II) **(PdC4)**: Following procedure (**P2**), **PdC4** was synthesized by reacting 0.5 mmol (113.63 mg) of **L4** and 0.25 mmol

(56.13 mg) of palladium acetate (Pd $(OAc)_2$). The complex was obtained as orange crystals (109.1 mg, 78%; mp: 271.2 – 272.5°C (> 280°C = Decomposition)): ^{1}H NMR (400 MHz, $CDCl_3$) δppm: 3.91 (s, 6H, -**H$_a$**-), 6.25 (d, 2H, *J* = 8.54 Hz, -**H$_k$**-), 6.53 (t, 2H, *J* = 7.24 Hz, -**H$_i$**-), 6.96 (d + $CDCl_3$, 6H, *J* = 8.83 Hz, -**H$_c$**-), 7.15 - 7.19 (m, 4H, -**H$_{j\ \&\ h}$**-), 7.27 - 7.29 (m, 4H, -**H$_d$**-), 7.74 (s, 2H, -**H$_f$**-).^{13}C NMR (100 MHz, $CDCl_3$) δppm: 55.64 (-**C$_a$**-), 113.25 (-**C$_c$**-), 115.10 (-**C$_k$**-), 120.28 (-**C$_g$**-), 120.63 (-**C$_i$**-), 125.59 (-**C$_d$**-), 134.39 (-**C$_h$**-), 135.05 (-**C$_j$**-), 142.78 (-**C$_e$**-), 158.13 (-**C$_l$**-), 162.72 (-**C$_b$**-), 165.16 (-**C$_f$**-).. FTIR (Liquid neat) cm^{-1}: 34439.25 (ν $_{O-H}$), 1658.67 (ν $_{HC=N}$), 1421.91 (ν $_{C=C}$), 1311.12 (ν $_{C-N}$), 1029.80 (ν $_{C-O}$). TOF- MS ES$^+$ $[M + Na]^+$, *m/z* = 581.07 (calculated *m/z* = 558.93).

4.3.1.5 Synthesis of *Bis ((E)-2-(((4-fluorophenyl)imino)methyl) phenol) Palladium (II)* (PdC5)

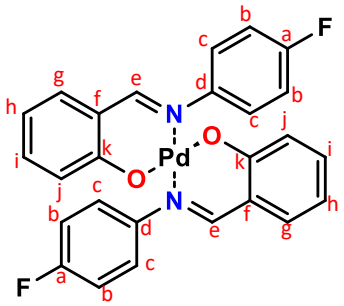

Bis ((E)-2-(((4-fluorophenyl)imino)methyl) phenol) Palladium (II) **(PdC5)**: Following procedure (**P2)**, complex **PdC5** was synthesized by reacting 0.5 mmol (107.62 mg) of **L5** and 0.25 mmol (56.13 mg) of palladium acetate (Pd $(OAc)_2$). The complex was obtained as orange crystals (114.6 mg, 86%; mp: 334.6 – 335.3°C (> 340°C = Decomposition)): ^{1}H NMR (400 MHz, $CDCl_3$) δppm: 7.21 (d, 2H, *J* = 8.91 Hz, -**H$_j$**-), 6.55 (t, 2H, *J* = 7.41 Hz, -**H$_h$**-), 7.10 - 7.20 (m, 8H, -**H$_{c\ \&\ b}$**-), 7.28 - 7.32 (m, 8H, -**H$_{i\ \&\ g}$**-), 7.75 (s, 2H, -**H$_e$**-). ^{13}C NMR (100 MHz, $CDCl_3$) δppm: 114.94 (-**C$_j$**-), 115.39 (-**C$_b$**-), 119.91 (-**C$_f$**-), 120.66 (-**C$_h$**-), 126.17 (-**C$_c$**-), 134.53 (-**C$_g$**-), 135.50 (-**C$_i$**-), 145.38 (-**C$_d$**-), 160.21 (-**C$_k$**-), 163.07 (-**C$_a$**-), 165.11 (-**C$_e$**-). FTIR (Liquid neat) cm^{-1}: 3431.99 (ν $_{O-H}$), 1657.75 (ν $_{HC=N}$), 1421.53 (ν $_{C=C}$), 1312.12 (ν $_{C-N}$), 1026.97 (ν $_{C-O}$). TOF-MS ES$^+$ $[M + Na]^+$, *m/z* = 557.03 (calculated *m/z* = 534.86).

4.3.1.6 Synthesis of *Bis ((E)-2-(((4-bromophenyl)imino)methyl) phenol) Palladium (II)* (PdC6)

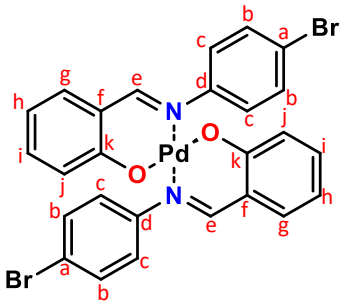

Bis ((E)-2-(((4-bromophenyl)imino)methyl) phenol) Palladium (II) **(PdC6)**: Following procedure (**P2**), **PdC6** was synthesized by reacting 0.5 mmol (138.07 mg) of **L6** and 0.25 mmol (56.13 mg) of palladium acetate (Pd $(OAc)_2$). The complex was obtained as orange crystals (133.3, 81%; mp: 283.1 – 284.6°C (> 290°C = Decomposition)): ^{1}H NMR (400 MHz, $CDCl_3$) δppm: 6.22 (d, 2H, J = 8.32 Hz, -**H$_j$**-), 6.57 (t, 1H, J = 7.01 Hz, -**H$_h$**-), 7.19 - 7.24 (m, 8H, -**H$_c$**, **i & g**-), 7.56 - 7.58 (m, 4H, -**H$_b$**-), 7.73 (s, 2H, -**H$_e$**-). ^{13}C NMR (100 MHz, $CDCl_3$) δppm: 115.50 (-**C$_j$**-), 119.90 (-**C$_f$**-), 119.97 (-**C$_h$**-), 120.78 (-**C$_a$**-), 126.42 (-**C$_c$**-), 131.20 (-**C$_g$**-), 134.58 (-**C$_i$**-), 135.71 (-**C$_b$**-), 148.34 (-**C$_d$**-), 162.92 (-**C$_k$**-), 165.15 (-**C$_e$**-). FT-IR (Liquid neat) cm^{-1}: 3440.48 (ν $_{O-H}$), 1658.71 (ν $_{HC=N}$), 1422.14 (ν $_{C=C}$), 1311.65 (ν $_{C-N}$), 1030.95 (ν $_{C-O}$). TOF - MS ESI$^+$ [M + H_2O]$^+$, *m/z* = 674.30 (calculated *m/z* = 656.67).

4.3.1.7 Synthesis of *Bis ((E)-4-((2-hydroxybenzylidene)amino) benzonitrile) Palladium (II)* (PdC7)

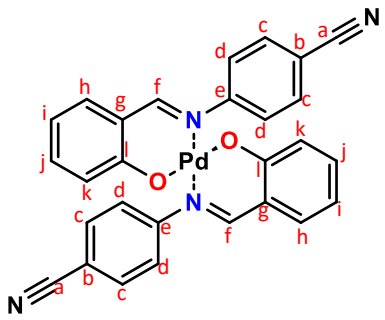

Bis ((E)-4-((2-hydroxybenzylidene)amino) benzonitrile) Palladium (II) **(PdC7)**: Following procedure (**P2**), **PdC7** was synthesized by reacting 0.5 mmol (111.13 mg) of **L7** and 0.25 mmol (56.13 mg) of palladium acetate (Pd $(OAc)_2$). The complex was obtained as orange crystals (125.2 mg, 91%; mp: 289.4 – 290.1°C (> 295°C = Decomposition)): ^{1}H NMR (400MHz, $CDCl_3$) δppm: 6.10 (d, 2H, *J* = 8.54 Hz, -**H$_k$**-), 6.59 (t, 2H, *J* = 7.37 Hz, -**H$_i$**-), 7.20 - 7.25 (m, 4H, -**H$_d$**-), 7.45 - 7.47 (m, 4H, -**H$_c$**-), 7.73 (s, 2H, -**H$_f$**-), 7.75 - 7.77 (m, 4H, -**H$_{h\ \&\ j}$**-). ^{13}C NMR (100 MHz, $CDCl_3$) δppm: 110.36 (-**C$_b$**-), 115.99 (-**C$_k$**-), 118.67 (-**C$_g$**-), 119.62 (-**C$_a$**-), 120.78 (-**C$_i$**-), 125.87 (-**C$_d$**-), 132.33 (-**C$_h$**-), 134.81 (-**C$_j$**-), 136.38 (-**C$_c$**-), 153.01 (-**C$_e$**-), 163.04 (-**C$_l$**-), 165.13 (-**C$_f$**-). FTIR (Liquid neat) cm^{-1}: 3426.91 (ν_{O-H}), 1657.90 ($\nu_{HC=N}$), 1421.44 ($\nu_{C=C}$), 1313.16 (ν_{C-N}), 1025.10 (ν_{C-O}). TOF-MS ES$^+$ $[M + H]^+$, *m/z* = 549.05 (calculated *m/z* = 548.90).

4.4 Synthesis of sodium borate salt

4.4.1 Synthetic procedure of the sodium borate salt (P3)

In a 1 neck 100 mL round-bottom flask equipped with a magnetic stirrer bar, 5 ml of toluene was added and heated to 100°C. Once the toluene reached this temperature, 2 g of boronic acid was completely dissolved in the hot toluene. Subsequently, concentrated sodium hydroxide (NaOH) was added dropwise until no further precipitate formed. The hot solution was then filtered with suction to yield the product without further purification.

4.4.1.1 Synthesis of sodium (trihydroxy)phenylborate salt (115)

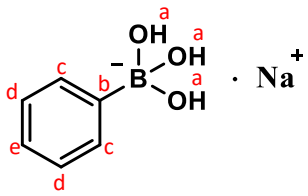

sodium (trihydroxy)phenylborate (115): Following procedure **(P3),** borate salt **(115)** was obtained as a fluffy white solid (159.2 mg g, 98%): ^{1}H NMR (400MHz, D_2O) δppm: 7.18 - 7.24 (m, 1H, -**H$_e$**-), 7.29 (t, 2H, *J* = 7.19 Hz, -**H$_d$**-), 7.55 (d, 2H, *J* = 7.34 Hz, -**H$_c$**-). ^{13}C NMR (100 MHz, D_2O) δppm: 125.77 (-**C$_e$**-), 127.33 (-**C$_d$**-), 131.27 (-**C$_c$**-), 168.10 (-**C$_b$**-). ^{11}b NMR (128 MHz) δppm: 2.95. TOF-MS ES$^+$ $[M + H]^+$, *m/z* = 162.05 (calculated *m/z* = 161.93).

4.5 Synthesis of biaryls

4.5.1 Synthetic procedure of biaryls (P4)

In a 2 neck 50 ml round-bottom flask equipped with a magnetic stirrer bar, reflux condenser, and a rubber septum, 1 mmol (161.93 mg) of sodium (trihydroxy)phenylborate, 1 mmol (0.12 ml) of 4-bromotoluene, 2 mol% of (**PdC2 - PdC7**), 3 ml of ethanol, and 3 drops of distilled water were added. Before initiating the reaction, the contents in the round-bottom flask were degassed under nitrogen gas and refluxed while stirred at 60 °C with a continuous flow of nitrogen gas for 24 hours to yield a crude product. The resulting crude product was purified by plug column chromatography using a 90:10 (hexane/ethyl acetate) solvent system. Further

purification was achieved by chromatotron with the same solvent system (90:10 hexane/ethyl acetate) to obtain the desired product.

4.5.1.1 Synthesis of 4-methylbiphenyl (117)

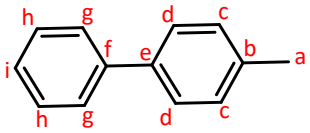

4-methylbiphenyl (117): Following procedure (**P4**), **117** was obtained as white crystals (30.8 - 53.8 mg, 18% - 32%): ^{1}H NMR (400MHz, $CDCl_3$) δppm: 2.42 (s, 3H, -**H$_a$**-), 7.27 (d, 2H, *J* = 7.25 Hz, -**H$_c$**-), 7.33 - 7.37 (m, 1H, -**H$_i$**), 7.45 (t, 2H, *J* = 7.45 Hz, -**H$_h$**-), 7.52 (d, 2H, *J* = 8.03 Hz, -**H$_d$**-), 7.60 - 7.62 (m, 2H, -**H$_g$**-),. ^{13}C NMR (100 MHz, $CDCl_3$) δppm: 29.70 (-**C$_a$**-), 126.97 (-**C$_{d\ \&\ g}$**-), 126.99 (-**C$_i$**-), 128.70 (-**C$_h$**-), 129.47 (-**C$_c$**-), 137.01 (-**C$_b$**-), 138.38 (-**C$_c$**-), 141.18 (-**C$_f$**-). GC-MS: Retention time = 12.939 minutes, Similarity Index (SI) = 95, $[M - H]^-$, *m/z* = 167 (calculated *m/z* = 168.09).

4.5.2. Synthetic procedure of biaryl ketones (P5)

In a 2 neck 50 ml round-bottom flask equipped with a magnetic stirrer bar, reflux condenser, and a rubber septum, 1 mmol (161.93 mg) of sodiumphenylboric acid, 1.1 mmol (0.13 ml) of benzoyl chloride, 2 mol% of (**PdC2 & PdC6**), 3 ml of toluene, and 3 drops of distilled water were added. Before starting the reaction, the contents in the round-bottom flask were degassed under nitrogen gas. The mixture was refluxed while stirred at 60 °C with a continuous flow of nitrogen gas for 24 hours to yield a crude product which was purified by plug column chromatography using a 90:10 (hexane/ethyl acetate) solvent system. Further purification was achieved by chromatotron with the same solvent system (90:10 hexane/ethyl acetate) and afforded the desired product.[3]

4.5.2.1 Synthesis of benzophenone (119)

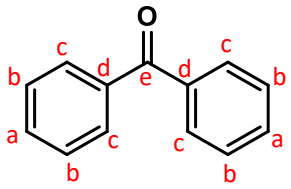

Benzophenone (119): Following procedure (**P5**), **119** was obtained as a colourless paste (28.2-55.0 mg, 15% - 30%): ^{1}H NMR (400MHz, $CDCl_3$) δppm: 7.50 (t, 4H, J = 7.65 Hz -**H$_b$**-), 7.61 (t, 2H, J = 7.42 Hz, -**H$_a$**-), 7.83 (d, 2H, J = 7.82 Hz, -**H$_d$**-). ^{13}C NMR (100 MHz, $CDCl_3$) δppm: 128.28 (-**C$_b$**-), 130.05 (-**C$_c$**-), 132.41 (-**C$_a$**-), 137.64 (-**C$_d$**-), 196.74 (-**C$_e$**-), 137.01 GC-MS: Retention time = 14.204 minutes, Similarity Index (SI) = 97, $[M - H]^-$, *m/z* = 181 (calculated *m/z* = 182.22).

References

1. Z. D. Petrović, J. Đorović, D. Simijonović, V. P. Petrović and Z. Marković, *RSC Advances*, 5(31), 24094-24100 (**2015**).
2. S.O. Akiri, S.O. and Ojwach, *Journal of Organometallic Chemistry*, 942, 121812 (**2021**).
3. S. Sithebe, and P. Molefe, *Journal of Organometallic Chemistry*, 846, 305-311 (**2017**).

APPENDIX

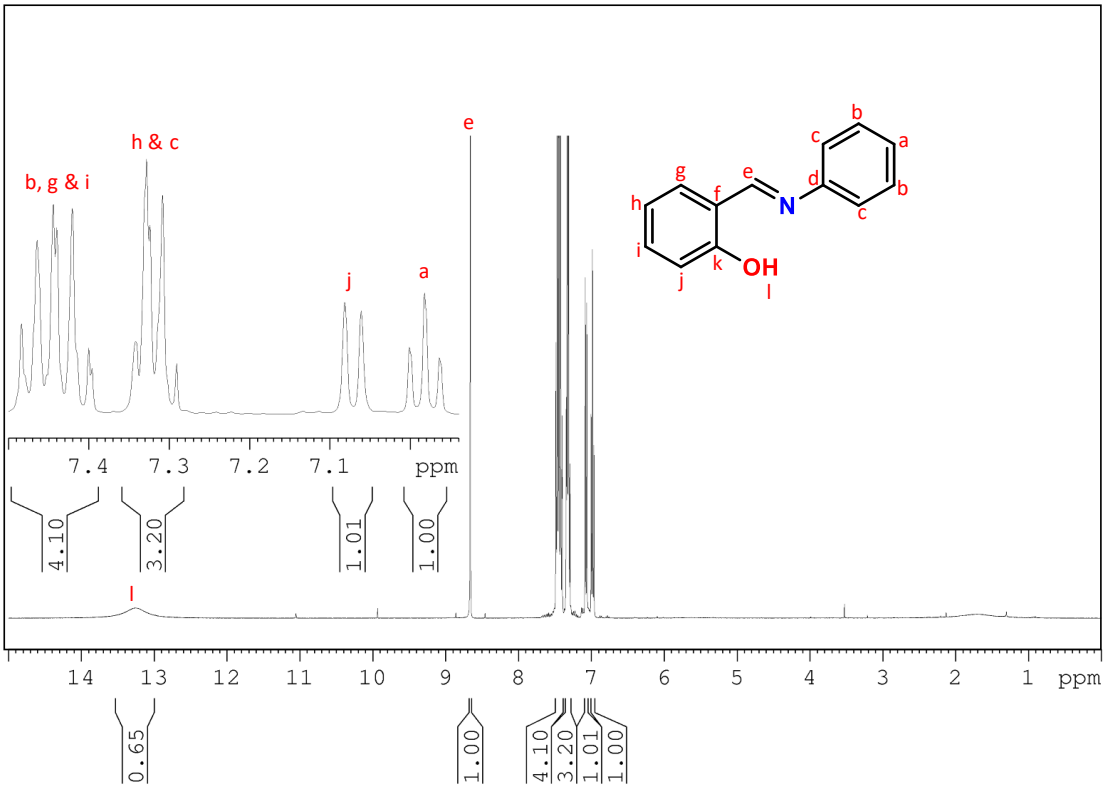

Figure A1: ^{1}H NMR spectrum of **L1**.

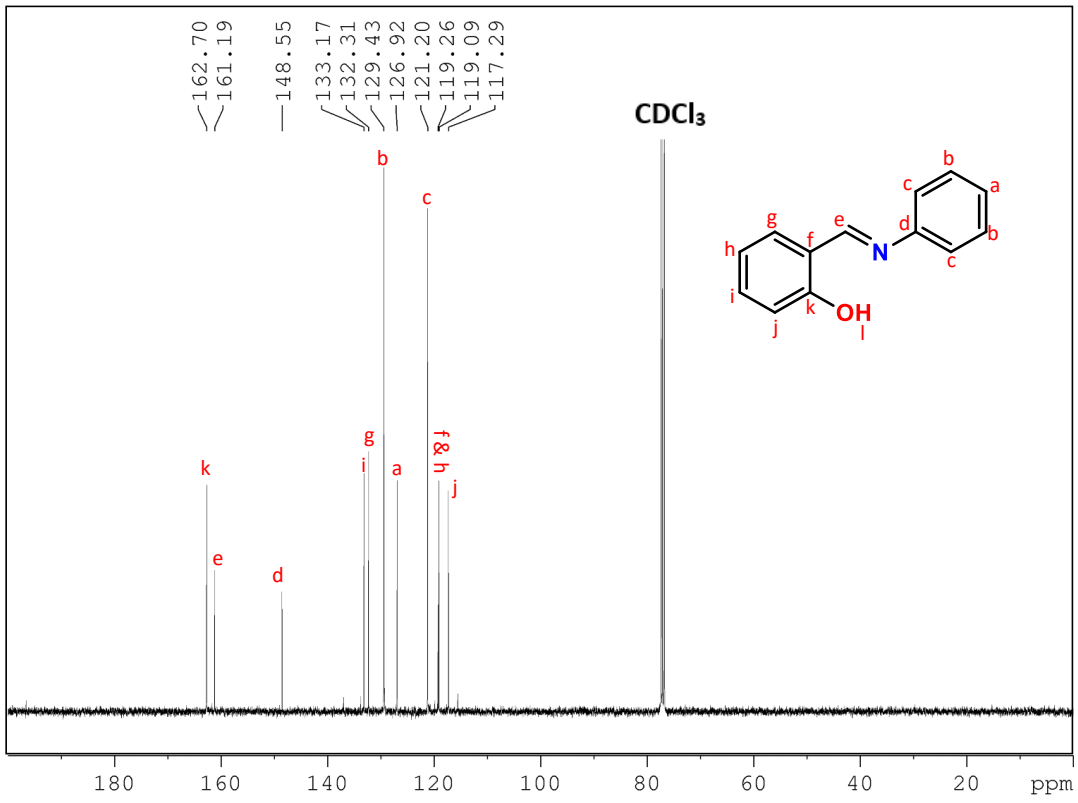

Figure A2: ^{13}C NMR spectrum of **L1**.

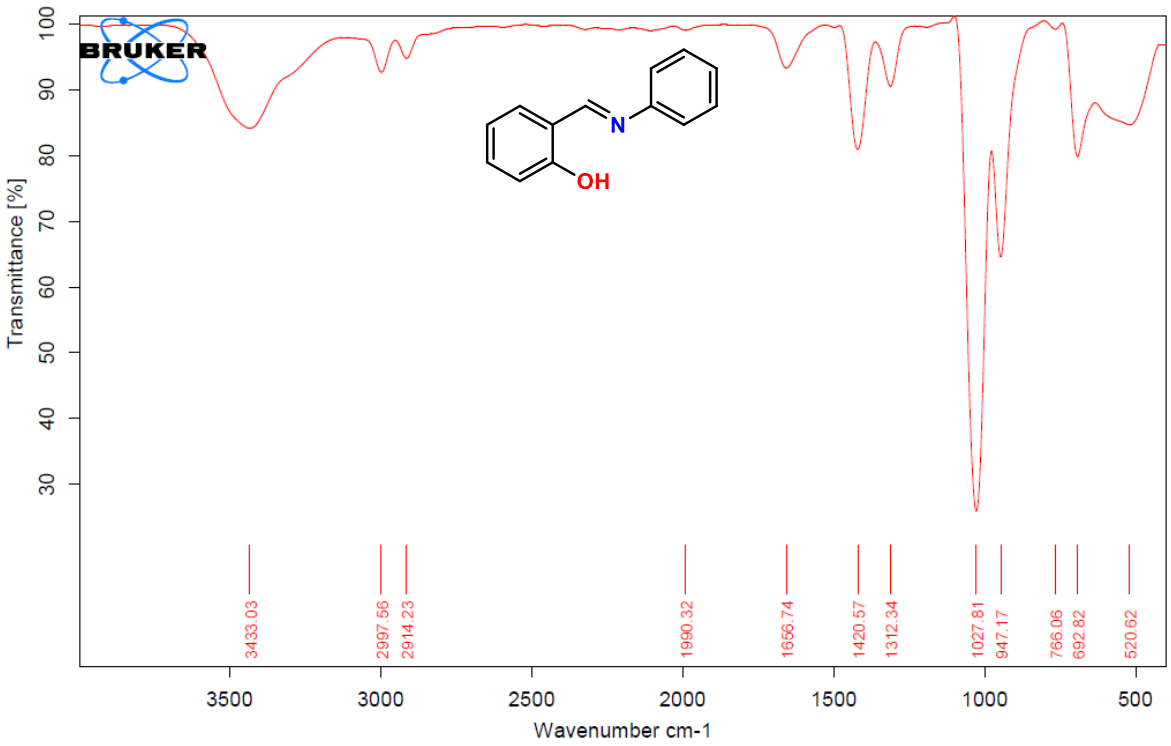

Figure A3: FTIR spectrum of **L1**.

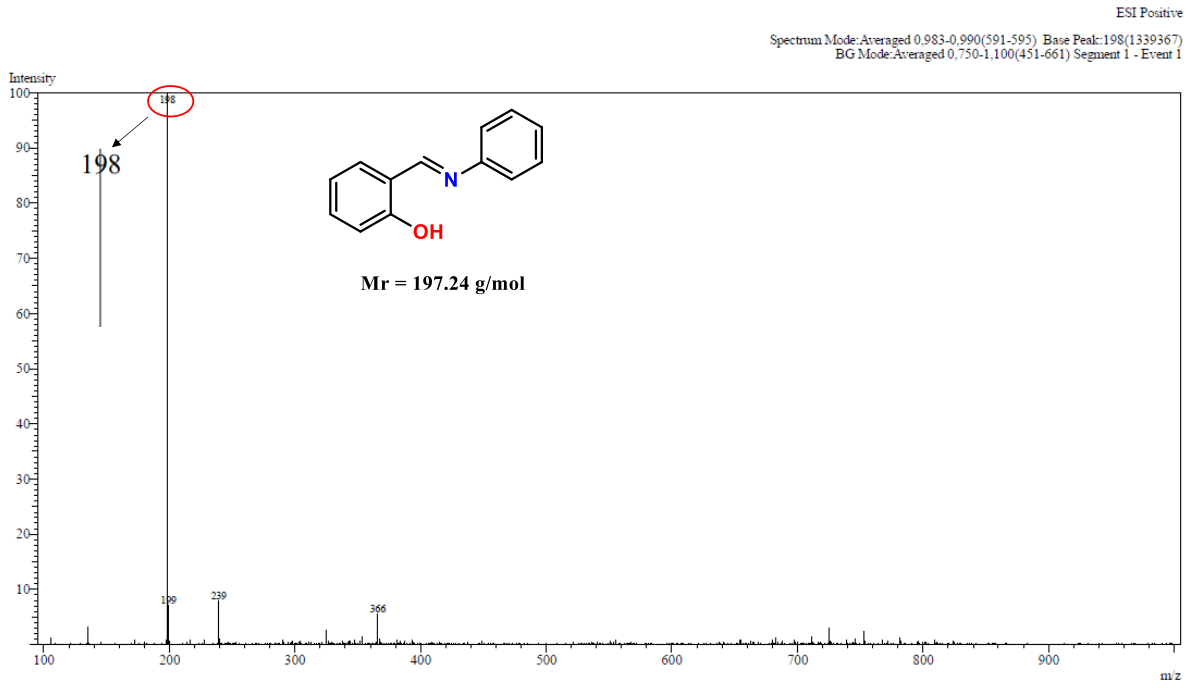

Figure A4: ESI^{+}- MS spectrum of **L1**.

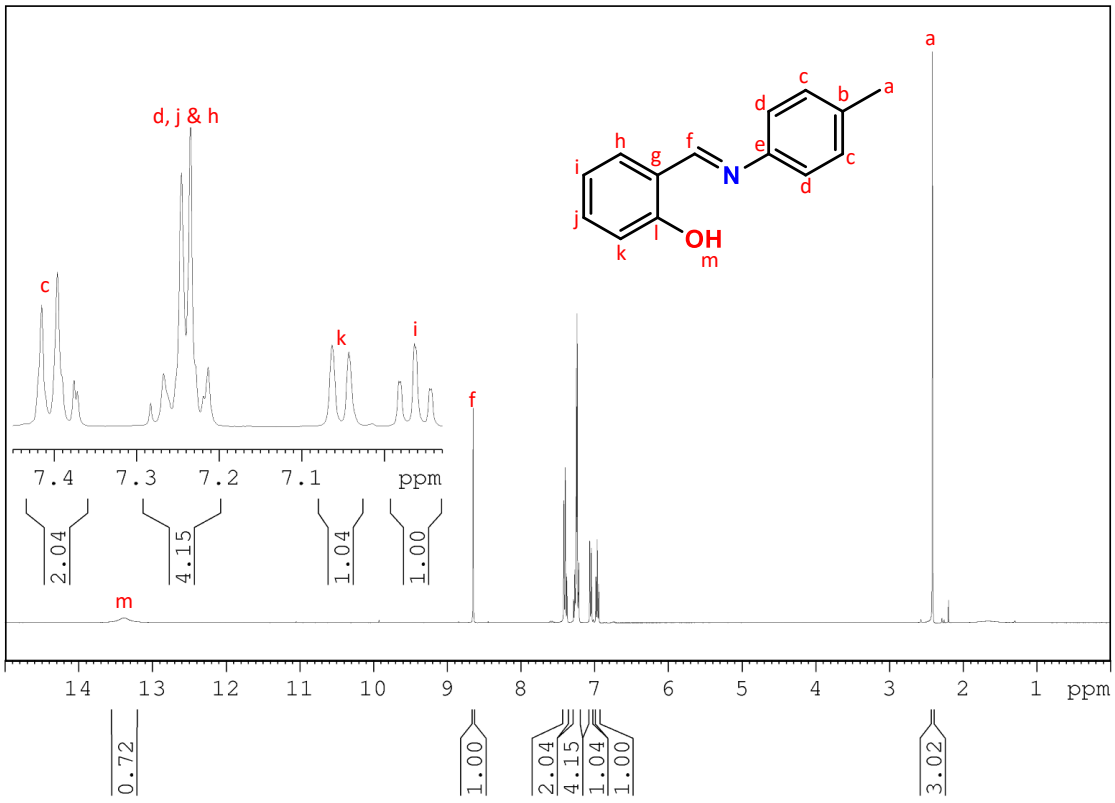

Figure A5: ^{1}H NMR spectrum of **L2**.

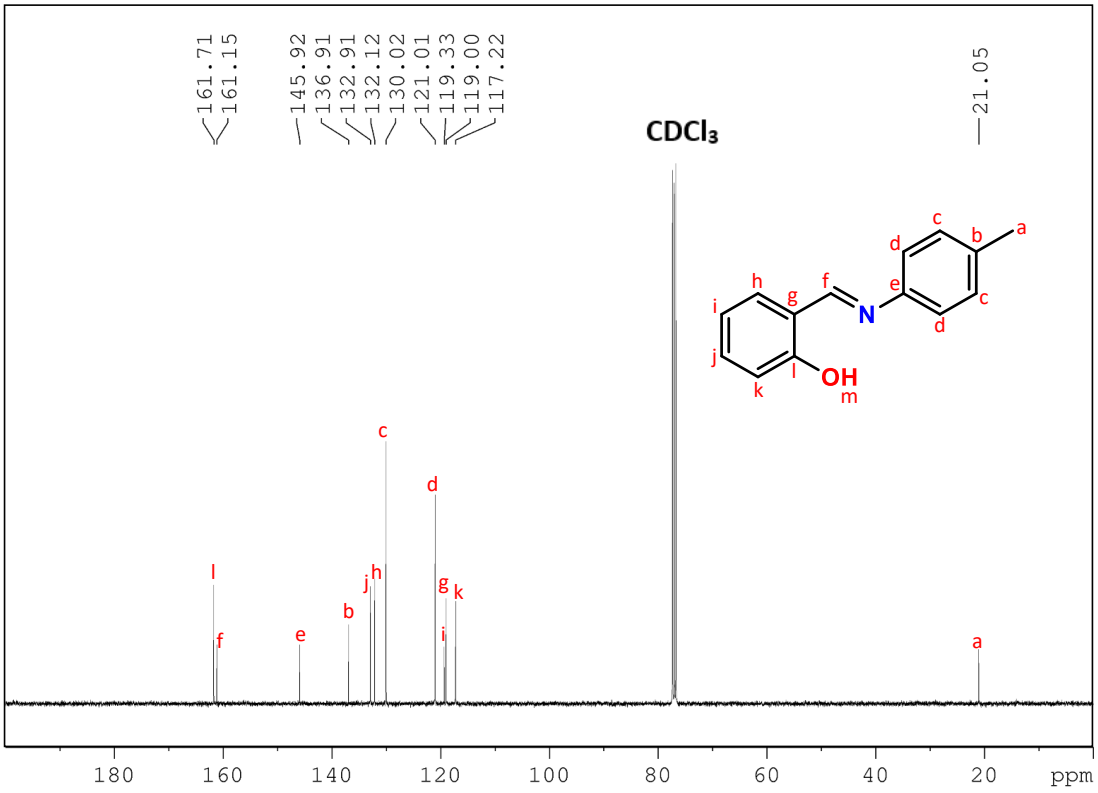

Figure A6: ^{13}C NMR spectrum of **L2**.

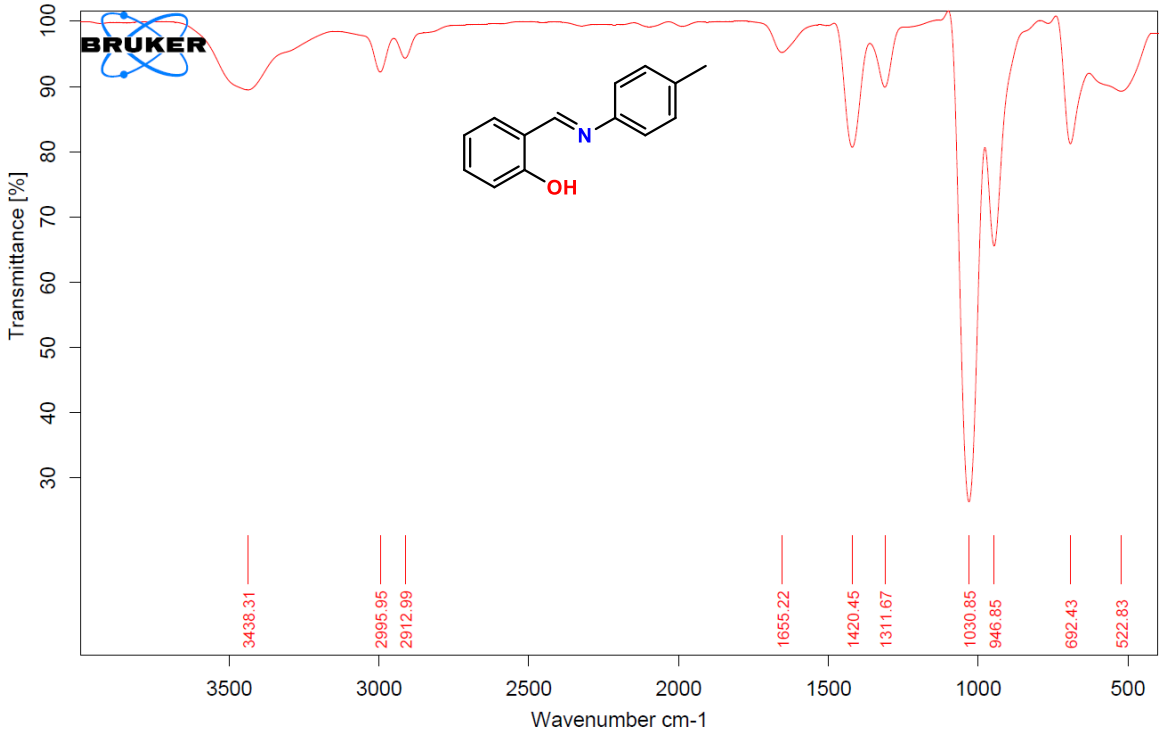

Figure A7: FTIR spectrum of **L2**.

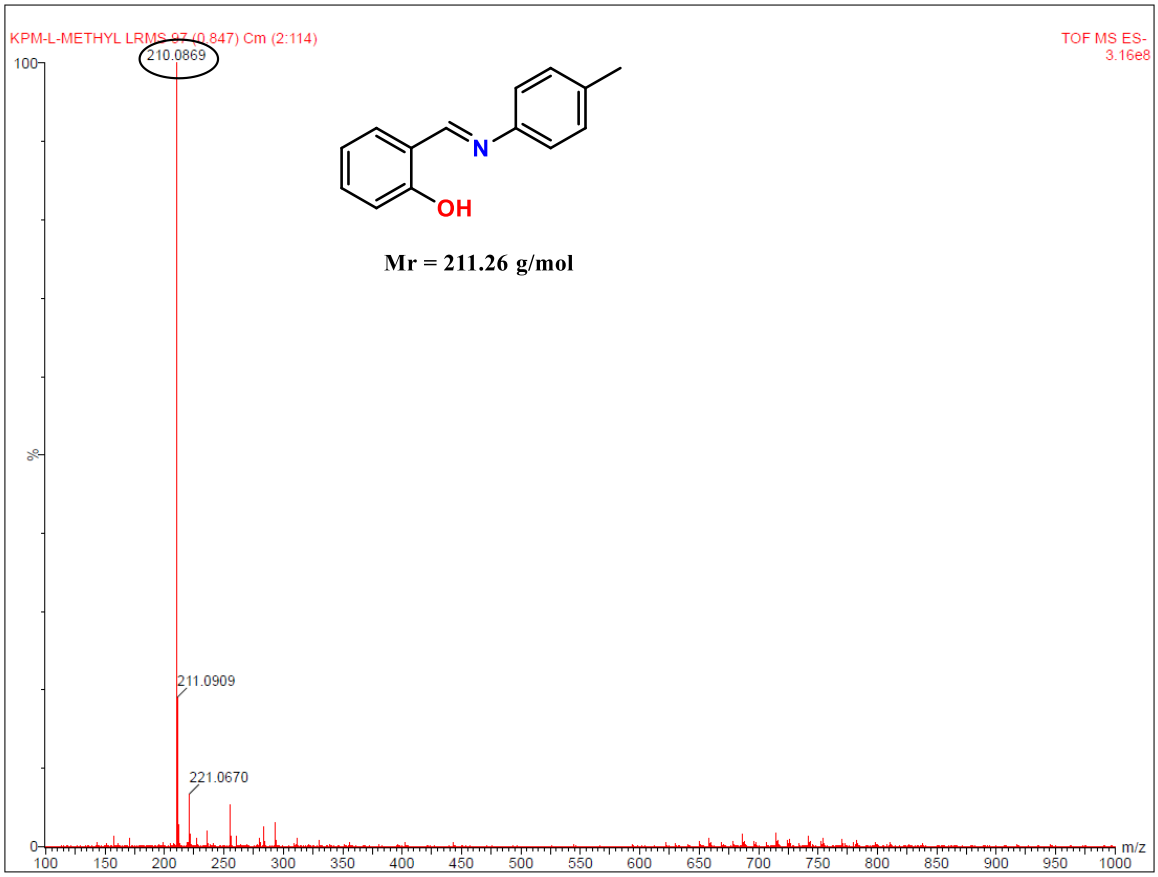

Figure A8: TOF-MS ES$^-$ spectrum of **L2**.

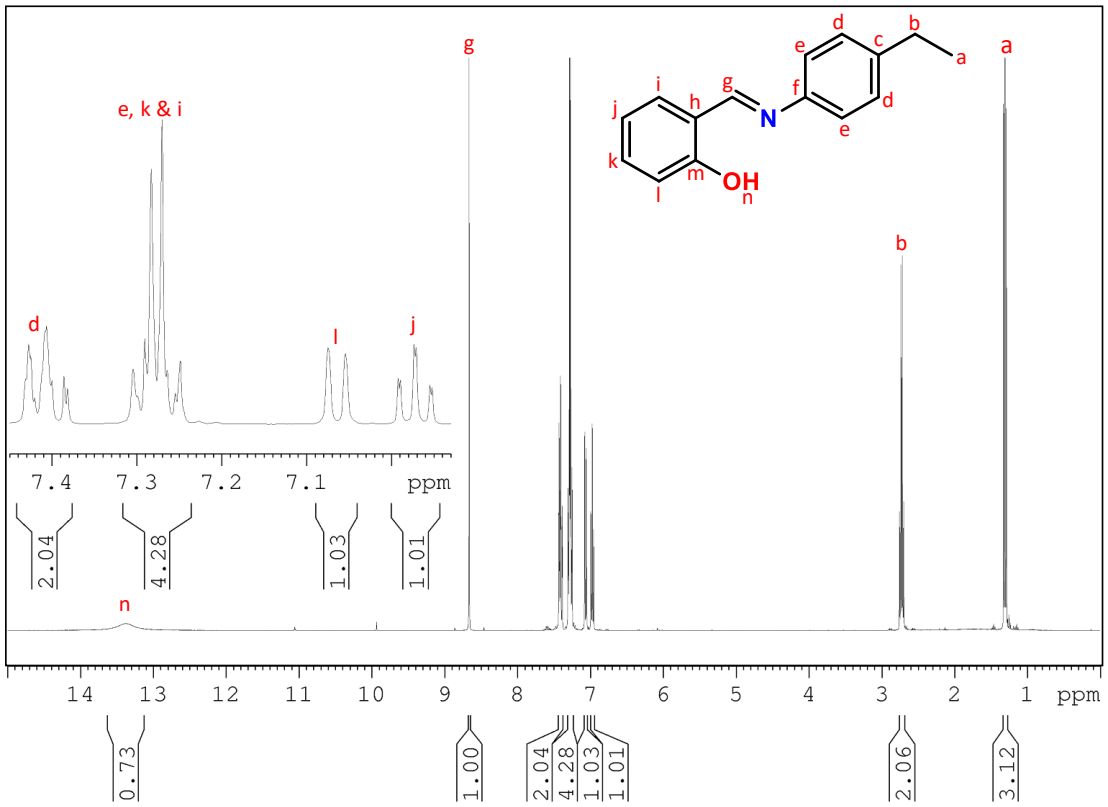

Figure A9: ^{1}H NMR spectrum of **L3**.

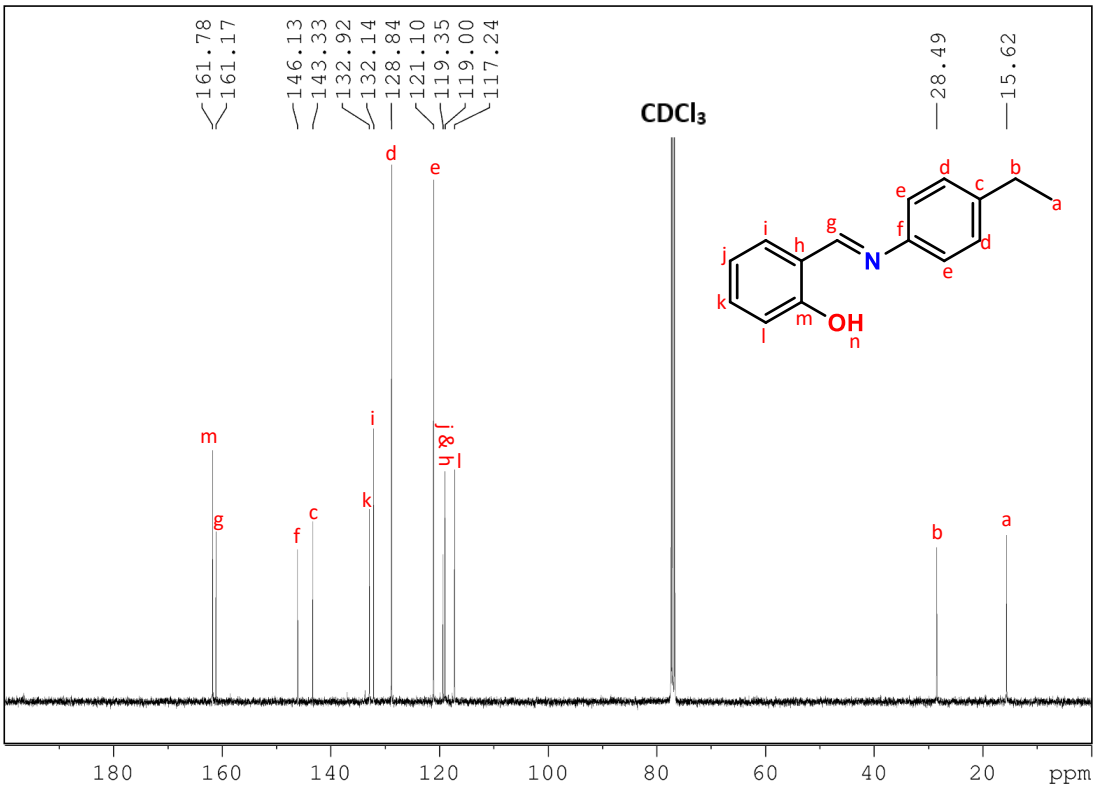

Figure A10: ^{13}C NMR spectrum of **L3**.

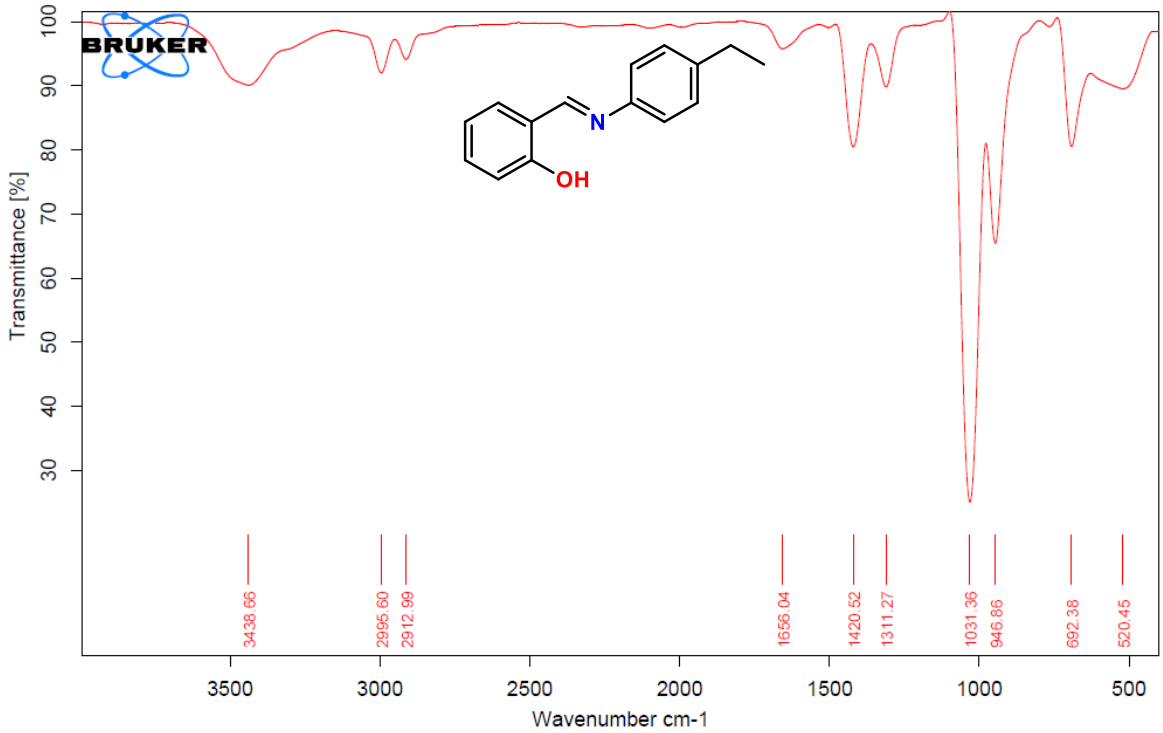

Figure A11: FTIR spectrum of **L3**.

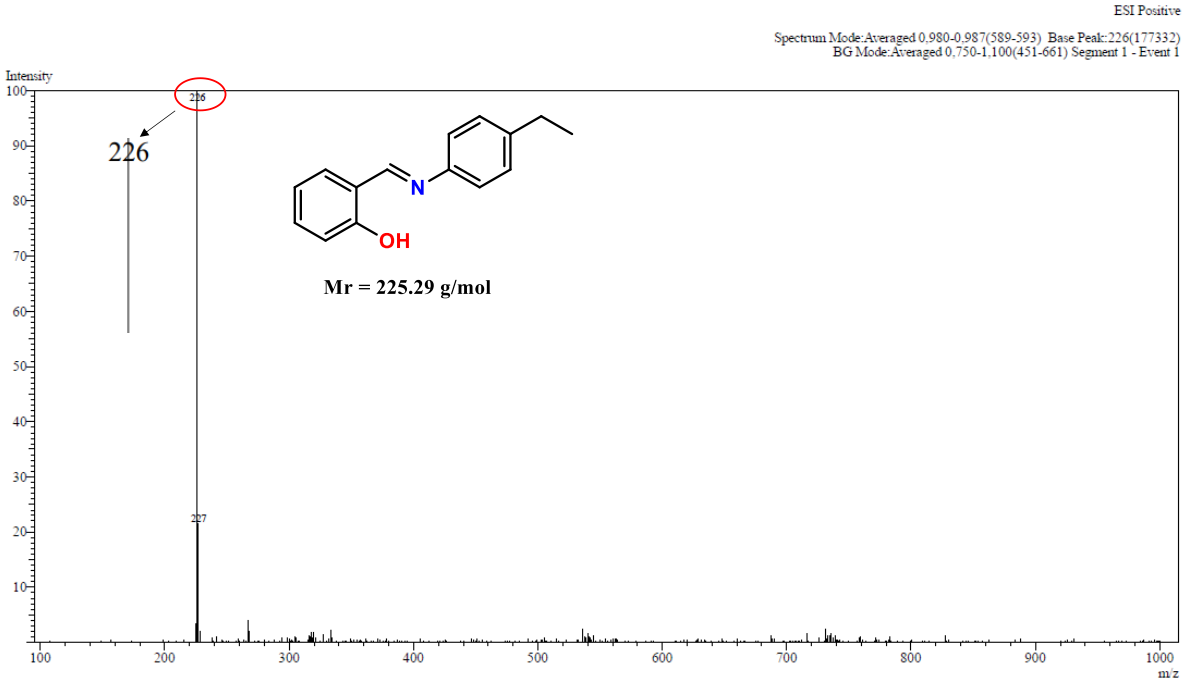

Figure A12: ESI^{+}- MS spectrum of **L3**.

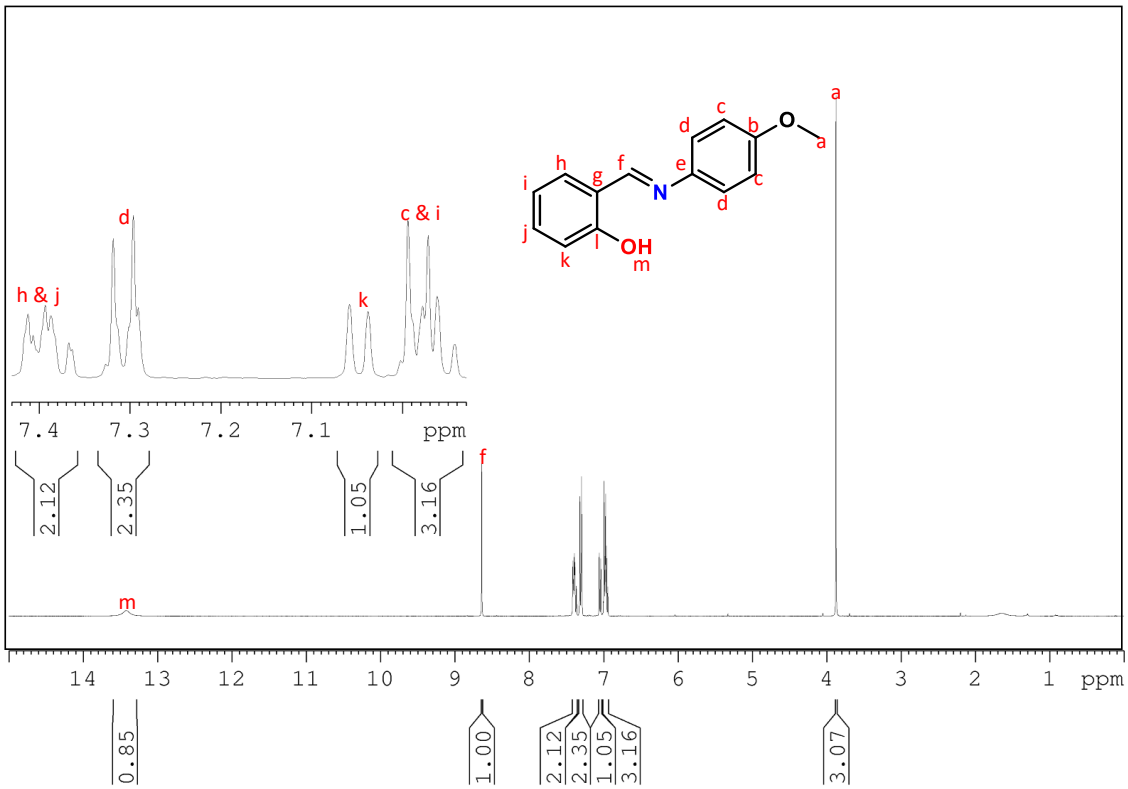

Figure A13: ^{1}H NMR spectrum of **L4**.

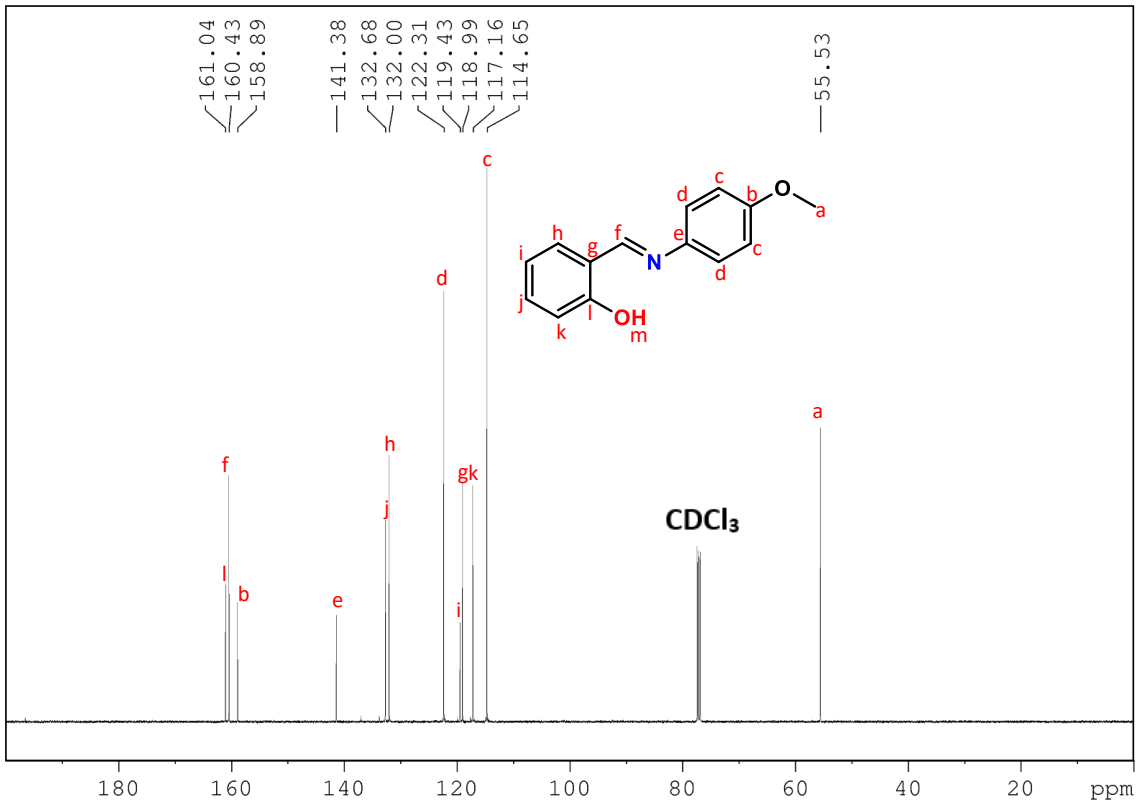

Figure A14: ^{13}C NMR spectrum of **L4**.

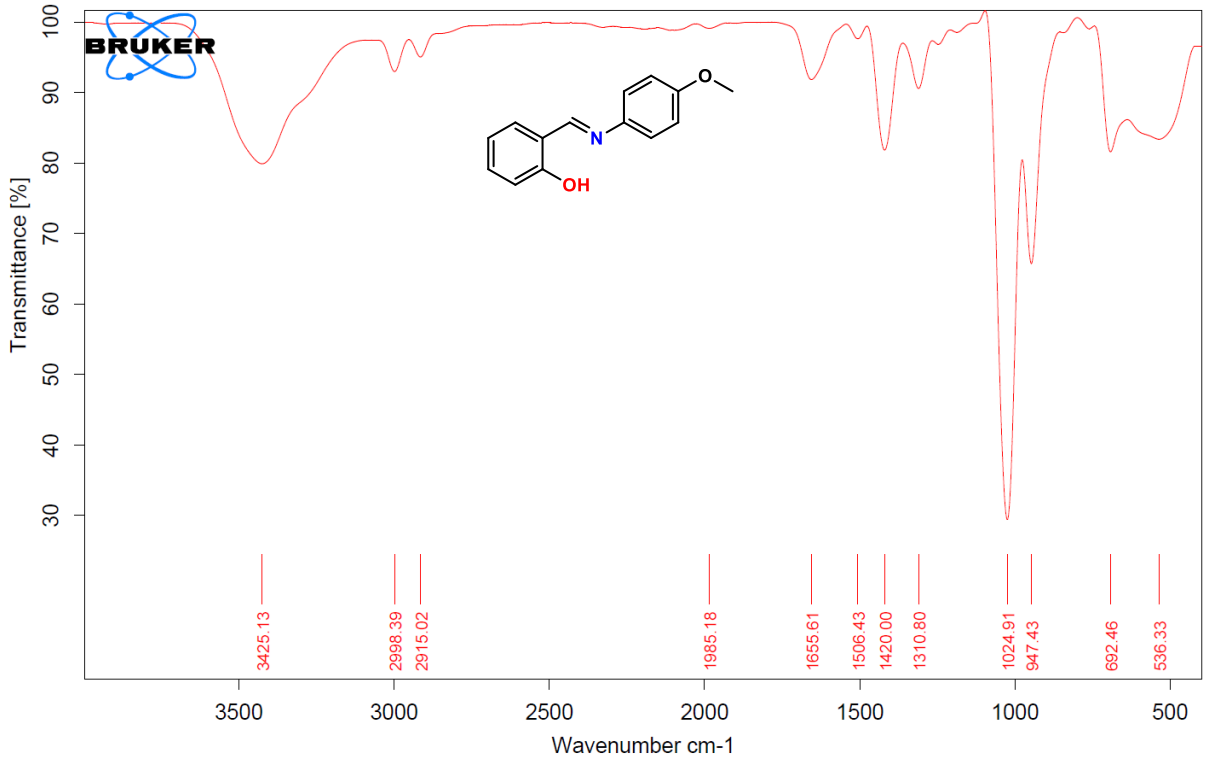

Figure A15: FTIR spectrum of **L4**.

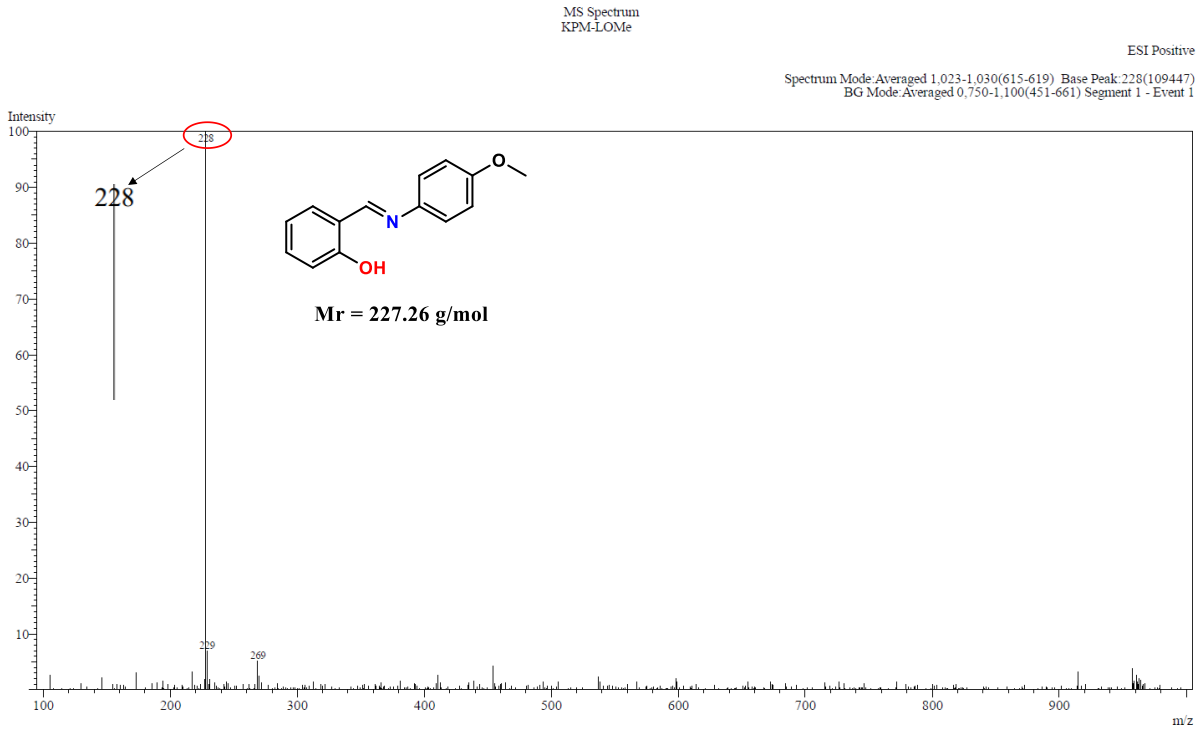

Figure A16: ESI^{+}- MS spectrum of **L4**.

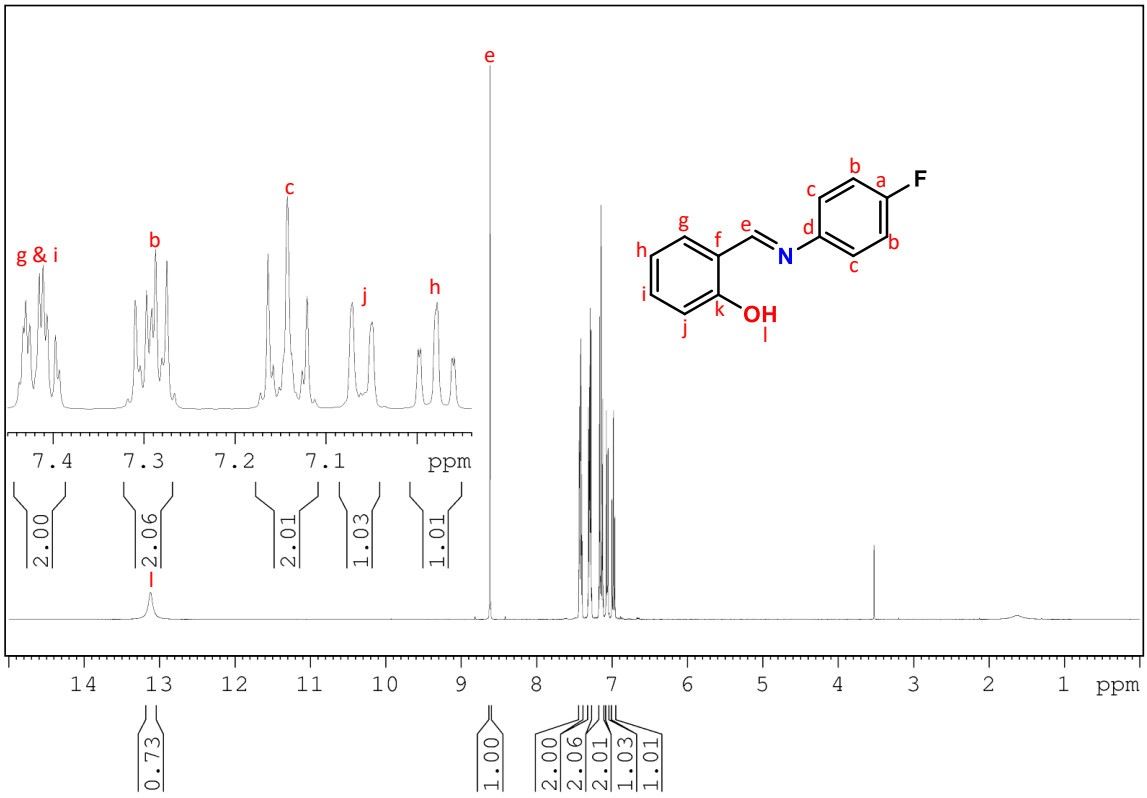

Figure A17: ^{1}H NMR spectrum of **L5**.

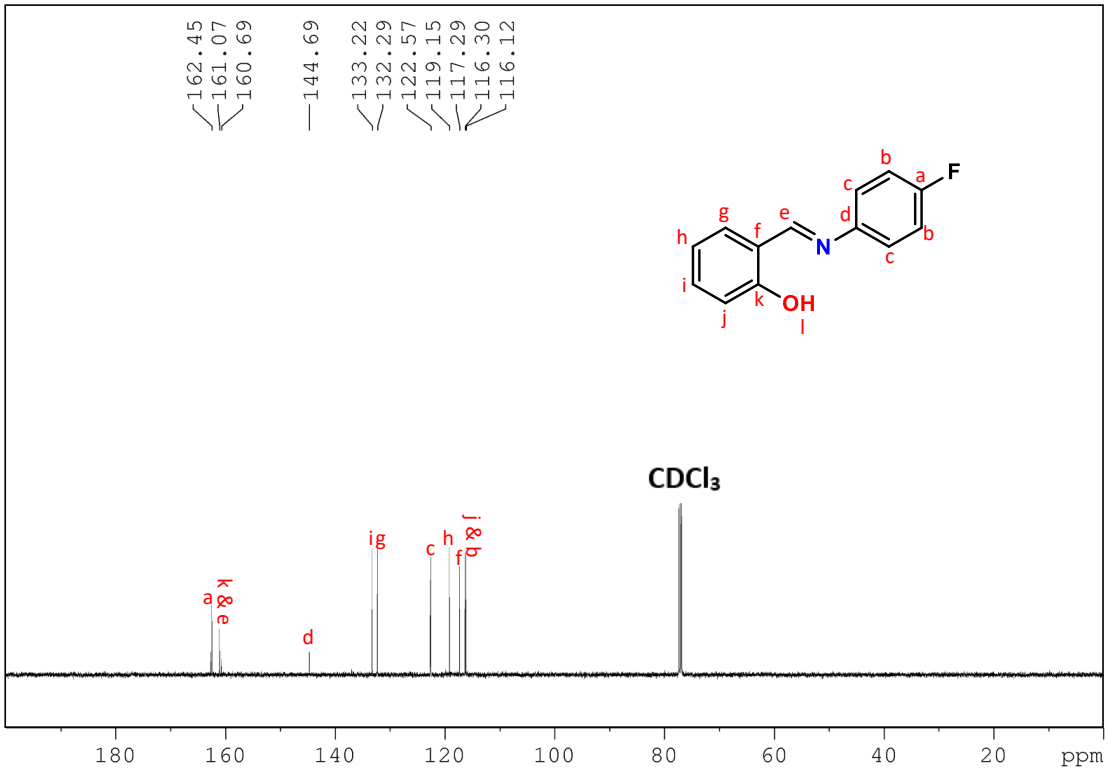

Figure A18: ^{13}C NMR spectrum of **L5**.

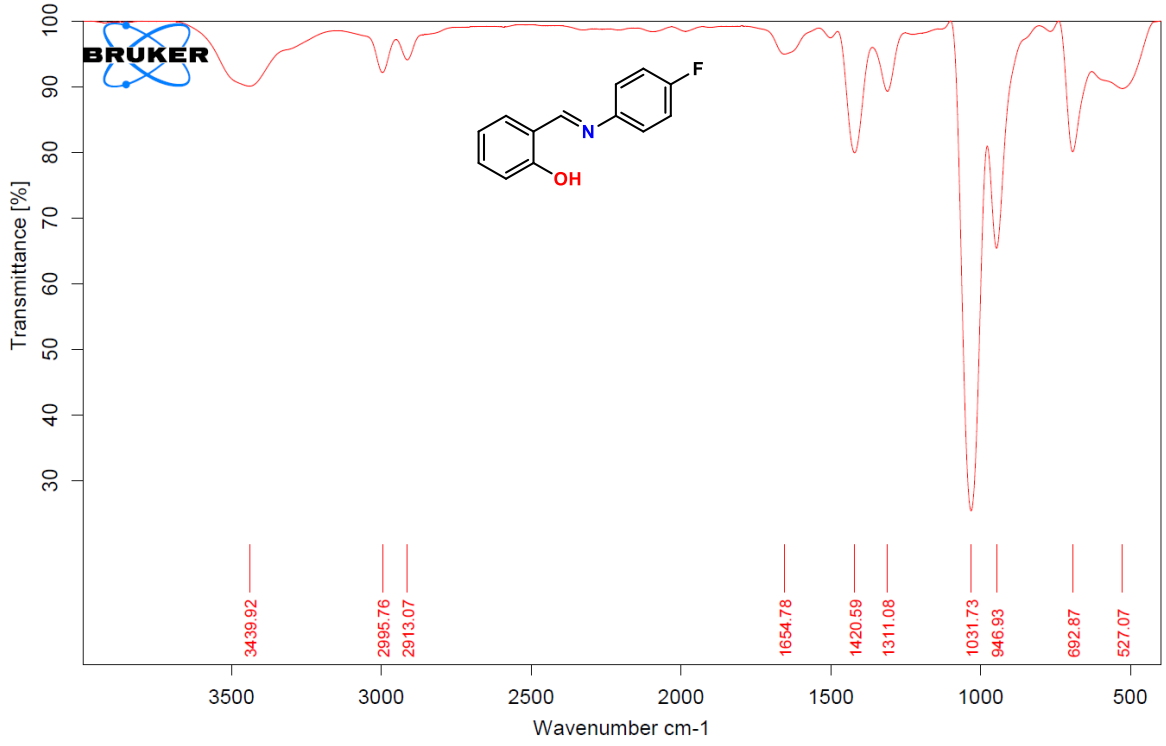

Figure A19: FTIR spectrum of **L5**.

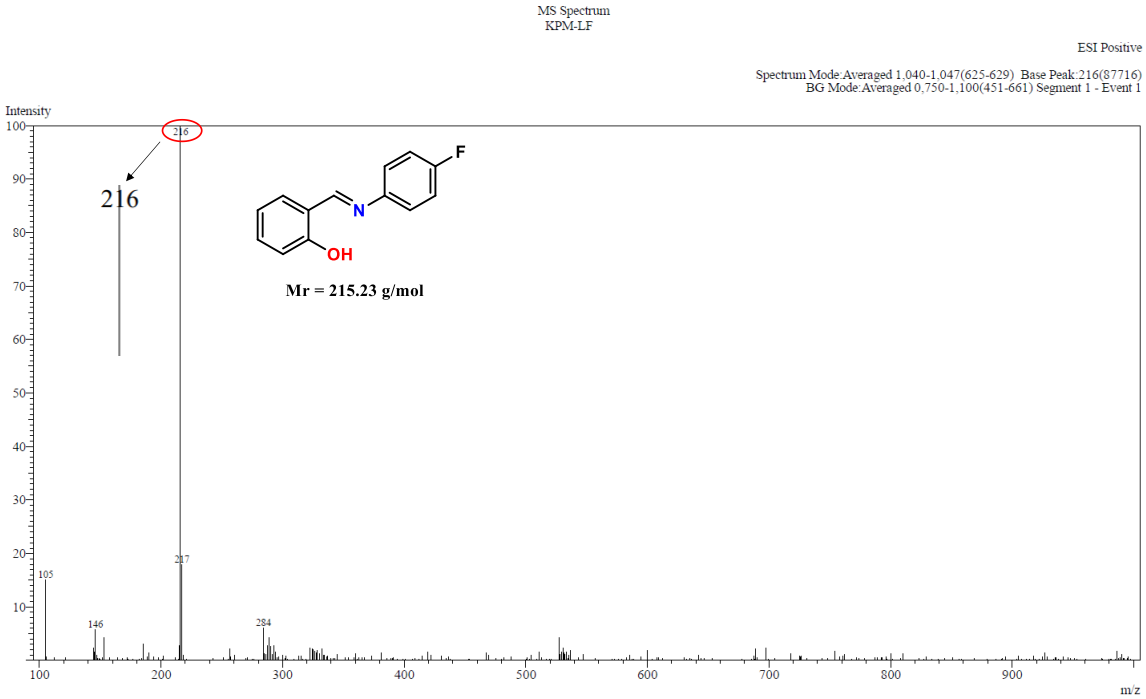

Figure A20: ESI^{+}- MS spectrum of **L5**.

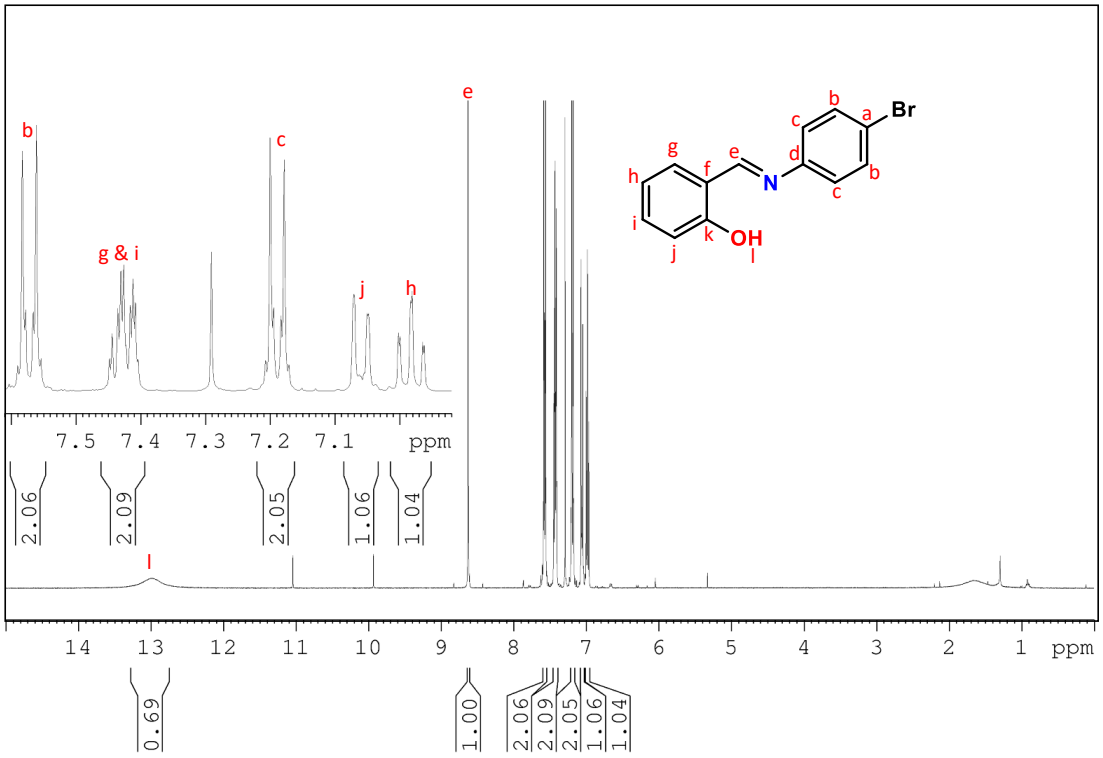

Figure A21: ^{1}H NMR spectrum of **L6**.

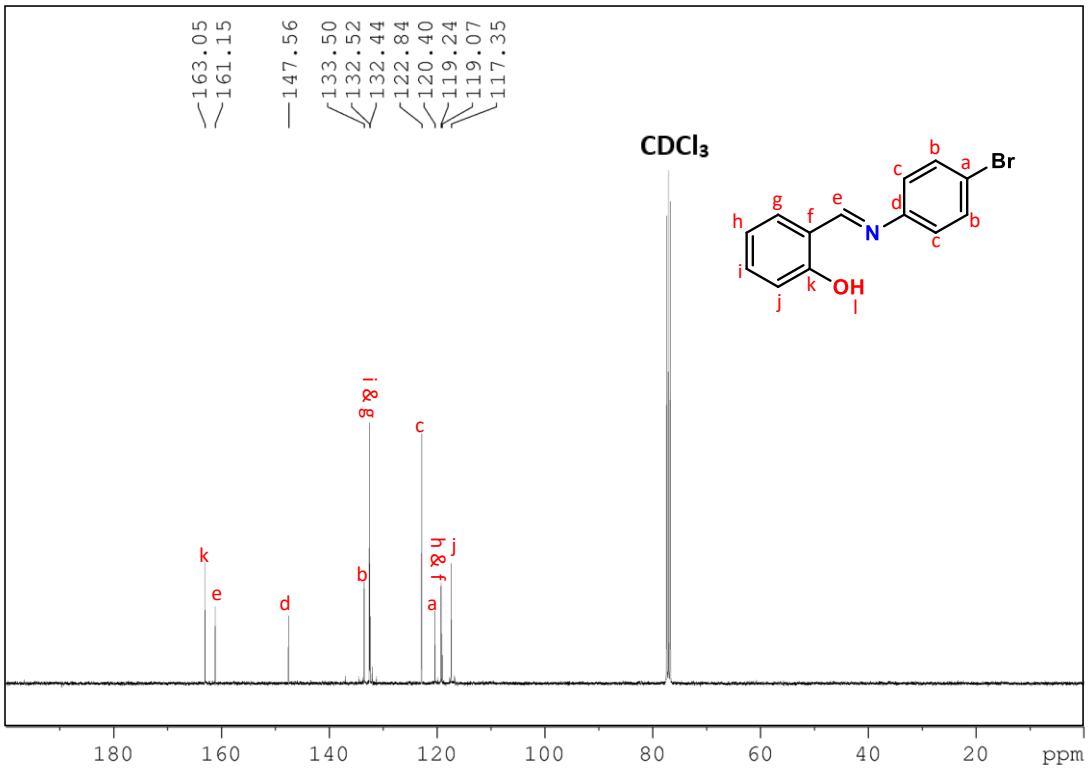

Figure A22: ^{13}C NMR spectrum of **L6**.

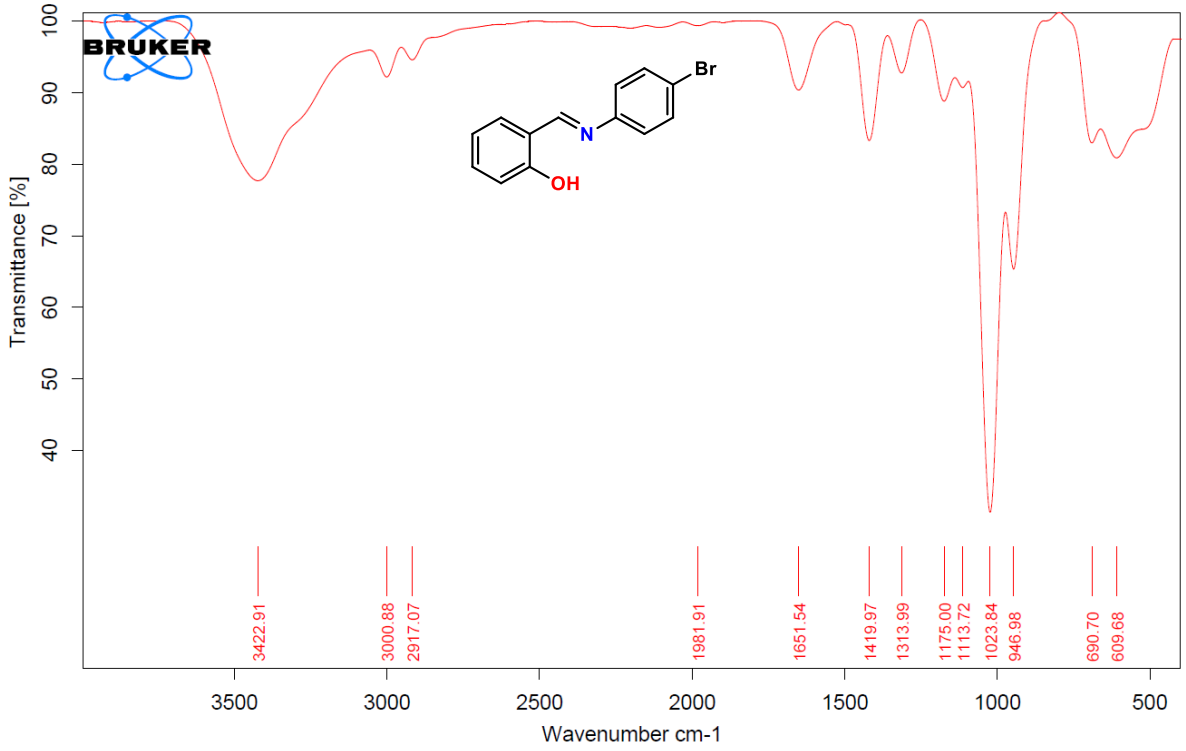

Figure A23: FTIR spectrum of **L6**.

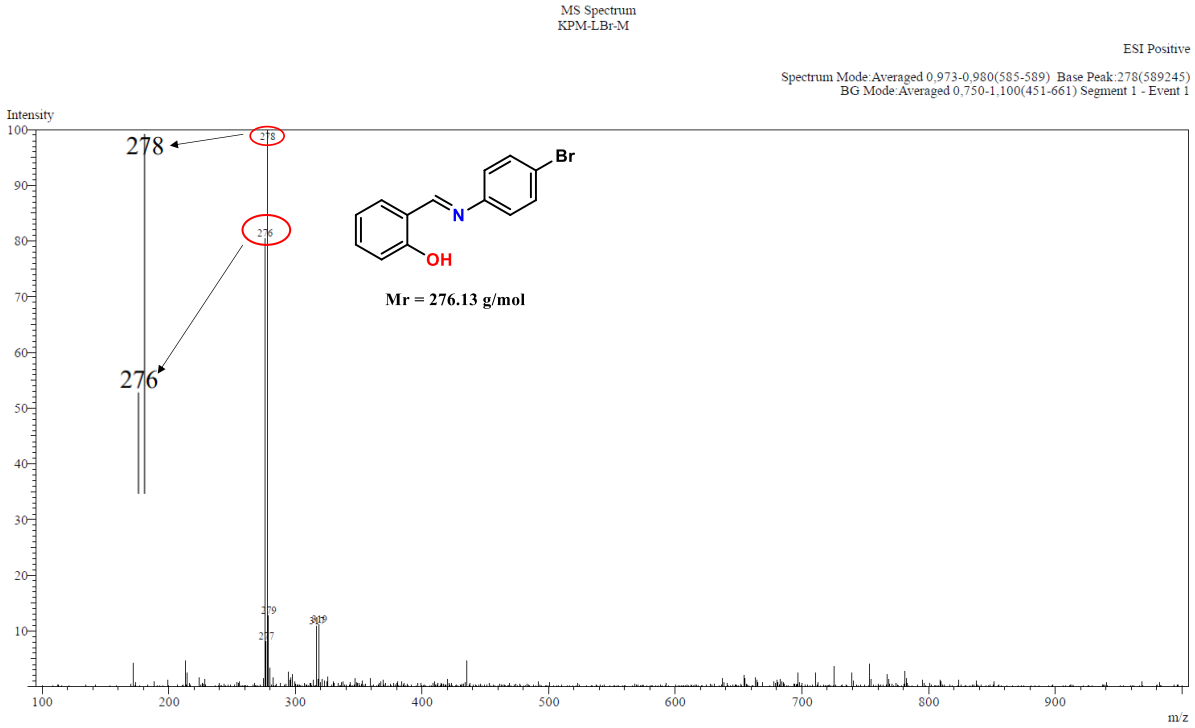

Figure A24: ESI^{+}- MS spectrum of **L6**.

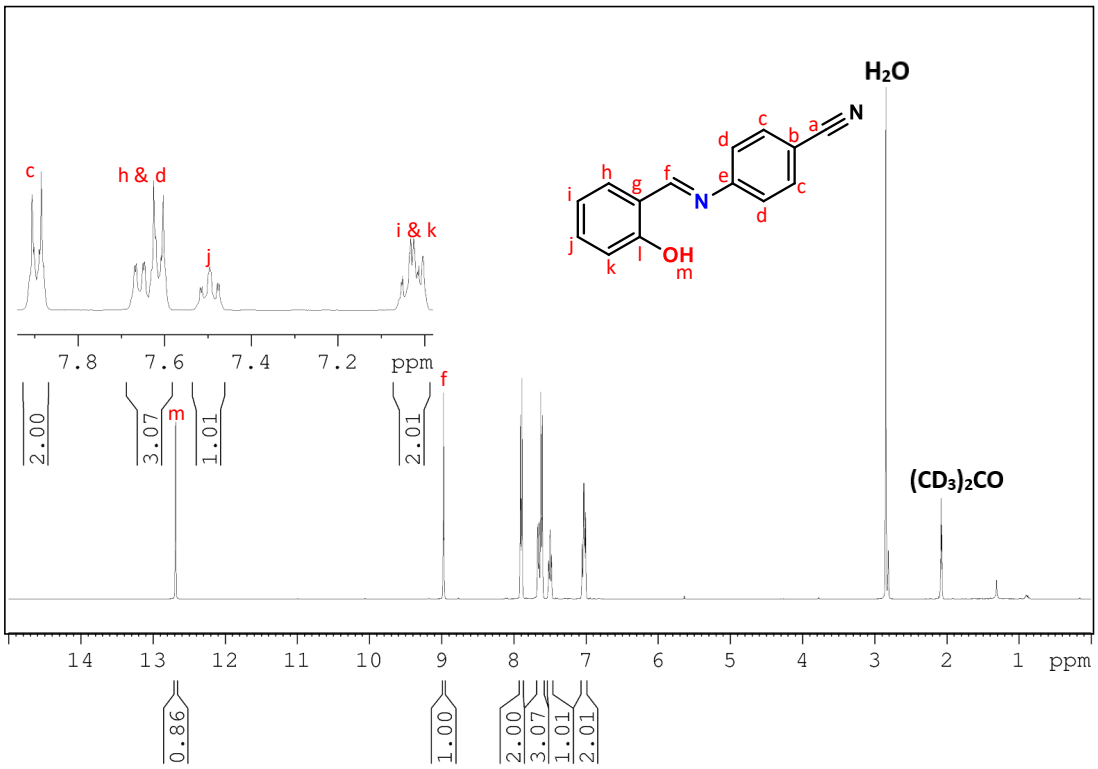

Figure A25: ^{1}H NMR spectrum of **L7**.

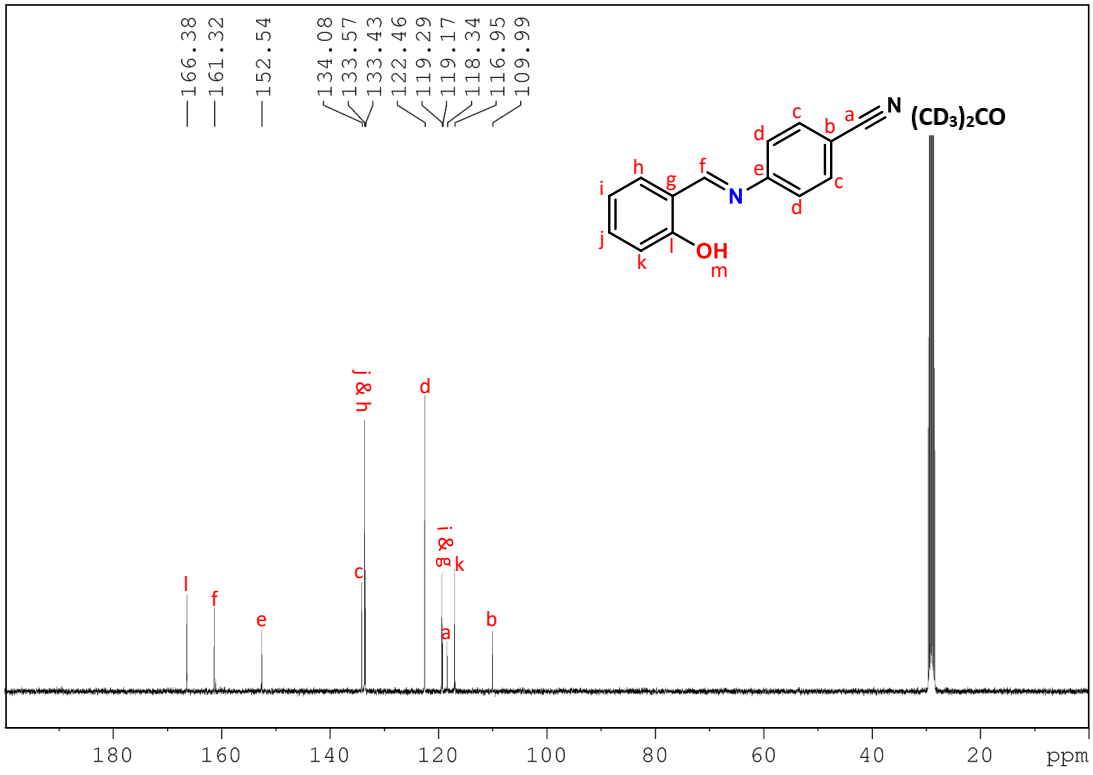

Figure A26: ^{13}C NMR spectrum of **L7**.

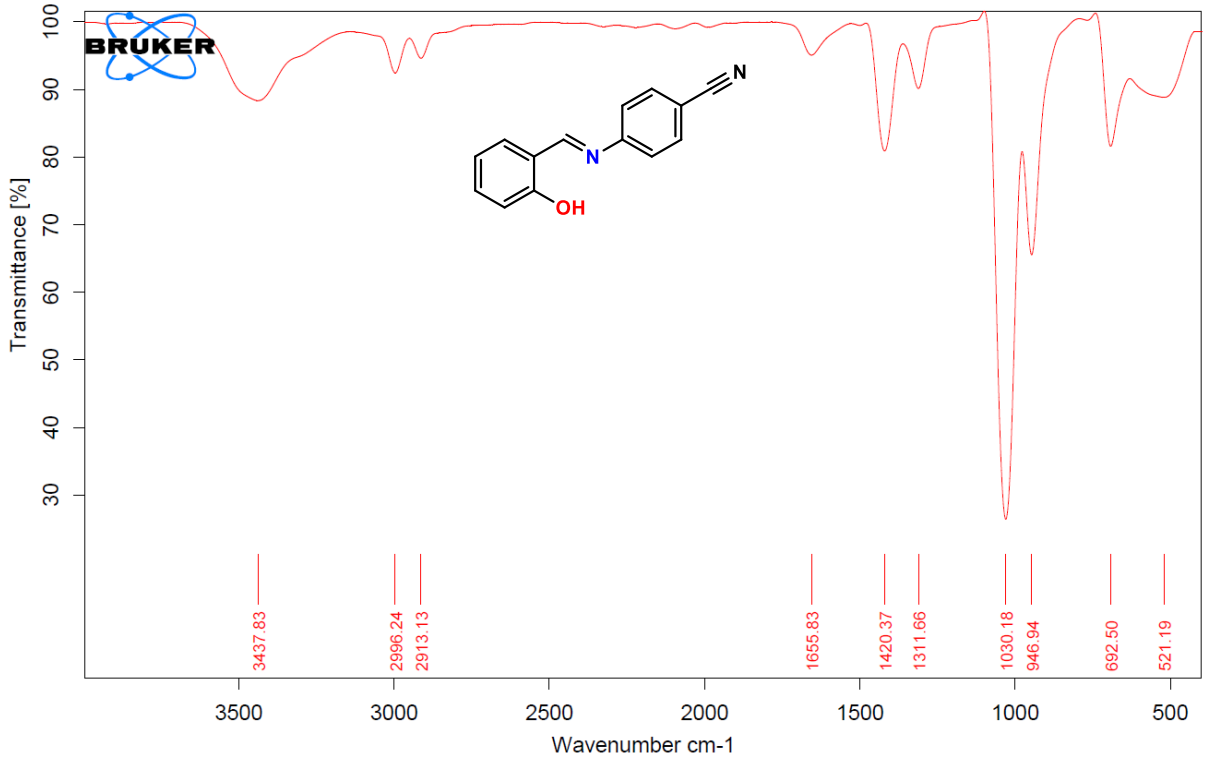

Figure A27: FTIR spectrum of **L7**.

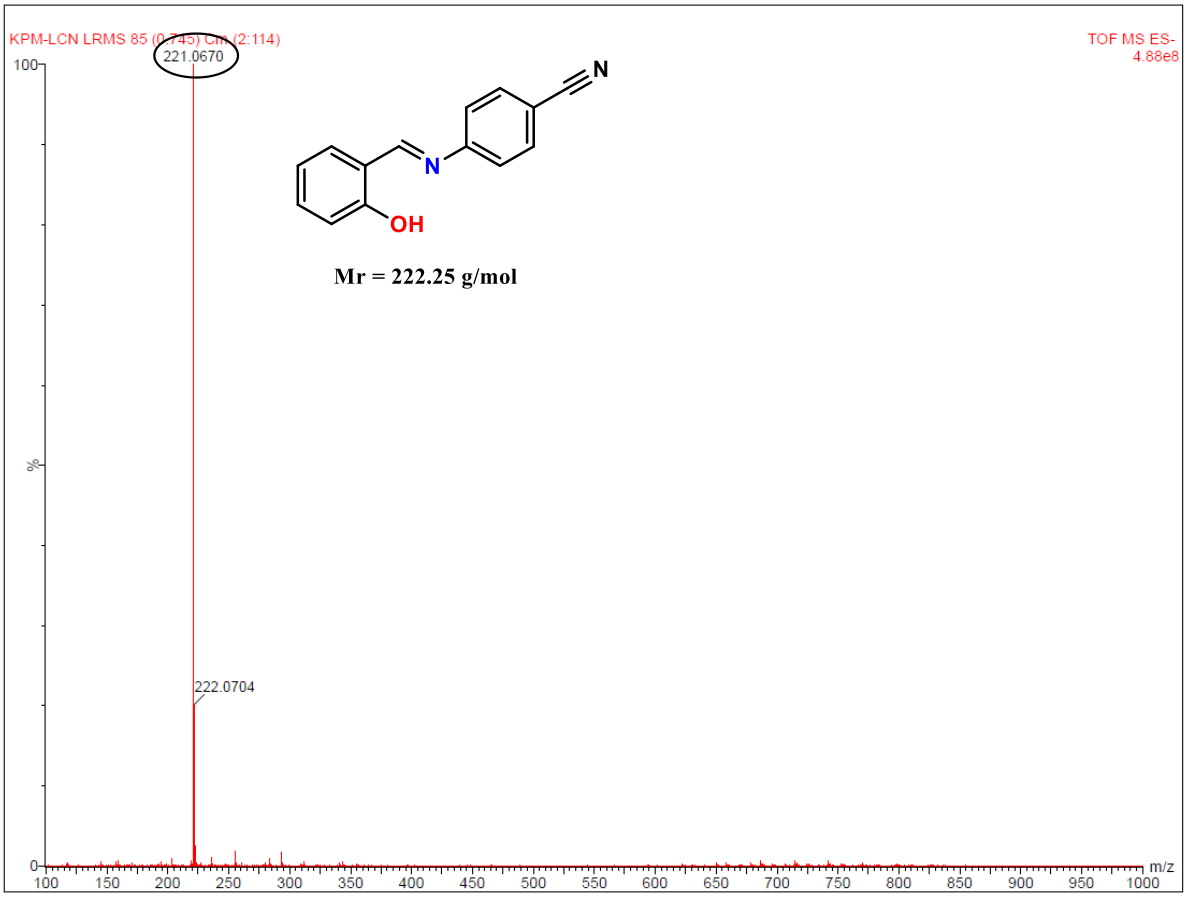

Figure A28: TOF-MS ES$^-$ spectrum of **L7**.

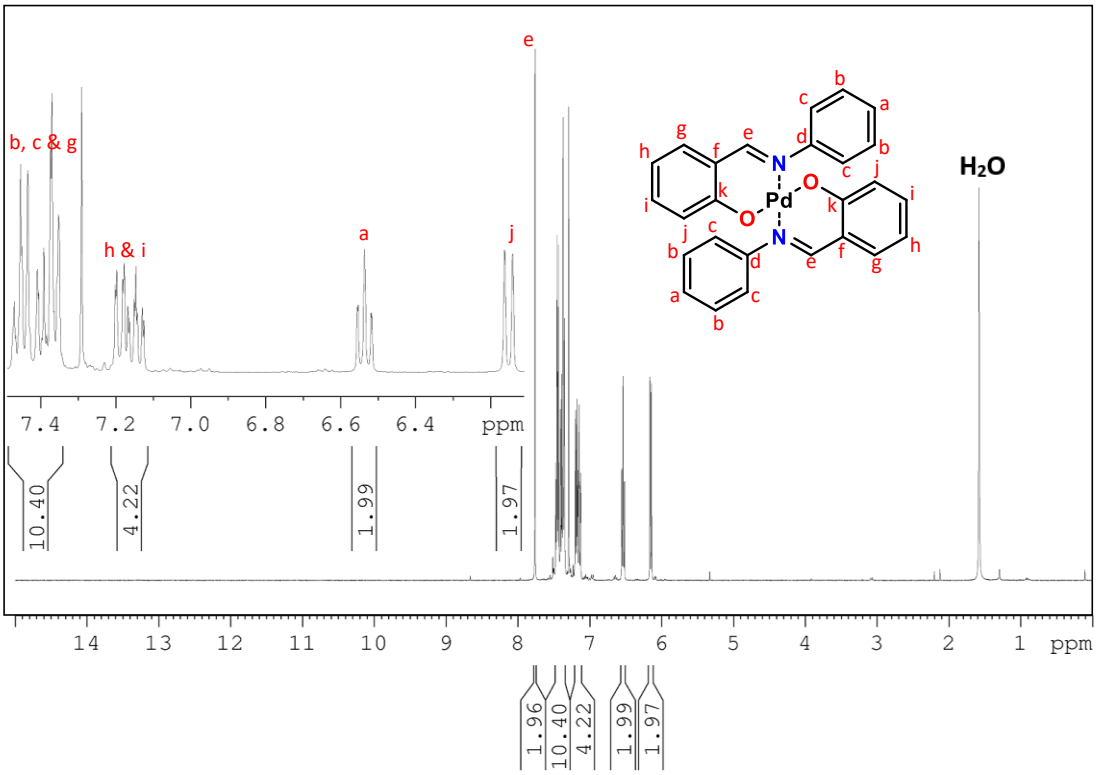

Figure A29: ^{1}H NMR spectrum of **PdC1**.

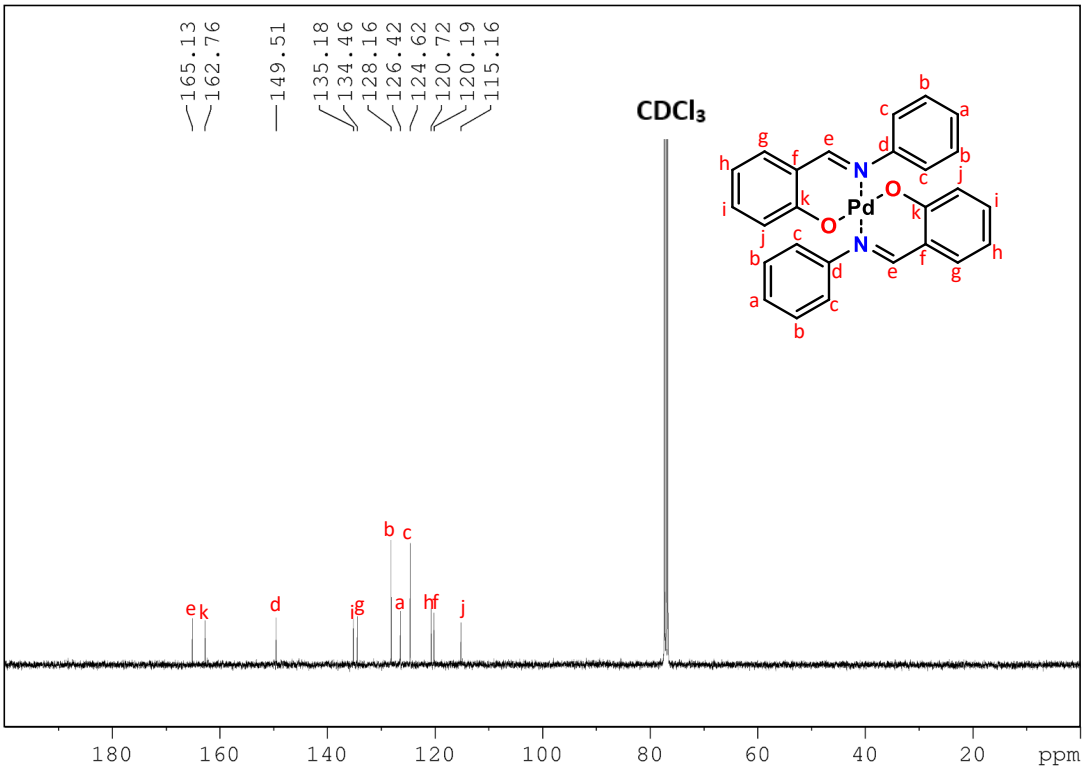

Figure A30: ^{13}C NMR spectrum of **PdC1**.

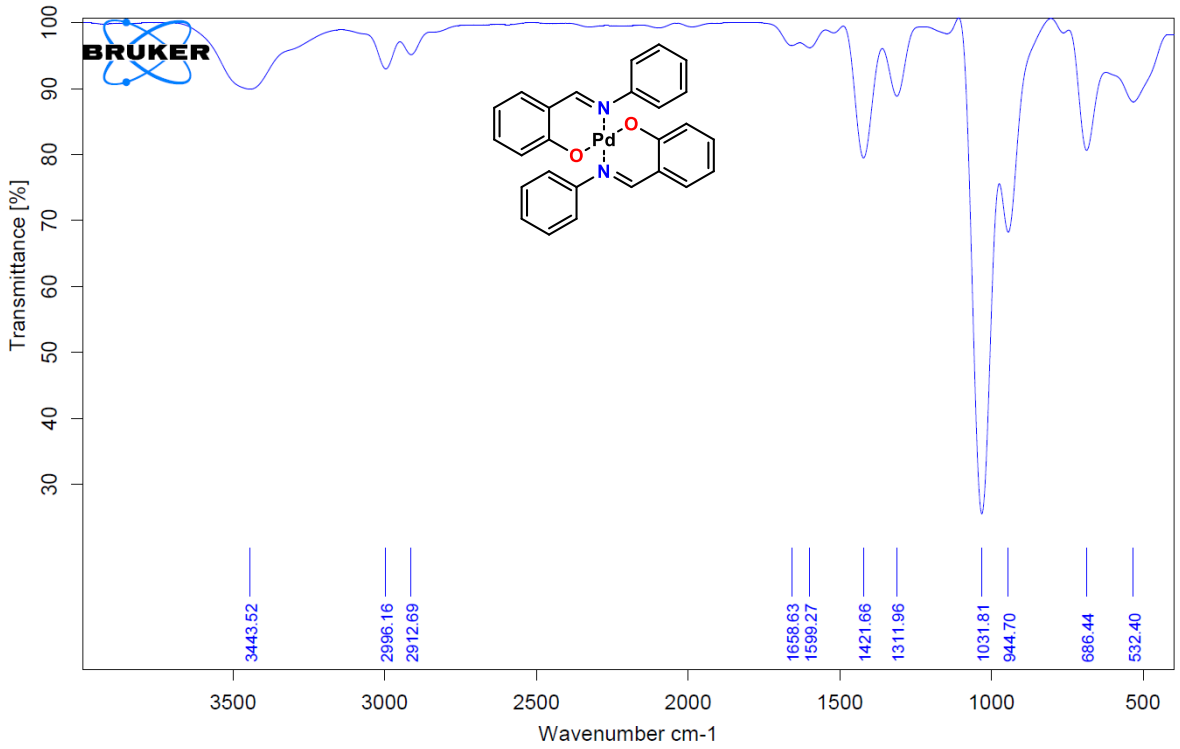

Figure A31: FTIR spectrum of **PdC1**.

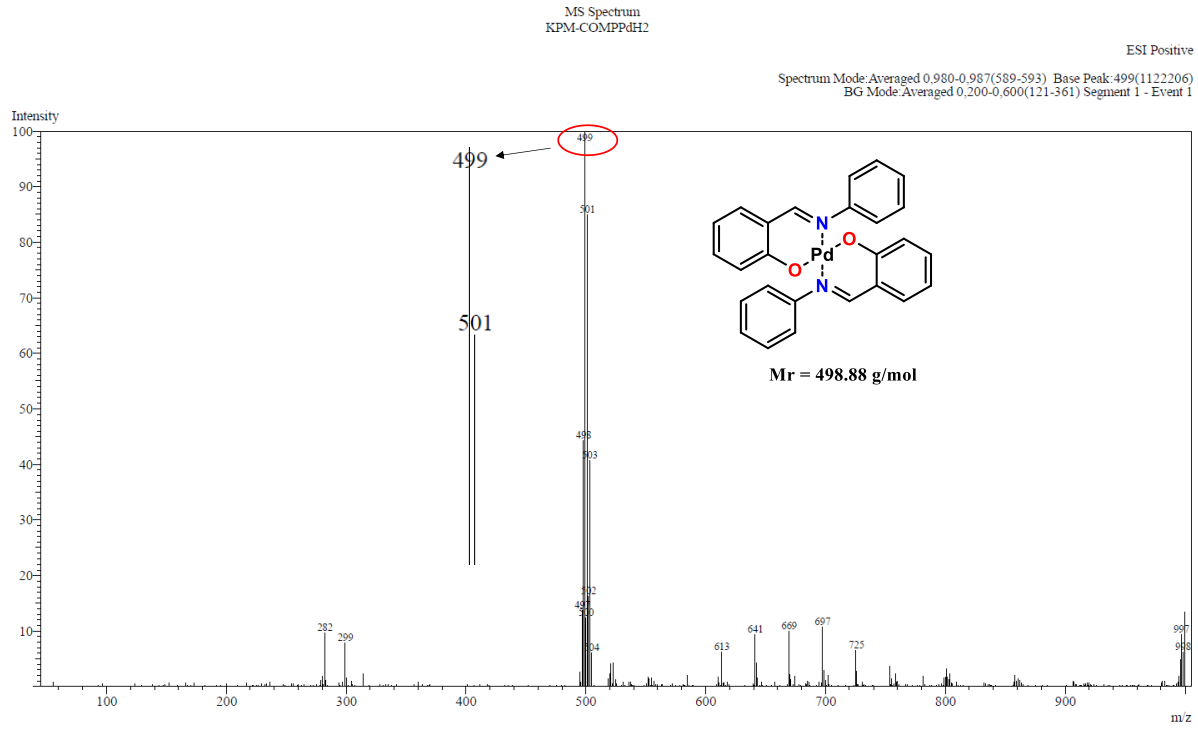

Figure A32: ESI^{+}- MS spectrum of **PdC1**.

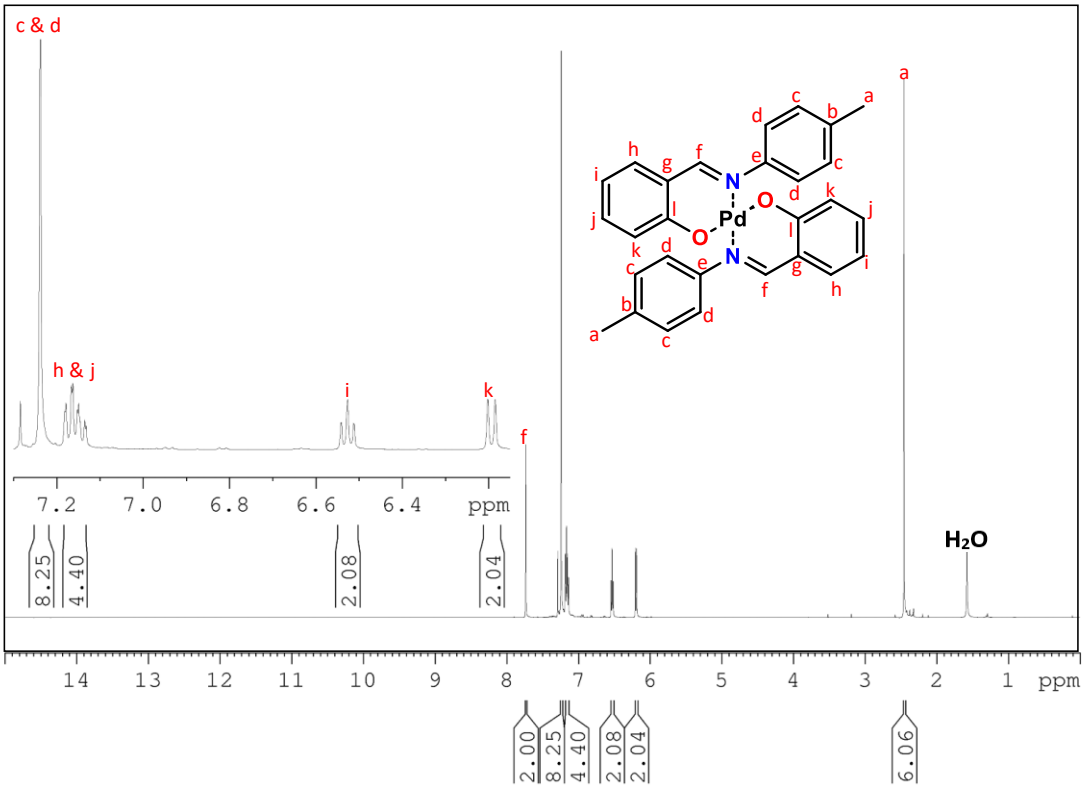

Figure A33: ^{1}H NMR spectrum of **PdC2**.

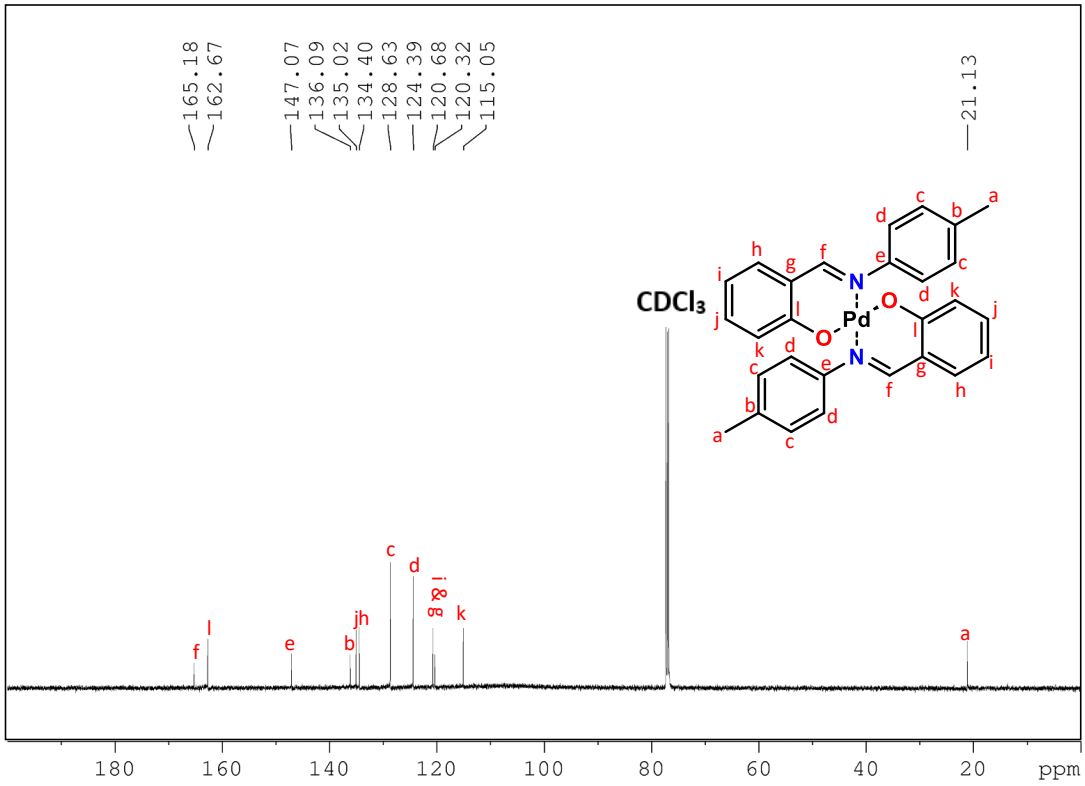

Figure A34: ^{13}C NMR spectrum of **PdC2**.

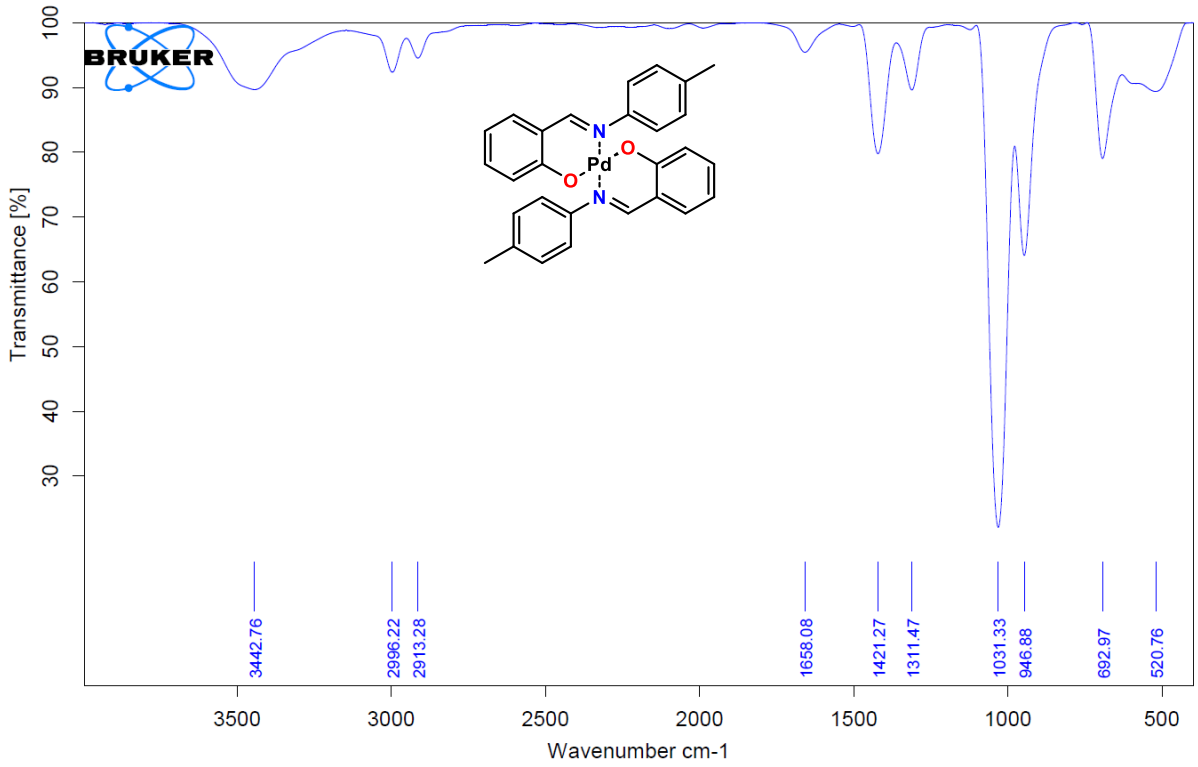

Figure A35: FTIR NMR spectrum of **PdC2**.

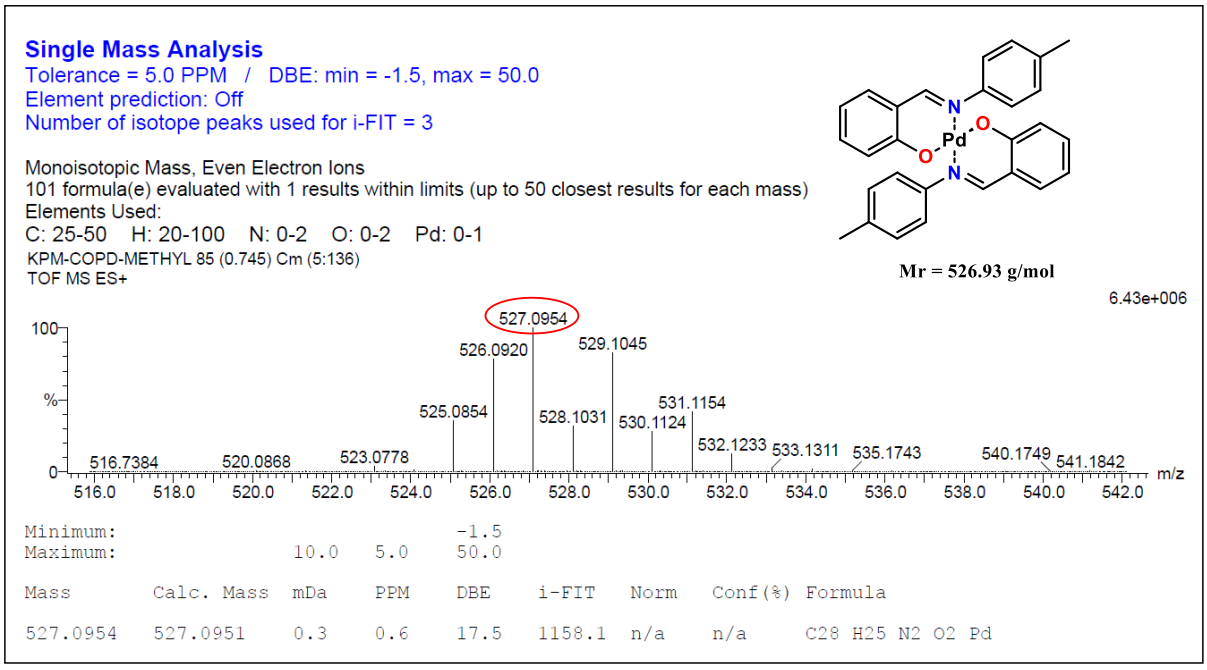

Figure A36: TOF-MS ES^+ spectrum of **PdC2**.

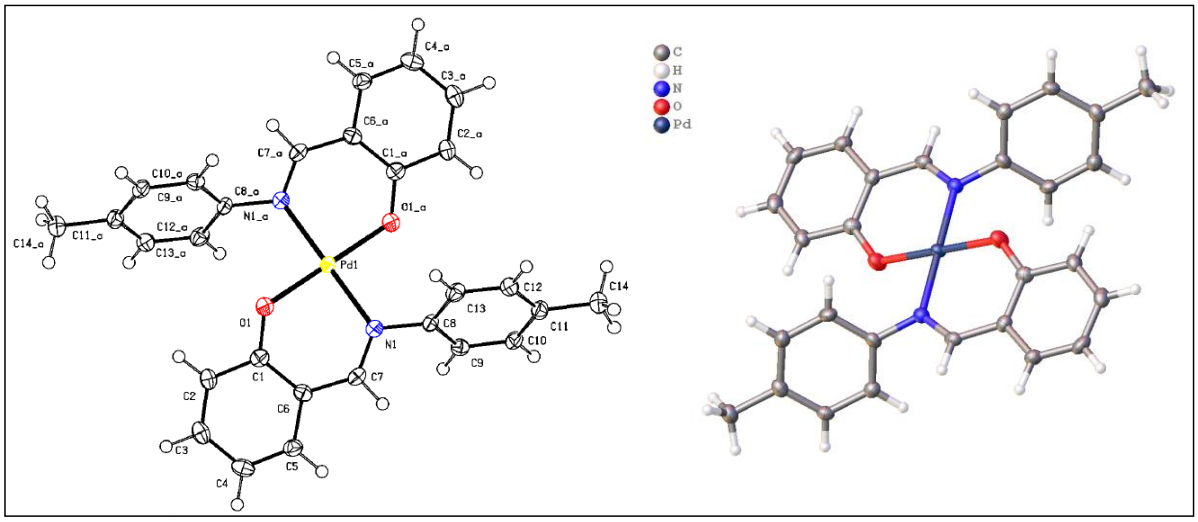

Figure A37: X-ray crystallographic structure of **PdC2**.

Table A1: Crystallographic bond angles of **PdC2**.

Atom	Atom	Atom	Angle/°	Atom	Atom	Atom	Angle/°
O1	Pd1	O1[1]	180.0	C4	C5	C6	121.6(3)
O1	Pd1	N1	91.36(10)	C12	C13	C8	119.4(3)
O1[1]	Pd1	N1	88.64(10)	C13	C12	C11	121.8(3)
O1[1]	Pd1	N1[1]	91.36(10)	C5	C6	C7	117.1(3)
O1	Pd1	N1[1]	88.64(10)	C5	C6	C1	118.9(3)
N1	Pd1	N1[1]	180.00(13)	C1	C6	C7	123.8(3)
C1	O1	Pd1	125.8(2)	O1	C1	C6	123.8(3)
C8	N1	Pd1	120.10(19)	O1	C1	C2	117.7(3)
C7	N1	Pd1	123.7(2)	C2	C1	C6	118.4(3)
C7	N1	C8	116.0(3)	C3	C2	C1	120.3(3)
C9	C8	N1	119.7(3)	C10	C11	C14	120.8(3)
C9	C8	C13	120.1(3)	C12	C11	C10	117.8(3)
C13	C8	N1	120.2(3)	C12	C11	C14	121.4(3)
C9	C10	C11	121.1(3)	C2	C3	C4	121.8(3)
N1	C7	C6	126.9(3)	C5	C4	C3	118.9(3)
C8	C9	C10	119.7(3)				

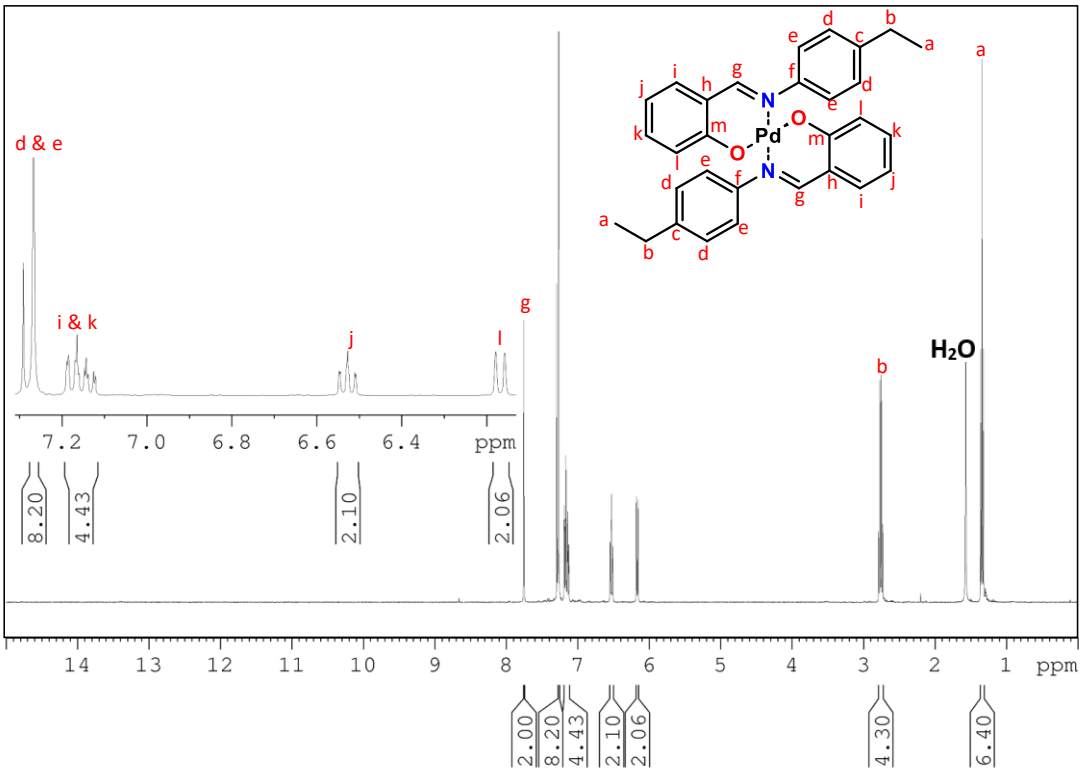

Figure A38: ^{1}H NMR spectrum of **PdC3**.

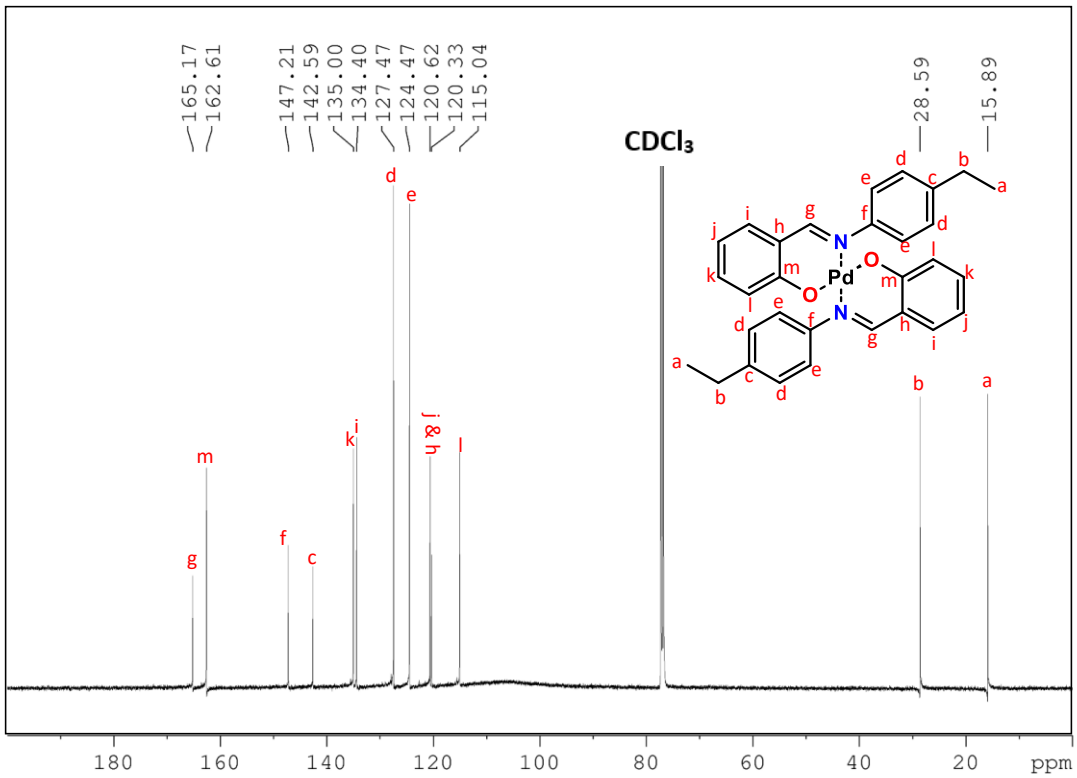

Figure A39: ^{13}C NMR spectrum of **PdC3**.

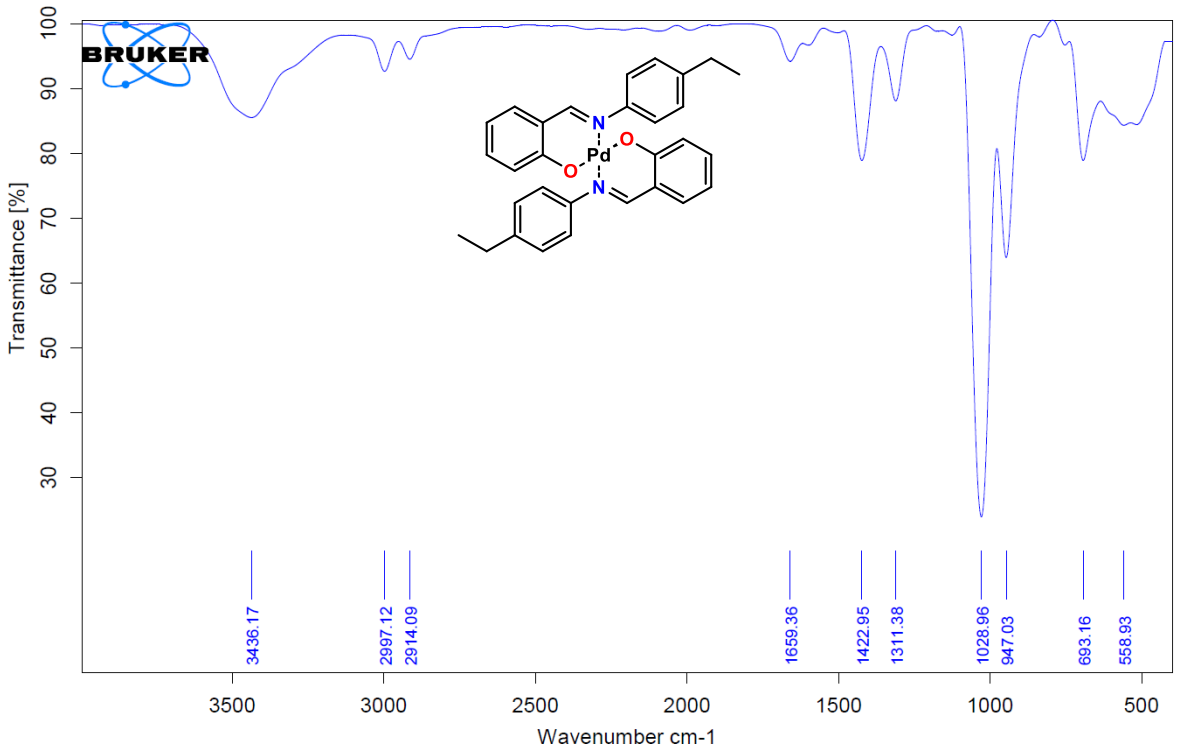

Figure A40: FTIR spectrum of **PdC3**.

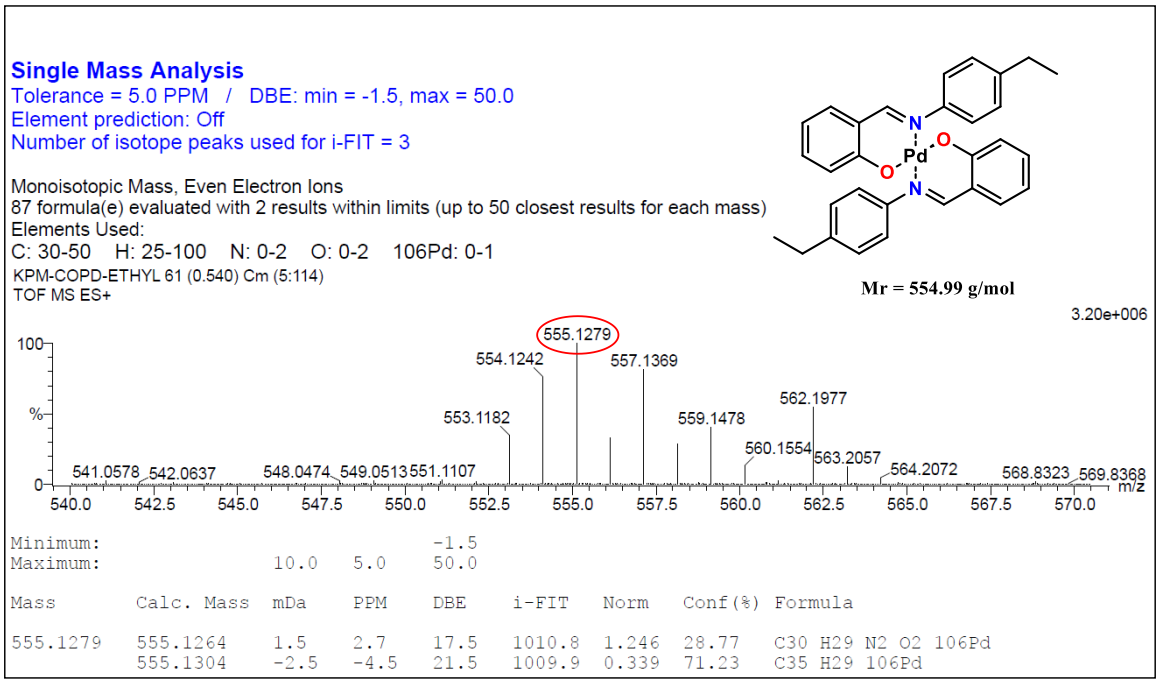

Figure A41: TOF- MS ES^+ spectrum of **PdC3**.

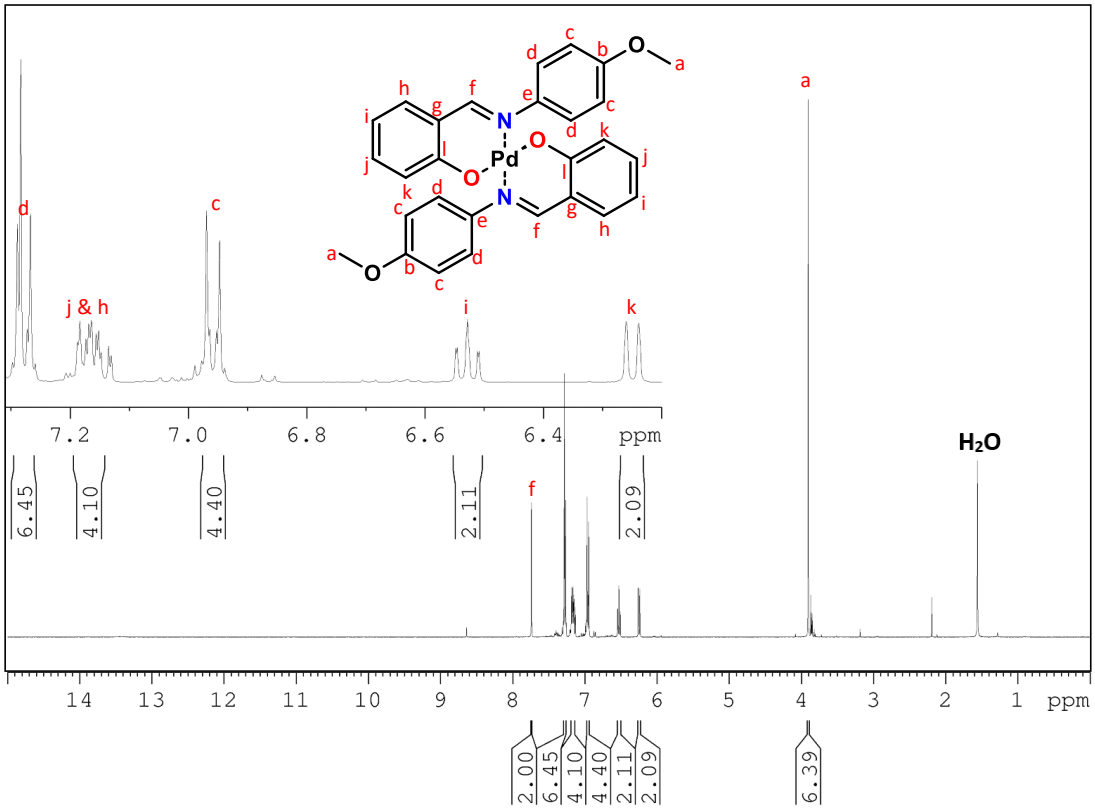

Figure A42: ^{1}H NMR spectrum of **PdC4**.

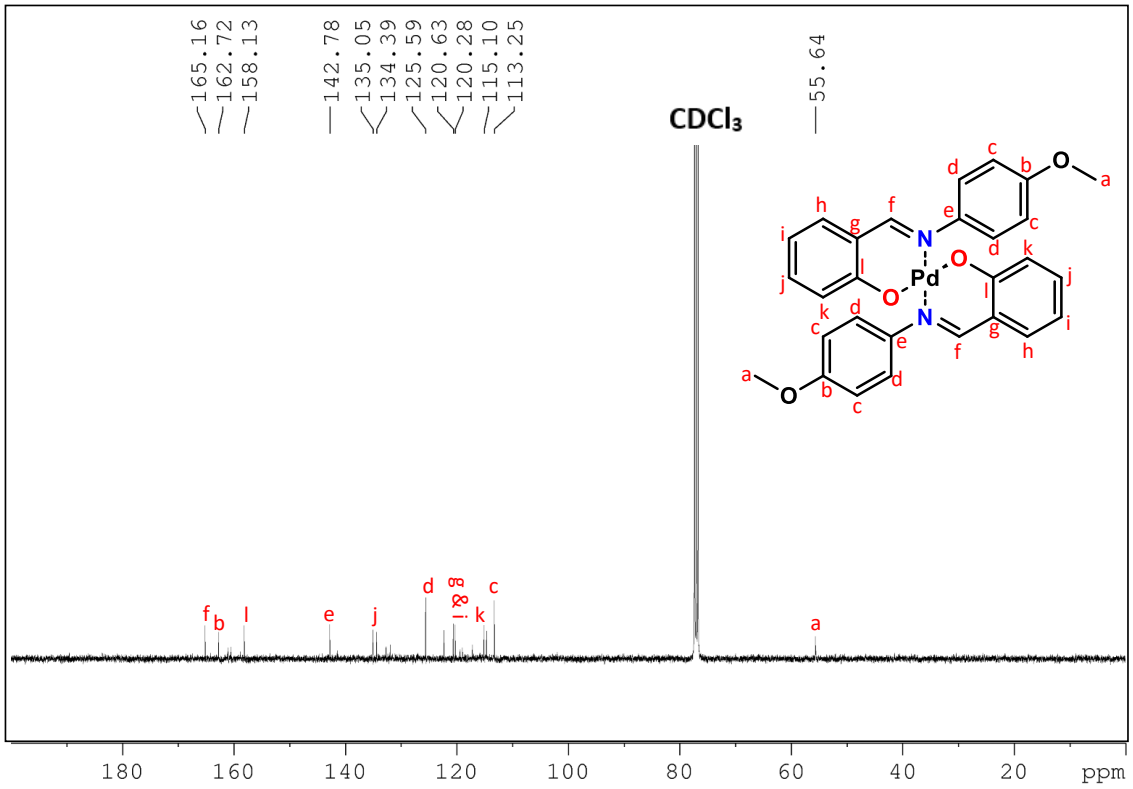

Figure A43: ^{13}C spectrum of **PdC4**.

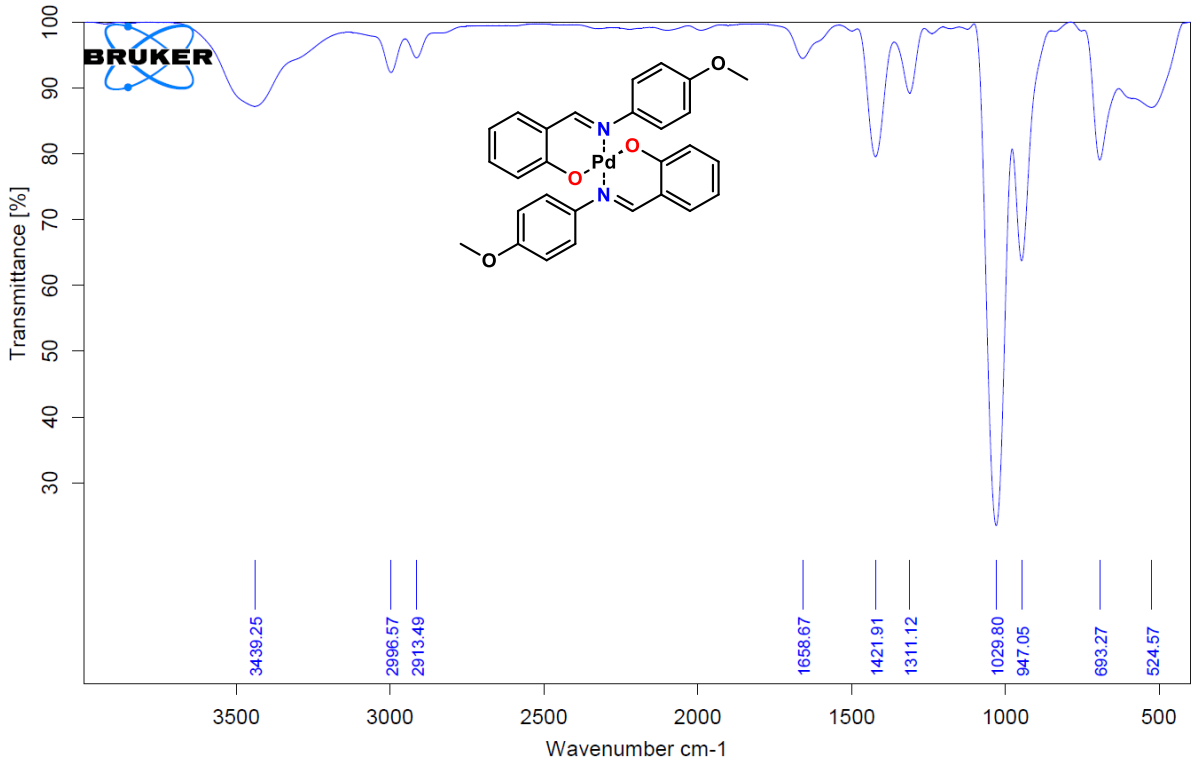

Figure A44: FTIR spectrum of **PdC4**.

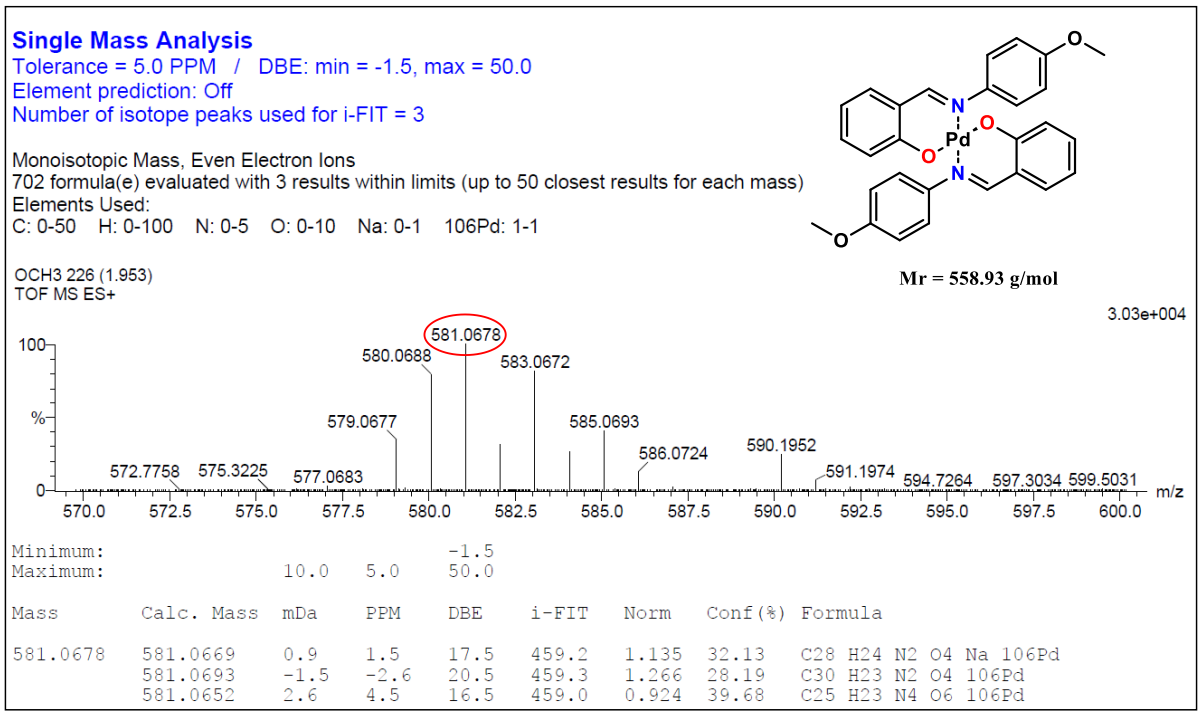

Figure A45: TOF- MS ES$^+$ spectrum of **PdC4**.

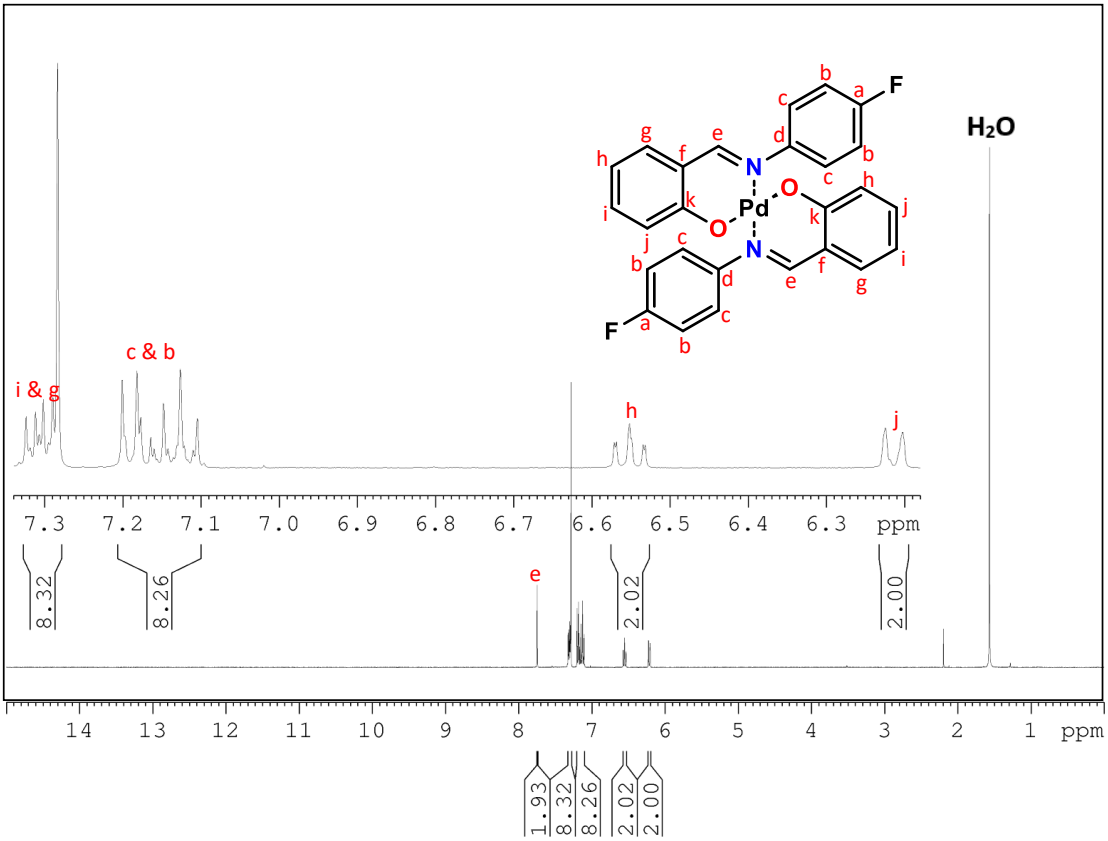

Figure A46: ^{1}H NMR spectrum of **PdC5**.

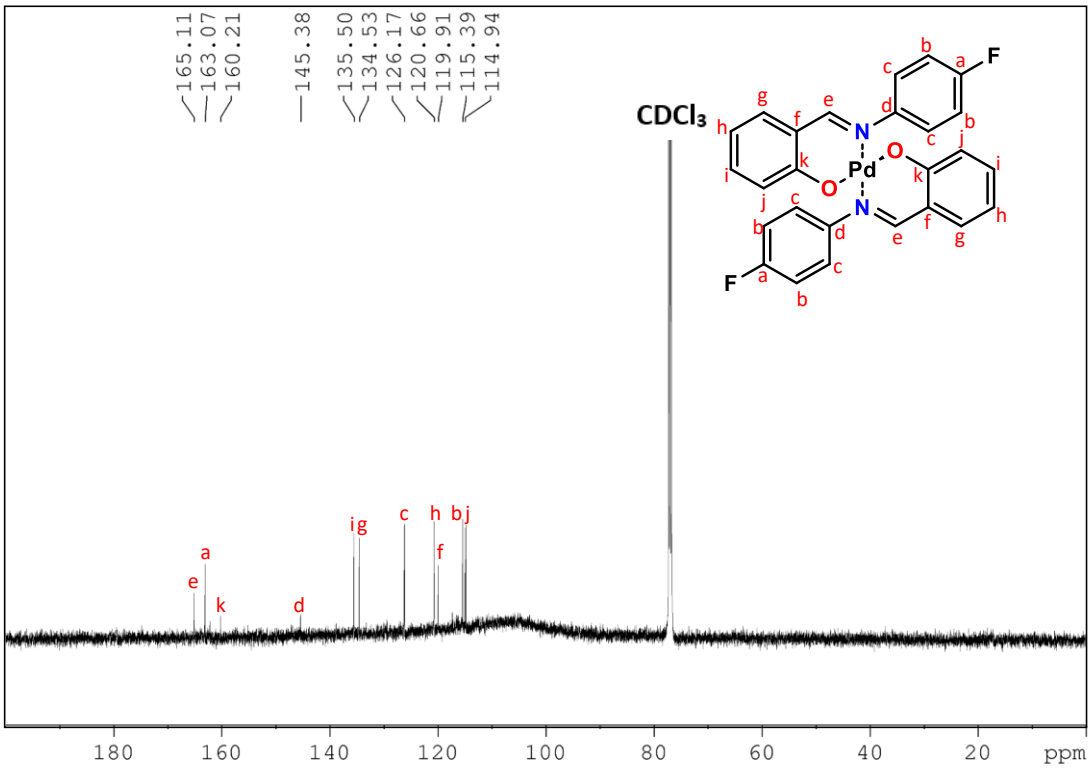

Figure A47: ^{13}C NMR spectrum of **PdC5**.

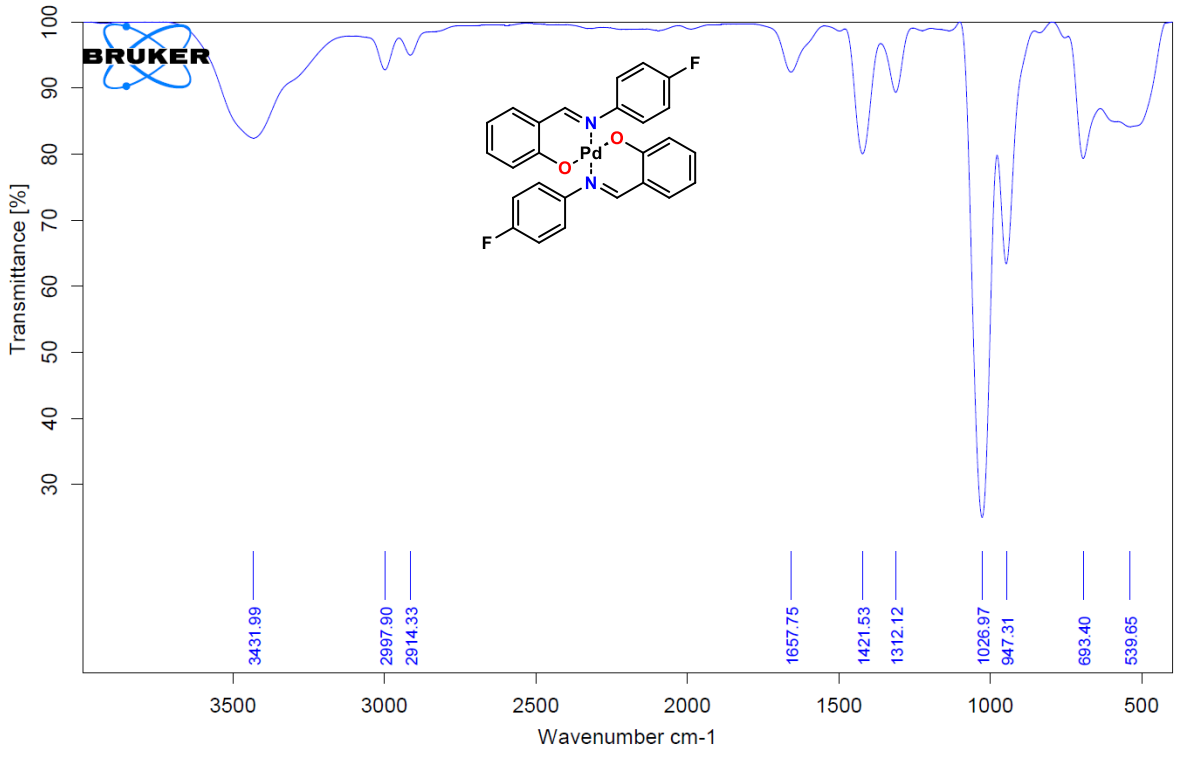

Figure A48: FTIR spectrum of **PdC5**.

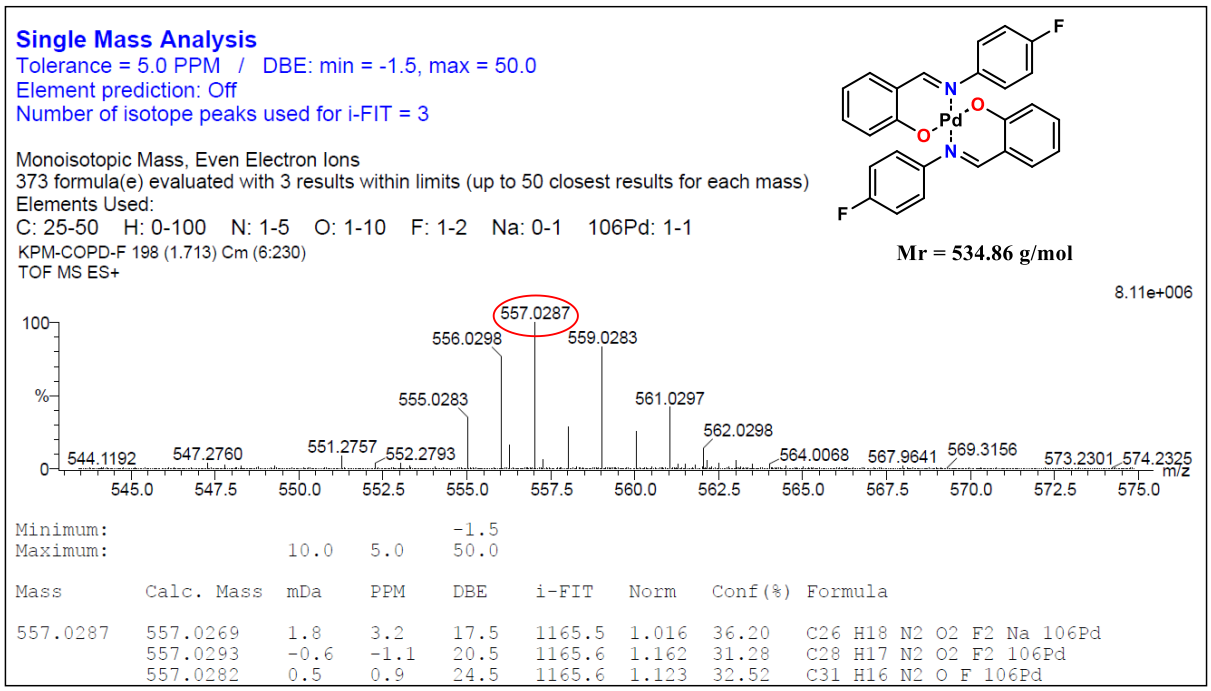

Figure A49: TOF- MS ES$^+$ spectrum of **PdC5**.

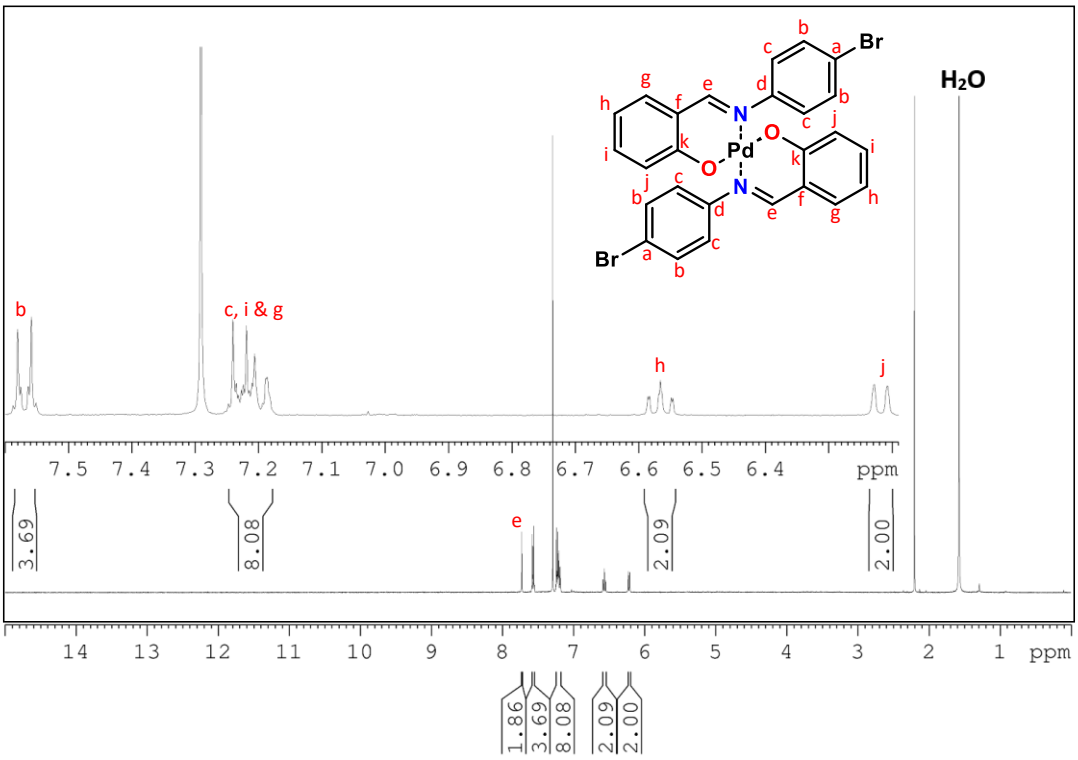

Figure A50: ^{1}H NMR spectrum of **PdC6**.

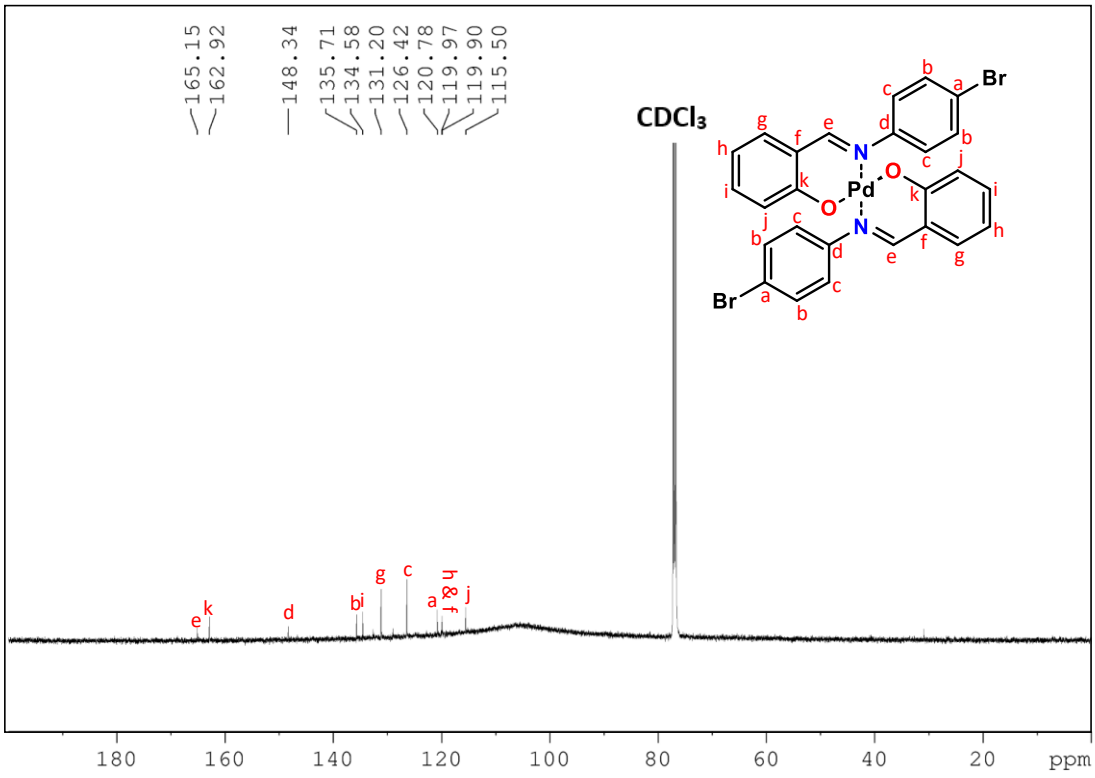

Figure A51: ^{13}C NMR spectrum of **PdC6**.

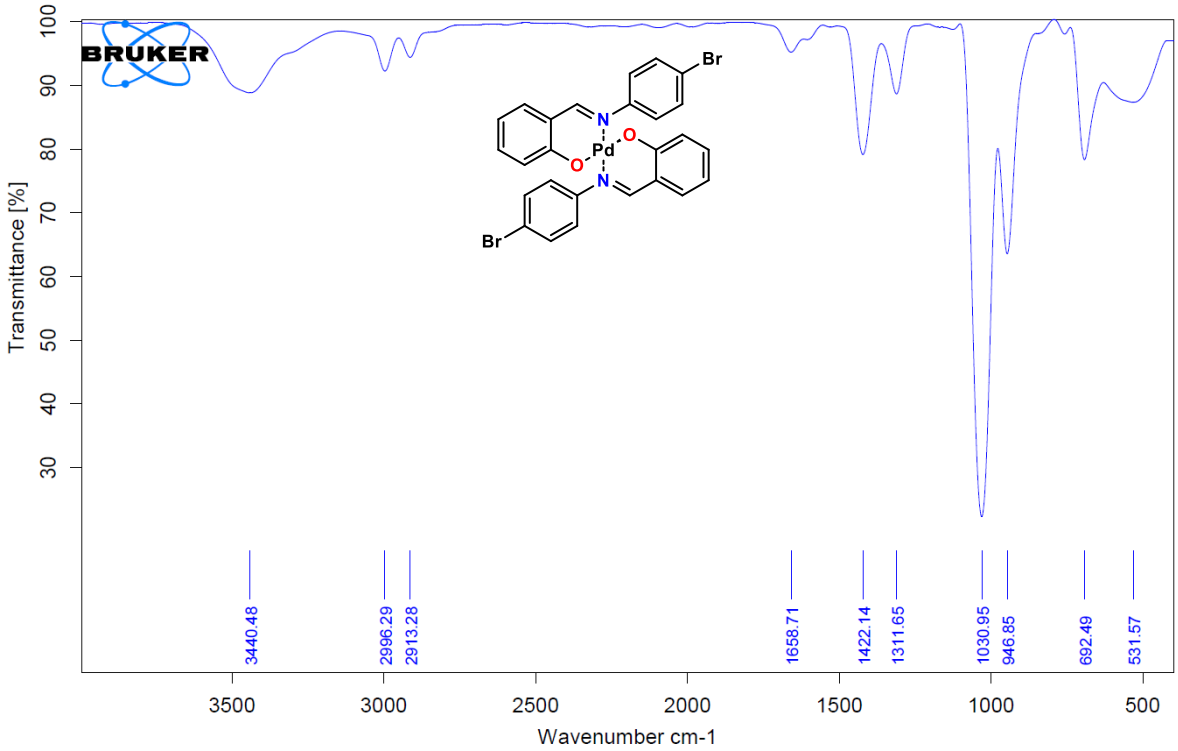

Figure A52: FTIR spectrum of **PdC6**.

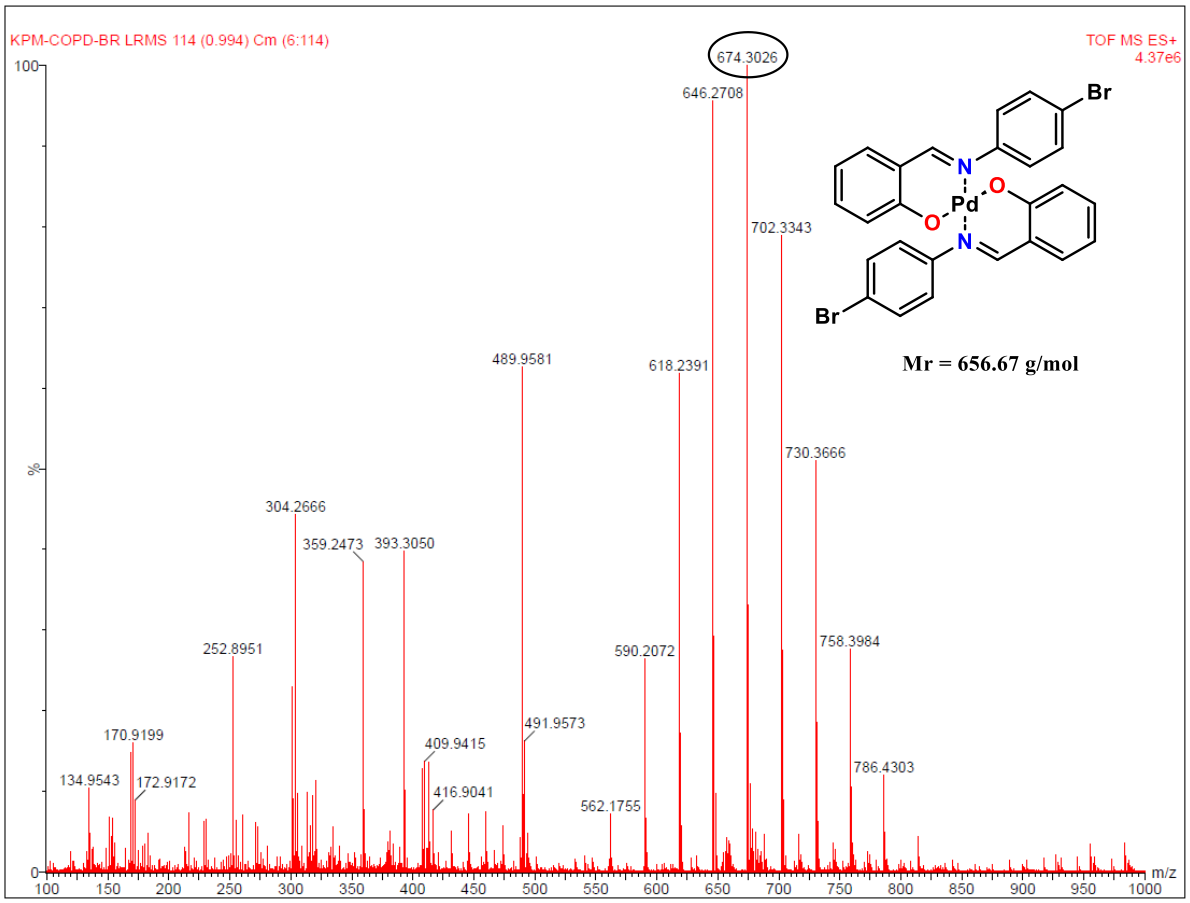

Figure A53: TOF- MS ESI^{+} spectrum of **PdC6**.

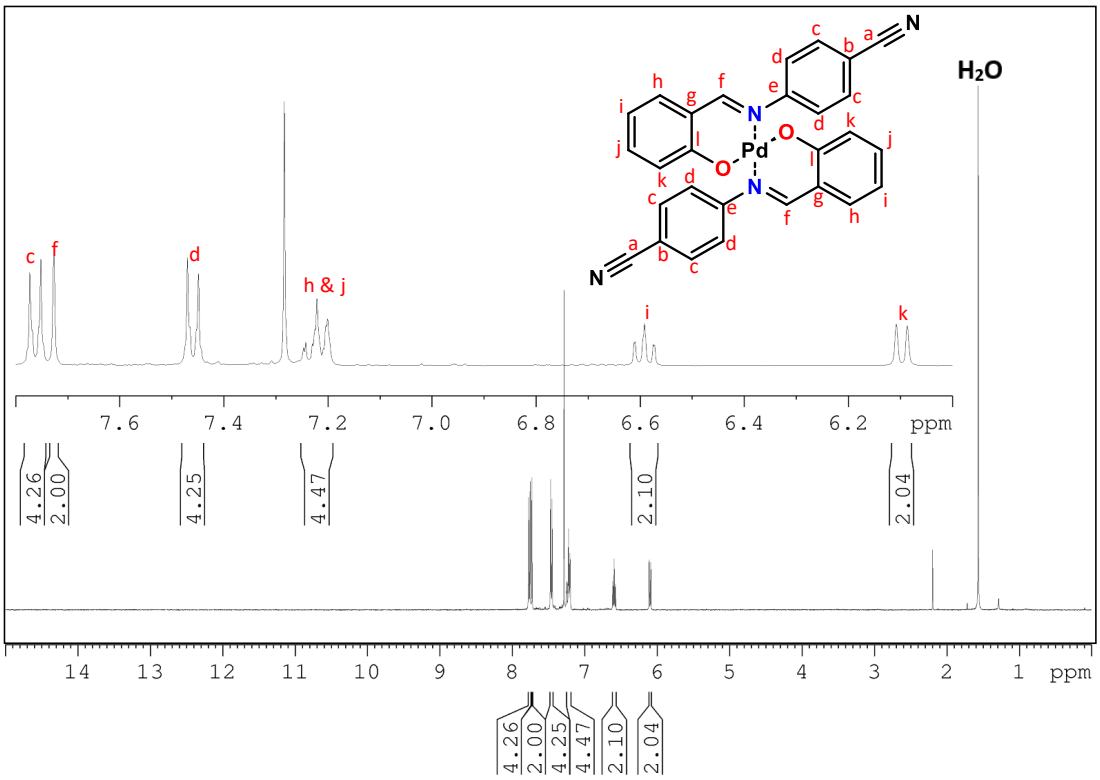

Figure A54: ^{1}H NMR spectrum of **PdC7**.

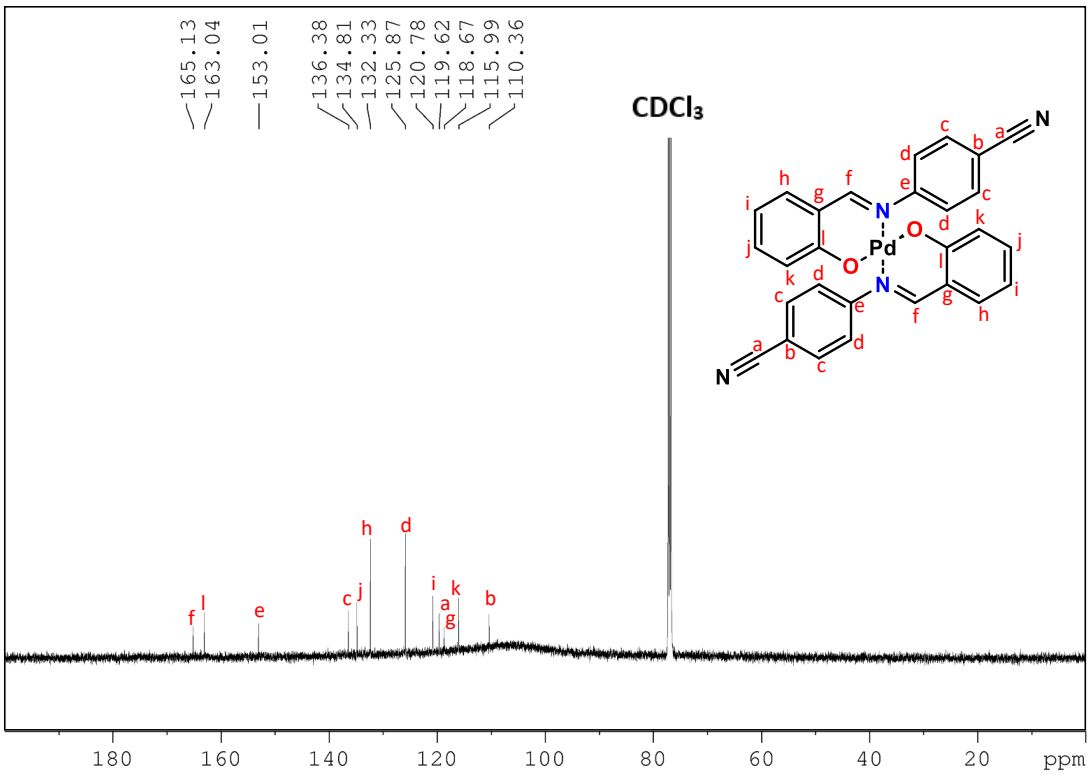

Figure A55: ^{13}C NMR spectrum of **PdC7**.

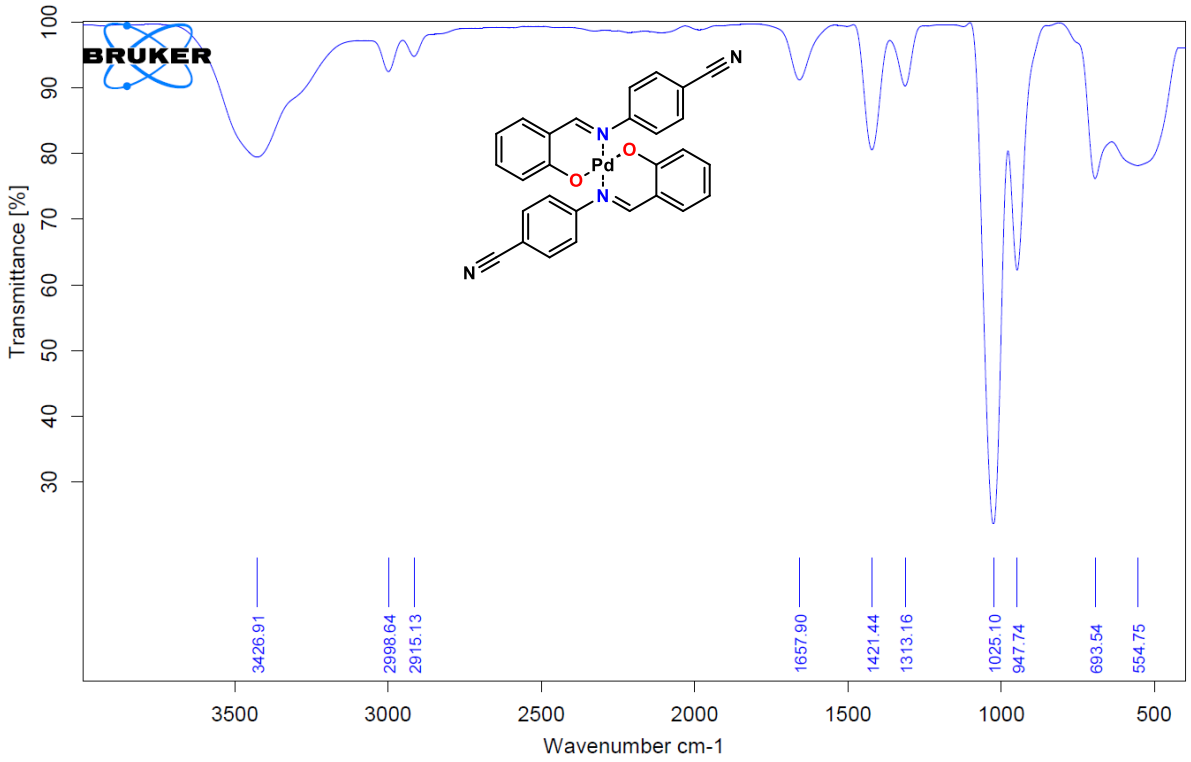

Figure A56: FTIR spectrum of **PdC7**.

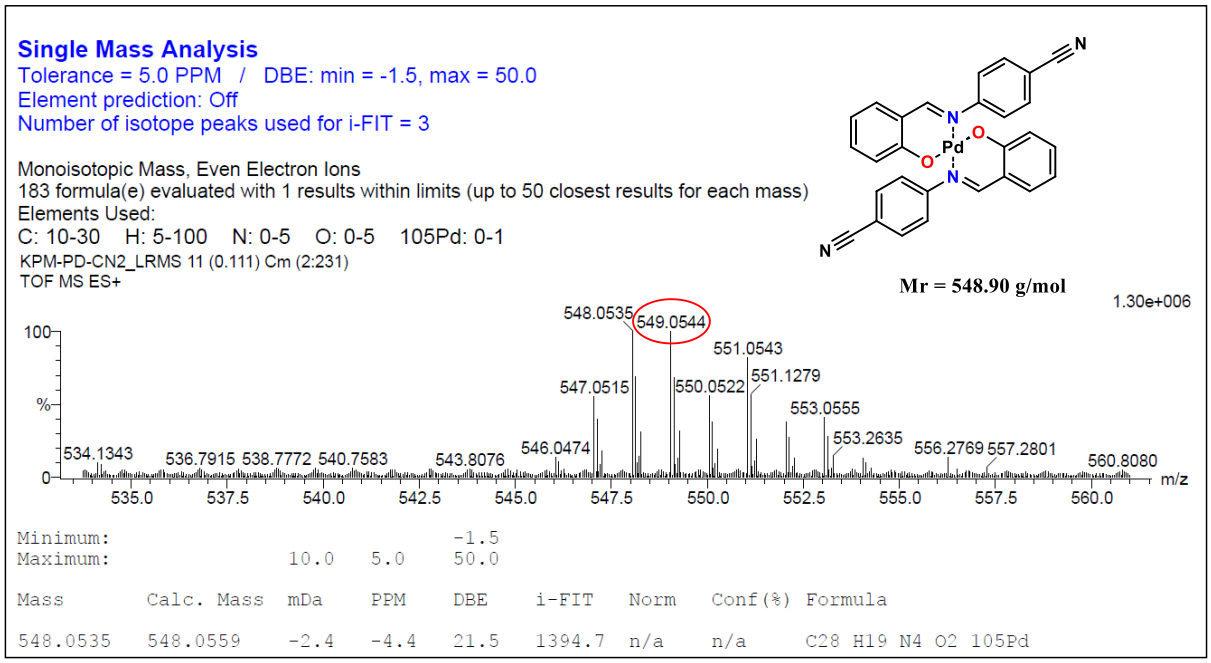

Figure A57: TOF-MS ES^+ spectrum of **PdC7**.

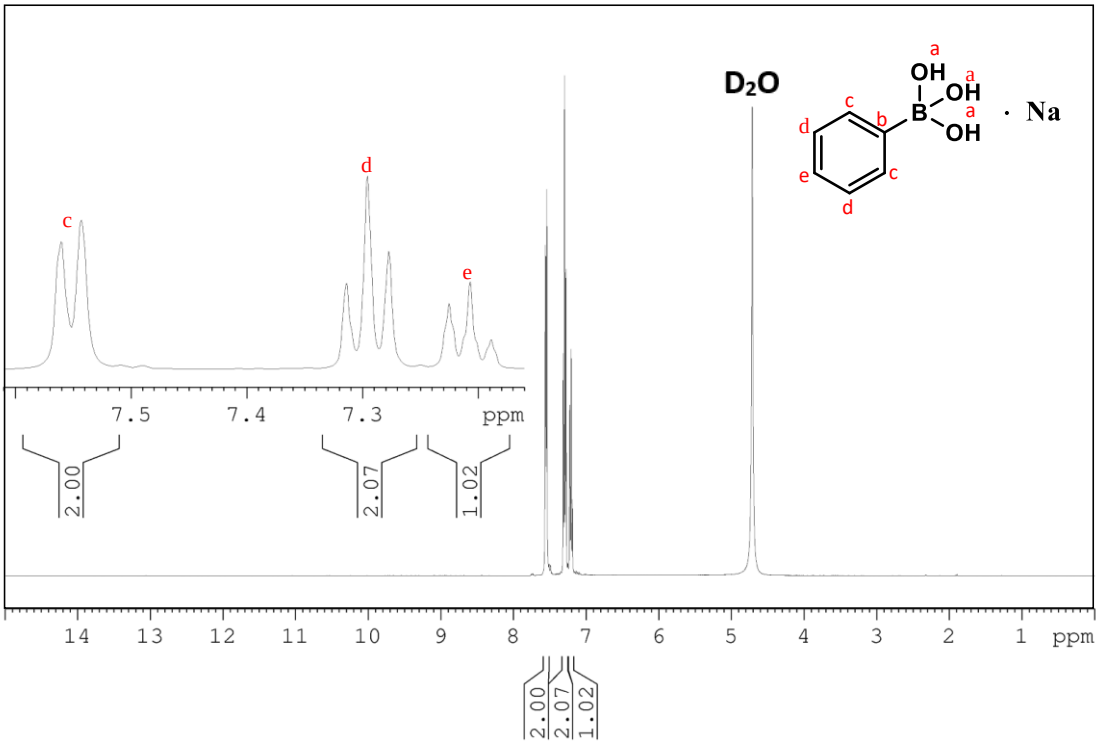

Figure A58: ^{1}H NMR spectrum of Sodiumphenylboric acid **115**.

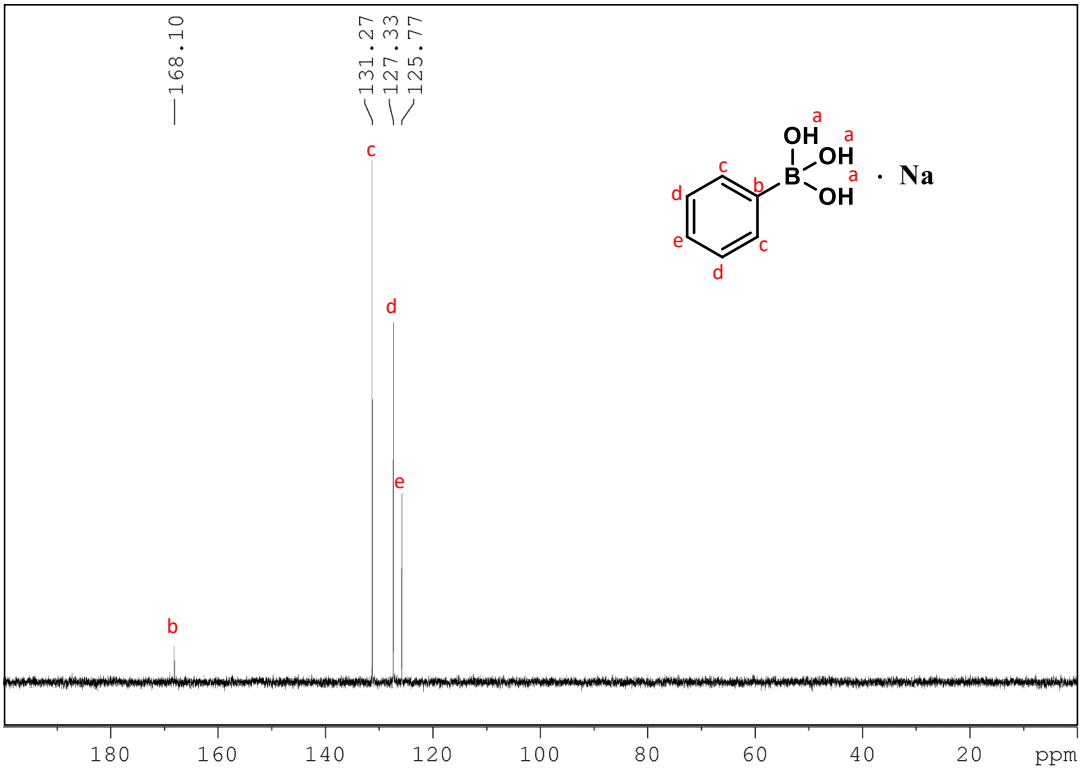

Figure A59: ^{13}C NMR spectrum of Sodiumphenylboric acid **115**.

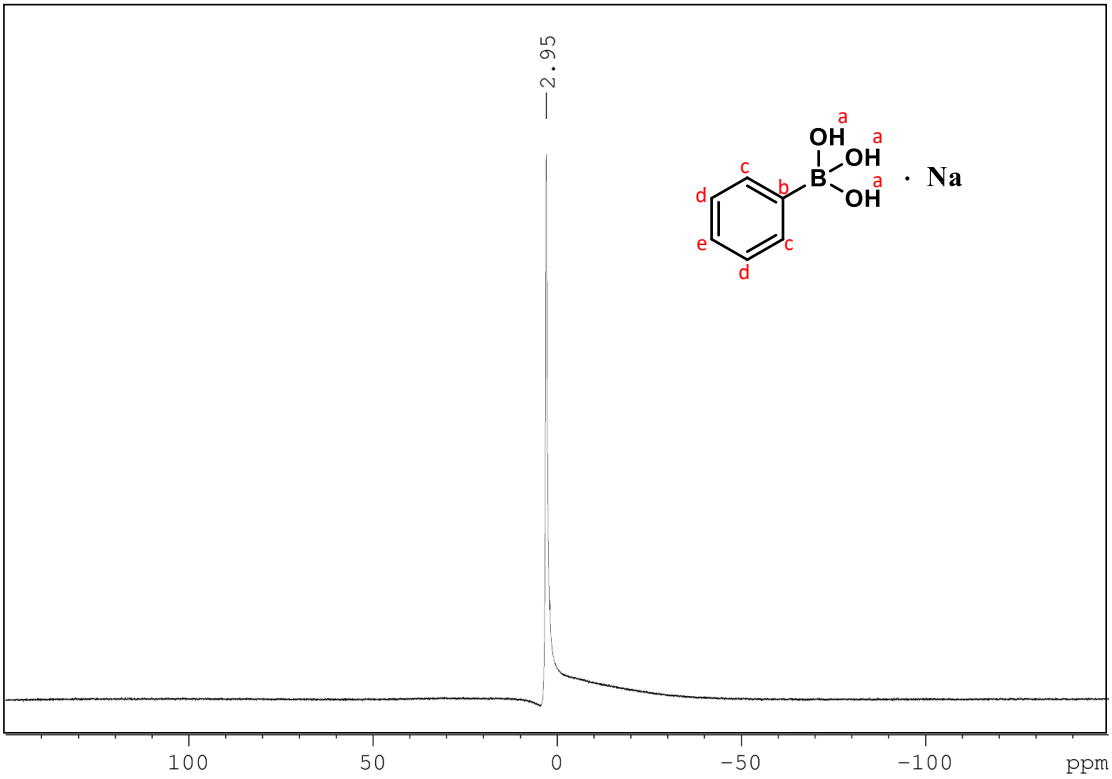

Figure A60: ^{11}B NMR spectrum of Sodiumphenylboric acid **115**.

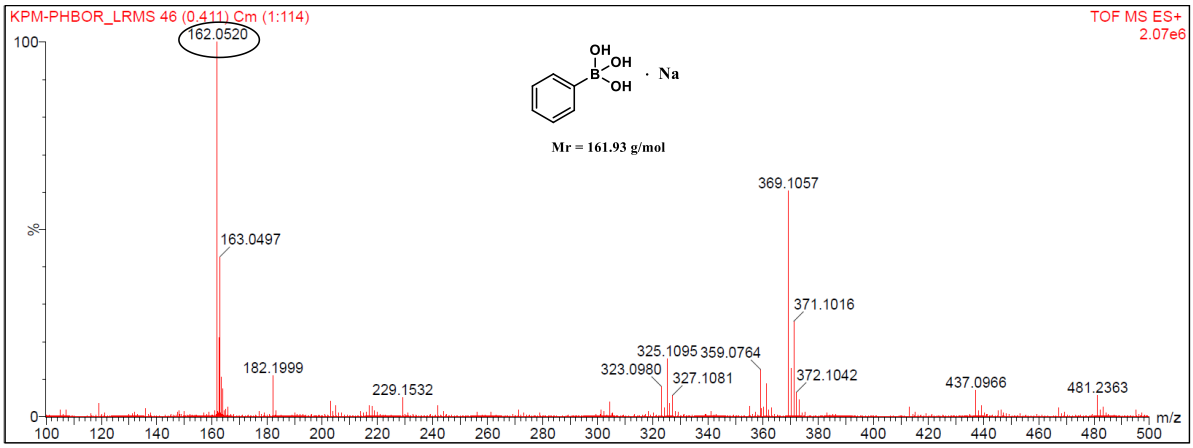

Figure A61: TOF- MS ESI^{+} spectrum of Sodiumphenylboric acid **115**.

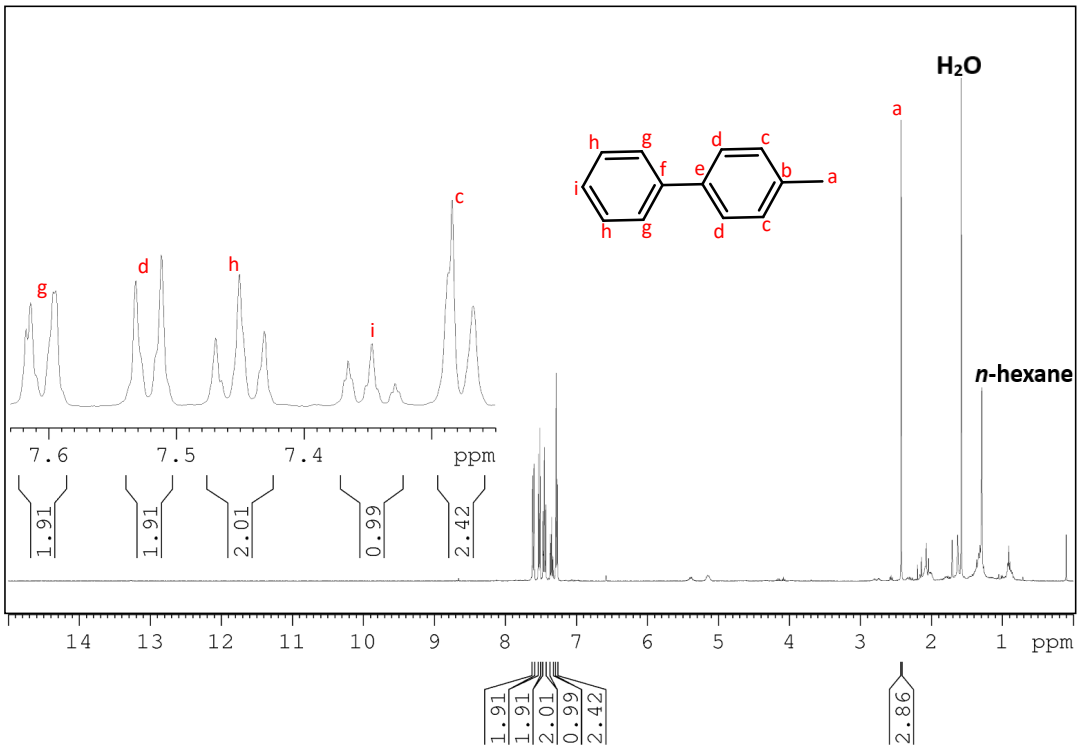

Figure A62: ^{1}H NMR spectrum of 4-Methyl biphenyl **117**.

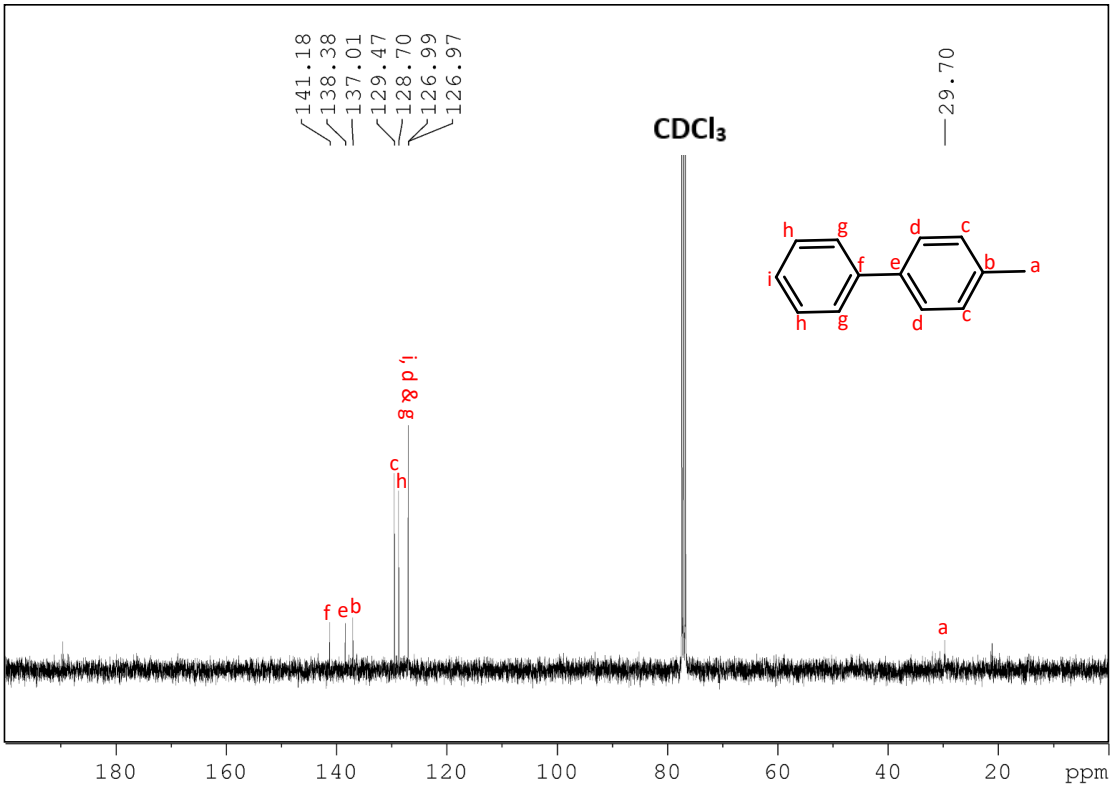

Figure A63: ^{13}C NMR spectrum of 4-Methyl biphenyl **117**.

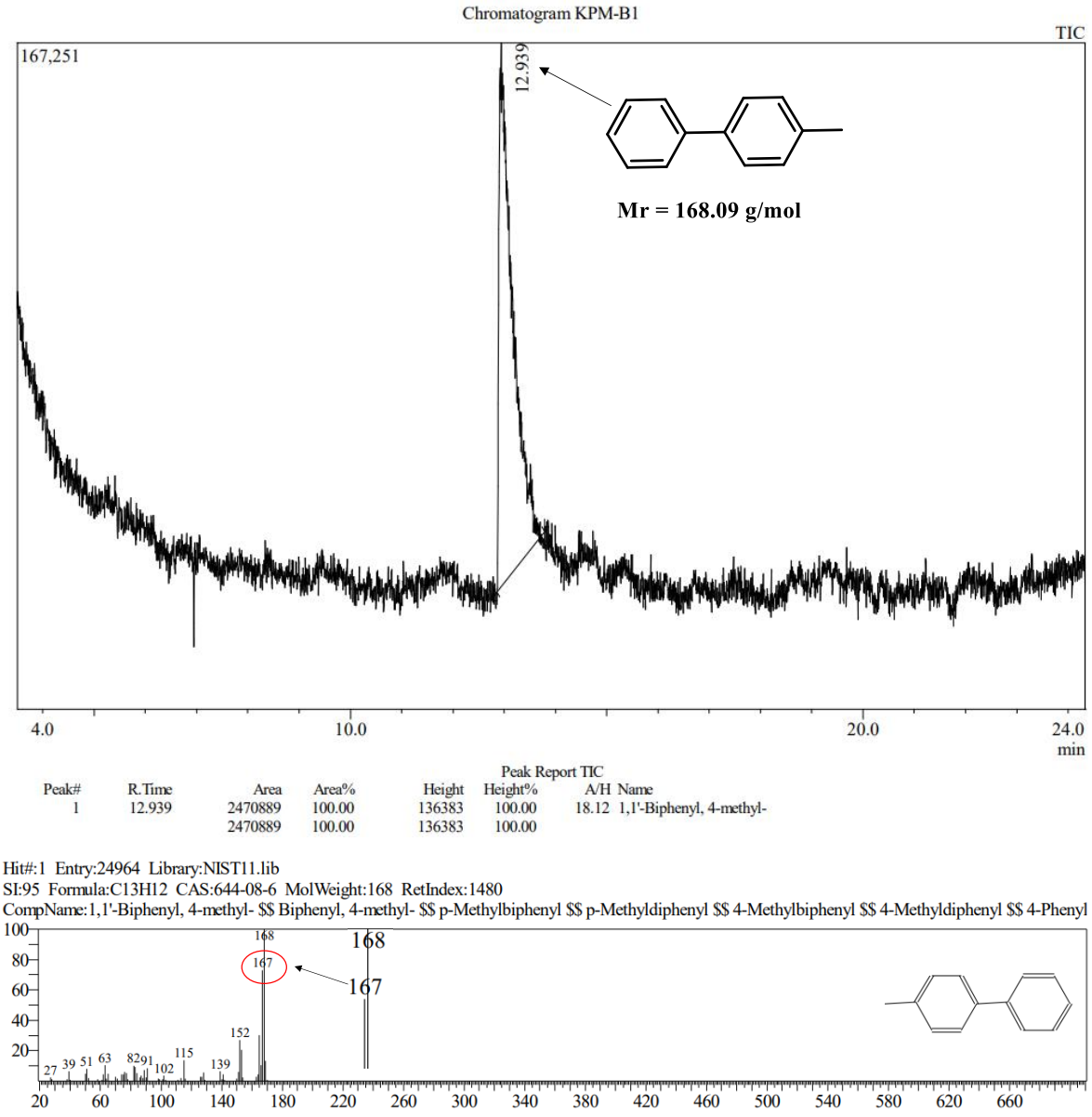

Figure A64: GC-MS chromatogram and MS spectrum of **117**.

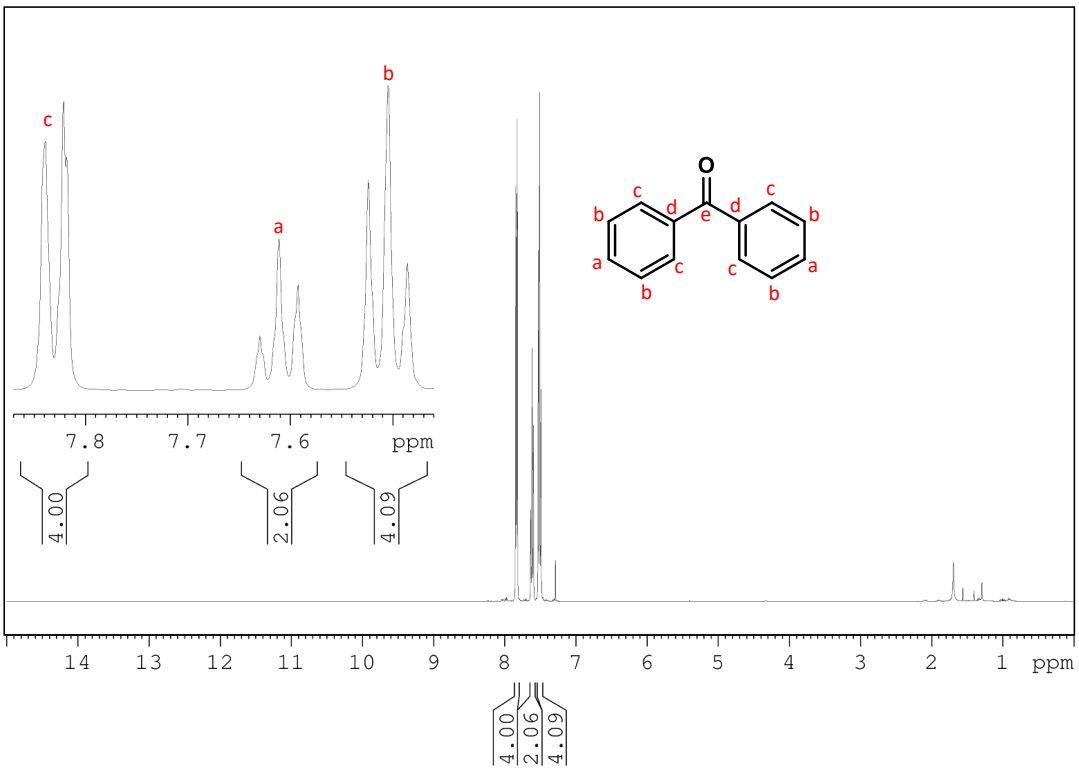

Figure A65: ^{1}H NMR of **119**.

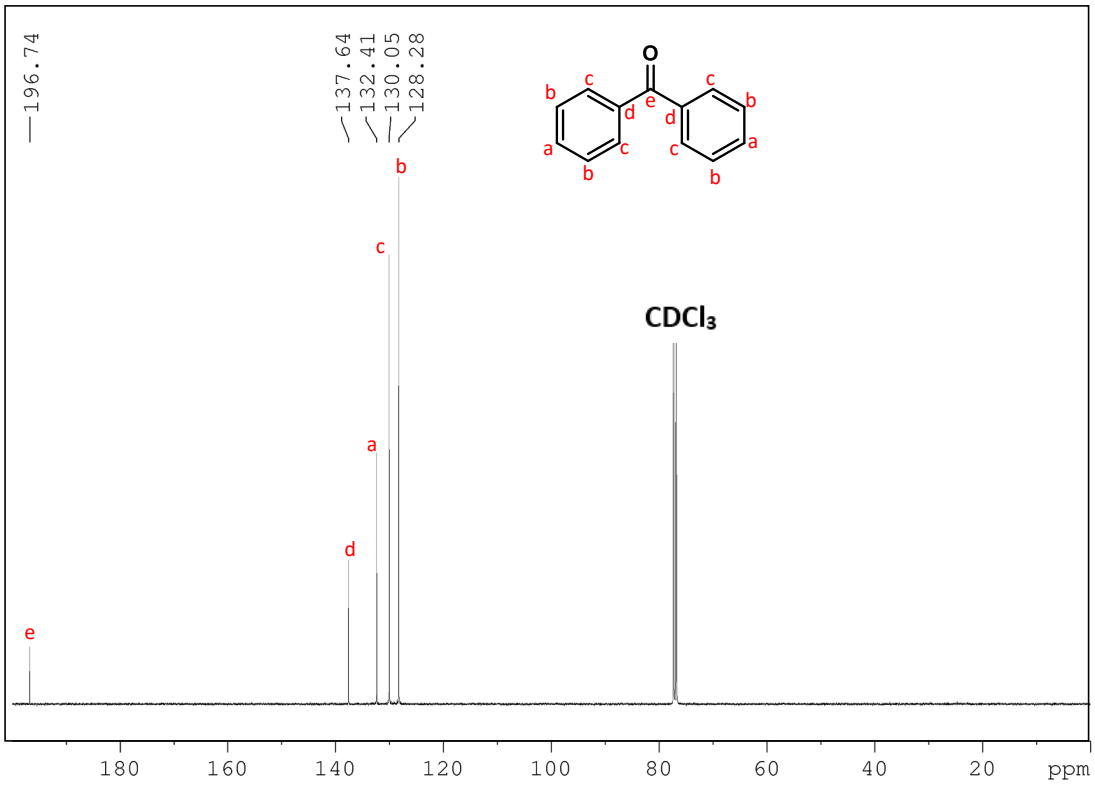

Figure A66: ^{13}C NMR of **119**.

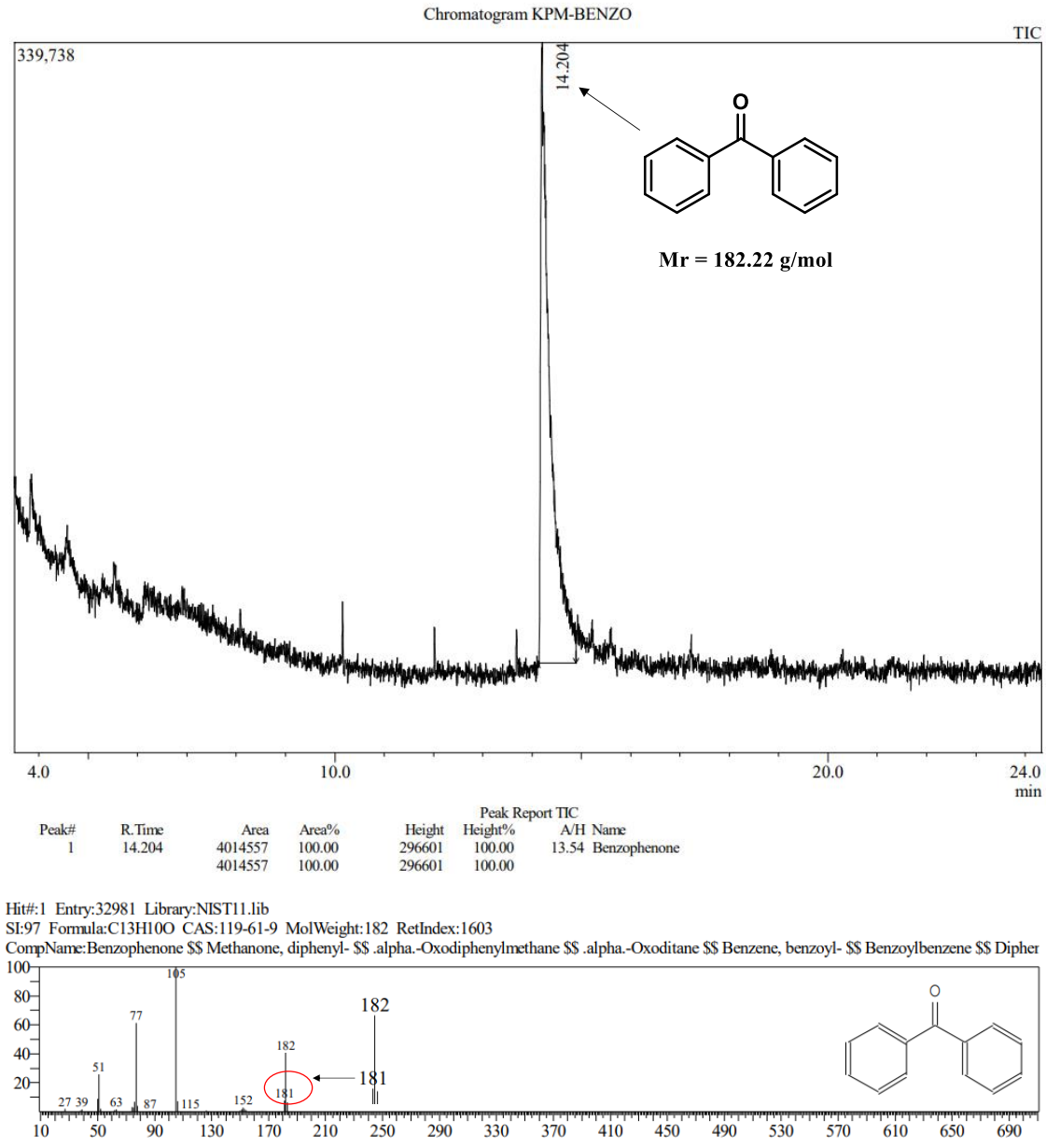

Figure A67: GC-MS chromatogram and MS spectrum of **119**.